

REPLACING ANIMAL EXPERIMENTS

**IN DEVELOPMENTAL TOXICITY TESTING OF PHENOLS
BY COMBINING IN VITRO ASSAYS WITH PHYSIOLOGICALLY
BASED KINETIC (PBK) MODELLING**

Marije Strikwold

Thesis committee

Promotors

Prof. Dr I.M.C.M. Rietjens
Professor of Toxicology
Wageningen University

Prof. Dr R.A. Woutersen
Professor of Translational Toxicology
Wageningen University

Co-promotor

Dr A. Punt
Food Toxicologist, Rikilt Wageningen
University and Research Centre

Other members

Prof. Dr S.C. de Vries, Wageningen University
Prof. Dr B.J. Blaauboer, Utrecht University
Prof. Dr N.P.E. Vermeulen, VU University Amsterdam
Dr E.D. Kroese, TNO, Zeist

This research was conducted under the auspices of the Graduate School VLAG (Advanced studies in Food Technology, Agrobiotechnology, Nutrition and Health Sciences).

REPLACING ANIMAL EXPERIMENTS

IN DEVELOPMENTAL TOXICITY TESTING OF PHENOLS
BY COMBINING IN VITRO ASSAYS WITH PHYSIOLOGICALLY
BASED KINETIC (PBK) MODELLING

Marije Strikwold

Thesis

submitted in fulfilment of the requirements for the degree of doctor
at Wageningen University

by the authority of the Rector Magnificus

Prof. Dr A.P.J. Mol,

in the presence of the

Thesis Committee appointed by the Academic Board

to be defended in public

on Friday 29 April 2016

at 4 p.m. in the Aula.

Marije Strikwold

Replacing animal experiments in developmental toxicity testing of phenols by combining in vitro assays with physiologically based kinetic (PBK) modelling
172 pages.

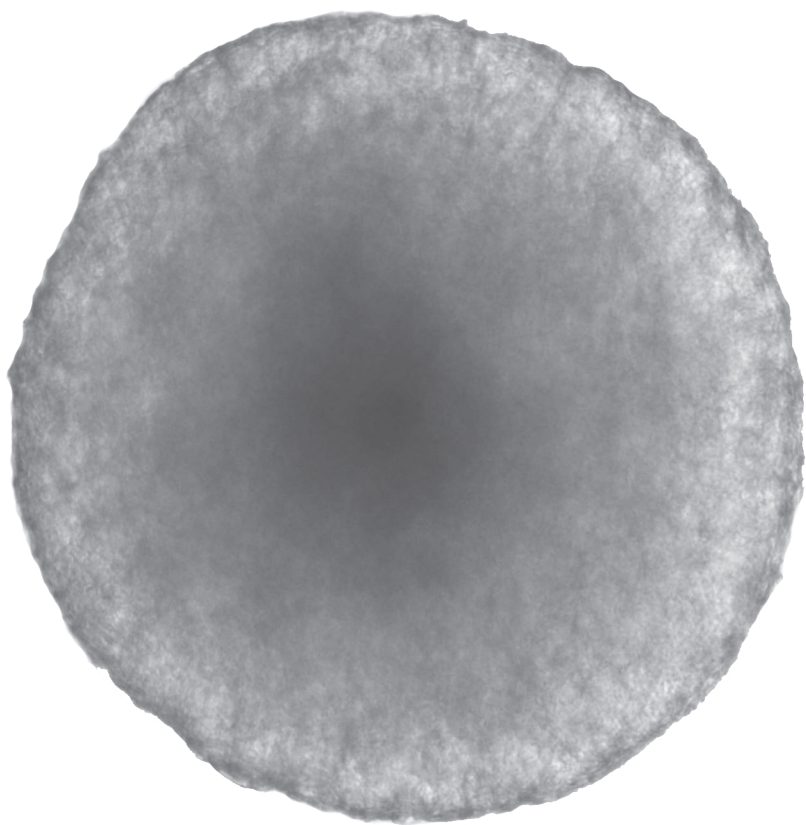
PhD thesis Wageningen University, Wageningen, NL (2016)

With references, with summary in English

ISBN: 978-94-6257-692-6

CONTENTS

CHAPTER 1	7
General introduction	
CHAPTER 2	27
Relative embryotoxic potency of p-substituted phenols in the embryonic stem cell test (EST) and comparison to their toxic potency in vivo and in the whole embryo culture (WEC) assay	
CHAPTER 3	47
Combining in vitro embryotoxicity data with physiologically based kinetic (PBK) modelling to define in vivo dose-response curves for developmental toxicity of phenol in rat and human	
CHAPTER 4	77
Integrating in vitro data and physiologically based kinetic (PBK) modelling to assess the in vivo potential developmental toxicity of a series of phenols	
CHAPTER 5	109
Development of a combined in vitro physiologically based kinetic (PBK) and Monte Carlo modelling approach to predict interindividual human variation in phenol induced developmental toxicity	
CHAPTER 6	133
General discussion and future perspectives	
CHAPTER 7	157
Summary	
ACKNOWLEDGEMENTS	161
ABOUT THE AUTHOR	165



CHAPTER 1

General introduction

RISK ASSESSMENT OF CHEMICALS

In the past century, major events such as the industrial revolution and World War I and II took place, which resulted in a significant increase of the development and production of chemicals. Many of these chemicals are beneficial for our life as they for example facilitate the production of crops as fertiliser or protect them from pests, they are used as pharmaceuticals, applied to produce a wide variety of consumer goods, or are used in chemical synthesis. Consequently, chemical exposure has become ubiquitous in daily life, from the moment of conception until death. Exposure to chemicals, however, may also lead to adverse health effects. A classical example is the synthetic hormone diethylstilbestrol (DES) which was prescribed to millions of women around the world, predominantly in the period of 1940 till late 1970s (Troisi et al. 2007), to prevent miscarriages and premature labour (National Toxicology Program 2011). It was considered safe and effective until the United States Environmental Protection Agency (EPA) advised physicians in 1971 to discontinue prescribing DES due to a link to a rare vaginal cancer in female offspring (Anon. 1972). Now, millions of people, both DES mothers and their (grand)children suffer from or are at increased risk to a variety of adverse health effects, like vaginal and cervical cancer (Verloop et al. 2010), breast cancer (Hoover et al. 2011; Titus-Ernstoff et al. 2001), infertility (Senekjian et al. 1988; Verloop et al. 2010) and urogenital abnormalities (Klip et al. 2002). This event and many other incidences reported in the previous century have initiated a more thorough pre-market testing and safety evaluation of novel chemicals.

Over time, dozens of regulations and directives on the safety of compounds have come into force within Europe, like the European regulation on food additives (EC 2008), the European regulation on pesticides (EC 2009a) and the directive on pharmacovigilance (EC 2010). In Europe, health and safety tests for industrial chemicals did not become compulsory until 1981 (Čihák, 2009). As a result, more than 100,000 chemicals have been marketed in Europe prior to 1981, which have not yet been (fully) tested on safety (Čihák, 2009). A more or less similar situation is encountered in the US; since the late 1970s about 84,000 industrial chemicals that are manufactured and/or processed in the USA are listed on the US Toxic Substances Control Act (TSCA) inventory (EPA 2015), but chemical companies were not obliged to provide specific toxicological evaluations although this information may be required by the EPA (National Research Council 2006). From the time the TSCA was enacted in 1976 until 2009, additional toxicity information was required for only less than 200 chemicals (GOA 2013), leaving a large number of chemicals for which no adequate toxicological data are available. Insight into the possible health effects of these chemicals is therefore highly desirable. With the enforcement of the European Registration, Evaluation, Authorisation and restriction of CHemicals (REACH) regulation in 2007 (EC 2007), the EU aims to collect chemical safety information of chemicals that are produced or imported at levels > 1 tonne/

yr, in the period from 2007-2018. The estimated number of chemicals to be registered under REACH lays within 68,000-100,000 (Rovida and Hartung 2009).

Traditionally, human health risk assessment consists of four steps, the hazard identification, dose-response assessment, exposure assessment and risk characterisation (National Research Council 1983), and enables estimation of the probability of adverse health effects in humans due to a chemical exposure. At the current state-of-the-art both the hazard identification and the dose-response assessment of chemicals rely heavily on the results of *in vivo* toxicity studies in experimental animals. To be able to fill the data gaps on the safety information of industrial chemicals, millions of animals would be required. Rovida and Hartung (2009) estimated that for the implementation of REACH, 114 million vertebrate animals might be needed. The greatest contribution to the total number of animals required has been estimated to come from three toxicity tests only, namely the developmental toxicity screening test (28.13%), the two-generation reproduction toxicity test (31.95%) and the long-term fish toxicity test (26.62%) (Rovida and Hartung 2009). The use of such a high number of experimental animals for safety testing of chemicals is generally regarded unethical, and not acceptable from a financial point of view (Rovida and Hartung 2009) and it would also require an enormous capacity of laboratories to carry out that many animal tests within the proposed period of time (IEH 2001). Because of these drawbacks, the application of alternatives to animal experiments is enforced within REACH (EC 2007) and the Cosmetic Products Regulation (EC 2009b). Moreover, a US National Research Council report on toxicity testing in the 21st century (National Research Council 2007) describes a transition in toxicity testing from relying on apical endpoints determined in *in vivo* studies towards application of *in vitro* tests to assess perturbations of toxicity pathways that are relevant for human biology. These initiatives promote that the safety evaluation of chemicals is evolving from using standalone animal toxicity tests towards the application of innovative non-animal based *in vitro* approaches to predict toxicity.

Over the past decades many efforts have been undertaken to develop alternatives to animal testing for a wide range of toxicological endpoints and parameters. *In vitro* toxicity assays are mainly used to screen and prioritise chemicals for further toxicity testing. Translation of *in vitro* toxicity data to the *in vivo* situation is an important, but limiting step for the use of *in vitro* toxicity outcomes in the regulatory risk assessment of chemicals, as *in vitro* derived outcomes of toxicity screening data do not always reflect *in vivo* toxicity ranking values (Blaauboer 2010). Moreover, the potential of *in vitro* tests to provide adequate quantitative toxicity values for the hazard and risk assessment of chemicals is limited. An important reason underlying this limitation is that an *in vitro* assay cannot provide a complete *in vivo* dose-response curve from which a point of departure (PoD) for risk assessment, like the no observed adverse effect level (NOAEL) or the 95% lower confidence limit of the benchmark dose (BMDL), can be derived. To overcome this constraint, *in vitro* toxicity tests

could be combined with physiologically based kinetic (PBK) modelling (Forsby and Blaauboer 2007; Louisse et al. 2010; Verwei et al. 2006). PBK models describe the absorption, distribution, metabolism and excretion (ADME) of a compound and may provide the link between in vitro derived toxicity data and in vivo toxicity values. Information describing the ADME characteristics can be obtained from in vivo kinetic studies, which have formed the basis for many PBK model parameters (Clewell and Clewell III 2008; Krewski et al. 1994). Along with the development of in vitro toxicity assays, in vitro and in silico approaches describing ADME processes have received increasing attention over the past years and may be used to parameterise PBK models (Rietjens et al. 2011). Combining in vitro toxicity data with PBK models, using in silico and in vitro derived kinetic parameters and information reported in the literature can be a next step to optimally contribute to a replacement, reduction and refinement (3Rs) of animal testing for the qualitative and quantitative safety assessment of chemicals.

Deriving human guidance values for chemicals is an important step for the risk assessment of chemicals and as outlined above frequently relies on animal data. Besides that alternatives to animal testing are required for ethical and financial reasons, alternative approaches might also provide better toxicity estimates for the human situation. At present, for non-genotoxic compounds PoDs derived from animal toxicity studies are extrapolated to human guidance values by applying default uncertainty factors that account for the inter- and intraspecies kinetic and dynamic differences (IPCS 2005). The default uncertainty factors often used amount to 10 for interspecies differences and another factor 10 for intraspecies variation (IPCS 2010). The interspecies safety factor is composed of a factor of $10^{0.6}$ (=4.0) accounting for kinetic differences and $10^{0.4}$ (=2.5) for dynamic differences, where the intraspecies safety factor is composed of a factor of $10^{0.5}$ (=3.16) accounting for human interindividual variability in toxicokinetics and a factor $10^{0.5}$ (=3.16) for human interindividual variability in toxicodynamics (IPCS 2005). The EPA and the United States Food and Drug Administration (FDA) use allometric scaling to account for interspecies differences. Two methods are often applied, namely allometry based on differences in body size (US FDA 2005) and allometry based on differences in physiological parameters (US EPA 2005) for which a body weight based allometric exponent of $2/3$ and $3/4$ is used, respectively. After applying intra- and interspecies uncertainty factors, the resulting guidance value can be applied for the general population, depending on the use of the chemical. However, these general factors do not always adequately resemble compound specific interindividual kinetic and dynamic differences. For example, response to environmental chemicals can vary between individuals or population groups as a result of multiple factors, i.e. age, life style, genotype, disease status and use of drugs. Insight into the sensitivity towards chemicals within the human population may be valuable as it can help to define specific groups that might be at higher risk, and thereby facilitate the risk assessment of compounds. Combining PBK modelling

with a statistical sampling technique (i.e. Monte Carlo simulation) may allow to evaluate variability and/or uncertainty in model inputs to variability and or uncertainty in model outputs, which potentially allows to quantify interindividual variability in chemical induced toxicity (Bois et al. 2010).

AIM OF THIS THESIS

The aim of the present thesis was to demonstrate the potential of a combined in vitro PBK based approach to translate in vitro data to in vivo toxicity values for rat and human predicting in vivo dose-response curves that allow definition of a PoD for risk assessment. This translation was carried out by applying PBK-based reverse dosimetry, using in silico and in vitro defined kinetic parameters, and by combining the in vitro PBK approach with Monte-Carlo simulations to assess interindividual variability.

The toxicity endpoint chosen for the studies was developmental toxicity because in vivo assays for this endpoint require one of the highest numbers of experimental animals in toxicity testing. Simple phenolic congeners were selected as model compounds based on the availability of in vitro and in vivo data for this endpoint.

DEVELOPMENTAL IN VITRO TOXICITY TESTING

Currently, several methods to predict human developmental toxicity are listed in the EURL database on alternative methods to animal experimentation (DM-ALM) (ECVAM DB-ALM 2014). Different species or tissue fractions or cells from different organisms, including mice and rats are used. Despite the fact that these assays are recorded in the database on alternative methods DM-ALM, they differ with respect to their contribution to the 3Rs. For example, in the whole embryo culture (WEC) assay, the frog embryo teratogenesis assay-xenopus (FETAX) test and the chicken embryotoxicity test, whole embryos are used (in culture), while the murine embryonic stem cell test (EST) uses a permanent cell line (Spielmann et al. 2006). Moreover, the alternatives included in the database on alternative methods DM-ALM cover a variety of (developmental) endpoints, i.e. effects of chemicals on differentiation, morphology, viability and/or functional parameters. So far the EST, WEC assay and micromass (MM) test are scientifically validated by ECVAM. From these three assays, the EST is the only test that does not require experimental animals, as it uses a permanent mouse cell line which makes it a promising assay for high-throughput screening of compounds (Spielmann et al. 2006). Therefore, the EST was chosen to assess the embryotoxic potency

of phenols in vitro in the present thesis. The differentiation assay of EST studies the embryotoxic potential of chemicals and is based on the assumption that chemicals block the spontaneous development of embryonic cells into beating cardiomyocyte clusters (Seiler et al. 2006). It is presumed that it covers critical endpoints in embryotoxicity (Adler et al. 2011). Based on different (pre)validation test that were performed it was stated that the EST was a reliable in vitro method to test embryotoxicity in vitro (Seiler et al. 2006). However, another validation study reported a low predictivity of the assay (Marx-Stoelting et al. 2009).

PBK MODELLING

PBK modelling is a mathematical technique to describe the ADME of a compound in an organism. In a PBK model, organs and tissues are represented as compartments, which are defined by anatomical (i.e. organ and tissue weights), physiological (i.e. blood flows), physico-chemical (i.e. blood:tissue coefficients) and kinetic (i.e. metabolic constants) parameters (Chiu et al. 2007; Krewski et al. 1994). The concentration of a compound and/or its metabolites in the compartment of interest in time is calculated using a set of mass-balance differential equations (Krewski et al. 1994; Rietjens et al. 2011).

Traditionally, PBK models have been applied to estimate the internal exposure to a chemical, i.e. a blood or tissue concentration, after being externally exposed for example orally or via inhalation. This type of prediction is called forward dosimetry (Clewell et al. 2008). The inverse, estimating external dose levels based on internal concentrations is called reverse dosimetry (Clewell et al. 2008) and was applied in the present thesis to translate in vitro effect concentrations to in vivo external dose levels in our so-called in vitro PBK approach.

PBK models can be developed for different species, for specific populations and even for individuals. When PBK models are linked with Monte Carlo simulations, then the impact of interindividual variation regarding for example physiological or biochemical parameters, on the distribution of internal (plasma) concentrations of a compound across a population can be simulated.

PBK MODEL PARAMETERISATION

Parameterisation of PBK models is an essential aspect of constructing a PBK model, because it can greatly affect the outcomes of the model. PBK model parameter values may be obtained from different sources. Anatomical and physiological parameter values for the species to be modelled (e.g. rat, mouse, human) are to a large extent available in the literature (Brown et al. 1997; Delp et al. 1998; ICRP 2003), especially when this concerns anatomical and physiological values that should represent the average of a population. In contrast, in vivo derived physico-chemical and kinetic data are scarce because in vivo ADME studies have not

regularly been conducted. Moreover, due to restrictions on animal testing under recent regulations like REACH (EC 2007) and the Cosmetic Products Regulation (EC 2009b) alternative approaches to predict physico-chemical and kinetic parameters are essential. Some key parameters in PBK modelling are discussed below.

Partition coefficients are physico-chemical parameters that are used in PBK models to estimate the distribution of a chemical over the specific body compartments or blood, such as for example the partitioning of a chemical between liver tissue and plasma. In vivo derived values for partition coefficients are obtained by taking the ratio of measured in vivo tissue and plasma concentrations at steady state conditions. An alternate approach is to determine these values in vitro, applying separation techniques including vial equilibration (Jepson et al. 1994; Murphy et al. 1995), ultra filtration (Tremblay et al. 2012), dialysis (Pacifci and Viani 1992) or solid-phase microextraction (Artola-Garicano et al. 2000), which accomplish partitioning of the test chemical between two or more compartments that represent the matrices of interest, for example the tissue and blood. Chemical analysis of the compartments at equilibrium provides information to calculate the partition coefficients. In addition to these in vitro approaches, numerous algorithms that estimate a chemical specific partition coefficient for certain compartments have been proposed in the past decades. Some have been established empirically (Meulenberg and Vijverberg 2000), while others are mechanistically defined using descriptors including the octanol-water partition coefficient and protein binding (Berezhkovskiy 2004; DeJongh et al. 1997; Payne and Kenny 2002; Poulin et al. 2001; Poulin and Krishnan 1996a; Poulin and Krishnan 1996b; Poulin and Theil 2000; Rodgers et al. 2005; Rodgers and Rowland 2006).

Frequently used kinetic data in PBK models include the oral absorption coefficient and kinetic constants for biotransformation reactions of a chemical. Non-animal based systems to study intestinal permeation include cell based drug transport studies (Alqahtani et al. 2013; Balimane and Chong 2005), isolated membrane vesicles (Hillgren et al. 1995), the Parallel Artificial Membrane Permeability Assay (PAMPA) (Kansy et al. 1998) and ex vivo and in situ models, for instance everted gut sacs (Wilk-Zasadna et al. 2015). Information on metabolism may be predicted using hepatocytes (Vellonen et al. 2014), tissue-slices (De Graaf et al. 2010), subcellular fractions like microsomes (Punt et al. 2008), or embryonic and induced pluripotent stem cells (Mann 2015; Takebe et al. 2013), each with its specific benefits and drawbacks (Wilk-Zasadna et al. 2015). In silico approaches to predict metabolism vary from rule-based expert systems that predict chemical sites liable for metabolism and the resulting metabolites (T'Jollyn et al. 2011), to Quantitative Structure-Activity Relationships (QSARs) to estimate metabolic constants such as K_m and V_{max} (Pirovano et al. 2014). The availability of alternative methods to quantify ADME characteristics, however, depends on the tissue, or barrier studied as well as the species.

Despite recent developments in non-animal approaches to estimate ADME properties,

PBK models for toxicological risk assessment purposes have often been developed based on animal data. Thus, exploring the development of PBK models that are (only) based on *in vitro* and *in silico* approaches, as was carried out in the present thesis may provide new perspectives for advancing PBK modelling as a method in alternatives to animal testing.

Selecting an applicable approach or assay to parameterise a PBK model requires consideration about the purpose of the PBK model, the age group, gender and species to be modelled, the physico-chemical properties of the compound of interest, the predictive power of the ADME assay and its applicability domain. For instance, to select the appropriate algorithm for predicting a partition coefficient, the species and the tissues to be modelled, as well as the chemical lipophilicity should be considered (Payne and Kenny 2002). Parameters generated with *in silico* or *in vitro* approaches may often not directly represent the *in vivo* system, and hence extrapolation of *in vitro* data to the *in vivo* situation (IVIVE) is imperative, to enable use of the generated output in the PBK model.

GENERAL OUTLINE OF THE IN VITRO PBK APPROACH USING REVERSE DOSIMETRY

The *in vitro* PBK approach applied in the present thesis is schematically represented in Figure 1 and encompasses 5 steps. The first step is the establishment of an *in vitro* concentration-response curve defined by effective concentrations (EC_x) of the test compound *in vitro*. For this purpose, different concentrations of a chemical are tested in an *in vitro* toxicity assay that is regarded to represent a specific *in vivo* toxicity outcome. In the present thesis this was the EST. This assay provided a series of EC_x values from which a concentration-response curve could be derived.

The second step is the development of a PBK model describing kinetic properties of the test compound *in vivo*, including the derivation of the required PBK model parameters. The present thesis took into account the principle of parsimony for the development of the PBK models, meaning that models should be as simple as possible but with sufficient explanatory power to fulfil their purpose (Clewell and Clewell III 2008). In the present thesis, model compartments were selected based on the target tissue of the toxicant and discriminating ADME properties that affect the fate of the test compound. Other tissues were lumped together in one compartment. Anatomical and physiological parameter values were obtained from literature. Physico-chemical and kinetic parameters were mainly derived with *in vitro* and *in silico* approaches to contribute to the 3Rs in the most optimal way.

Step three encompasses evaluation of the PBK model. The performance of the PBK model can be evaluated by comparing plasma concentrations predicted with the PBK model, with *in vivo* plasma concentrations of the compound reported in literature. For this purpose, PBK

model predictions were performed by applying similar dose administrations as reported in the in vivo studies used for the evaluation. Evaluation of the PBK models also comprised a sensitivity analysis to identify the sensitivity of the model outcome to changes in parameter values or model structures and aid the model interpretation and the decision if additional testing (of parameters) is required.

In the fourth step, in vitro EC_x values are translated into in vivo external dose levels (ED_x) generating dose-response curves for the toxic endpoint of interest in vivo, using PBK model based reverse dosimetry (Figure 1).

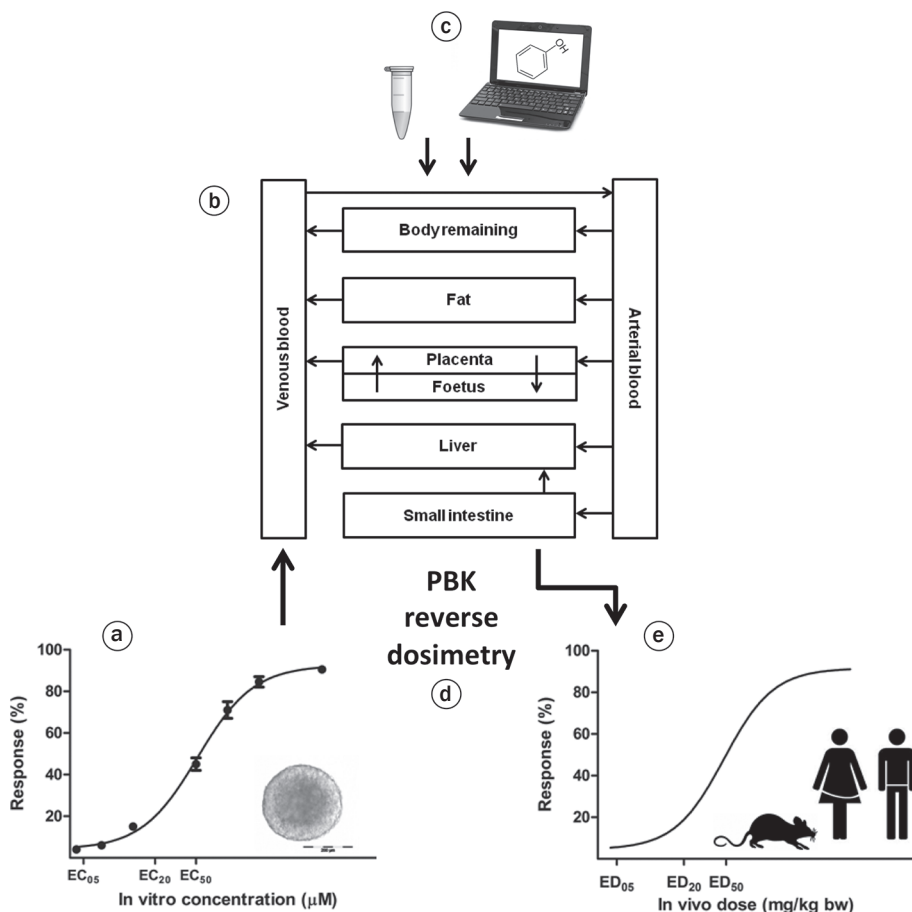


Figure 1 Principle of the in vitro PBK-based reverse dosimetry approach applied in the present thesis to predict developmental toxicity in vivo. Key elements of the approach that are visualised are (a) establishment of in vitro effect concentrations with the EST, (b) development of a PBK model, (c) parameterisation of the model using in vitro and in silico data, (d) applying reverse dosimetry and hence (e) generating in vivo effective dose levels and a dose-response curve.

For the reverse dosimetry step, in vitro EC_x values are set equal to internal plasma or tissue concentrations. Before applying this step, the influence of in vitro biokinetic processes i.e. evaporation or binding of the test chemical to components of the in vitro test system, like plastic or serum albumin should be identified as this may affect the bioavailability of a test compound in vitro and hence the EC_x values. Extrapolating in vitro effect concentrations towards values equivalent to in vivo EC_x values should be made, whenever possible. Use of the (corrected) in vitro EC_x values in the PBK model when applying PBK-based reverse dosimetry, will provide in vivo external dose levels (ED_x), from which a dose-response curve and hence a PoD or an effective dose level for the safety assessment of the compound under study can be derived.

In the final step, the in vitro PBK approach is evaluated by comparing the predicted dose-response curves and the PoD with in vivo data obtained from the literature.

PROBABILISTIC RISK ASSESSMENT AND MONTE CARLO SIMULATION

In the present thesis PBK modelling was also combined with Monte Carlo simulations to obtain insight in interindividual variation within the human population. This is of interest given that risk is a probability to develop an adverse health effect after being exposed towards a chemical (IPCS 2004).

For human health risk assessment, it has been recommended to distinguish uncertainty from individual variability (National Research Council 1994). The estimation of risk may be subject to uncertainties which may have different origins in the four step paradigm of risk assessment. For example, uncertainty may arise from experimental procedures, sampling and storage conditions of the chemical, definition of the adversity of the effect, model selection to define a PoD, extrapolation of animal data to human, and definition of exposure to the chemical (National Research Council 1994; Ramsey 2009). Variability can be defined as the spread of the true value of a quantified variable and is a property of a population, where uncertainty is the contribution to the estimated distribution that comes from imperfect knowledge (Kelly and Campbell 2000).

Monte Carlo is a statistical sampling technique to evaluate variability and/or uncertainty in model inputs to variability and or uncertainty in model outputs. Model inputs can be defined by probability distributions. In Monte Carlo simulations, situations or events (i.e. an exposure assessment) are simulated many times (i.e. 1000 times) thereby randomly sampling a parameter value from its probability distribution. Such a sampling can be performed for a single parameter as well as for multiple parameters in one simulation. The result of applying Monte Carlo simulations is an output distribution (i.e. a distribution of estimated exposures).

In the present thesis, the Monte Carlo simulation technique was linked to the PBK model for phenol (Figure 2) to obtain insight in interindividual variation in phenol induced development toxicity within the human population. Samples were randomly drawn repeatedly from distributions representing human interindividual variability in input parameters of the PBK model (i.e. metabolic constants and oral absorption coefficient). The input data sets generated by these Monte Carlo simulations were entered in the PBK model. After performing the PBK model calculations, an output distribution was generated representing variability in the phenol plasma concentrations for the human population. Differences in the phenol plasma concentrations for the average and the sensitive individual were used to define a chemical specific adjustment factor (CSAF) for interindividual kinetic differences, which is an alternative to the default uncertainty factor that accounts for human interindividual variability in toxicokinetics (IPCS 2005). The CSAF can be applied to the PoD to derive a safe guidance value for the risk assessment of chemicals (IPCS 2005).

Estimated input distributions

Estimated output distribution

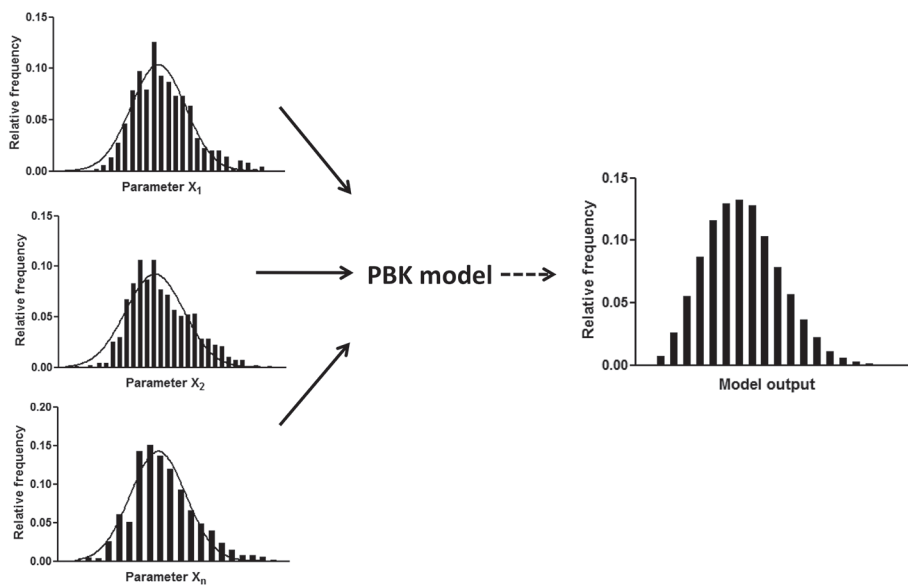


Figure 2 Schematic representation of the combination of Monte Carlo simulations with PBK modelling. The solid arrows indicate repeated drawings of samples from distributions of specified input parameters of the PBK model, generating a model output distribution after performing the PBK model calculations.

MODEL COMPOUNDS OF THE PRESENT THESIS: PHENOLS

To demonstrate the potential of a combined in vitro PBK model based approach to translate in vitro toxicity data to in vivo toxicity values and define a PoD for risk assessment the studies presented in the thesis used a series of phenol model compounds. Phenolic compounds are a wide class of compounds that are naturally present, i.e. in food, or are produced synthetically and are ubiquitous in our environment. Phenolic compounds contain an aromatic ring bearing one or more hydroxyl groups (Weber and Weber 2010). Phenols can be classified as simple phenols and polyphenols based on the number of phenol units in the molecule (Khoddami et al. 2013). The simplest form of a phenolic compound is hydroxybenzene generally referred to as phenol (Figure 3), which is a high volume production chemical with an annual production volume of about 9 million tons in 2008 world-wide (Weber and Weber 2010). The phenols selected for the present thesis are phenol and simple phenols with a substituent in the para position (Table 1). These compounds were selected based on their potential developmental toxicity reported in in vivo models (Argus 1997; Kavlock 1990) and/or in vitro models (Bernardini et al. 1996; Chapman et al. 1994; Oglesby et al. 1992; Paisio et al. 2009) and/or based on the fact that developmental toxicity was identified as the critical effect for defining guidance values for these compounds (Environment Agency 2009; WHO 1994).

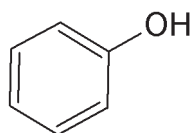
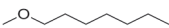
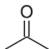


Figure 3 Chemical structure of phenol.

Table 1 Chemical name, p-substituent and CAS number of phenols used in the present thesis.

Chemical name	p-substituent	CAS
phenol	—H	108-95-2
p-fluorophenol	—F	371-41-5
p-heptyloxyphenol		13037-86-0
p-mercaptophenol	—SH	637-89-8
p-methylketophenol		99-93-4

ABSORPTION, DISTRIBUTION, METABOLISM AND EXCRETION OF PHENOLS

In vivo studies in rat and man reported a rapid uptake of phenol via the oral, inhalation and dermal routes (Hughes and Hall 1995; Piotrowski 1971). Dermal absorption was also reported for p-heptyloxyphenol in rats (Hughes and Hall 1997). Phenol is mainly transported in plasma, partly bound to albumin or other macromolecules (Liao and Oehme 1981) and is retained mainly in the highly perfused tissues, although concentrations were low (Hughes and Hall 1995; Liao and Oehme 1981).

Due to the presence of the hydroxyl moiety on the aromatic ring, the phenols selected for the present thesis may undergo direct conjugation catalyzed by sulfotransferases (SULT) and uridine diphosphate glucuronyltransferases (UGT) requiring the cofactors 3'-phosphoadenosine-5'-phosphosulfate (PAPS) and uridine 5'-diphosphoglucuronic acid (UDPGA), respectively (see Figure 4). Generally, these conjugations serve as a detoxification step and represent the major metabolic pathways of these phenols. In vivo, phase I hydroxylation of phenol mainly occurs at high concentrations and is known to occur via cytochromes P450 producing hydroquinone (Hiser et al. 1994). However, this is not a major metabolic pathway and hydroquinone has been found in urine as its glucuronide conjugate (Hiser et al. 1994).

Depending on the substituent on the phenol ring, other metabolic conversions may occur, i.e. elimination of the halogen may lead to the formation hydroquinone or benzoquinone which consecutively may be rapidly converted to hydroquinone (Ohe et al. 1997), but these metabolic pathways are regarded as minor routes compared to the conjugation while the resulting metabolites may also be detoxified by conjugation. Commonalities that are often found in the metabolic pathways of the simple phenols selected in the present thesis are included in Figure 4. Glucuronidation and sulfation of phenol have been identified as the major elimination pathways both in rodents (Capel et al. 1972; Edwards et al. 1986; Koster et al. 1981; Mulder and Meerman 1978) and in man (Capel et al. 1972; Hiser et al. 1994). First pass conjugation of phenol in rat was identified in the intestine, liver and the pulmonary system (Kothare and Zimmerman 2002; Powell et al. 1974), although pulmonary first pass metabolism has been questioned given that Dickinson and Taylor (1996) could not demonstrate this in vitro or in vivo. Metabolism of phenol and p-substituted phenols may also occur in the kidney as glucuronidation of p-nitrophenol was identified in kidney homogenates in vitro (Machida et al. 1982).

Excretion of phenol, mainly as conjugates, occurs in rat and human predominantly via urine (Capel et al. 1972; Hiser et al. 1994; Hughes and Hall 1995) and is, upon single oral and intravenous dosing, nearly complete within 12 hours (Hughes and Hall 1995; Hughes and Hall 1997). This was also found for phenol and a group of p-substituted phenols including p-heptyloxyphenol, after dermal and intraperitoneal administration of these compounds in young female rats (Hughes and Hall 1997), although p-heptyloxyphenol was retained in small

amounts in the carcasses (7-10% of the dose) after ip injection after 120 hours (Hughes and Hall 1997). This study also showed that excretion of p-heptyloxyphenol also occurs partly via faeces, though excretion via urine was reported to be still greater. The glucuronide conjugate of p-heptyloxyphenol may be subject to biliary secretion and hence elimination via the faeces, because its molecular weight is higher than 300 Da (Hughes and Hall 1997). Biliary excretion was observed in vivo for the glucuronide conjugate of p-methylketophenol, which has a molecular weight of 312 Da (Machida et al. 1982).

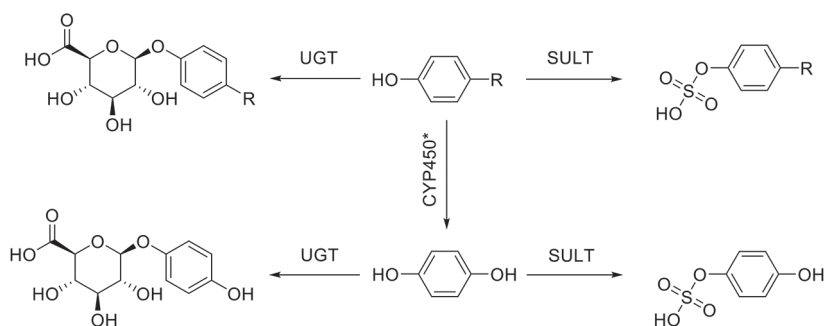


Figure 4 Commonalities in metabolic pathways of phenol and p-substituted phenols. The R represents the p-substituent included in Table 1. SULT and UGT represent sulfotransferases and uridine diphosphate glucuronyltransferases which are responsible for direct conjugation of the phenols with a glucuronide or sulfate moiety representing the major metabolic pathways. The reaction indicated by the asterisk represents hydroxylation of phenol by CYP450, accompanied by dehalogenation in the case of p-fluorophenol resulting in the formation of hydroquinone or benzoquinone that can subsequently be chemically reduced to hydroquinone, which are regarded minor metabolic pathways (see text for more details).

OUTLINE OF THIS THESIS

The aim of the present thesis was to demonstrate the potential of a combined in vitro PBK model based approach to translate in vitro toxicity data to in vivo toxicity values for rat and human predicting in vivo dose-response curves that allow definition of a PoD for risk assessment. Chapter 1 provides background information on alternatives to animal testing, gives a brief description of PBK modelling, Monte Carlo simulations and a short overview of some important ADME characteristics of phenols, the model compounds of the present thesis. This chapter also outlines the in vitro PBK-based reverse dosimetry approach to translate in vitro effective concentrations towards in vivo toxicity data. Chapter 2 describes the results of the EST which were used to identify the in vitro relative embryotoxic potency of the selected phenolic congeners. These results were compared to the outcomes of the ex vivo WEC assay and in vivo developmental toxicity values for the phenols, to provide insight into the applicability of the EST as an alternative for in vivo developmental toxicity testing. Chapter 3 describes the development of the PBK model of phenol and the extrapolation of in

in vitro EC_x values obtained in the EST to an in vivo dose-response curve, applying PBK-based reverse dosimetry. The prediction was evaluated against available in vivo toxicity data. In chapter 4 it was investigated whether the in vitro PBK approach was able to correctly predict the developmental toxic potency of the selected series of phenolic congeners in vivo. In chapter 5 we demonstrated a modelling approach that integrated in vitro toxicity data, PBK modelling and Monte Carlo simulations to derive chemical specific safety factors that cover interindividual human kinetic variation, with phenol induced developmental toxicity as the endpoint of interest. Chapter 6 presents the discussion of the results obtained within the present thesis and suggestions for future research.

REFERENCES

- Adler S, Basketter D, Creton S, Pelkonen O, van Benthem J, Zuang V, Andersen KE, Angers-Loustau A, Aptula A, Bal-Price A, Benfenati E, Bernauer U, Bessems J, Bois FY, Boobis A, Brandon E, Bremer S, Broschard T, Casati S, Coecke S, Corvi R, Cronin M, Daston G, Dekant W, Felter S, Grignard E, Gundert-Remy U, Heinonen T, Kimber I, Kleinjans J, Komulainen H, Kreiling R, Kreysa J, Leite SB, Loizou G, Maxwell G, Mazzatorta P, Munn S, Pfuhrer S, Phrakonkham P, Piersma A, Poth A, Prieto P, Repetto G, Rogiers V, Schoeters G, Schwarz M, Serafimova R, Täthi H, Testai E, van Delft J, van Loveren H, Vinken M, Worth A, Zaldivar JM (2011) Alternative (non-animal) methods for cosmetics testing: current status and future prospects-2010. *Arch Toxicol* 85:367-485
- Alqahtani S, Mohamed LA, Kaddoumi A (2013) Experimental models for predicting drug absorption and metabolism. *Expert Opin Drug Metab Toxicol* 9:1241-1254
- Anon. (1972) Selected item from the FDA drug bulletin-november 1971: diethylstilbestrol contraindicated in pregnancy. *Calif Med* 116:85-86
- Argus (1997) Oral (gavage) developmental toxicity study of phenol in rats. Protocol Number: Argus 916-011. Argus Research Laboratories, Inc., Horsham, PA
- Artola-Garicano E, Vaes WHJ, Hermens JLM (2000) Validation of negligible depletion solid-phase microextraction as a tool to determine tissue/blood partition coefficients for semivolatile and nonvolatile organic chemicals. *Toxicol Appl Pharmacol* 166:138-144
- Balimane PV and Chong S (2005) Cell culture-based models for intestinal permeability: a critique. *Drug Discov today* 10:335-343
- Berezhkovskiy LM (2004) Volume of distribution at steady state for a linear pharmacokinetic system with peripheral elimination. *J Pharm Sci* 93:1628-1640
- Bernardini G, Spinelli O, Presutti C, Vismara C, Bolzacchini E, Orlandi M, Settimi R (1996) Evaluation of the developmental toxicity of the pesticide MCPA and its contaminants phenol and chlorocresol. *Environ Toxicol Chem* 15:754-760
- Blaauboer BJ (2010) Biokinetic modeling and in vitro-in vivo extrapolations. *J Toxicol Environ Health, Part B* 13:242-252
- Bois FY, Jamei M, Clewell HJ (2010) PBPK modelling of inter-individual variability in the pharmacokinetics of environmental chemicals. *Toxicology* 278:256-267
- Brown RP, Delp MD, Lindstedt SL, Rhomberg LR, Beliles RP (1997) Physiological parameter values for physiologically based pharmacokinetic models. *Toxicol Ind Health* 13:407-484
- Capel ID, French MR, Millburn P, Smith RL, Williams RT (1972) The fate of [¹⁴C]phenol in various species. *Xenobiotica* 2:25-34
- Chapman DE, Namkung MJ, Juchau MR (1994) Benzene and benzene metabolites as embryotoxic agents: effects on cultured rat embryos. *Toxicol Appl Pharmacol* 128:129-137
- Chiu WA, Barton HA, DeWoskin RS, Schlosser P, Thompson CM, Sonawane B, Lipscomb JC, Krishnan K (2007) Evaluation of physiologically based pharmacokinetic models for use in risk assessment. *J Appl Toxicol* 27:218-237
- Čihák R (2009) REACH - an overview. *Interdisc Toxicol* 2:42-44
- Clewell HJ, Tan YM, Campbell JL, Andersen ME (2008) Quantitative interpretation of human biomonitoring data. *Toxicol Appl Pharmacol* 231:122-133

- Clewell RA and Clewell III HJ (2008) Development and specification of physiologically based pharmacokinetic models for use in risk assessment. *Regul Toxicol Pharmacol* 50:129-143
- De Graaf IAM, Olinga P, de Jager MH, Merema MT, de Kanter R, van de Kerkhof EG, Groothuis GMM (2010) Preparation and incubation of precision-cut liver and intestinal slices for application in drug metabolism and toxicity studies. *Nat Protoc* 5:1540-1551
- DeJongh J, Verhaar HJM, Hermens JLM (1997) A quantitative property-property relationship (QPPR) approach to estimate in vitro tissue-blood partition coefficients of organic chemicals in rats and humans. *Arch Toxicol* 72:17-25
- Delp MD, Evans MV, Duan C (1998) Effects of aging on cardiac output, regional blood flow, and body composition in Fischer-344 rats. *J Appl Physiol* 85:1813-1822
- Dickinson PA and Taylor G (1996) Pulmonary first-pass and steady-state metabolism of phenols. *Pharm Res* 13:744-748
- EC (2007) Corrigendum to Regulation (EC) No 1907/2006 of the European Parliament and of the Council of 18 December 2006 concerning the Registration, Evaluation, Authorisation and Restriction of Chemicals (REACH), establishing a European Chemicals Agency, amending Directive 1999/45/EC and repealing Council Regulation (EEC) No 793/93 and Commission Regulation (EC) No 1488/94 as well as Council Directive 76/769/EEC and Commission Directives 91/155/EEC, 93/67/EEC, 93/105/EC and 2000/21/EC. *Off J Eur Union* L136: 3-280
- EC (2008) Regulation (EC) No 1333/2008 of the European parliament and of the council of 16 December 2008 on food additives. *Off J Eur Union* L354:16-33
- EC (2009a) Regulation (EC) No 1107/2009 of the European parliament and of the council of 21 October 2009 concerning the placing of plant protection products on the market and repealing Council Directives 79/117/EEC and 91/414/EEC. *Off J Eur Union* L309:1-50
- EC (2009b) Regulation (EC) No 1223/2009 of the European parliament and of the council of 30 November 2009 on cosmetic products. *Off J Eur Union* L342:59-209
- EC (2010) Directive 2010/84/EU of the European parliament and of the council of 15 December 2010 amending, as regards pharmacovigilance, Directive 2001/83/EC on the Community code relating to medicinal products for human use. *Off J Eur Union* L348:74-99
- ECVAM DB-ALM (2014) EURL ECVAM. DataBase service on ALternative Methods to animal experimentation (DB-ALM). Available at: <http://ecvam-dbalm.jrc.ec.europa.eu/beta/>.
- Edwards VT, Jones BC, Hutson DH (1986) A comparison of the metabolic fate of phenol, phenyl glucoside and phenyl 6-O-malonyl-glucoside in the rat. *Xenobiotica* 16:801-807
- Environment Agency (2009) Contaminants in soil: updated collation of toxicological data and intake values for humans. Phenol. Science Report SC050021 / TOX9. Environment Agency, Bristol
- EPA (2015) Toxic Substances Control Act Chemical Substance Inventory (TSCA Inventory) Available at: <http://www.epa.gov/tsca-inventory>
- Forsby A and Blaauboer B (2007) Integration of in vitro neurotoxicity data with biokinetic modelling for the estimation of in vivo neurotoxicity. *Hum Exp Toxicol* 26:333-338
- GOA (2013) Chemical Regulation: Observations on the Toxic Substances Control Act and EPA Implementation. GAO-13-696T. U.S. Government Accountability Office, Washington D.C.
- Hillgren KM, Kato A, Borchardt RT (1995) In vitro systems for studying intestinal drug absorption. *Med Res Rev* 15:83-109
- Hiser MF, Kropscott BE, McQuirk RJ, Bus JS (1994) Pharmacokinetics, metabolism and distribution of ¹⁴C-phenol in Fischer 344 rats after gavage, drinking water and inhalation exposure. OTS0557473. Study ID: K-002727-022. Dow Chemical Company. Submitted to U.S. Environmental Protection Agency under TSCA Section 8D
- Hoover RN, Hyer M, Pfeiffer RM, Adam E, Bond B, Cheville AL, Colton T, Hartge P, Hatch EE, Herbst AL, Karlan BY, Kaufman R, Noller KL, Palmer JR, Robboy SJ, Saal RC, Strohsnitter W, Titus-Ernstoff L, Troisi R (2011) Adverse health outcomes in women exposed in utero to diethylstilbestrol. *N Engl J Med* 365:1304-1314
- Hughes MF and Hall LL (1995) Disposition of phenol in rat after oral, dermal, intravenous, and intratracheal administration. *Xenobiotica* 25:873-883
- Hughes MF and Hall LL (1997) In vivo disposition of p-substituted phenols in the young rat after intraperitoneal and dermal administration. *Food Chem Toxicol* 35:697-704
- ICRP (2003) Basic anatomical and physiological data for use in radiological protection: reference values. ICRP Publication 89. Pergamon, Oxford
- IEH (2001) Testing requirements for proposals under the EC white paper 'strategy for a future chemicals policy'. Web Report W6. Institute for Environment and Health, Leicester, UK
- IPCS (2004) IPCS risk assessment terminology. Part 1: IPCS/OECD key generic terms used in chemical hazard/risk assessment. Part 2: IPCS glossary of key exposure

- assessment terminology. World Health Organization, Geneva
- IPCS (2005) Chemical-specific adjustment factors for interspecies differences and human variability: guidance document for use of data in dose/concentration-response assessment. World Health Organization, Geneva
- IPCS (1999) Principles for the assessment of risks to human health from exposure to chemicals. World Health Organization, Geneva
- Jepson GW, Hoover DK, Black RK, McCafferty JD, Mahle DA, Gearhart JM (1994) A partition coefficient determination method for nonvolatile chemicals in biological tissues. *Fundam Appl Toxicol* 22:519-524
- Kansy M, Senner F, Gubernator K (1998) Physicochemical high throughput screening: Parallel artificial membrane permeation assay in the description of passive absorption processes. *J Med Chem* 41:1007-1010
- Kavlock RJ (1990) Structure-activity relationships in the developmental toxicity of substituted phenols: in vivo effects. *Teratology* 41:43-59
- Kelly EJ and Campbell K (2000) Separating variability and uncertainty in environmental risk assessment - Making choices. *Human Ecol Risk Assess* 6:1-13
- Khoddami A, Wilkes MA, Roberts TH (2013) Techniques for analysis of plant phenolic compounds. *Molecules* 18:2328-2375
- Klip H, Verloop J, van Gool JD, Koster META, Burger CW, van Leeuwen FE (2002) Hypospadias in sons of women exposed to diethylstilbestrol in utero: a cohort study. *Lancet* 359:1102-1107
- Koster H, Halsema I, Scholtens E, Knippers M, Mulder GJ (1981) Dose-dependent shifts in the sulfation and glucuronidation of phenolic compounds in the rat in vivo and in isolated hepatocytes. The role of saturation of phenol-sulfotransferase. *Biochem Pharmacol* 30:2569-2575
- Kothare PA and Zimmerman CL (2002) Intestinal metabolism: the role of enzyme localization in phenol metabolite kinetics. *Drug Metab Dispos* 30:586-594
- Krewski D, Withey JR, Ku LF, Andersen ME (1994) Applications of physiologic pharmacokinetic modeling in carcinogenic risk assessment. *Environ Health Perspect* 102:37-50
- Liao TF and Oehme FW (1981) Tissue distribution and plasma protein binding of [¹⁴C]phenol in rats. *Toxicol Appl Pharmacol* 57:220-225
- Louise J, de Jong E, van de Sandt JJM, Blaauboer BJ, Woutersen RA, Piersma AH, Rietjens IMCM, Verwei M (2010) The use of in vitro toxicity data and physiologically based kinetic modeling to predict dose-response curves for in vivo developmental toxicity of glycol ethers in rat and man. *Toxicol Sci* 118:470-484
- Machida M, Morita Y, Hayashi M, Awazu S (1982) Pharmacokinetic evidence for the occurrence of extrahepatic conjugative metabolism of p-nitrophenol in rats. *Biochem Pharmacol* 31:787-791
- Mann DA (2015) Human induced pluripotent stem cell-derived hepatocytes for toxicology testing. *Expert Opin Drug Metab Toxicol* 11:1-5
- Marx-Stoelting P, Adriaens E, Ahr HJ, Bremer S, Garthoff B, Gelbke HP, Piersma A, Pellizzer C, Reuter U, Rogiers V, Schenk B, Schwengberg S, Seiler A, Spielmann H, Steemans M, Stedman DB, Vanparrys P, Vericat JA, Verwei M, van de Water F, Weimer M, Schwarz M (2009) A review of the implementation of the embryonic stem cell test (EST). The report and recommendations of an ECVAM/ReProTect Workshop. *Altern Lab Anim* 37:313-328
- Meulenberg CJW and Vijverberg HPM (2000) Empirical relations predicting human and rat tissue:air partition coefficients of volatile organic compounds. *Toxicol Appl Pharmacol* 165:206-216
- Mulder JG and Meerman JHN (1978) Glucuronidation and sulphation in vivo and in vitro: selective inhibition of sulphation by drugs and deficiency of inorganic sulphate. In: Aitio A. (ed.) *Conjugation reactions in drug biotransformation*. Elsevier/North-Holland Biomedical Press, Amsterdam, pp 389-397
- Murphy JE, Janszen DB, Gargas ML (1995) An in vitro method for determination of tissue partition coefficients of non-volatile chemicals such as 2,3,7,8-tetrachlorodibenzo-p-dioxin and estradiol. *J Appl Toxicol* 15:147-152
- National Research Council (1983) Risk assessment in the federal government: managing the process. The National Academy Press, Washington, DC
- National Research Council (1994) Science and judgment in risk assessment. National Academy Press, Washington, DC
- National Research Council (2006) Toxicity testing for assessment of environmental agents: interim report. The National Academy Press, Washington, DC
- National Research Council (2007) Toxicity testing in the 21st century: a vision and a strategy. The National Academy Press, Washington, DC
- National Toxicology Program (2011) Report on carcinogens, twelfth edition. Diethylstilbestrol pp 159-161. U.S. Department of Health and Human Services, Public Health Service, Research Triangle Park, NC

- Oglesby LA, Ebron-McCoy MT, Logsdon TR, Copeland F, Beyer PE, Kavlock RJ (1992) In vitro embryotoxicity of a series of para-substituted phenols: structure, activity, and correlation with in vivo data. *Teratology* 45:11-33
- Ohe T, Mashino T, Hirobe M (1997) Substituent elimination from p-substituted phenols by cytochrome P450 ipso-substitution by the oxygen atom of the active species. *Drug Metab Dispos* 25:116-122
- Pacifici GM and Viani A (1992) Methods of determining plasma and tissue binding of drugs. Pharmacokinetic consequences. *Clin Pharmacokinetics* 23:449-468
- Paisio CE, Agostini E, González PS, Bertuzzi ML (2009) Lethal and teratogenic effects of phenol on *Bufo arenarum* embryos. *J Hazard Mater* 167:64-68
- Payne MP and Kenny LC (2002) Comparison of models for the estimation of biological partition coefficients. *J Toxicol Environ Health - Part A* 65:897-931
- Piotrowski JK (1971) Evaluation of exposure to phenol: absorption of phenol vapour in the lungs and through the skin and excretion of phenol in urine. *Br J Ind Med* 28:172-178
- Pirovano A, Huijbregts MAJ, Ragas AMJ, Veltman K, Hendriks AJ (2014) Mechanistically-based QSARs to describe metabolic constants in mammals. *Altern Lab Anim* 42:59-69
- Poulin P and Krishnan K (1996a) A mechanistic algorithm for predicting blood:air partition coefficients of organic chemicals with the consideration of reversible binding in hemoglobin. *Toxicol Appl Pharmacol* 136:131-137
- Poulin P and Krishnan K (1996b) A tissue composition-based algorithm for predicting tissue:air partition coefficients of organic chemicals. *Toxicol Appl Pharmacol* 136:126-130
- Poulin P, Schoenlein K, Theil FP (2001) Prediction of adipose tissue:plasma partition coefficients for structurally unrelated drugs. *J Pharm Sci* 90:436-447
- Poulin P and Theil FP (2000) A priori prediction of tissue:plasma partition coefficients of drugs to facilitate the use of physiologically-based pharmacokinetic models in drug discovery. *J Pharm Sci* 89:16-35
- Powell GM, Miller JJ, Olavesen AH, Curtis CG (1974) Liver as major organ of phenol detoxication? *Nature* 252:234-235
- Punt A, Freidig AP, Delatour T, Scholz G, Boersma MG, Schilter B, van Bladeren PJ, Rietjens IMCM (2008) A physiologically based biokinetic (PBBK) model for estragole bioactivation and detoxification in rat. *Toxicol Appl Pharmacol* 231:248-259
- Ramsey MH (2009) Uncertainty in the assessment of hazard, exposure and risk. *Environ Geochem Health* 31:205-217
- Rietjens IMCM, Lousse J, Punt A (2011) Tutorial on physiologically based kinetic modeling in molecular nutrition and food research. *Mol Nutr Food Res* 55:941-956
- Rodgers T, Leahy D, Rowland M (2005) Physiologically based pharmacokinetic modeling 1: predicting the tissue distribution of moderate-to-strong bases. *J Pharm Sci* 94:1259-1276
- Rodgers T and Rowland M (2006) Physiologically based pharmacokinetic modelling 2: predicting the tissue distribution of acids, very weak bases, neutrals and zwitterions. *J Pharm Sci* 95:1238-1257
- Rovida C and Hartung T (2009) Re-evaluation of animal numbers and costs for in vivo tests to accomplish REACH legislation requirements for chemicals - a report by the transatlantic think tank for toxicology (t⁴). *ALTEX* 26:187-208
- Seiler AEM, Buesen R, Visan A, Spielmann H (2006) Use of murine embryonic stem cells in embryotoxicity assays. The embryonic stem cell test. *Methods Mol Biol* 329:371-395
- Senekjian EK, Potkul RK, Frey K, Herbst AL (1988) Infertility among daughters either exposed or not exposed to diethylstilbestrol. *Am J Obstet Gynecol* 158:493-498
- Spielmann H, Seiler A, Bremer S, Hareng L, Hartung T, Ahr H, Faustman E, Haas U, Moffat GJ, Nau H, Vanparys P, Piersma A, Sintes JR, Stuart J (2006) The practical application of three validated in vitro embryotoxicity tests. *Altern Lab Anim* 34:527-538
- T'Jolyn H, Boussery K, Mortishire-Smith RJ, Coe K, De Boeck B, Van Bocxlaer JF, Mannens G (2011) Evaluation of three state-of-the-art metabolite prediction software packages (Meteor, MetaSite, and StarDrop) through independent and synergistic use. *Drug Metab Dispos* 39:2066-2075
- Takebe T, Sekine K, Enomura M, Koike H, Kimura M, Ogaeri T, Zhang RR, Ueno Y, Zheng YW, Koike N, Aoyama S, Adachi Y, Taniguchi H (2013) Vascularized and functional human liver from an iPSC-derived organ bud transplant. *Nature* 499:481-484
- Titus-Ernstoff L, Hatch EE, Hoover RN, Palmer J, Greenberg ER, Ricker W, Kaufman R, Noller K, Herbst AL, Colton T, Hartge P (2001) Long-term cancer risk in women given diethylstilbestrol (DES) during pregnancy. *Br J Cancer* 84:126-133
- Tremblay RT, Kim D, Fisher JW (2012) Determination of tissue to blood partition coefficients for nonvolatile herbicides, insecticides, and fungicides using negligible

depletion solid-phase microextraction (nd-SPME) and ultrafiltration. *J Toxicol Environ Health, Part A* 75:288-298

Troisi R, Hatch EE, Titus-Ernstoff L, Hyer M, Palmer JR, Robboy SJ, Strohsnitter WC, Kaufman R, Herbst AL, Hoover RN (2007) Cancer risk in women prenatally exposed to diethylstilbestrol. *Int J Cancer* 121:356-360

US EPA (2005) Guidelines for Carcinogen Risk Assessment. EPA/630/P-03/001F

US FDA (2005) Guidance for industry. Estimating the maximum safe starting dose in initial clinical trials for therapeutics in adult healthy volunteers. U.S. Department of Health and Human Services, Food and Drug Administration Center for Drug Evaluation and Research (CDER), Rockville, MD

Vellonen KS, Malinen M, Mannermaa E, Subrizi A, Toropainen E, Lou YR, Kidron H, Yliperttula M, Urtti A (2014) A critical assessment of in vitro tissue models for ADME and drug delivery. *J Controlled Release* 190:94-114

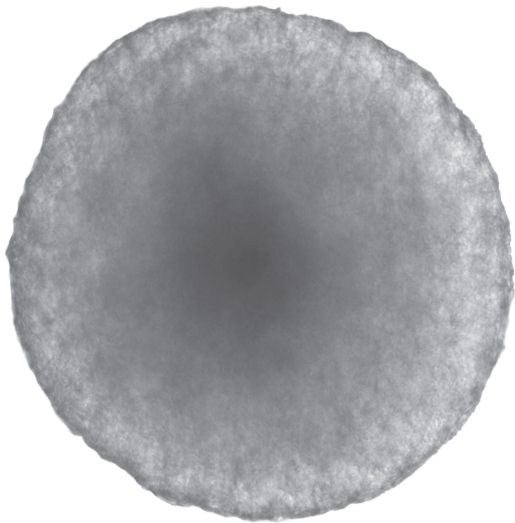
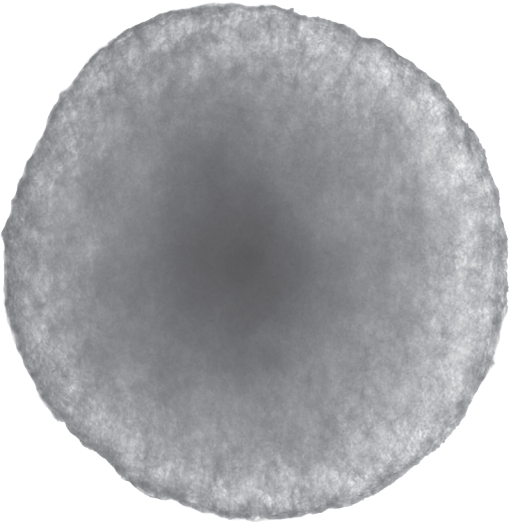
Verloop J, van Leeuwen FE, Helmerhorst TJM, van Boven HH, Rookus MA (2010) Cancer risk in DES daughters. *Cancer Causes Control* 21:999-1007

Verwei M, van Burgsteden JA, Krul CAM, van de Sandt JJM, Freidig AP (2006) Prediction of in vivo embryotoxic effect levels with a combination of in vitro studies and PBPK modelling. *Toxicol Lett* 165:79-87

Weber M and Weber M (2010) Phenols. In: Pilato L (ed.) *Phenolic resins: a century of progress*. Springer, Berlin Heidelberg, pp 9-23

WHO (1994) Phenol. *Environmental Health Criteria* 161. World Health Organization, Geneva

Wilk-Zasadna I, Bernasconi C, Pelkonen O, Coecke S (2015) Biotransformation in vitro: An essential consideration in the quantitative in vitro-to-in vivo extrapolation (QIVIVE) of toxicity data. *Toxicology* 332:8-19



CHAPTER 2

**Relative embryotoxic potency of
p-substituted phenols in the
embryonic stem cell test (EST)
and comparison to their toxic
potency in vivo and in the whole
embryo culture (WEC) assay**

**Marije Strikwold, Ruud A Woutersen, Bert Spenkelink, Ans Punt, Ivonne MCM Rietjens
Based on: Toxicology Letters (2012) 213:235-242**

ABSTRACT

The applicability of the embryonic stem cell test (EST) as an alternative for in vivo embryotoxicity testing was evaluated for a series of five p-substituted phenols. To this purpose, the potency ranking for this class of compounds derived from the inhibition of cardiomyocyte differentiation in the EST was compared to in vivo embryotoxic potency data obtained from literature and to the potency ranking defined in the in vitro whole embryo culture (WEC) assay. From the results obtained it appears that the EST was able to identify the embryotoxic potential for p-substituted phenols, providing an identical potency ranking compared to the WEC assay. However, the EST was not able to predict an accurate ranking for the phenols compared to their potency observed in vivo. Only phenol, the least potent compound within this series, was correctly ranked. Furthermore, p-mercaptophenol was correctly identified as a relative potent congener of the phenols tested, but its ranking was distorted by p-heptyloxyphenol, of which the toxicity was overestimated in the EST. It is concluded that when attempting to explain the observed disparity in potency rankings between in vitro and in vivo embryotoxicity, the in vitro models should be combined with a kinetic model describing in vivo absorption, distribution, metabolism and excretion processes of the compounds.

INTRODUCTION

Embryotoxicity is considered a critical step in reproductive toxicity (Adler, 2011). For this endpoint, so far, three scientifically validated rodent based *in vitro* assays are available, which have been evaluated for discriminating between non, weak and strong embryotoxic compounds (Genschow et al. 2002). These assays are the postimplantation rat whole-embryo culture test (WEC), the limb bud micromass test and the embryonic stem cell test (EST). Each of these assays has its advantages and limitations. Briefly, in the WEC, embryo's dissected at gestational day (GD) 10 are cultured and exposed to the test compound for two days, whereupon they are examined and evaluated for developmental anomalies (ECVAM, 2010a). An advantage of the WEC is that the model system comprises a whole organism. A drawback, however, resides in the fact that it only covers a limited period of organogenesis (Augustine-Rauch et al. 2010). Both, the limb bud micromass test and the EST are more simplified methods to evaluate embryotoxicity compared to the WEC. In principle, the limb bud micromass test studies the interference of a compound with the formation of foci of chondrocytes *in vitro*, but still requires embryos, though less than the WEC (ECVAM, 2010b). The EST is based on the principle that chemicals may affect the spontaneous development of embryonic cells into beating cardiomyocyte clusters (Seiler et al. 2006). An important advantage of the EST, compared to both the WEC and the limb bud micromass test, is the use of a permanent cell line (Spielmann et al. 2006), permitting nearly indefinite propagation of the embryonic stem cells *in vitro*, thereby greatly supporting reduction, refinement, and replacement (3 Rs) in animal testing. Moreover, this feature allows high-throughput screening of chemical compounds (Spielmann et al. 2006), which makes the EST a promising tool to screen compounds on potential embryotoxicity.

In a validation study lead by the European Centre for the Validation of Alternative Methods (ECVAM), the EST demonstrated a good correlation between *in vitro* and *in vivo* data, providing a correct classification of 78% of a test set of twenty chemicals into three distinct embryotoxic classes (non, weak and strong embryo toxicants) (Genschow et al. 2004). However, in a second study only two of thirteen additional selected chemicals were correctly classified with the EST, which raises concern about the applicability of the prediction model that was applied in both studies to classify compounds in non, weak and strong embryo toxicants (Marx-Stoelting et al. 2009). An explanation for this poor predictivity might be the absence of a carefully defined applicability domain and the limited number of compounds that was used to develop the prediction model, thereby restricting the application of the EST for regulatory purposes (Marx-Stoelting et al. 2009).

To overcome this limitation, additional information on the performance of the EST with different chemical classes is needed (de Jong et al. 2011a). Therefore, the aim of the present study was to evaluate the applicability of the EST for a series of *p*-substituted phenols, a novel

chemical class to be studied with the EST, as an alternative for in vivo embryotoxicity testing.

Phenol is a high production volume chemical with an annual production of nearly 9 million tons world-wide in 2008 (Weber and Weber, 2010). Phenol is used as an intermediate in the chemical industry and as a disinfectant, slimicide and in medicinal drugs (ATSDR, 2008). Many phenols, including p-substituted phenols, are applied in pesticides, resins, textiles, dyes and/or drugs. In addition, 4-methylketophenol is a natural occurring and chemically synthesised flavouring compound (FAO, 2010). Several studies demonstrated an embryotoxic potential of phenol and/or p-substituted phenols in vivo (Argus, 1997; Kavlock, 1990) and in vitro (Chapman et al. 1994; Oglesby et al. 1992).

In the present study, results obtained for a selected series of phenols in the EST, were compared to the in vivo benchmark dose (BMD₁₀) values derived for their effects reported in in vivo developmental toxicity studies as well as to outcomes already reported in the literature for their effects in the WEC assay. This in order to evaluate the performance of the EST for this novel chemical class not tested before in this in vitro assay for embryotoxicity.

MATERIALS AND METHODS

COMPOUNDS AND CELLS

Phenol (99%), p-fluorophenol (99%), p-heptyloxyphenol (97%), p-mercaptophenol (97%), p-methylketophenol (99%), p-hydroxyphenol (99%), p-aminophenol (99%), ascorbic acid, glutathione and β-mercaptoethanol were purchased from Sigma Aldrich (Steinheim, Germany). Methanol (HPLC supra-gradient) was obtained from Biosolve (Valkenswaard, The Netherlands). Dimethylsulfoxide was obtained from Acros Organics (Geel, Belgium). Murine embryonic stem cells (ES-D3 cells) were kindly provided by Johnson & Johnson (Beerse, Belgium). Dulbecco's Modified Eagle Medium (DMEM), L-glutamine, non-essential amino acids and penicillin and streptomycin are from Gibco and were purchased from Fisher Emergo (Landsmeer, The Netherlands). Foetal calf serum was obtained from Lonza (Verviers, Belgium) and mouse leukemia inhibitory factor from Chemicon International (Temecula, CA).

PHENOL STABILITY

The chemical stability in time of phenol and six p-substituted phenols in ES-D3 cell culture medium was tested prior to experiments with the EST. Stability of the compounds was tested at concentrations to be tested in the EST, which were initially selected based on in vitro cytotoxicity data from literature (Kendig and Tarloff, 2007; Selassie et al. 2005; Verma et al. 2003; Zhou et al. 2009). These final test concentrations were 3.16 mM for phenol, 1.0 mM for p-fluorophenol, p-mercaptophenol and p-aminophenol, 0.024 mM for p-heptyloxyphenol, 0.5 mM for p-methylketophenol and 0.316 mM for p-hydroxyphenol. ES-D3 cell culture

medium with the test compound, but without cells, was maintained in 24 well plates under similar test conditions as applied in the differentiation assay of the EST (for details see Sections Cell culture and Differentiation assay). Samples were taken on days 0, 1, 2 and 5 and analysis of the compound in culture medium was performed on a Waters Alliance HPLC-system using an Alltima C18, 5 μm column, 150 mm x 4.6 mm (Grace Alltech, Breda, The Netherlands). The mobile phase was made of nanopure water (A) and pure methanol (B) using a gradient (A:B) of 100:0 for the first 10 min, changing to 90:10 in 5 min and then to 10:90 within another 5 min, maintaining this ratio for 2 min, then changing to 100:0 in 1 min and maintaining this ratio for 10 min. The flow rate was 1 ml/min. Phenol, p-fluorophenol, p-heptyloxyphenol, p-mercaptophenol, p-methylketophenol, p-aminophenol and p-hydroxyphenol were detected and quantified based on their peak areas at their maximum wavelength, using a photodiode array detector.

CELL CULTURE

Embryotoxicity of phenol and four p-substituted phenols (Figure 1) was assessed using the murine embryonic stem cell differentiation assay (ES-D3 cells) performed essentially as previously described (De Smedt et al. 2008). Briefly, ES-D3 cells, which were stored in liquid nitrogen, were thawed and cultured for 3 days in ES-D3 culture medium, consisting of Dulbecco's Modified Eagle Medium, supplemented with 20% (v/v) foetal calf serum, 2 mM L-glutamine, 1% (v/v) non-essential amino acids, penicillin/streptomycin (50 U/ml / 50 μg /ml) and 0.1 mM β -mercaptoethanol. Cells were maintained undifferentiated by adding 1000 U/ml mouse leukemia inhibitory factor.

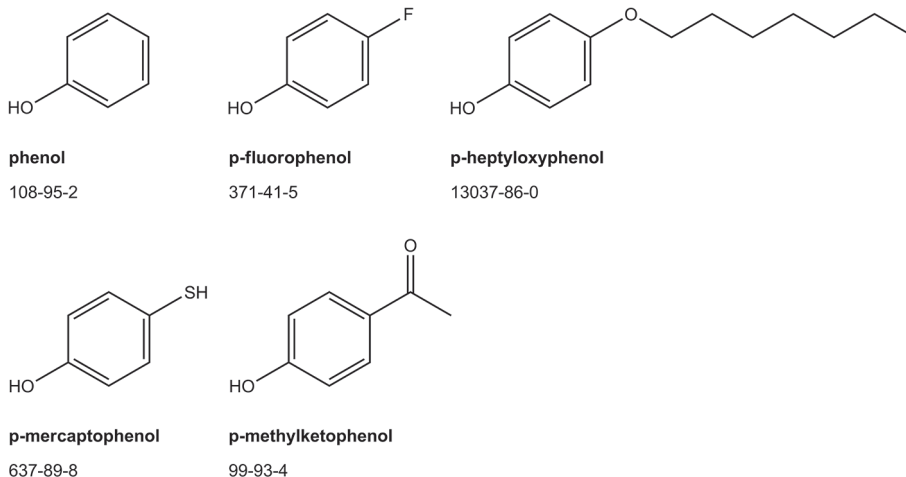


Figure 1 Chemical structure, chemical name and CAS number of phenol and four p-substituted phenols used in the present study.

DIFFERENTIATION ASSAY

The differentiation assay was started by culturing 20 μl drops (45 drops totally) of an embryonic stem cell suspension (3.75×10^4 cells/ml medium) on the inner side of the lid of a 96 well microtiter plate (Corning, The Netherlands) according to the hanging drop technique allowing cells to form embryoid bodies. After 3 days, embryoid bodies were transferred to 6 cm non-adherent petri dishes (Greiner Bio-one, Hungary) and incubated for 2 days. Then, one embryoid body was placed in each well of a 24 well tissue culture plate (one plate per test concentration) and cultured for 5 more days. After that, differentiation of the embryoid bodies into contracting cardiomyocytes was evaluated visually with an Olympus CKX41 inverted microscope. During culturing, cells were constantly kept in a 5% CO_2 -humidified atmosphere at 37 °C and were continuously exposed to the test compound. Stock solutions and compound dilutions were prepared in dimethylsulfoxide and added to ES-D3 culture medium. The final dimethylsulfoxide concentration in culture medium was 0.25% (v/v) and a solvent control was tested in each experiment. ES-D3 medium including the compound was refreshed on days 0, 3 and 5 of the differentiation assay.

The differentiation assay was considered valid if a blank resulted in beating cardiomyocyte clusters in at least 21 out of 24 wells. The inhibition of differentiation by the test compound was defined and presented as the fraction of wells with undifferentiated embryoid bodies in a 24 well plate. For each phenol, multiple independent assays were performed ($n=2-5$ as indicated), using different test concentrations (Figure 2).

SELECTION OF IN VIVO AND IN VITRO TOXICITY DATA

A literature search was performed to identify available in vivo and in vitro studies on reproductive and developmental toxicity of phenol and the p-substituted phenol model compounds of the present study. A study was selected if it included at least three dose groups, because this would enable analysis by the benchmark dose (BMD) approach and possible establishment of a BMD value. Developmental endpoints were considered relevant if the compound showed a dose or concentration depended effect and a BMD value could be derived. In addition, in vivo maternal effects were evaluated, when available from the selected developmental toxicity studies.

DATA COMPUTATION

For each phenol that was tested in the EST, in vitro concentration-response curves for embryotoxicity were derived to calculate benchmark concentrations at which 50 percent (BMC_{50}) of the embryoid bodies did not differentiate into contracting cardiomyocytes. To this purpose, different dichotomous concentration-response models were fitted to the embryotoxicity data obtained with the EST. The data of the independent assays were combined prior to the curve-fitting. Models included in the evaluation were the gamma, (log)



logistic, (log) probit, multistage and the Weibull model. For each BMC calculation an extra risk at a benchmark response above background was considered (Davis et al. 2011). The performance of each model fit was consecutively evaluated for the global goodness-of-fit ($p > 0.1$), the model with the smallest scaled residual at the concentration-response curve closest to the calculated BMC_{50} and a visual inspection of the fitted concentration-response curves (Davis et al. 2011). In case no goodness-of-fit with $p > 0.1$ was obtained for any model, an additional curve-fitting was performed using average response values for each concentration tested. If the model-fit of two or more models was accepted according the criteria described above, then the model with the smallest Akaike's Information Criterion (AIC) was regarded superior (Davis et al. 2011). Hence, the BMC_{50} was selected from the model that provided the best fit.

For continuous *in vivo* data a benchmark response of 10% adverse effect of the studied maternal and developmental toxicity endpoints was used (Barnes et al. 1995). Continuous data were fit to the exponential, polynomial, power, linear, and hill models. The dose-response curves were included in further evaluation if they showed a significant ($p < 0.05$) dose dependent response and if the variance (constant or non-homogeneous) was adequately modelled ($p > 0.05$). Subsequently, the evaluation of the model fit was performed according to the same criteria as described for the dichotomous models. Finally, the BMD_{10} was selected from the model that provided the best fit.

All benchmark dose and benchmark concentration calculations were performed with the Environmental Protection Agency's (EPA) Benchmark Dose Software (BMDS) version 2.2. Concentration-response curves were plotted with GraphPad Prism (version 5, GraphPad Software, San Diego, CA) applying a four-parameter logistic fit.

POTENCY RANKING

Phenols tested in the EST were ranked for embryotoxic potency according to their BMC_{50} value, from the one with the highest to that with the lowest toxic potency. This ranking was compared to *in vitro* embryotoxic potency (ranking) data obtained from literature and to ranking based on BMD_{10} values derived in the present study from *in vivo* data on developmental toxicity of the phenols reported in the literature. In addition, embryotoxicity was compared to maternal toxicity.

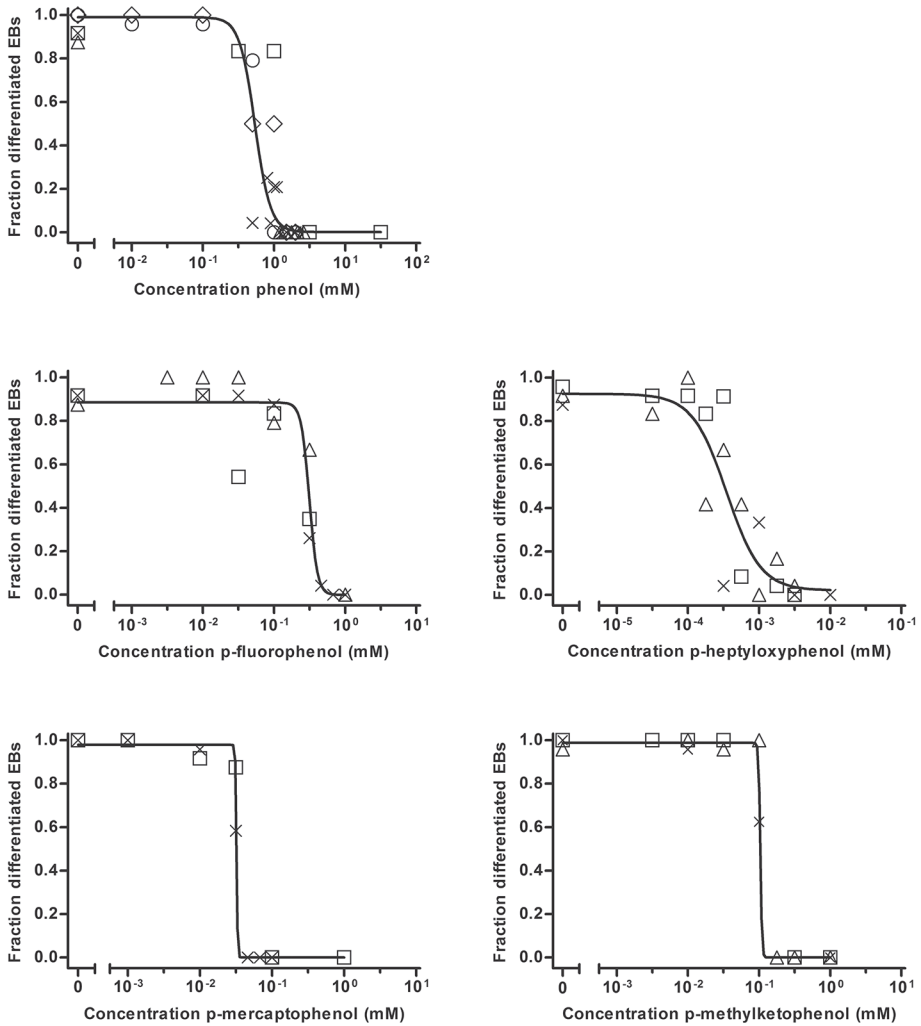


Figure 2 Concentration-response curves for phenol, p-fluorophenol, p-heptyloxyphenol, p-mercaptophenol and p-methylketophenol. Each figure represents the inhibition of differentiation of the embryonic bodies (EBs) by the compound at the specified concentrations. Different symbols represent independent assays.

RESULTS

STABILITY OF THE TEST COMPOUNDS

Results from the chemical stability tests of the phenols are presented in Figure 3. From these data it can be derived that the compounds p-heptyloxyphenol, p-mercaptophenol and p-methylketophenol, were stable during the 5 days of incubation. Phenol and p-fluorophenol showed some decrease in the test concentration in time. For phenol 75, 62 and 27% of the original test concentration was detected in culture medium after 1, 2 and 5 days of incubation, respectively, with an area under the curve ($AUC_{0-5days}$) from 0 to 5 days amounting 57.9% of what would be expected without decrease in the initial concentration. For p-fluorophenol these values amounted to 86, 74 and 39% with an $AUC_{0-5days}$ amounting 68.5% of what would be expected without decrease in the initial concentration. Stability was regarded sufficient to include these compounds in the EST. Both, p-hydroxyphenol and p-aminophenol could not be detected after 1 day of incubation, probably due to auto-oxidation of these compounds. To prevent auto-oxidation, both ascorbic acid and glutathione were added to the culture medium at 1 mM and 5 mM, respectively. However, both glutathione and ascorbic acid appeared to be toxic to ES-D3 cells at these concentrations (data not shown). Hence, p-hydroxyphenol and p-aminophenol were not included in the EST.

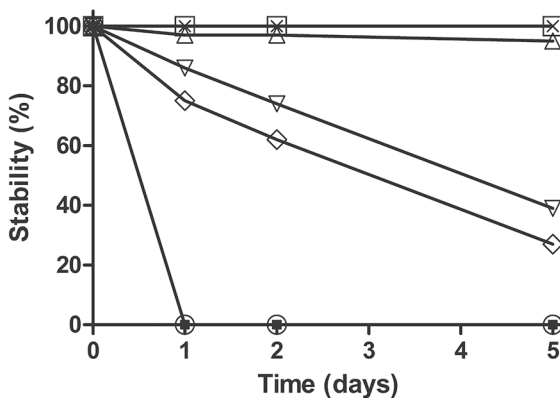


Figure 3 Chemical stability expressed as the percentage of the initial test concentration ($t=0$) of phenol (◇), p-fluorophenol (▽), p-heptyloxyphenol (×), p-mercaptophenol (△), p-methylketophenol (□), p-aminophenol (○) and p-hydroxyphenol (■) left in ES-D3 assay medium, in time (day).

Table 1 BMC₅₀ values of phenols tested in the EST as determined by a BMD analysis of the data of Figure 2, ranked from high to low potency.

Phenol	BMC ₅₀ (mM)
p-heptyloxy	0.00038
p-mercapto	0.035
p-methylketo	0.12
p-fluoro	0.31
phenol	0.59 ^a

^a Model fit: 0.05 < p < 0.1.

DIFFERENTIATION OF EMBRYONIC STEM CELLS TO BEATING CARDIOMYOCYTES

Figure 2 presents the concentration-response curves for the phenols tested in the EST. From these results it appears that each phenol inhibited differentiation of ES-D3 cells into beating cardiomyocytes in a concentration dependent manner. Both, p-mercaptophenol and p-methylketophenol show a steep concentration-response curve. The BMC₅₀ values derived from the concentration response data of the different phenols are presented in Table 1. The most potent phenol tested is p-heptyloxyphenol, followed by p-mercaptophenol, p-methylketophenol, p-fluorophenol and phenol. The choice of the dose-response model and the benchmark response value appeared not to affect the ranking (data not shown). The difference in the BMC₅₀ values of the least and the most potent chemical, phenol and p-heptyloxyphenol respectively, is three orders of magnitude. The difference between the BMC₅₀ value of phenol and the BMC₅₀ values of the other p-substituted phenols is less, namely, 16.9, 4.9 and 1.9-fold for p-mercaptophenol, p-methylketophenol and p-fluorophenol respectively. Figure 4 graphically presents these potency differences and compares them to the potency differences derived from the data reported in the literature for these phenols in the WEC and in vivo assay as described in the next sections.

POTENCY RANKING WEC ASSAY

Phenol, p-fluorophenol and p-heptyloxyphenol have been tested in the WEC assay by Oglesby et al. (1992) and assessed on both growth retardation (somite number, crown rump length and DNA content) and structural defects (fore and hind limb bud absence, hypoplasia of 1st arch, bifurcated tails and total tail defects). In general, the potency ranking for phenol, p-fluorophenol and p-heptyloxyphenol was similar for each of the endpoints tested in the WEC assay (Oglesby et al. 1992). A few phenols did not cause a toxic effect for some of the endpoints. The most potent of the three compounds in the WEC assay was p-heptyloxyphenol,

followed by p-fluorophenol and phenol. Based on the concentrations needed to reduce the somite number by 10% relative to the concurrent control (Oglesby et al. 1992), a 31.2-fold potency difference between the most and the least toxic chemical in the WEC assay was calculated, and a 4.1-fold potency difference between phenol and p-fluorophenol. The first potency difference is smaller compared to the potency difference in the EST while the latter is somewhat larger (Figure 4).

Oglesby et al. (1992) obtained a different potency ranking for the phenols tested in a WEC assay co-cultured with hepatocytes compared to the WEC system without hepatocytes (Table 2). The presence of hepatocytes diminished toxicity for p-heptyloxyphenol and p-fluorophenol, but enhanced toxicity for phenol (Oglesby et al. 1992). For the endpoints total tail defects and reduction in somite number this resulted in an altered ranking, which became phenol, p-fluorophenol and p-heptyloxyphenol (Oglesby et al. 1992). Modelling the free concentration instead of the total concentration did not change the ranking for p-heptyloxyphenol and phenol (Oglesby et al. 1992).

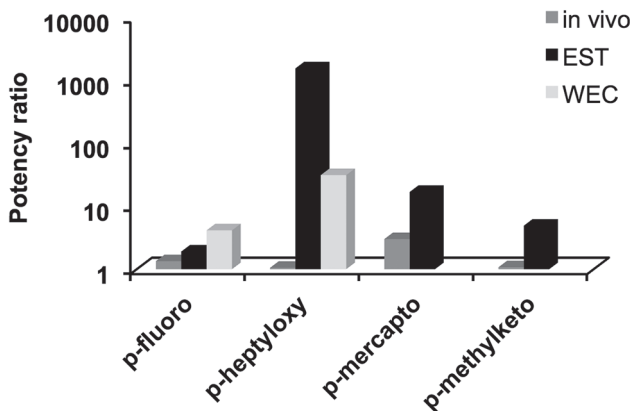


Figure 4 Potency of p-substituted phenols relative to phenol expressed as a potency ratio (potency ratio = potency phenol / potency p-substituted phenol), specified for litter biomass on postnatal day 6 in vivo (BMD_{10}), the EST (BMC_{50}) and the WEC assay (based on reduction in somite number by 10% relative to the concurrent control (Oglesby et al. 1992)). No potency data are available for p-mercaptophenol and p-methylketophenol from the WEC assay.

Table 2 Summary of toxic potency ranking, from high to low potency, of phenol, p-fluorophenol, p-heptyloxyphenol, p-mercaptophenol and p-methylketophenol tested in the EST, in vivo (postnatal day 6) and in the WEC assay, with a specification of the embryotoxic endpoints considered. Additionally, a toxic potency ranking is included for the WEC assay in the presence of hepatocytes and based on the free concentration.

EST ^a	In vivo ^b	In vivo ^b	In vivo ^c	WEC ^d	WEC ^d + hepatocytes	WEC ^d free conc.
Inhibition of differentiation	Change litter size	Reduction litter biomass	Perinatal loss	Diverse (see text)	Total tail defects & somite number	3 endpoints ^e
p-heptyloxy	p-mercapto	p-mercapto	p-mercapto	p-heptyloxy	phenol	p-heptyloxy
p-mercapto	p-fluoro	p-fluoro	p-methylketo	p-fluoro	p-fluoro	phenol
p-methylketo	p-heptyloxy	p-methylketo	p-heptyloxy	phenol	p-heptyloxy ^f	
p-fluoro	p-methylketo	p-heptyloxy	phenol			
phenol	phenol ^g	phenol	p-fluoro ^h			

^a Ranking based on BMC₅₀ as derived from the EST from the present study.

^b Ranking based on BMD₁₀, as derived from in vivo data from Kavlock (1990).

^c Ranking according Kavlock (1990).

^d Ranking according Oglesby et al. (1992).

^e Endpoints considered are reduction in somite number, crown-rump length and total DNA content.

^f No incidence was obtained for p-heptyloxyphenol on total tail defects.

^g No significant dose-related trend could be fit.

^h No perinatal loss observed at highest dose group for p-fluorophenol.

IN VIVO TOXICITY DATA

Table 3 presents a summary of the in vivo developmental toxicity data for phenol. From this overview it emerges that for phenol, the most common critical developmental endpoint in vivo is reduced foetal body weight. A number of studies reported the incidence of malformations due to phenol (Argus, 1997; Jones-Price et al. 1983a; Jones-Price et al. 1983b; Kavlock, 1990; Narotsky and Kavlock, 1995). In all but one study (Jones-Price et al. 1983a), developmental effects were accompanied by maternal effects, mostly by a decrease in maternal weight change. In general, the developmental no observed adverse effect levels (NOAELs) reported for phenol in the different studies are in agreement with each other.

Table 3 Summary of in vivo developmental toxicity data of phenol described in the literature.

Species and strain	Exposure day(s)	Dose (mg/kg bw/day) ^a	Developmental endpoint	Developmental NOAEL ^b (mg/kg bw/day)	Reference
Sprague-Dawley rat	GD 11	0, 100, 333, 667, 1000	Malformations ^c reported at two highest doses ^d	333	Kavlock (1990)
Sprague-Dawley rat	GD 6-15	0, 30, 60, 120	Decreased average foetal bw/litter	60	Jones-Price et al. (1983a)
Sprague-Dawley rat	GD 6-15	0, 60, 120, 360	Decreased foetal bw Decreased ossification sites metatarsals ^e	120	Argus (1997)
Fischer rat	GD 6-19	0, 40, 53.3	Increased prenatal loss Reduced litter size 2 cases of kinked tails in one litter ^d	40	Narotsky and Kavlock (1995)
Sprague-Dawley rat	10-11 weeks prior to mating through weaning	0, 200, 1000, 5000 ppm (= 0, 20, 93, 350 mg/kg/d)	Decreased pup survival Decreased bw/growth delay Increased organ to bw ratios Delay in landmarks of sexual maturation	93	Ryan et al. (2001) ^g
CD-1 mice	GD 6-15	0, 70, 140, 280	Decreased average foetal bw/litter Increased incidence in cleft palate at high dose ^f	140	Jones-Price et al. (1983b)

^a In each study phenol was administered by oral gavage, except in the study of Ryan et al. (2001) at which phenol was administered via drinking water.

^b NOAELs were taken from cited studies, except the NOAEL from the study of Kavlock (1990) which is derived in the present study based on malformations.

^c Hindlimb paralysis and/or short kinky tails.

^d Not analysed on statistical significance.

^e Significant effect, but biological significance questioned.

^f Not statistical significant.

^g Effects possibly related to decreased maternal water intake due to flavour aversion.

One in vivo study in rats was available on developmental effects for the other phenolic congeners, including phenol as well (Kavlock, 1990). In this rat study, in which compounds were administered orally at GD11, all five phenols were classified as active developmental toxicants (Kavlock, 1990). Developmental toxicity endpoints quantitatively assessed included perinatal loss, change in pup weight, litter size, and litter biomass. For the latter two endpoints dose-response curves with a significant dose-related trend were obtained enabling calculation of a BMD₁₀ value, with the exception of phenol for the endpoint litter size for which no significant dose-related trend could be established (Table 4). Table 2 summarizes the potency

ranking based on the BMD₁₀ values obtained and in addition the potency ranking for perinatal loss from Kavlock (1990). From this overview it appears that each in vivo endpoint considered resulted in a different potency ranking (Table 2). Though, at each endpoint, p-mercaptophenol was the most potent compound and phenol the least toxic, except for perinatal loss where phenol is the second least toxic compound in the potency ranking. The ranking for p-methylketophenol, p-heptyloxyphenol and p-fluorophenol differs between the in vivo endpoints in a non-systematic way (Table 2). The potency difference between phenol and p-substituted phenols tested in vivo is less than the potency difference observed in the EST (Figure 4).

From the developmental toxicity study from Kavlock (1990), dose-response curves and BMD₁₀ values for maternal weight change were obtained as well (Table 4). For each phenol, except for p-methylketophenol, a significant dose-response relationship could be established. In general, embryotoxicity occurs at similar (p-mercaptophenol) or somewhat higher dose levels (5.7, 2.0 and 1.5-fold higher for p-heptyloxyphenol, p-fluorophenol and phenol respectively) than maternal toxicity.

Table 4 BMD₁₀ values (mg/kg) of phenols for maternal effect 72 h after dosing and developmental effects on postnatal day 6, calculated from in vivo data from Kavlock (1990), ranked from high to low developmental potency of the endpoint litter size.

Phenol	BMD ₁₀ (mg/kg)	BMD ₁₀ (mg/kg)	
	Maternal	Developmental	
	Weight change	Litter size	Litter biomass
p-mercapto	<333 ^a	<333 ^a	<333 ^a
p-fluoro	369	719	747
p-heptyloxy	168	946	951
p-methylketo	>1000 ^b	979	932 ^c
phenol	667 ^a	>1000 ^b	>1000 ^a

^a Data not adequate for BMD modelling. Instead, the NOAEL is presented.

^b No significant dose-related trend could be fit. Instead, the maximum tested dose is presented.

^c Model fit: 0.05 < p < 0.1.

DISCUSSION

The aim of the present study was to evaluate the applicability of the EST for a series of p-substituted phenols, as an alternative for in vivo embryotoxicity testing. The EST showed concentration dependent response curves for the inhibition of differentiation of the embryoid bodies for all tested compounds, demonstrating the embryotoxic potential of the phenols.

The test concentration of both phenol and p-fluorophenol in the EST decreased in time. As the reported BMC₅₀ values for inhibition of differentiation of the embryoid bodies were

derived from the initial total test concentrations ($t=0$), the actual BMC_{50} might be lower than the concentration reported in this study for these two compounds. In the EST, phenol is the least toxic compound followed by p-fluorophenol. Hence, a lower BMC_{50} of these compounds in vitro could potentially affect the potency ranking of the phenols. It is unknown, however, if the toxic effects of phenol and p-fluorophenol in vitro occur due to a peak concentration or as the result of a prolonged exposure above a certain concentration. In addition, the critical exposure period in the 10-day EST is also unknown. Therefore, correcting the initial BMC_{50} towards an actual effective BMC_{50} in vitro was not possible and hence not applied in the present study. However, correcting the initial BMC_{50} for the percentage of the compound that was stable for 5 days using the AUC_{0-5} , could provide insight in the effect of the chemical loss on the potency. This correction resulted in the reduction of BMC_{50} values from 0.59 mM towards 0.34 mM for phenol and from 0.31 mM towards 0.21 mM for p-fluorophenol. After this correction, phenol remained the least toxic compound, followed by p-fluorophenol, which is equal to the ranking based on the initial concentration. Even a correction for the maximum decrease, as was measured on day 5, would not alter the potency ranking. Hence, the potency ranking as presented in the present study is considered valid.

The potency ranking of the phenols, based on the BMC_{50} values derived from the EST, is identical to the potency ranking from the WEC assay of Oglesby et al. (1992). This finding is in accordance with Louisse et al. (2011) who found a similar potency ranking between both in vitro test systems for a series of retinoids. However, for a series of six 1,2,4-triazoles, de Jong et al. (2011a) found only a moderate correlation between the potency of the tested compounds in the EST and the WEC assay. It was found that p-heptyloxyphenol is relatively more potent in the EST compared to the WEC assay. This may (partly) be explained by differences in serum content between both in vitro assays, which is 20% in the EST and 50% in the WEC assay. Moreover, it has been shown that p-heptyloxyphenol readily binds to serum albumin and may accumulate in the embryo in the WEC assay possibly due to its high lipophilicity (Fisher et al. 1993). Similar phenomena might occur in the EST and, in conjunction with the lower serum content in the EST than the WEC assay, may explain the relative high toxicity of p-heptyloxyphenol in the present EST study.

In order to evaluate the applicability of the EST as an alternative for in vivo embryotoxicity testing, the potency of the phenols in the EST was compared to the potency of the compounds in vivo. It was found that the potency ranking in the EST differs from the in vivo developmental toxicity potency ranking for perinatal loss, reduction litter biomass and change litter size. None of these three in vivo endpoints was best mimicked by the EST. Only phenol, the least potent compound from the phenols tested, was correctly ranked when compared to in vivo litter biomass and litter size. Furthermore, p-mercaptophenol was correctly identified as a relative potent congener within the series of phenols, but its ranking was distorted by p-heptyloxyphenol, of which the toxicity was overestimated in the EST. Again, differences in

serum albumin levels, which are higher *in vivo* in the rat than in the EST (Verwei et al. 2006), may cause the difference in the ranking for p-heptyloxyphenol. Moreover, the ranking for p-methylketophenol, p-heptyloxyphenol and p-fluorophenol differs between the *in vivo* endpoints in a non-systematic way. The disparity in potency ranking between the EST and *in vivo* embryotoxicity is in accordance to what has been found for two other chemical classes, namely a series of 1,2,4-triazoles (de Jong et al. 2011a) and a series of retinoids (Louisse et al. 2011). However, the EST predicted a correct potency ranking for a series of glycol ether alkoxy acid metabolites compared to the potency ranking of parent glycol ether compounds *in vivo* (de Jong et al. 2009). A good predictive property of the EST was also found for valproic acid analogues (de Jong et al. 2011b; Riebeling et al. 2011).

The relative poor predictivity of the EST for the embryotoxic potency *in vivo* for the p-substituted phenols tested might also be due to differences in biotransformation between the *in vitro* and the *in vivo* system. In the present study, only parent phenolic compounds were tested as the ES-D3 cells are expected to have no or hardly any metabolic capacity. However, in the *in vivo* situation, maternal metabolism can play a key role in (de)activating the compound before reaching the embryo. For phenol and p-substituted phenols the major metabolic pathways *in vivo* are sulfation and glucuronidation reducing toxicity of the phenols, whereas cytochrome P450 mediated bioactivation may result in the formation p-hydroxyphenol (Bollard et al. 1996; Capel et al. 1972; Hoffmann et al. 1999; Koster et al. 1981; Mulder and Meerman, 1978). The latter compound appeared to be the most potent compound of the p-substituted phenols tested in the WEC assay (Oglesby et al. 1992). It was not possible, however, to test the latter compound in the EST due to a rapid auto-oxidation of the compound and the toxicity of anti-oxidants, which could prevent auto-oxidation. From data of Oglesby et al. (1992) it appeared that adding a metabolic system to the *in vitro* WEC assay, to mimic maternal metabolism *in vivo*, could not overcome the disparity between embryotoxicity *in vitro* and *in vivo* for the phenols. In the WEC assay co-cultured with hepatocytes, phenol became more potent for the endpoints total tail defects and reduction in somite number, while the toxic potency of p-heptyloxyphenol and p-fluorophenol was diminished by the hepatocytes (Oglesby et al. 1992). The diminished potency of the latter two compounds may reflect the *in vivo* situation where glucuronidation and sulfation result in detoxification. However, the increased potency of phenol in the co-cultured system is not in agreement with the *in vivo* potency ranking where phenol is the least potent compound. A possible explanation for this observation may be differences between *in vitro* kinetics and *in vivo* kinetics. To illustrate this, from an *in vitro* incubation experiment of 1 h with 3 mM phenol using freshly isolated rat hepatocytes (Schrenk and Bock, 1990) the formation of 19.3% p-hydroxyphenol, 29.8% phenylsulfate and 41.4% phenylglucuronide was derived. However, the fraction of the toxic metabolite p-hydroxyphenol (measured as p-hydroxyphenol conjugates) formed *in vivo* in the rat is much lower, namely 3% in 24-hour urine (Capel et al. 1972), providing a possible



explanation for the difference between the potency ranking in the WEC assay co-cultured with hepatocytes and the in vivo situation. Instead, combining in vitro embryotoxicity data with kinetic modelling of in vivo absorption, distribution, metabolism and excretion (ADME) processes is expected to more closely mimic the in vivo embryotoxicity as has been demonstrated recently for other developmentally toxic model compounds (Louisse et al. 2010; Verwei et al. 2006).

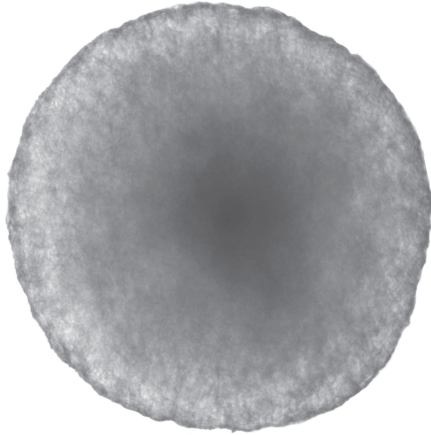
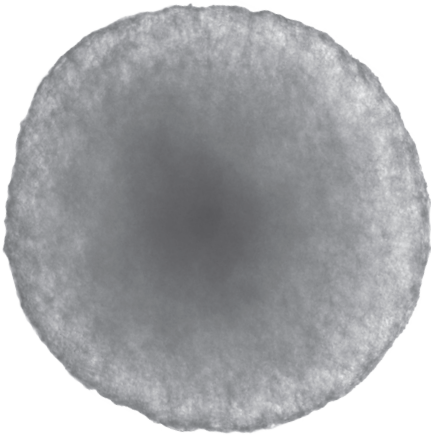
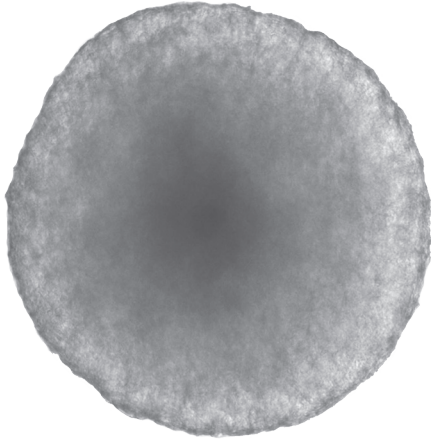
The BMD₁₀ values for embryotoxic effects in vivo were similar or somewhat higher than the BMD₁₀ values for reduction in maternal weight change, except for methylketophenol which showed a lower developmental BMD₁₀. These findings might raise the question whether embryotoxic effects observed in vivo are due to indirect maternal effects or are induced by a more direct action of the compound. In line with the in vivo maternal-developmental correlations observed in this study, a positive correlation was found between four of seven embryotoxic endpoints for phenols in the WEC assay and maternal weight reduction in vivo by Oglesby et al. (1992), who pointed out that this correlation might reflect some general mechanisms, but stated that the maternal and embryotoxic endpoints are clearly dissimilar. This is supported by the different physico-chemical properties that were able to predict maternal and developmental toxicity in vivo for a large group of p-substituted phenols (Kavlock, 1990). Furthermore, it is important to take into account that in vivo kinetics could greatly reduce the concentration actually reaching the embryo, and hence the embryotoxic effect in vivo. This demonstrates the necessity to combine in vitro embryotoxicity data with in vivo ADME processes, which could be achieved by extrapolating in vitro effect concentrations towards in vivo dose levels, using physiologically based kinetic models.

In conclusion, the EST was able to identify the embryotoxic potential for phenol and p-substituted phenols, providing an identical potency ranking compared to the WEC assay. However, the EST was not able to predict an accurate ranking for the phenols compared to their potency observed in vivo and hence is not yet able to serve as a standalone assay to replace animal testing, even not for the purpose of prioritising a closely related group of chemicals on their embryotoxicity like the p-substituted phenols. The reason for this disparity might be the kinetic difference between the in vitro and the in vivo system. Therefore, it is essential to combine in vitro embryotoxicity data with kinetic modelling of in vivo ADME processes in the evaluation of the true in vivo embryotoxic potential of a compound, thereby enhancing the power of the EST in the potency ranking and risk assessment of this class of chemicals. To this purpose, our laboratory is currently investigating whether combining in vitro toxicity levels obtained from the EST together with a physiologically based kinetic model for phenol, would actually lead towards a better prediction of in vivo embryotoxicity of these compounds.

REFERENCES

- Adler S, Basketter D, Creton S, Pelkonen O, van Benthem J, Zuang V, Andersen KE, Angers-Loustau A, Aptula A, Bal-Price A, Benfenati E, Bernauer U, Bessems J, Bois FY, Boobis A, Brandon E, Bremer S, Broschard T, Casati S, Coecke S, Corvi R, Cronin M, Daston G, Dekant W, Felter S, Grignard E, Gundert-Remy U, Heinonen T, Kimber I, Kleinjans J, Komulainen H, Kreiling R, Kreysa J, Leite SB, Loizou G, Maxwell G, Mazzatorta P, Munn S, Pfuhrer S, Phrakonkham P, Piersma A, Poth A, Prieto P, Repetto G, Rogiers V, Schoeters G, Schwarz M, Serafimova R, Täthi H, Testai E, van Delft J, van Loveren H, Vinken M, Worth A, Zaldivar JM (2011) Alternative (non-animal) methods for cosmetics testing: current status and future prospects-2010. *Arch Toxicol* 85:367-485
- Argus (1997) Oral (gavage) developmental toxicity study of phenol in rats. Protocol Number: Argus 916-011. Argus Research Laboratories, Inc., Horsham, PA
- ATSDR (2008) Toxicological profile for phenol. US Department of Health and Human Services, Public Health Service, Agency for Toxic Substances and Disease Registry (ATSDR), Atlanta, GA
- Augustine-Rauch K, Zhang CX, Panzica-Kelly JM (2010) In vitro developmental toxicology assays: a review of the state of the science of rodent and zebrafish whole embryo culture and embryonic stem cell assays. *Birth Defects Research Part C* 90:87-98
- Barnes DG, Daston GP, Evans JS, Jarabek AM, Kavlock RJ, Kimmel CA, Park C, Spitzer HL (1995) Benchmark dose workshop: criteria for use of a benchmark dose to estimate a reference dose. *Regul Toxicol Pharm* 21:296-306
- Bollard ME, Holmes E, Blackledge CA, Lindon, JC, Wilson ID, Nicholson JK (1996) ¹H and ¹⁹F-nmr spectroscopic studies on the metabolism and urinary excretion of mono- and disubstituted phenols in the rat. *Xenobiotica* 26:255-273
- Capel ID, French MR, Millburn P, Smith RL, Williams RT (1972) The fate of [¹⁴C]phenol in various species. *Xenobiotica* 2:25-34
- Chapman DE, Namkung MJ, Juchau MR (1994) Benzene and benzene metabolites as embryotoxic agents: effects on cultured rat embryos. *Toxicol Appl Pharmacol* 128:129-137
- Davis JA, Gift JS, Zhao QJ (2011) Introduction to benchmark dose methods and US EPA's benchmark dose software (BMDS) version 2.1.1. *Toxicol Appl Pharmacol* 254:181-191
- De Jong E, Barenys M, Hermsen SAB, Verhoef A, Ossendorp BC, Bessems JGM, Piersma AH (2011a) Comparison of the mouse Embryonic Stem cell Test, the rat Whole Embryo Culture and the Zebrafish Embryotoxicity Test as alternative methods for developmental toxicity testing of six 1,2,4-triazoles. *Toxicol Appl Pharmacol* 253:103-111
- De Jong E, Doedée AMCM, Reis-Fernandes MA, Nau H, Piersma AH (2011b) Potency ranking of valproic acid analogues as to inhibition of cardiac differentiation of embryonic stem cells in comparison to their in vivo embryotoxicity. *Reprod Toxicol* 31:375-382
- De Jong E, Louisse, J Verwei M, Blaauboer BJ, van de Sandt JJM, Woutersen RA Rietjens, IMCM Piersma, AH (2009) Relative developmental toxicity of glycol ether alkoxy acid metabolites in the embryonic stem cell test as compared with the in vivo potency of their parent compounds. *Toxicol Sci* 110:117-124
- De Smedt A, Steemans M, De Boeck M, Peters AK, van der Leede B, Van Goethem F, Lampo A, Vanparys P (2008) Optimisation of the cell cultivation methods in the embryonic stem cell test results in an increased differentiation potential of the cells into strong beating myocard cells. *Toxicol in Vitro* 22:1789-1796
- ECVAM (2010a) INVITTOX protocol no 123. Embryotoxicity testing in post-implantation whole embryo culture (WEC) - method of Piersma. Available at: <http://ecvam-dbal.m.jrc.ec.europa.eu/>
- ECVAM (2010b) INVITTOX protocol no 122. The micromass test - method of Brown. Available at: <http://ecvam-dbal.m.jrc.ec.europa.eu/>
- FAO (2010) Compendium of food additive specifications. Joint FAO/WHO Expert Committee on Food Additives, 73rd Meeting 2010 FAO JECFA Monographs 10 Food and Agriculture Organization of the United Nations, Rome
- Fisher HL, Sumler MR, Shrivastava SP, Edwards B, Oglesby LA, Ebron-McCoy MT, Copeland F, Kavlock RJ, Hall LL (1993) Toxicokinetics and structure-activity relationships of nine para-substituted phenols in rat embryos in vitro. *Teratology* 48:285-297
- Genschow E, Spielmann H, Scholz G, Pohl I, Seiler A, Clemann N, Bremer S, Becker K (2004) Validation of the embryonic stem cell test in the international ECVAM validation study on three in vitro embryotoxicity tests. *Altern Lab Anim* 32:209-244
- Genschow E, Spielmann H, Scholz G, Seiler A, Brown N, Piersma A, Brady M, Clemann N, Huuskonen H, Paillard F, Bremer S, Becker K (2002) The ECVAM international validation study on in vitro embryotoxicity tests: results of the definitive phase and evaluation of prediction models. *Altern Lab Anim* 30:151-176

- Hoffmann MJ, Ji S, Hedli CC, Snyder R (1999) Metabolism of [¹⁴C]phenol in the isolated perfused mouse liver. *Toxicol Sci* 49:40-47
- Jones-Price C, Ledoux TA, Reel JR, Fisher PW, Langhoff-Paschke L, Marr MC, Kimmel CA (1983a) Teratologic evaluation of phenol (CAS No. 108-95-2) in CD rats. NTP Study TER81104. Research Triangle Institute, Research Triangle Park, NC
- Jones-Price C, Ledoux TA, Reel JR, Langhoff-Paschke L, Marr MC, Kimmel CA (1983b) Teratologic evaluation of phenol (CAS No. 108-95-2) in CD-1 mice. NTP Study TER80129. Research Triangle Institute, Research Triangle Park, NC
- Kavlock RJ (1990) Structure-activity relationships in the developmental toxicity of substituted phenols: in vivo effects. *Teratology* 41:43-59
- Kendig DM and Tarloff JB (2007) Inactivation of lactate dehydrogenase by several chemicals: implications for in vitro toxicology studies. *Toxicol in Vitro* 21:125-132
- Koster H, Halsema I, Scholtens E, Knippers M, Mulder GJ (1981) Dose-dependent shifts in the sulfation and glucuronidation of phenolic compounds in the rat in vivo and in isolated hepatocytes. The role of saturation of phenol-sulfotransferase *Biochem Pharmacol* 30:2569-2575
- Louisse J, de Jong E, van de Sandt JJM, Blaauboer BJ, Woutersen RA, Piersma AH, Rietjens IMCM, Verwei M (2010) The use of in vitro toxicity data and physiologically based kinetic modeling to predict dose-response curves for in vivo developmental toxicity of glycol ethers in rat and man. *Toxicol Sci* 118:470-484
- Louisse J, Gönen S, Rietjens IMCM, Verwei M (2011) Relative developmental toxicity potencies of retinoids in the embryonic stem cell test compared with their relative potencies in in vivo and two other in vitro assays for developmental toxicity. *Toxicol Lett* 203:1-8
- Marx-Stoelting P, Adriaens E, Ahr HJ, Bremer S, Garthoff B, Gelbke HP, Piersma A, Pellizzer C, Reuter U, Rogiers V, Schenk B, Schwengberg S, Seiler A, Spielmann H, Steemans M, Stedman DB, Vanparys P, Vericat JA, Verwei M, van de Water F, Weimer M, Schwarz M (2009) A review of the implementation of the embryonic stem cell test (EST). The report and recommendations of an ECVAM/ReProTect Workshop. *Altern Lab Anim* 37:313-328
- Mulder GJ and Meerman JHN (1978) Glucuronidation and sulphation in vivo and in vitro: selective inhibition of sulphation by drugs and deficiency of inorganic sulphate, in: Aitio, A (ed.), *Conjugation Reactions in Drug Biotransformation*, Elsevier/North-Holland Biomedical Press, Amsterdam, pp 389-397
- Narotsky MG and Kavlock RJ (1995) A multidisciplinary approach to toxicological screening: II. Developmental toxicity. *J Toxicol Environ Health* 45:145-171
- Oglesby LA, Ebron-McCoy MT, Logsdon TR, Copeland F, Beyer PE, Kavlock RJ (1992) In vitro embryotoxicity of a series of para-substituted phenols: structure, activity, and correlation with in vivo data. *Teratology* 45:11-33
- Riebeling C, Pirow R, Becker K, Buesen R, Eikel D, Kaltenhäuser J, Meyer F, Nau H, Slawik B, Visan A, Voland J, Spielmann H, Luch A, Seiler A (2011) The embryonic stem cell test as tool to assess structure-dependent teratogenicity: the case of valproic acid. *Toxicol Sci* 120:360-370
- Ryan BM, Selby R, Gingell R, Waechter Jr JM, Butala JH, Dimond SS, Dunn BJ, House R, Morrissey R (2001) Two-generation reproduction study and immunotoxicity screen in rats dosed with phenol via the drinking water. *Int J Toxicol* 20:121-142
- Schrenk D and Bock KW (1990) Metabolism of benzene in rat hepatocytes. Influence of inducers on phenol glucuronidation. *Drug Metab Dispos* 18:720-725
- Seiler AE, Buesen R, Visan A, Spielmann H (2006) Use of murine embryonic stem cells in embryotoxicity assays. The embryonic stem cell test. *Methods Mol Biol* 329:371-395
- Selassie CD, Kapur S, Verma RP, Rosario M (2005) Cellular apoptosis and cytotoxicity of phenolic compounds: a quantitative structure-activity relationship study. *J Med Chem* 48:7234-7242
- Spielmann H, Seiler A, Bremer S, Hareng L, Hartung T, Ahr H, Faustman E, Haas U, Moffat GJ, Nau H, Vanparys P, Piersma AH, Sintes JR, Stuart J (2006) The practical application of three validated in vitro embryotoxicity tests. *Altern Lab Anim* 34:527-538
- Verma RP, Kapur S, Barberena O, Shusterman A, Hansch CH, Selassie CD (2003) Synthesis, cytotoxicity, and QSAR analysis of X-thiophenols in rapidly dividing cells. *Chem Res Toxicol* 16:276-284
- Verwei M, van Burgsteden JA, Krul CAM, van de Sandt JJM, Freidig AP (2006) Prediction of in vivo embryotoxic effect levels with a combination of in vitro studies and PBPK modelling. *Toxicol Lett* 165:79-87
- Weber M and Weber, M (2010) Phenols. In: Pilato L (ed.), *Phenolic resins: a century of progress*. Springer, Berlin Heidelberg, pp 9-23
- Zhou H, Kepa JK, Siegel D, Miura S, Hiraki Y, Ross D (2009) Benzene metabolite hydroquinone up-regulates chondromodulin-I and inhibits tube formation in human bone marrow endothelial cells. *Mol Pharmacol* 76:579-587



CHAPTER 3

Combining in vitro embryotoxicity data with physiologically based kinetic (PBK) modelling to define in vivo dose-response curves for developmental toxicity of phenol in rat and human

**Marije Strikwold, Bert Spenkelink, Ruud A Woutersen, Ivonne MCM Rietjens, Ans Punt
Based on: Archives of Toxicology (2013) 87:1709-1723**

ABSTRACT

In vitro assays are often used for the hazard characterisation of compounds, but their application for quantitative risk assessment purposes is limited. This is because in vitro assays cannot provide a complete in vivo dose-response curve from which a point of departure (PoD) for risk assessment can be derived, like the no observed adverse effect level (NOAEL) or the 95% lower confidence limit of the benchmark dose (BMDL). To overcome this constraint, the present study combined in vitro data with a physiologically based kinetic (PBK) model applying reverse dosimetry. To this end, embryotoxicity of phenol was evaluated in vitro using the embryonic stem cell test (EST), revealing a concentration dependent inhibition of differentiation into beating cardiomyocytes. In addition, a PBK model was developed on the basis of in vitro and in silico data and data available from the literature only. After evaluating the PBK model performance, effective concentrations (EC_x) obtained with the EST served as an input for in vivo plasma concentrations in the PBK model. Applying PBK-based reverse dosimetry provided in vivo external effective dose levels (ED_x) from which an in vivo dose-response curve and a PoD for risk assessment were derived. The predicted PoD lies within the variation of the NOAELs obtained from in vivo developmental toxicity data from the literature. In conclusion, the present study showed that it was possible to accurately predict a PoD for the risk assessment of phenol using in vitro toxicity data combined with reverse PBK modelling.

INTRODUCTION

In vitro toxicity assays play an important role in screening chemicals for their possible hazards and prioritising them for further toxicity testing. The implementation of in vitro assays in quantitative risk assessment, however, is limited. An important reason underlying this limitation is that in vitro assays cannot provide a complete in vivo dose-response curve from which a point of departure (PoD) for risk assessment can be derived, like the no observed adverse effect level (NOAEL) or the 95% lower confidence limit of the benchmark dose (BMDL). To overcome this constraint, toxicological in vitro data can be combined with physiologically based kinetic (PBK) modelling, applying reverse dosimetry (Louisse et al. 2010; Verwei et al. 2006). With PBK-based reverse dosimetry, external dose levels are estimated from internal concentrations, i.e. plasma or tissue concentrations, using a PBK model describing the kinetics of a compound. Concentration-response information obtained from an in vitro assay, represented by different effective concentrations (EC_x), may serve as a surrogate for in vivo internal effect concentrations in the PBK model. Applying PBK-based reverse dosimetry will then provide external effective dose levels (ED_x) from which an in vivo dose-response curve and a PoD for risk assessment can be derived. Identifying whether this in vitro PBK approach with reverse dosimetry can actually be applied in quantitative risk assessment of chemicals, requires insight into its predictive performance for different compounds (Rietjens et al. 2011; Punt et al. 2011).

The objective of the present study was to demonstrate the capability of the in vitro PBK approach to predict in vivo dose-response curves and hence a PoD for risk assessment from experimentally derived in vitro toxicity data, with phenol as the selected model compound. PBK models for rat and human were developed on the basis of only in vitro and in silico data and data available from the literature to contribute to the 3Rs principle for the replacement, reduction and refinement of animal testing in the most optimal way.

Phenol is a high production volume chemical and is an important compound in many production processes, like the manufacturing of bisphenol-A and phenolic resins (Weber and Weber 2010). Phenol is present in various commercially available (household) products and has a number of clinical applications as well (ATSDR 2008; Landau 2007; Kheder and Nair 2012). Exposure to phenol can occur occupationally, domestically as well as clinically, i.e. via inhalation, ingestion of contaminated drinking water, or via dermal contact (ATSDR 2008). The compound is also a major intermediate metabolite of benzene and exposure can therefore also occur due to benzene exposure (Rothman et al. 1998). Uptake of phenol itself occurs rapidly via all routes (Hughes and Hall 1995). Animal studies revealed adverse effects on the kidney, liver, and the immunological and neurological system upon exposure (Bruce et al. 2001). Moreover, several studies demonstrated the embryotoxic potential of phenol in vivo (Argus 1997; Kavlock 1990) and in vitro (Chapman et al. 1994; Oglesby et al. 1992;

Strikwold et al. 2012). In vivo developmental toxicity has been used as endpoint to derive a PoD for the risk assessment of phenol (Baars et al. 2001; Environment Agency 2009; WHO 1994). In the present study, it will be evaluated whether such a PoD could also be adequately predicted with the combined in vitro PBK approach using the in vitro embryonic stem cell test (EST) for determining the embryotoxic potential of phenol.

MATERIALS AND METHODS

COMPOUNDS AND BIOLOGICAL MATERIALS

Phenol (99%), tetra-n-butylammonium bromide, phenylglucuronide ($\geq 99\%$), ammonium acetate ($\geq 98\%$), sulfamic acid (99.3%), uridine 5'-diphosphoglucuronic acid (UDPGA), alamethicin ($\geq 98\%$), sulfatase (from *Helix pomatia*), 3'-phosphoadenosine-5'-phosphosulfate (PAPS) and tris(hydroxymethyl)aminomethane (Tris) ($\geq 99.9\%$) were purchased from Sigma Aldrich. Dimethyl sulfoxide (DMSO) ($\geq 99.9\%$) was obtained from Acros Organics (Geel, Belgium), acetonitrile (ULC/MS grade) and methanol (HPLC supra-gradient) from BioSolve (Valkenswaard, The Netherlands), and trifluoroacetic acid (TFA) ($\geq 99.8\%$) from J.T. Baker (Philipsburg, NJ, USA). Glacial acetic acid, sodium acetate trihydrate (99.5%), hydrochloride acid (37%) pyridine and magnesium chloride hexahydrate ($\geq 99\%$) were purchased from VWR International GmbH (Darmstadt, Germany).

Pooled liver microsomes and cytosol from male Sprague-Dawley rats were obtained from BD Biosciences Gentest (Woburn, MA, USA). Pooled small intestinal microsomes and pooled small intestinal, kidney and lung cytosols, all from male Sprague-Dawley rats, and pooled human mixed gender small intestinal microsomes and cytosols were obtained from BioPredic (Rennes, France). Pooled male rat kidney and lung microsomes, pooled human mixed gender liver microsomes and cytosol, and pooled human mixed gender lung and kidney S9 were obtained from XenoTech (Lenexa, KS, USA).

SYNTHESIS OF PHENYLSULFATE

Phenylsulfate was synthesised as the potassium salt, from phenol and sulfamic acid in pyridine according to the method of Yamaguchi (1959). The synthesised phenylsulfate was required as a reference standard to quantify phenylsulfate from the incubation experiments, using LC-ESI-MS/MS. The product of synthesis was analysed by a Waters Alliance HPLC system using a Supelcosil LC-18 25 cm x 4.6 mm 5 μm column connected to a photodiode array detector (PDA, Waters). The isocratic eluent consisted of methanol and nanopure water (50:50) containing 0.05 M tetra-n-butylammonium bromide and 0.2% (v/v) acetic acid, and elution was performed at a flow of 0.8 ml/min. The amount of phenylsulfate in the synthesised product was quantified by the comparison of HPLC-PDA data to those for phenylglucuronide,

which has similar UV characteristics. Peak areas of phenylsulfate and phenylglucuronide were quantified at a wavelength of 262 nm. The retention times of phenylglucuronide and phenylsulfate were 4.6 and 9.9 min, respectively.

GENERAL OUTLINE IN VITRO PBK APPROACH

The in vitro PBK approach to predict in vivo dose-response curves and a PoD for risk assessment using in vitro toxicity data consisted of the following steps: (1) establishment of in vitro effective concentrations (EC_x) of phenol in the EST, (2) development of PBK models describing in vivo kinetic properties of phenol in rat and human and derivation of PBK model parameters, (3) evaluation of the PBK models, (4) translation of in vitro EC_x into in vivo external dose levels (ED_x) generating dose-response curves for developmental toxicity in rat and human and deriving a PoD for risk assessment, and (5) evaluation of the in vitro PBK approach.

IN VITRO EMBRYOTOXICITY DATA AND THE AREA UNDER THE CURVE OF PHENOL IN THE EST

Embryotoxicity data of phenol derived using the murine embryonic stem cell differentiation assay (ES-D3 cells) by Strikwold et al. (2012) were used as a starting point for the in vitro PBK approach to translate in vitro embryotoxicity data to in vivo toxicity values. The assay encompassed five independently performed experiments in which the inhibition of differentiation of ES-D3 cells into beating cardiomyocyte clusters was the toxicity endpoint that was studied. Cytotoxicity in ES-D3 cells and fibroblasts, which represent additional endpoints in the validated EST when used for embryotoxic potency classification (Genschow et al. 2004), was not quantified and is not required for the present study, since the aim was to convert a concentration-response curve of an in vitro developmental toxicity endpoint to an in vivo dose-response curve.

A compound may exert its toxic effect either by the peak concentration in blood (C_{max}) or by its concentration in blood over a specific time period, represented by the area under the blood concentration-time curve (AUC). The current study evaluated both metrics in the in vitro PBK approach. The area under the curve of phenol in the 10-day EST (AUC_{0-10d}) was obtained by measuring the course of the phenol concentration in the cell culture medium of the EST. This was evaluated for two test concentrations, namely 0.2 and 0.6 mM phenol. To this end, the embryonic stem cell differentiation assay was performed as described by Strikwold et al. (2012), but DMEM containing phenol red was replaced by phenol red-free DMEM to prevent interference of peaks in the chromatogram of phenol during analysis. Samples of the EST culture medium were taken immediately after refreshing the culture medium at days 3 and 5 of the EST and at $t=0, 1, 2, 4$ and 24 h after starting the EST, then followed by a time interval of 24 h for the remaining test period. The samples were stored at -20°C until analysis of the

phenol concentration by UPLC-PDA (see Quantification of phenol, phenylglucuronide and phenylsulfate section).

IN VITRO ASSAYS FOR GLUCURONIDATION AND SULFATION OF PHENOL BY RAT AND HUMAN TISSUE SAMPLES

At first, the ability of rat and human tissue samples to glucuronidate and/or sulfate phenol was identified using incubations in 50 mM Tris-HCl buffer (pH 7.4 including 10 mM MgCl₂) with liver, intestinal, kidney and lung tissue fractions (microsomes, cytosol or S9) containing (final concentrations) 1 mg protein/ml, 10 mM UDPGA or 0.6 mM PAPS, for a maximum of 2-h incubation.

Subsequently, incubations with pooled rat and pooled human microsomes, cytosol or S9 were performed to determine kinetic constants, namely the maximum enzyme reaction rate (V_{max}) and the Michaelis-Menten constant (K_m), for glucuronidation and sulfation of phenol for the metabolising organs. Conditions were optimised to obtain linear metabolism reaction rates with respect to incubation time and protein concentration and non-limiting cofactor levels were applied.

For glucuronidation, the rat incubation mixtures consisted of 50 mM Tris-HCl buffer (pH 7.4) with 10 mM MgCl₂, containing (final concentrations) 2 mM UDPGA and 0.2 mg microsomal protein/ml for incubations with rat liver microsomes and 10 mM UDPGA and 0.7, 0.8, and 0.8 mg microsomal protein/ml for incubations with rat small intestinal, lung, and kidney microsomes, respectively. The incubation mixtures with human microsomes or S9 consisted of 50 mM Tris-HCl buffer (pH 7.4) with 10 mM MgCl₂, containing (final concentrations) 10 mM UDPGA and 0.8 mg microsomal or S9 protein/ml, except for the incubations with human liver tissue fractions for which 0.5 mg microsomal protein/ml was used. To obtain maximum glucuronidation activity, the microsomes were activated by preincubating the incubation mixture with 0.025 mg/ml alamethicin added from a 200 times concentrated stock solution in methanol, during 15 min on ice (Fisher et al. 2000). Subsequently, the incubations were started after a 1-min preincubation at 37 °C by the addition of the substrate phenol from a 200 times concentrated stock solution in DMSO and left in a shaking water bath of 37 °C for 10, 20, 20 and 45 min for incubations with rat liver, intestinal, kidney and lung microsomes, respectively. Incubations with human liver microsomes were carried out for 10 min and those with human intestinal microsomes and kidney S9 for 45 min. The reactions were terminated by the addition of ice-cold acetonitrile (20% v/v). Subsequently, the reaction mixtures were put on ice. In the blank incubation mixtures, UDPGA was omitted.

For sulfation, the incubation mixtures consisted of 50 mM Tris-HCl buffer (pH 7.4), containing (final concentrations) 0.4 mM PAPS and 0.2 mg cytosolic protein/ml for incubations with rat liver cytosol and 0.4 mg cytosolic protein/ml for incubations with human liver cytosol and human intestinal cytosol. After a 1-min preincubation at 37 °C, the reactions were started by

the addition of the substrate phenol from a 100 times concentrated stock solution in DMSO and left in a shaking water bath of 37 °C for 30 min for incubations with rat liver cytosol and 20 min for incubations with human liver and intestinal cytosol. The reactions were terminated by the addition of ice-cold acetonitrile (20% v/v). Subsequently the reaction mixtures were put on ice. In the blank incubation mixtures, PAPS was omitted.

The formation of phenylsulfate in the sulfation assays was confirmed by enzymatic deconjugation using sulfatase. A 60 µl volume of 0.1 M sodium acetate (pH 5.2) and 6 µl of sulfatase (400 units/ml) were added to 90 µl of the incubation mixtures of the sulfation assays (that was not stopped by the addition of ice-cold acetonitrile) and incubated overnight in a shaking water bath at 37 °C. Control samples were treated under the same conditions, but without sulfatase.

QUANTIFICATION OF PHENOL, PHENYLGLUCURONIDE AND PHENYLSULFATE

Samples of the EST culture medium were thawed after which ice-cold acetonitrile was added (50% v/v). Subsequently, the samples were vortexed and left on ice for 20 min after which they were centrifuged at 10,000 g for 10 min. The samples of the incubation mixtures of the glucuronidation assay were centrifuged for 5 min at 14,000 rpm. Next, 3.5 µl of the supernatant of each sample was analysed by UPLC (Waters Acquity) using a Waters BEH C18 1.7 µm column, 2.1 x 50 mm, with nanopure water (0.1% TFA) (A) and pure acetonitrile (B) applying a gradient elution. The start condition was 100:0 (A:B), changing to 90:10 from 1 to 2 min, then to 10:90 from 2 to 4 min, remaining at this ratio for 0.5 min and then rapidly declining to the start condition. The flow rate was 0.6 ml/min. Peaks of phenol and phenylglucuronide were detected with a photodiode array detector (PDA, Waters) at a wavelength of 270 and 266 nm, respectively. The retention times of phenol and phenylglucuronide were 2.6 and 2.4 min, respectively. Phenol and phenylglucuronide were quantified based on their peak areas using a linear calibration curve ($R^2 > 0.999$) prepared from commercially available reference compounds.

The incubation mixtures from the sulfation assay were centrifuged at 14,000 rpm for 5 min, after which 5 µl of the supernatant of each sample was analysed by LC-ESI-MS/MS. High-performance liquid chromatography separation (PerkinElmer 200 series, Waltham, MA, USA) was performed using a Zorbax Extend-C18 column, 2.1 x 50 mm, 3.5 µm, with Zorbax guard column. The mobile phase consisted of 5 mM ammonium acetate solution (A) and methanol (B). The start condition was 80:20 (A:B) for 2 min, changing to 5:95 in 0.1 min and kept at this elution for 2.4 min, and then declining to the start condition in 0.1 min, which was maintained for 2.9 min. A flow rate of 0.2 ml/min was applied and the retention time of phenylsulfate was 1.51 min. The LC effluent was split using a valve (Valco Instruments Co. Inc.) to divert the effluent to waste for the period that phenylsulfate was not eluting to prevent contamination of the ionisation source. The HPLC was connected to an API-3000 triple-

quadrupole mass spectrometer with a turbo ionspray (Applied Biosystems, Foster City, CA, USA). Nitrogen gas was used as the nebuliser gas. Sample analysis was performed in the negative ionisation mode, using multiple reaction monitoring (MRM). Transitions for phenylsulfate with m/z 173→93 and 173→80 (Kikuchi et al. 2010) were monitored and used for quantification and identity confirmation, respectively. The ionspray voltage was -4200 V, the nebuliser gas pressure was 10 psi, the curtain gas pressure was 8 psi, the collision gas pressure was 5 psi, and the ion source temperature was 350 °C. The declustering potential was -37 V, the focussing potential -200 V, the entrance potential -12 V, and the collision cell exit potential -15 V. The collision energies were -34 and -26 eV for transitions 173→93 and 173→80, respectively. The dwell time was 25 ms. Phenylsulfate was quantified based on its peak area using a linear calibration curve ($R^2 > 0.997$) prepared from the in the present study synthesised phenylsulfate. The data were processed with the Analyst software, version 1.5 (Applied Biosystems).

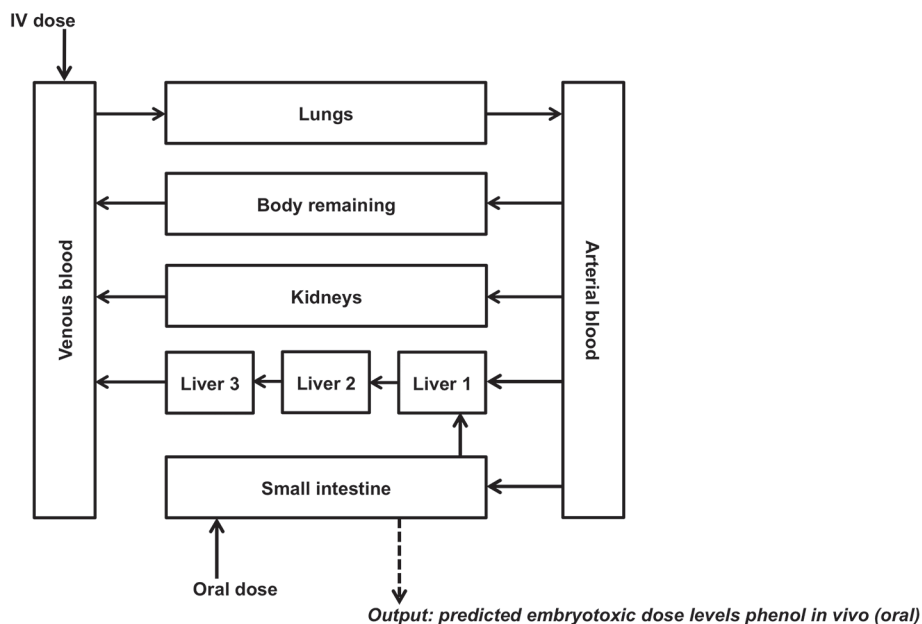


Figure 1 Schematic presentation of the PBK model for phenol in rat and human.

PBK MODEL RAT AND HUMAN

A perfusion rate-limited distribution was used to describe the disposition of unconjugated phenol and its metabolites between plasma and tissue, an assumption that is in line with

data reported for rats exposed to phenol (Liao and Oehme 1981). The conceptual structure of the PBK model for unconjugated phenol is illustrated in Figure 1. A set of differential equations describes the kinetics of unconjugated phenol (supplementary data A). Liver, small intestine, kidney and lung were identified as metabolising organs in the present study. The liver was divided in 3 metabolic zones namely (1) the periportal zone, (2) the midzone and (3) the perivenous zone. Sulfation was assigned to be evenly distributed across the zones and glucuronidation was assigned to zone 3 (Pang et al. 2008). Fat was not included as a separate compartment, because relative low concentrations of phenol appear in fat containing tissues (Liao and Oehme 1981) and due to corresponding calculated partition coefficients with the other body tissues (data not shown). Therefore, fat was lumped together with all other body tissues. Simple phenolic compounds may readily pass the placental barrier (Abu-Qare et al. 2000; Gray and Kavlock 1990). Therefore, the concentration reaching the embryo was set equal to the maternal plasma concentration and no separate embryonic compartment was distinguished. Following exposure, a high recovery of phenol in urine has been reported, predominantly as phenol metabolites (Hiser et al. 1994; Capel et al. 1972; Weitering et al. 1979). Only minor excretion of unconjugated phenol was observed via faeces and no or hardly any via exhalation (Hiser et al. 1994). Hence, metabolism was considered as the only excretion pathway in the present PBK model. At high-dose levels, phenol has been reported to be partly converted to hydroquinone, which is excreted as hydroquinone glucuronide (Hiser et al. 1994). The formation of hydroquinone is not included in the present model as it is not expected that hydroquinone contributes to the developmental toxicity of phenol. Namely, hydroquinone was not developmental toxic at low doses in vivo (Blacker et al. 1993; Krasavage et al. 1992; Murphy et al. 1992), only at a single high dose of 333 mg/kg bw (Kavlock 1990), but such a high level will probably not be reached due to the limited formation of hydroquinone after phenol exposure. Kinetic model calculations were performed applying Rosenbrock's algorithms for solving stiff systems (Berkeley Madonna, version 8.3.18, UC Berkeley, CA, USA).

All physiological parameters were obtained from Brown et al. (1997), except the fraction of blood flow to small intestine, which for rat was calculated using reported blood flow rates for the specific parts of the splanchnic system by Delp et al. (1998), whereas for human the value was taken from ICRP (2003). Physiological parameters are outlined in Table 1. Both, rat and human tissue:plasma partition coefficients were calculated by the algorithm of Berezhkovskiy (2004) requiring information on plasma protein binding, lipophilicity and acid-base properties. The olive oil:water partition coefficient was used to calculate the adipose tissue:plasma partition coefficient, and the octanol:water partition coefficient was used for the non-adipose tissues. The unbound fraction of phenol in plasma was 0.59 for the rat (Liao and Oehme 1981) and 0.47 for human (Judis 1982). The log Kow (pH 7.4) was 1.46 and the pKa was 9.99, which were obtained from the CHEMFATE database (<http://esc.syrres.com/esc/chemfate.htm>). The olive oil:water partition coefficient was calculated from the Kow

using the algorithm reported by Poulin and Theil (2002). The tissue:plasma partition coefficients for rat and human are presented in Table 2.

Table 1 Physiological data for rat and human applied in the PBK model.

Physiological parameter	Rat	Human
<i>Percentage of body weight</i>		
Small intestine	1.4	0.91
Liver	3.4	2.57
Kidney	0.70	0.44
Lung	0.50	0.76
Arterial blood	1.85	1.98
Venous blood	5.55	5.93
Body remaining	77.6	76.0
Cardiac output (l/h/kg bw ^{0.74})	15.0	15.0
<i>Percentage of cardiac output</i>		
Small intestine	7.5	10
Liver (without flow from small intestine)	17.5	12.7
Kidney	14.1	17.5
Body remaining	60.9	59.8

Table 2 Calculated tissue:plasma partition coefficients for rat and human.

Tissue	Partition coefficient	
	Rat	Human
Liver	0.97	1.13
Small intestine	1.18	1.26
Kidney	0.99	0.93
Lung	1.09	0.67
Body remaining	0.92	0.98

Kinetic parameters, namely V_{\max} and K_m , were derived from the in vitro metabolism data obtained in the present study. To this end, the in vitro data were fit to the Michaelis-Menten equation (GraphPad Prism 5.0 software, San Diego, CA, USA). The in vitro-derived V_{\max} values (nmol/min/mg protein) were scaled to the in vivo situation using reported protein yields for the liver, small intestine, kidney and lung (Table 3). The in vivo K_m values were assumed to equal the in vitro K_m values. The oral uptake rate (k_a) of phenol via small intestine was 7.62/h (Humphrey et al. 1980) for the rat. The same oral uptake rate value was applied in the human PBK model.

Table 3 Microsomal and cytosolic protein yields (mg/g organ) of different organs for rat and human.

Organ tissue fraction	Rat (mg/g)	Reference	Human (mg/g)	Reference
Liver microsomes	38	Chiu and Ginsberg (2011)	32	Barter et al. (2007)
Liver cytosol	87	Chiu and Ginsberg (2011)	80.7	Cubitt et al. (2011)
Intestinal microsomes	2.4	Van de Kerkhof et al. (2007)	20.6	Cubitt et al. (2009)
Intestinal cytosol	-		18	Gibbs et al. (1998)
Kidney microsomes	16	Bong et al. (1985)	16 ^a	
Lung microsomes	20	Medinsky et al. (1994)	-	

^a Value of rat kidney microsomes.

EVALUATION OF THE PBK MODEL PERFORMANCE

The performance of the PBK model for rat was examined by means of comparing predicted plasma concentrations of phenol with reported in vivo plasma levels. For the rat, this was evaluated for both the oral and the intravenous (IV) route of administration and at different dose levels, using in vivo rat data for phenol available from the literature (Table 4). The performance of the human PBK model was not evaluated due to the lack of data on the disposition of phenol in humans.

SENSITIVITY ANALYSIS OF THE PBK MODEL

For both the rat and human PBK models, a local parameter sensitivity analysis was carried out to identify influential parameters; each parameter was changed in turn keeping the other ones constant (Chiu et al. 2007). To this purpose, normalised sensitivity coefficients (SC) were calculated with respect to the maximum venous plasma concentrations of unconjugated phenol (C_{max}) using the algorithm:

$$SC = \frac{(C' - C)}{(P' - P)} * \left(\frac{P}{C}\right)$$

where C is the initial value of the model output, and C' is the output after a 1% parameter change. P is the initial parameter value and P' is the parameter value modified by an increase of 1%. The sensitivity analysis was conducted for an oral exposure to a single dose of 1.5 and 150 mg/kg bw.

TRANSLATION OF IN VITRO-DERIVED EMBRYOTOXICITY DATA TO AN IN VIVO POD FOR RISK ASSESSMENT

PBK reverse dosimetry was conducted to predict in vivo dose-response curves from in vitro concentration-response data. To this purpose, each nominal effective concentration (EC_x) of

phenol tested in the EST by Strikwold et al. (2012) was set equal to the maximum plasma concentration of unconjugated phenol (C_{max}) in the PBK model. In a second approach, the area under the curve of phenol in the 10-day EST (AUC_{0-10d}) was set equal to the in vivo AUC of phenol in plasma. No correction was applied to in vitro embryotoxic effect levels to account for different concentrations of free phenol in the EST culture medium and in plasma caused by different albumin levels in these matrices, since it was found that in vitro cytotoxicity of phenol tested with the fibroblast-like embryonic mouse cell line Balb/c 3T3 clone A31 was not affected by differences in bovine serum albumin levels reflecting the in vitro and in vivo situation (Gülden et al. 2002). Applying PBK-based reverse dosimetry with in vitro EC_x (or AUC response data) as an input for in vivo plasma levels provides in vivo effective dose levels (ED_x). From these ED_x values, an in vivo dose-response curve and a $BMDL_{05}$ (95% lower confidence limit of the benchmark dose at 5% benchmark response) were derived, using the Environmental Protection Agency's (EPA) Benchmark Dose Software (BMDS) version 2.2, applying the model that provided the best fit as described previously (Strikwold et al. 2012).

EVALUATION IN VITRO PBK APPROACH

In vivo dose-response curves for the rat predicted with the in vitro PBK approach were compared to individual data points representing the fraction of embryos affected at different experimental doses obtained from in vivo developmental toxicity studies (Table 5). To this purpose, the average continuous data for foetal weight/litter as reported by Argus (1997) were dichotomised using a 5% reduction in the foetal body weight from the mean foetal body weight/litter of the control group as a cut-off point. Based on this point, each foetal body weight/per litter was assigned affected or not affected, from which the fraction affected was calculated. In addition to this evaluation, the in vivo $BMDL_{05}$ predicted with the in vitro PBK approach was compared to NOAELs obtained from in vivo developmental toxicity studies from the literature.

To provide a sound evaluation of the in vitro PBK approach, exposure routes and scenarios (i.e. oral intake) from in vivo developmental toxicity studies for the rat available from literature (Table 5) were applied to the in vitro PBK approach. In most studies, phenol was tested during several consecutive days administering a single daily oral dose. As phenol was rapidly eliminated (<2 h) at a dose <350 mg/kg bw, only one single oral administration was modelled with the PBK model for unconjugated phenol. In the study of Ryan et al. (2001), rats were dosed via drinking water. The intake of drinking water by rats occurs in bouts (Zorrilla et al. 2005). The oral intake of phenol was calculated using a maximum intake amount of 6.6 ml water per bout (Zorrilla et al. 2005) multiplied by the concentration of phenol in drinking water to obtain maximum peak concentrations. Accumulation of phenol that could result from quick successive drinking water bouts was not considered.

RESULTS

IN VITRO EMBRYOTOXICITY DATA AND THE AREA UNDER THE CURVE OF PHENOL IN THE EST

Phenol inhibited differentiation of ES-D3 cells into beating cardiomyocytes in a concentration-dependent fashion (Figure 2). The in vitro BMC_{50} (benchmark concentration at 50% level of response) was 590 μM and the BMC_{1-99} ranged from 70 to 1520 μM (Strikwold et al. 2012).

It was found that the phenol concentration in the EST culture medium decreased rapidly in the first few hours of the EST resulting in hardly any exposure from day 0-3 in the EST. In the remaining days, phenol was relatively stable (Figure 2). The decrease of the phenol concentration in time follows a similar course for phenol concentrations of 0.2 and 0.6 mM and was on average 39% of the nominal concentration. The nominal AUC_{0-10d} of each concentration tested in the EST was reduced by 39% to calculate the actual AUC_{0-10d} , which then served as the surrogate for the in vivo plasma AUC in the PBK model.

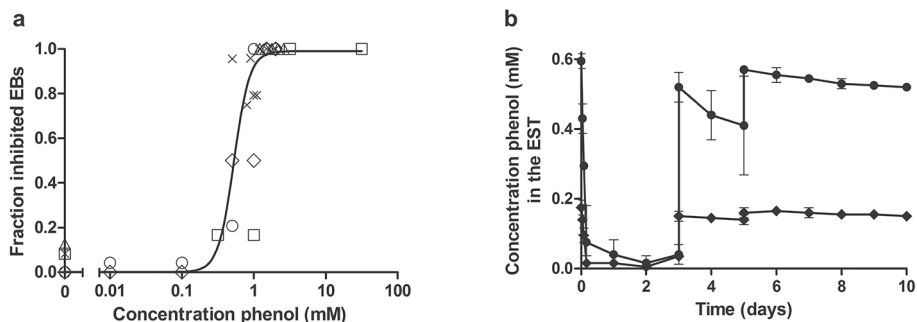


Figure 2 **a** Concentration-response curve for phenol representing the inhibition of differentiation of the embryoid bodies (EBs) at the specified concentrations, as previously obtained by Strikwold et al. (2012). Different symbols represent independent assays. **b** Course of the phenol concentration in the EST in time, tested at initial concentrations ($t = 0$) of 0.2 mM (\blacklozenge) and 0.6 mM (\bullet). Symbols represent mean values \pm SD.

IN VITRO KINETIC DATA FOR RAT AND HUMAN

Analysis of the incubations with phenol revealed that rat liver, small intestinal, kidney and lung microsomes were able to metabolise phenol towards phenylglucuronide and that rat liver cytosol was capable of forming phenylsulfate. For human samples, the incubations with phenol showed that liver and small intestinal microsomes and kidney S9 were able to glucuronidate phenol to phenylglucuronide and that both human liver and human small intestinal cytosol were able to form phenylsulfate. Sulfation was not detected in incubations with rat small intestinal cytosol, rat kidney and lung cytosol, and not with human kidney and lung S9 up to 2 h of incubation, neither was glucuronidation detected in incubations with human lung S9.

In each incubation with the relevant tissue fractions (microsomes, S9 or cytosol), metabolism followed Michaelis-Menten kinetics (Figure 3). The apparent K_m , V_{max} and the catalytic efficiencies ($V_{max(app)}/K_m$) of the tissue fractions are presented in Table 6, as well as the scaled $V_{max(app)}$ and the scaled catalytic efficiencies (scaled $V_{max(app)}/K_m$). In general, the scaled catalytic efficiencies (ml/h/g organ) for glucuronidation and sulfation of phenol obtained from human tissue fractions were lower compared to values obtained from rat tissue fractions. It appeared that the scaled catalytic glucuronidation efficiency was higher than the scaled catalytic sulfation efficiency for both rat and human liver, while the scaled catalytic sulfation efficiency in human intestinal tissue fraction was higher compared to the scaled catalytic glucuronidation efficiency. The liver was found to be the main metabolising organ for phenol in both rat and human. Rat liver tissue expressed a scaled catalytic glucuronidation efficiency of 440 ml/h/g liver, which is 6.4-fold higher compared to kidney tissue and 35.7- and 160.7-fold higher compared to lung tissue and small intestinal tissue, respectively. The ranking of human organs based on their scaled catalytic efficiencies is almost similar to the rat organs, identifying the liver as the main metabolising organ expressing a scaled catalytic efficiency of 59 ml/h/g liver, followed by kidney and small intestine that showed a 9.1- and a 23.0-fold lower catalytic efficiency compared to the liver. The scaled catalytic efficiency for sulfation in rat liver tissue was 636 ml/h/g liver and occurred with a relatively high affinity and low capacity resulting in saturation of this pathway at low doses. Human liver cytosol expressed a scaled catalytic sulfation efficiency of 17 ml/h/g liver, which is 1.4 times higher than the scaled catalytic efficiency determined with human intestinal cytosol. In case the catalytic efficiencies (ml/h/g liver) were scaled to a whole organ (ml/h/organ) using organ weights, then the ranking between the organs based on their catalytic efficiency would remain the same, both for rat and human (data not shown).

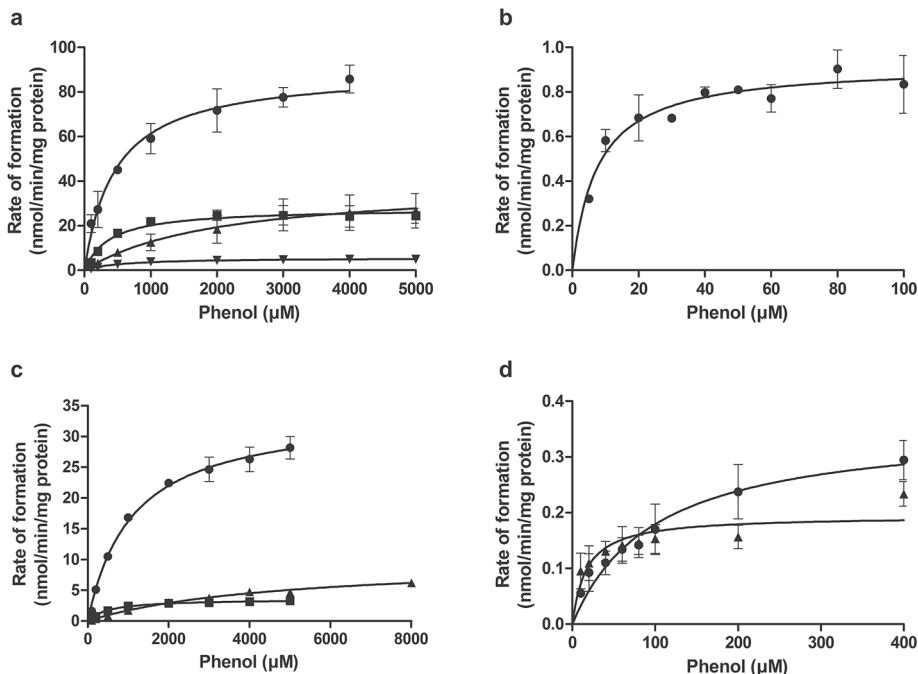


Figure 3 Concentration-dependent formation of phenylglucuronide (a and c) and phenylsulfate (b and d) by liver (●), small intestine (▲), kidney (■) and lung (▼) in incubations with relevant rat (a and b) and human (c and d) tissue fractions (microsomes, cytosol or S9). Individual symbols represent mean activities of ≥ 3 measurements \pm SD.

Table 4 Specifications of in vivo kinetic studies of phenol published in the literature and applied to evaluate the developed PBK model for phenol.

Species and strain	Body weight (kg)	Exposure route	Dose (mg/kg bw/d)	C_{max} PBK / C_{max} in vivo	AUC _{PBK} / AUC _{in vivo}	Remarks	Reference
Fischer 344 rat (male)	0.191 0.175	Oral	1.69 147	1.56 0.86	4.28 1.09	Bolus dose, volume administration 5 ml/kg	Hiser et al. (1994)
Sprague-Dawley rat (male)	0.263	Intraduodenal	0.4 1.5 4.5 15	- ^b	1.30 1.02 0.61 0.42		Cassidy and Houston (1984)
Sprague-Dawley rat (male)	0.263	IV	0.4 1.5 4.5 15	- ^b	1.49 1.48 1.21 1.05	0.01-h infusion (assumption)	Cassidy and Houston (1984)
Wistar rat (male)	0.286 ^a	IV	1.5	1.00	1.20	0.167-h infusion, volume administration 10 ml/kg	Dickinson and Taylor (1996)

^a Mean of the reported range of 0.241-0.330 kg.

^b No in vivo data available for first few minutes after dosing; therefore, no reliable C_{max} could be obtained from the in vivo data.

EVALUATION OF THE PBK MODEL PERFORMANCE

Figure 4 shows plasma concentration-time curves for unconjugated phenol in the rat predicted with the developed rat PBK model together with in vivo kinetic data obtained from the literature. The kinetic data show that phenol is rapidly absorbed in the body, resulting in a high peak concentration, after which phenol is readily excreted from the body, both at low and high doses. Figure 4 reveals that the PBK model accurately predicts the time course of changes in plasma concentrations of phenol for the oral route and for the IV route at the specified doses. The difference between the predicted and observed C_{max} for a single oral dose of 1.69 and 147 mg/kg bw was 1.56- and 0.86-fold, respectively, and for 10-min IV infusion of 1.5 mg/kg bw, there was no difference (1.0-fold) (Table 4). In addition, the difference between the AUC predicted with the PBK model for phenol and the AUC values obtained from the corresponding studies was small for most of the concentrations tested (Table 4). Only at the low single oral dose of 1.69 mg/kg bw, the model tends to overpredict the AUC expressing a 4.28-fold difference between the AUC predicted with the PBK model and the observed AUC obtained from the study of Hiser et al. (1994) (Table 4).

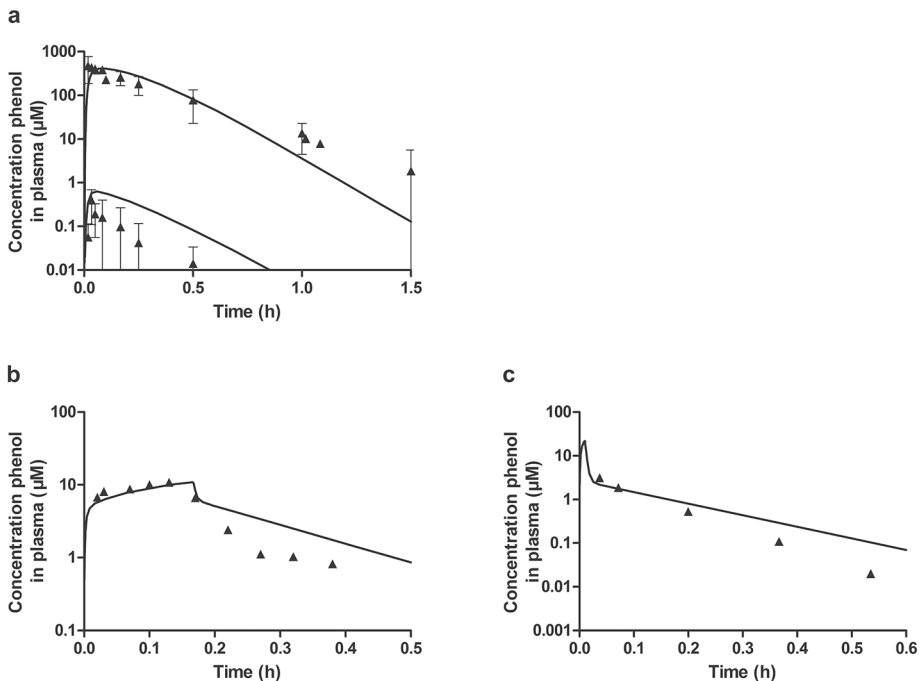


Figure 4 Plasma concentration-time profiles for phenol in rat predicted with the PBK model (solid lines) and published in vivo values (\blacktriangle) after a single oral dose of 1.69 and 147 mg/kg bw (a) (Hiser et al. 1994) and after IV dosing of 1.5 mg/kg bw with an infusion rate of 0.167/h (b) (Dickinson and Taylor 1996) and 0.4 mg/kg bw with presumed infusion rate of 0.01/h (c) (Cassidy and Houston 1984). a shows mean values \pm SD.

Table 5 In vivo developmental toxicity data of phenol obtained from the literature, used to evaluate the in vitro PBK approach.

Species and strain	Exposure day(s)	Dose (mg/kg bw/d) ^a	Developmental endpoint	Developmental NOAEL (mg/kg bw/d)	Reference
Sprague-Dawley rat	GD 11	0, 100, 333, 667, 1000	Malformations ^b reported at two highest doses ^c	333	Kavlock (1990)
Sprague-Dawley rat	GD 6-15	0, 30, 60, 120	Decreased average foetal bw/litter	60	Jones-Price et al. (1983a)
Sprague-Dawley rat	GD 6-15	0, 60, 120, 360 (3 doses/d; 0, 20, 40, 120 mg/kg bw/dosage)	Decreased average foetal bw/litter	120 (40)	Argus (1997)
Fischer rat	GD 6-19	0, 40, 53.3	Reduced live pups/litter and fraction litters fully resorbed	40	Narotsky and Kavlock (1995)
Sprague-Dawley rat	10-11 weeks prior to mating through weaning	0, 200, 1000, 5000 ppm (= 0, 20, 93, 350 mg/kg bw/d)	Fraction of offspring nonlive postnatal day 4 and postnatal day 7-21.	70 (males) 93 (females)	Ryan et al. (2001) ^d
CD-1 mice	GD 6-15	0, 70, 140, 280 (final study) 0, 100, 200, 230, 260, 275, 300, 400 (preliminary study)	Decreased average foetal bw/litter Fraction foetuses malformed	140	Jones-Price et al. (1983b)

^a In each study phenol was administered by oral gavage, except in the study of Ryan et al. (2001) in which phenol was administered via drinking water.

^b Hindlimb paralysis and/or short or kinky tails.

^c Not analysed on statistical significance.

^d Effects possibly related to decreased maternal water intake due to flavour aversion.

Table 6 Kinetic constants K_m and $V_{max} \pm SD$, and catalytic efficiencies of the formation of phase II metabolites phenylglucuronide and phenylsulfate of phenol in rat and human tissue fractions.

Species Organ	Glucuronidation						Sulfation					
	In vitro tissue fraction	K_m (app) ^a	V_{max} (app) ^b	Catalytic efficiency ^c	Scaled V_{max} (app) ^d	Scaled catalytic efficiency ^e	In vitro tissue fraction	K_m (app) ^a	V_{max} (app) ^b	Catalytic efficiency ^c	Scaled V_{max} (app) ^d	Scaled catalytic efficiency ^e
<i>Rat</i>												
Liver	microsomes	465 ± 66	90 ± 4	193	205	440	cytosol	7.6 ± 1.3	0.92 ± 0.03	122	4.8	636
Small intestine	microsomes	2061 ± 853	39 ± 7	19	5.6	2.7	cytosol	n.d.	n.d.	--	--	--
Kidney	microsomes	388 ± 70	28 ± 1	72	27	69	cytosol	n.d.	n.d.	--	--	--
Lung	microsomes	550 ± 77	5.6 ± 0.2	10	6.8	12	cytosol	n.d.	n.d.	--	--	--
<i>Human</i>												
Liver	microsomes	1105 ± 101	34 ± 1.0	31	66	59	cytosol	99 ± 22	0.36 ± 0.03	3.6	1.7	17
Small intestine	microsomes	4723 ± 785	9.9 ± 0.9	2.1	12	2.6	cytosol	17 ± 6	0.19 ± 0.01	12	0.2	12
Kidney	S9	529 ± 98	3.6 ± 0.2	6.8	3.4	6.5	S9	n.d.	n.d.	--	--	--
Lung	S9	n.d.	n.d.	--	--	--	S9	n.d.	n.d.	--	--	--

n.d. not detected

^a μM .^b nmol/min/mg protein in tissue fraction.^c μl /min/mg protein in tissue fraction.^d $\mu mol/h/g$ organ.^e ml/h/g organ.

SENSITIVITY ANALYSIS OF THE PBK MODEL

The sensitivity analysis (supplementary data B) revealed that the intestinal absorption coefficient, the volume of the liver, the maximum glucuronidation and sulfation rate in the liver and the liver cytosolic protein yield were the most influential parameters in the rat PBK model expressing normalised sensitivity coefficients >1 . The normalised sensitivity coefficients of most of the PBK model parameters were not dose-dependent, except for parameters related to sulfation in the rat liver (cytosolic protein yield and the Michaelis-Menten parameters K_m and V_{max}), which were more influential on C_{max} at low oral dose levels compared to high oral dose levels.

The sensitivity analysis of the human PBK model revealed that the intestinal absorption coefficient, the volume of the intestine, the microsomal protein yield in the intestine and the maximum glucuronidation rate in the intestine were the most influential parameters in the model, expressing normalised sensitivity coefficients >1 . The normalised sensitivity coefficients of several parameters of the human PBK model were dose-dependent, namely those for the body weight, the volume of the liver and the volume of the small intestine, the blood flow to the small intestine, the intestinal absorption coefficient, and parameters related to metabolism. Compared to the rat, parameters related to glucuronidation in human intestine were more influential at lower doses and parameters related to sulfation of phenol in the liver were not as influential in the human PBK model compared to the rat PBK model at low doses. These differences in sensitivity of the model parameters may be explained by the different catalytic efficiencies of the metabolising organs in rat and human.

TRANSLATION OF IN VITRO-DERIVED EMBRYOTOXICITY DATA TO AN IN VIVO POD FOR RISK ASSESSMENT

Figure 5 presents the predicted in vivo dose-response curves for developmental toxicity of phenol in the rat using the in vitro PBK approach, along with developmental toxicity data obtained from the literature. This figure shows that the predicted dose-response curves for the rat based on the C_{max} of phenol closely mimic most of the in vivo developmental toxicity values obtained from the literature, which is not the case for the dose-response curve based on the AUC_{0-10d} . The $BMDL_{05}$ derived from the dose-response curve for rat based on the C_{max} is 93.5 mg/kg bw/d and the $BMDL_{05}$ derived from the dose-response curve for rat based on the AUC_{0-10d} is 1890 mg/kg bw/d. From here onwards, the $BMDL_{05}$ derived from C_{max} is considered because this value matches the in vivo data better than the $BMDL_{05}$ derived from the AUC_{0-10d} . The NOAELs for the rat obtained from the available in vivo developmental toxicity studies are presented in Table 5. A 0.3- to 2.3-fold difference was observed between the in the present study predicted $BMDL_{05}$ and the in vivo-derived NOAELs. The predicted $BMDL_{05}$ lies within the range of the reported PoDs obtained from in vivo developmental toxicity studies (Figure 6). The $BMDL_{05}$ derived from the dose-response curve for human (Figure 5) based on the C_{max} is 26.9 mg/kg bw/d, which is 3.5-fold lower compared to the predicted $BMDL_{05}$ for the rat.

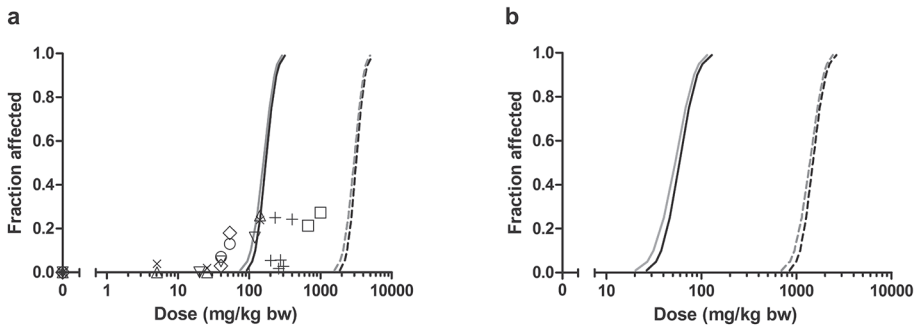


Figure 5 In vivo dose-response curves together with the 95% lower confidence limit for developmental toxicity of phenol in rat (a) and human (b) predicted by the in vitro PBK approach compared to in vivo developmental toxicity data reported in the literature. The solid lines represent the predicted dose-response curves based on the nominal test concentration of phenol relating C_{max} to developmental toxicity, and the dashed lines represent the predicted dose-response curves relating the AUC_{0-10d} of phenol to developmental toxicity. Symbols represent fraction of litters which had offspring with hindlimb paralysis and/or short or kinky tails (\square) (Kavlock 1990), fraction of offspring nonlive postnatal day 4 (Δ) and fraction of offspring nonlive postnatal day 7-21 (\times) (Ryan et al. 2001), fraction of litters with 5% reduction of foetal bw compared to average foetal bw/litter of the control group (∇) (Argus 1997), fraction litters fully resorbed (\circ), fraction nonlive pups per litter (compared to number of implants (average data)) (\diamond) (Narotsky and Kavlock 1995) and fraction foetuses malformed (+) (Jones-Price et al. 1983b). See Table 5 for specifications of the in vivo data.

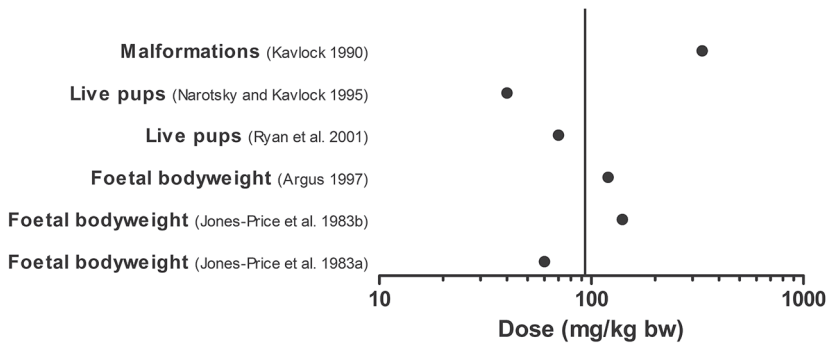


Figure 6 95% lower confidence limit of the benchmark dose ($BMDL_{05}$) for developmental toxicity of phenol in the rat predicted by the in vitro PBK approach (line) compared to NOAELs (\bullet) obtained from in vivo developmental toxicity studies of phenol. See Table 5 for specifications of the in vivo data.

DISCUSSION

The objective of the present study was to demonstrate the potential of a combined in vitro PBK approach to predict in vivo dose-response curves that allow definition of a PoD for risk assessment using in vitro-derived toxicity data combined with a PBK model, with phenol as the compound of interest. The current study demonstrated that combining in vitro toxicity data with a PBK model is a promising approach to derive safe exposure levels for the risk assessment of chemicals, predicting a BMDL₀₅ that lies within the variation of NOAELs obtained from in vivo developmental toxicity data from the literature. The maximum observed difference was 0.3-fold between the in vitro PBK predicted BMDL₀₅ of 93.5 mg/kg bw/d and the in vivo NOAELs with 333 mg/kg bw/d being the highest NOAEL. This result was achieved on the basis of in vitro and in silico data and data available from the literature only, thereby considerably contributing to the reduction, refinement and replacement (3Rs) in animal testing. In practice, there is a great demand for alternatives to animal experiments, as the use of animal testing is regulated in the new Cosmetic Products Regulation, which banned the testing of cosmetic ingredients on animals by March 2013 (EC 2009) and in the EU chemical legislation-Registration, Evaluation, Authorisation and restriction of Chemicals (REACH)-which states that animal testing may only be undertaken as a last resort (EC 2007). As only a few examples of the in vitro PBK approach are reported so far (Louisse et al. 2010; Verwei et al. 2006), more studies are required before the present approach can be regarded reliable and implemented in practice.

In most in vivo developmental toxicity studies, phenol was administered during several consecutive gestational days, resulting in a reduced foetal body weight. This adverse effect was not observed in the developmental screening study of Kavlock (1990) in which phenol was administered only on gestational day 11 up to a dose of 1000 mg/kg bw. Phenol is very rapidly eliminated from the body and does not accumulate after repeated daily dosing. The current study showed that the C_{max} was an appropriate metric to predict in vivo developmental toxicity of phenol for most endpoints including reduction in foetal body weight.

Physiological conditions of rat and human may change during pregnancy and may influence the kinetics of a compound. It has been reported that uridine diphosphate glucuronyltransferase (UDPGT) activity towards phenolic substrates in pregnant rats can be reduced by about 50% during pregnancy (Luquita et al. 2001). Glucuronidation is the dominant elimination pathway at higher dose levels of phenol. Using the approach developed in the present study it was calculated that a 50% reduction of the V_{max} for glucuronidation in the liver would result in a 1.6-fold lower BMDL₀₅ of 58.9 mg/kg bw/d. This predicted BMDL₀₅ still lies well within the observed variation of the in vivo PoDs for developmental toxicity, though evaluating pregnancy specific kinetic changes may be valuable to refine model predictions.

Glucuronidation and sulfation conjugates were considered to be the most important phenol metabolites in the PBK models for rat and human in analogy with the metabolic profiles obtained from reported *in vivo* kinetic studies. Sulfation of phenol in rat small intestine could not be identified *in vitro* in incubations with tissue fractions that were positively screened for sulfation activity with genistein as the control substrate. However, sulfation of phenol was demonstrated in intestinal *in situ* perfusion studies in the rat (Kothare and Zimmerman 2002; Powell et al. 1974) and in isolated rat intestinal cells and preparations (Shirkey et al. 1979; Powell et al. 1974). This discrepancy, however, would not affect the predicted dose-response curves (BMD_{1.99}) and the PoD for phenol to a large extent, as the observed developmental toxic effect occurs at high doses, far above levels at which sulfation becomes saturated and at which the glucuronidation pathway dominates metabolism.

The predicted BMDL₀₅ of 93.5 mg/kg bw/d for rat obtained using the *in vitro* PBK approach could theoretically be used as a PoD for risk assessment, applying a default uncertainty factor of 100, accounting for intra- and interspecies kinetic and dynamic differences (IPCS 2005). This would result in a human guidance value for the general population of 0.93 mg/kg bw/d. Applying the BMDL₀₅ of 26.9 mg/kg bw/d obtained with the human *in vitro* PBK approach allows for elimination of an uncertainty factor of 10^{0.6} that accounts for interspecies kinetic differences (IPCS 2005). This provides a guidance value of 1.07 mg/kg bw/d which is close to the guidance value of 0.93 mg/kg bw/d derived from the rat *in vitro* PBK approach. Thus, the interspecies kinetic differences elucidated with the present PBK model for rat and human are correctly covered with the default uncertainty factor for interspecies kinetic differences (IPCS 2005).

The present study used the EST to assess the potential of phenol to cause developmental toxic effects *in vivo*. It should be noted, however, that the endpoint inhibition of cardiomyocyte differentiation tested in the EST cannot reflect the whole array of developmental toxic effects that can be induced by compounds, as some compounds interfere with processes that are not present in the 10-day EST and hence some effects may remain undetected. Therefore, additional test systems reflecting extra endpoints *i.e.* neural differentiation may be considered when applying this *in vitro* PBK approach in practice. In addition, there may be uncertainty whether the sensitivity of an *in vitro* test system towards the compound accurately reflects the sensitivity *in vivo*. Applying an extra uncertainty factor that accounts for these differences in sensitivity may therefore be considered in case the current *in vitro* PBK approach is applied for risk assessment purposes. Finally, it may be noted that the EST was not able to correctly rank a series of *p*-substituted phenols to their *in vivo* potency, except phenol itself (Strikwold et al. 2012). A reason may be the kinetic differences between the *in vitro* and the *in vivo* situation (Strikwold et al. 2012). Applying the current *in vitro* PBK approach to this series of *p*-substituted phenols may provide a promising strategy to elucidate this aspect in the future.

Overall, this study shows that it is possible to accurately predict a PoD for the risk assessment of phenol, providing a PoD that lies within the range of the reported *in vivo* PoDs for developmental toxicity, using *in vitro*, *in silico* data and data from the literature only. It shows how combining different alternatives to animal testing such as *in vitro* and *in silico* methods can enlarge their application from screening and prioritising chemicals towards deriving safe exposure levels for the risk assessment of compounds. Although, the application of the presented *in vitro* PBK approach is still in its infancy, the positive results obtained in the present study may stimulate to explore its feasibility for other toxicological endpoints and a wide set of compounds.

REFERENCES

- Abu-Qare AW, Brownie CF, Abou-Donia MB (2000) Placental transfer and pharmacokinetics of a single oral dose of [¹⁴C]p-nitrophenol in rats. *Arch Toxicol* 74:388-396
- Argus (1997) Oral (gavage) developmental toxicity study of phenol in rats. Protocol Number: Argus 916-011. Argus Research Laboratories, Inc., Horsham, PA
- ATSDR (2008) Toxicological profile for phenol. U.S. Department of Health and Human Services, Public Health Service, Agency for Toxic Substances and Disease Registry (ATSDR), Atlanta (GA)
- Baars AJ, Theelen RMC, Janssen PJCM, Hesse JM, van Apeldoorn ME, Meijerink MCM, Verdam L, Zeilmaker MJ (2001) Re-evaluation of human-toxicological maximum permissible risk levels. Report no. 711701025. National Institute for Public Health and the Environment (RIVM), Bilthoven
- Barter ZE, Bayliss MK, Beaune PH, Boobis AR, Carlile DJ, Edwards RJ, Houston JB, Lake BG, Lipscomb JC, Pelkonen OR, Tucker GT, Rostami-Hodjegan A (2007) Scaling factors for the extrapolation of *in vivo* metabolic drug clearance from *in vitro* data: reaching a consensus on values of human microsomal protein and hepatocellularity per gram of liver. *Curr Drug Metab* 8:33-45
- Berezhkovskiy LM (2004) Volume of distribution at steady state for a linear pharmacokinetic system with peripheral elimination. *J Pharm Sci* 93:1628-1640
- Blacker AM, Schroeder RE, English JC, Murphy SJ, Krasavage WJ, Simon GS (1993) A two-generation reproduction study with hydroquinone in rats. *Fundam Appl Toxicol* 21:420-424
- Bong M, Laskowska-Klita T, Szymczyk T (1985) Effect of the benzene fraction of petroleum on protein content in rat liver and kidney. *Bull Environ Contam Toxicol* 34:45-54
- Brown RP, Delp MD, Lindstedt SL, Rhomberg LR, Beliles RP (1997) Physiological parameter values for physiologically based pharmacokinetic models. *Toxicol Ind Health* 13:407-484
- Bruce W, Meek ME, Newhook R (2001) Phenol: hazard characterization and exposure-response analysis. *J Environ Sci Health C Environ Carcinog Ecotoxicol Rev* 19:305-324
- Capel ID, French MR, Millburn P, Smith RL, Williams RT (1972) The fate of [¹⁴C]phenol in various species. *Xenobiotica* 2:25-34
- Cassidy MK and Houston JB (1984) *In vivo* capacity of hepatic and extrahepatic enzymes to conjugate phenol. *Drug Metab Dispos* 12:619-624
- Chapman DE, Namkung MJ, Juchau MR (1994) Benzene and benzene metabolites as embryotoxic agents: effects on cultured rat embryos. *Toxicol Appl Pharmacol* 128:129-137
- Chiu WA, Barton HA, DeWoskin RS, Schlosser P, Thompson CM, Sonawane B, Lipscomb JC, Krishnan K (2007) Evaluation of physiologically based pharmacokinetic models for use in risk assessment. *J Appl Toxicol* 27:218-237
- Chiu WA and Ginsberg GL (2011) Development and evaluation of a harmonized physiologically based pharmacokinetic (PBPK) model for perchloroethylene toxicokinetics in mice, rats, and humans - Supplementary Materials. *Toxicol Appl Pharmacol* 253:203-234
- Cubitt HE, Houston JB, Galetin A (2009) Relative importance of intestinal and hepatic glucuronidation-impact on the prediction of drug clearance. *Pharm Res* 26:1073-1083

- Cubitt HE, Houston JB, Galetin A (2011) Prediction of human drug clearance by multiple metabolic pathways: integration of hepatic and intestinal microsomal and cytosolic data. *Drug Metab Dispos* 39:864-873
- Delp MD, Evans MV, Duan C (1998) Effects of aging on cardiac output, regional blood flow, and body composition in Fischer-344 rats. *J Appl Physiol* 85:1813-1822
- Dickinson PA and Taylor G (1996) Pulmonary first-pass and steady-state metabolism of phenols. *Pharm Res* 13:744-748
- EC (2007) Corrigendum to Regulation (EC) No 1907/2006 of the European Parliament and of the Council of 18 December 2006 concerning the Registration, Evaluation, Authorisation and Restriction of Chemicals (REACH), establishing a European Chemicals Agency, amending Directive 1999/45/EC and repealing Council Regulation (EEC) No 793/93 and Commission Regulation (EC) No 1488/94 as well as Council Directive 76/769/EEC and Commission Directives 91/155/EEC, 93/67/EEC, 93/105/EC and 2000/21/EC. *Off J Eur Union* L136:3-280
- EC (2009) Regulation (EC) no 1223/2009 of the European parliament and of the council of 30 November 2009 on cosmetic products. *Off J Eur Union* L342:59-209
- Environment Agency (2009) Contaminants in soil: updated collation of toxicological data and intake values for humans. Phenol. Science Report SC050021 / TOX9. Environment Agency, Bristol
- Fisher MB, Campanale K, Ackermann BL, Vandenbranden M, Wrighton SA (2000) In vitro glucuronidation using human liver microsomes and the pore-forming peptide alamethicin. *Drug Metab Dispos* 28:560-566
- Genschow E, Spielmann H, Scholz G, Pohl I, Seiler A, Clemann N, Bremer S, Becker K (2004) Validation of the embryonic stem cell test in the international ECVAM validation study on three in vitro embryotoxicity tests. *Altern Lab Anim* 32:209-244
- Gibbs JP, Yang JS, Slattery JT (1998) Comparison of human liver and small intestinal glutathione S-transferase-catalyzed busulfan conjugation in vitro. *Drug Metab Dispos* 26:52-55
- Gray JA and Kavlock RJ (1990) A pharmacokinetic analysis of phenol in the pregnant rat: deposition in the embryo and maternal tissues. *Teratology* 41:561
- Gülden M, Mörchel S, Tahan S, Seibert H (2002) Impact of protein binding on the availability and cytotoxic potency of organochlorine pesticides and chlorophenols in vitro. *Toxicology* 175:201-213
- Hiser MF, Kropscott BE, McQuirk RJ, Bus JS (1994) Pharmacokinetics, metabolism and distribution of ¹⁴C-phenol in Fischer 344 rats after gavage, drinking water and inhalation exposure. OTS0557473. Study ID: K-002727-022. Dow Chemical Company. Submitted to U.S. Environmental Protection Agency under TSCA Section 8D
- Hughes MF and Hall LL (1995) Disposition of phenol in rat after oral, dermal, intravenous, and intratracheal administration. *Xenobiotica* 25:873-883
- Humphrey MJ, Filer CW, Jeffery DJ, Langley PF, Wadds GA (1980) The availability of carfecillin and its phenol moiety in rat and dog. *Xenobiotica* 10:771-778
- ICRP (2003) Basic anatomical and physiological data for use in radiological protection: reference values. ICRP Publication 89. Pergamon, Oxford
- IPCS (2005) Chemical-specific adjustment factors for interspecies differences and human variability: guidance document for use of data in dose/concentration-response assessment. World Health Organization, Geneva
- Jones-Price C, Ledoux TA, Reel JR, Fisher PW, Langhoff-Paschke L, Marr MC, Kimmel CA (1983a) Teratologic evaluation of phenol (CAS No. 108-95-2) in CD rats. NTP Study TER81104. Research Triangle Institute, Research Triangle Park, NC
- Jones-Price C, Ledoux TA, Reel JR, Langhoff-Paschke L, Marr MC, Kimmel CA (1983b) Teratologic evaluation of phenol (CAS No. 108-95-2) in CD-1 mice. NTP Study TER80129. Research Triangle Institute, Research Triangle Park, NC
- Judis J (1982) Binding of selected phenol derivatives to human serum proteins. *J Pharm Sci* 71:1145-1147
- Kavlock RJ (1990) Structure-activity relationships in the developmental toxicity of substituted phenols: in vivo effects. *Teratology* 41:43-59
- Kheder A and Nair KPS (2012) Spasticity: pathophysiology, evaluation and management. *Pract Neurol* 12:289-298
- Kikuchi K, Itoh Y, Tateoka R, Ezawa A, Murakami K, Niwa T (2010) Metabolomic search for uremic toxins as indicators of the effect of an oral sorbent AST-120 by liquid chromatography/tandem mass spectrometry. *J Chromat B, Analyt Technol Biomed Life Sci* 878:2997-3002
- Kothare PA and Zimmerman CL (2002) Intestinal metabolism: the role of enzyme localization in phenol metabolite kinetics. *Drug Metab Dispos* 30:586-594
- Krasavage WJ, Blacker AM, English JC, Murphy SJ (1992) Hydroquinone: a developmental toxicity study in rats. *Fundam Appl Toxicol* 18:370-375
- Landau M (2007) Cardiac complications in deep chemical peels. *Dermatol Surg* 33:190-193

- Liao TF and Oehme FW (1981) Tissue distribution and plasma protein binding of [14 C]phenol in rats. *Toxicol Appl Pharmacol* 57:220-225
- Louisse J, de Jong E, van de Sandt JJM, Blaauboer BJ, Woutersen RA, Piersma AH, Rietjens IMCM, Verwei M (2010) The use of in vitro toxicity data and physiologically based kinetic modeling to predict dose-response curves for in vivo developmental toxicity of glycol ethers in rat and man. *Toxicol Sci* 118:470-484
- Luquita MG, Catania VA, Sánchez Pozzi EJ, Veggí LM, Hoffman T, Pellegrino JM, Ikushiro SI, Emi Y, Iyanagi T, Vore M, Mottino AD (2001) Molecular basis of perinatal changes in UDP-glucuronosyltransferase activity in maternal rat liver. *J Pharmacol Exp Ther* 298:49-56
- Medinsky MA, Leavens TL, Csanády GA, Gargas ML, Bond JA (1994) In vivo metabolism of butadiene by mice and rats: a comparison of physiological model predictions and experimental data. *Carcinogenesis* 15:1329-1340
- Murphy SJ, Schroeder RE, Blacker AM, Krasavage WJ, English JC (1992) A study of developmental toxicity of hydroquinone in the rabbit. *Fundam Appl Toxicol* 19:214-221
- Narotsky MG and Kavlock RJ (1995) A multidisciplinary approach to toxicological screening: II. Developmental toxicity. *J Toxicol Environ Health* 45:145-171
- Oglesby LA, Ebron-McCoy MT, Logsdon TR, Copeland F, Beyer PE, Kavlock RJ (1992) In vitro embryotoxicity of a series of para-substituted phenols: structure, activity, and correlation with in vivo data. *Teratology* 45:11-33
- Pang KS, Morris ME, Sun H (2008) Formed and preformed metabolites: facts and comparisons. *J Pharm Pharmacol* 60:1247-1275
- Poulin P and Theil FP (2002) Prediction of pharmacokinetics prior to in vivo studies. 1. Mechanism-based prediction of volume of distribution. *J Pharm Sci* 91:129-156
- Powell GM, Miller JJ, Olavesen AH, Curtis CG (1974) Liver as major organ of phenol detoxication? *Nature* 252:234-235
- Punt A, Schiffelers MJWA, Jean Horbach G, van de Sandt JJM, Groothuis GMM, Rietjens IMCM, Blaauboer BJ (2011) Evaluation of research activities and research needs to increase the impact and applicability of alternative testing strategies in risk assessment practice. *Regul Toxicol Pharmacol* 61:105-114
- Rietjens IMCM, Louisse J, Punt A (2011) Tutorial on physiologically based kinetic modeling in molecular nutrition and food research. *Mol Nutr Food Res* 55:941-956
- Rothman N, Bechtold WE, Yin SN, Dosemeci M, Li GL, Wang YZ, Griffith WC, Smith MT, Hayes RB (1998) Urinary excretion of phenol, catechol, hydroquinone, and muconic acid by workers occupationally exposed to benzene. *Occup Environ Med* 55:705-711
- Ryan BM, Selby R, Gingell R, Waechter JM Jr, Butala JH, Dimond SS, Dunn BJ, House R, Morrissey R (2001) Two-generation reproduction study and immunotoxicity screen in rats dosed with phenol via the drinking water. *Int J Toxicol* 20:121-142
- Shirkey RJ, Kao J, Fry JR, Bridges JW (1979) A comparison of xenobiotic metabolism in cells isolated from rat liver and small intestinal mucosa. *Biochem Pharmacol* 28:1461-1466
- Strikwold M, Woutersen RA, Spenkelink B, Punt A, Rietjens IMCM (2012) Relative embryotoxic potency of p-substituted phenols in the embryonic stem cell test (EST) and comparison to their toxic potency in vivo and in the whole embryo culture (WEC) assay. *Toxicol Lett* 213:235-242
- Van de Kerkhof EG, de Graaf IAM, Groothuis GMM (2007) In vitro methods to study intestinal drug metabolism. *Curr Drug Metab* 8:658-675
- Verwei M, van Burgsteden JA, Krul CAM, van de Sandt JJM, Freidig AP (2006) Prediction of in vivo embryotoxic effect levels with a combination of in vitro studies and PBPK modelling. *Toxicol Lett* 165:79-87
- Weber M and Weber M (2010) Phenols. In: Pilato L. (ed) *Phenolic resins: a century of progress*. Springer, Berlin Heidelberg, pp 9-23
- Weitering JG, Krijgsheld KR, Mulder GJ (1979) The availability of inorganic sulphate as a rate limiting factor in the sulphate conjugation or xenobiotics in the rat? Sulphation and glucuronidation of phenol. *Biochem Pharmacol* 28:757-762
- WHO (1994) Phenol. Environmental health criteria 161. World Health Organization, Geneva
- Yamaguchi S (1959) Sulfuric acid esters. I. Synthesis of sulfuric acid esters with sulfamic acid. *Nippon Kagaku Zasshi* 80:171-173, Chem. Abstr. 27666 (1961)
- Zorrilla EP, Inoue K, Fekete ÉM, Tabarín A, Valdez GR, Koob GF (2005) Measuring meals: structure of prandial food and water intake of rats. *Am J Physiol Regul Integr Comp Physiol* 288:R1450-R1467

SUPPLEMENTARY DATA A

MASS BALANCE EQUATIONS AND PARAMETER SPECIFICATIONS OF THE PBK MODEL FOR PHENOL IN THE RAT

COMPOUND	ABBREVIATION
phenol	ph
phenylglucuronide	pg
phenylsulfate	ps

COMPARTMENT (TISSUE (T))	ABBREVIATION
Small intestine	I
Liver	L
Lung	P
Kidney	K
Remaing body	B
Arterial	A
Venous	V

VARIABLE	UNIT	ABBREVIATION
Blood flow rate to tissue	$l\ h^{-1}$	Q(T)
Cardiac output	$l\ h^{-1}$	QC
Concentration phenol in tissue or blood	μM	C(T) _{ph}
Partition coefficient tissue:blood phenol	-	P(T) _{ph}
Volume of tissue or blood	l	V(T)
Amount phenol in tissue or blood	μmol	A(T) _{ph}
Maximum rate of formation metabolite (m) in tissue	$\mu mol\ h^{-1}$	Vmax(T) _m
Michaelis-Menten constant for formation metabolite (m) in tissue	μM	Km(T) _m
Uptake rate phenol intestine	h^{-1}	ka
Amount phenol taken up from the gut lumen	μmol	Uptake _{ph}
Amount phenol remaining in the gut lumen	μmol	AGL _{ph}

SMALL INTESTINE

$$\frac{dAI_{ph}}{dt} = \frac{dUptake_{ph}}{dt} + QI * \left(CA_{ph} - \frac{CI_{ph}}{PI_{ph}} \right) - \frac{VmaxI_{pg} * \frac{CI_{ph}}{PI_{ph}}}{KmI_{pg} + \frac{CI_{ph}}{PI_{ph}}}$$

Uptake phenol from gut lumen

$$\frac{dUptake_{ph}}{dt} = -\frac{dAGL_{ph}}{dt} = ka * AGL_{ph}$$

$$AGL_{ph}(0) = \text{Oral dose}$$

$$CI_{ph} = \frac{AI_{ph}}{VI}$$

LIVER COMPARTMENT 1

$$\frac{dAL1_{ph}}{dt} = QL * CA + QI * \frac{CI_{ph}}{PI_{ph}} - (QL + QI) * \frac{CL1_{ph}}{PL_{ph}} - \frac{VmaxL_{ps}/3 * \frac{CL1_{ph}}{PL_{ph}}}{KmL_{ps} + \frac{CL1_{ph}}{PL_{ph}}}$$

$$CL1_{ph} = \frac{AL1_{ph}}{VL/3}$$

LIVER COMPARTMENT 2

$$\frac{dAL2_{ph}}{dt} = (QL + QI) * \frac{CL1_{ph}}{PL_{ph}} - (QL + QI) * \frac{CL2_{ph}}{PL_{ph}} - \frac{VmaxL_{ps}/3 * \frac{CL2_{ph}}{PL_{ph}}}{KmL_{ps} + \frac{CL2_{ph}}{PL_{ph}}}$$

$$CL2_{ph} = \frac{AL2_{ph}}{VL/3}$$

LIVER COMPARTMENT 3

$$\frac{dAL_{3ph}}{dt} = (Q_L + Q_I) * \frac{CL_{2ph}}{P_{Iph}} - (Q_L + Q_I) * \frac{CL_{3ph}}{P_{Lph}} - \frac{Vmax_{Lpg} * \frac{CL_{3ph}}{P_{Lph}}}{Km_{Lpg} + \frac{CL_{3ph}}{P_{Lph}}} - \frac{Vmax_{Lps}/3 * \frac{CL_{3ph}}{P_{Lph}}}{Km_{Lps} + \frac{CL_{3ph}}{P_{Lph}}}$$

$$CL_{3ph} = \frac{AL_{3ph}}{VL/3}$$

LUNG COMPARTMENT

$$\frac{dAP_{ph}}{dt} = QC * \left(CV_{ph} - \frac{CP_{ph}}{P_{Pph}} \right) - \frac{Vmax_{Ppg} * \frac{CP_{ph}}{P_{Pph}}}{Km_{Ppg} + \frac{CP_{ph}}{P_{Pph}}}$$

$$CP_{ph} = \frac{AP_{ph}}{VP}$$

KIDNEY COMPARTMENT

$$\frac{dAK_{ph}}{dt} = QK * \left(CA_{ph} - \frac{CK_{ph}}{P_{Kph}} \right) - \frac{Vmax_{Kpg} * \frac{CK_{ph}}{P_{Kph}}}{Km_{Kpg} + \frac{CK_{ph}}{P_{Kph}}}$$

$$CK_{ph} = \frac{AK_{ph}}{VK}$$

REMAINING BODY TISSUE

$$\frac{dAB_{ph}}{dt} = QB * \left(CA_{ph} - \frac{CB_{ph}}{P_{Bph}} \right)$$

$$CB_{ph} = \frac{AB_{ph}}{VB}$$

ARTERIAL BLOOD COMPARTMENT

$$\frac{dAA_{ph}}{dt} = QC * \left(\frac{CP_{ph}}{PP_{ph}} - CA_{ph} \right)$$

$$CA_{ph} = \frac{AA_{ph}}{VA}$$

VENOUS BLOOD COMPARTMENT

$$\frac{dAV_{ph}}{dt} = (QL + QI) * \frac{CL3_{ph}}{PL_{ph}} + QK * \frac{CK_{ph}}{PK_{ph}} + QB * \frac{CB_{ph}}{PB_{ph}} - QC * CV_{ph}$$

$$CV_{ph} = \frac{AV_{ph}}{VV}$$

SUPPLEMENTARY DATA B

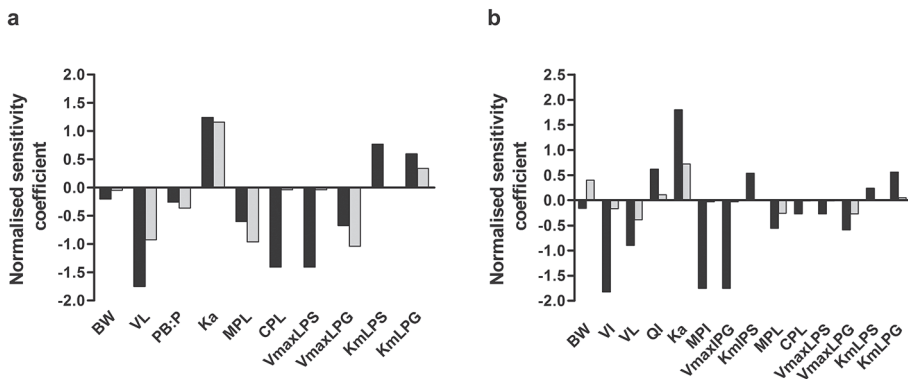
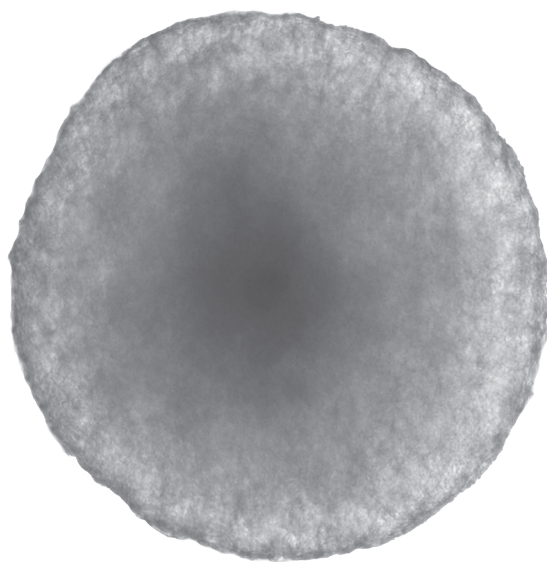
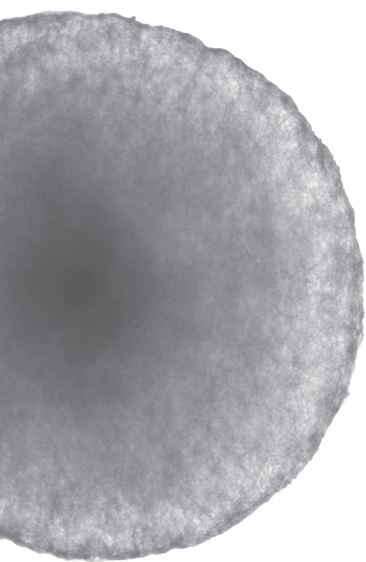
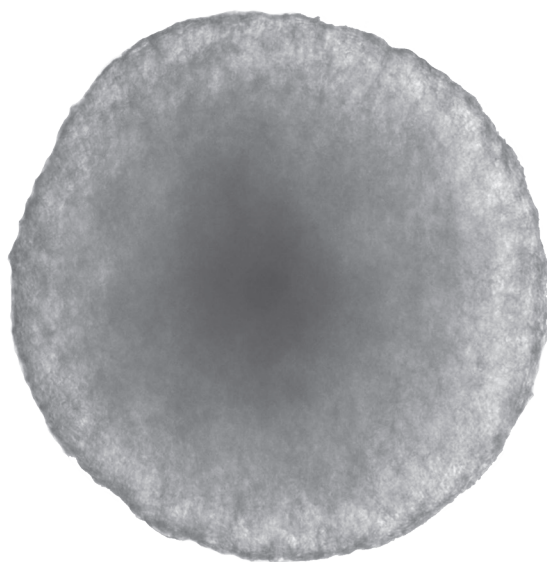
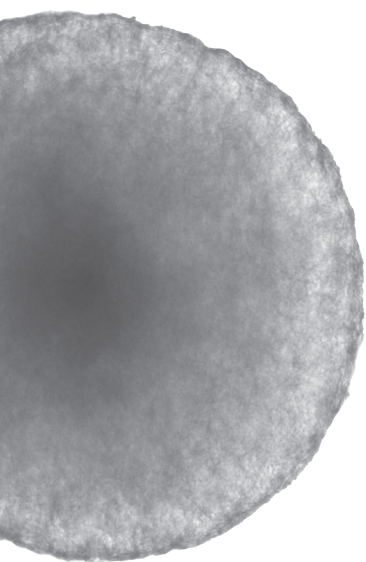


Figure S1 Normalised sensitivity coefficients for parameters of the PBK model for rat (a) and human (b) based on C_{max} values from a single oral dose of 1.5 mg/kg bw (black bars) and 150 mg/kg bw (grey bars). Normalised sensitivity coefficients ≥ 0.2 are presented. BW=body weight, VI=fraction small intestine, VL=fraction liver tissue, QI=fraction blood flow to small intestine, PB:P=partitioning coefficient body remaining:plasma, Ka=intestinal absorption coefficient, MPI=small intestinal microsomal protein yield, MPL=liver microsomal protein yield, CPL=liver cytosolic protein yield, VmaxLPS=unscaled maximum rate of sulfation of phenol in liver, VmaxLPG=unscaled maximum rate of glucuronidation of phenol in intestine, KmLPS=Michaelis-Menten constant for sulfation of phenol in small intestine, VmaxLPG=unscaled maximum rate of glucuronidation of phenol in liver, KmLPS=Michaelis-Menten constant for sulfation of phenol in liver, KmLPG=Michaelis-Menten constant for glucuronidation of phenol in liver.



CHAPTER 4

Integrating in vitro data and physiologically based kinetic (PBK) modelling to assess the in vivo potential developmental toxicity of a series of phenols

**Marije Strikwold, Bert Spengelink, Laura HJ de Haan, Ruud A Woutersen, Ans Punt,
Ivonne MCM Rietjens
Submitted for publication**

ABSTRACT

In vitro derived toxicity outcomes do not always reflect in vivo toxicity values, which was previously observed for a series of phenols tested in the embryonic stem cell test (EST). Translation of in vitro data to the in vivo situation is therefore an important, but still limiting step for the use of in vitro toxicity outcomes in the safety assessment of chemicals. The aim of the present study was to translate in vitro embryotoxicity data for a series of phenols to in vivo developmental toxic potency values for the rat by physiologically based kinetic (PBK) modelling based reverse dosimetry. To this purpose, PBK models were developed for each of the phenols. The models were parameterised with in vitro derived values defining metabolism and transport of the compounds across the intestinal and placental barrier, and with in silico predictions and data from the literature. Using PBK-based reverse dosimetry, in vitro concentration-response curves from the EST were translated into in vivo dose-response curves from which points of departure (PoDs) were derived. The predicted PoDs differed less than 3.8-fold from PoDs derived from in vivo toxicity data for the phenols available in the literature. Moreover, the in vitro PBK-based reverse dosimetry approach could overcome the large disparity that was observed previously between the in vitro and the in vivo relative potency of the series of phenols. In conclusion, this study shows another proof-of-principle that the in vitro PBK approach is a promising strategy for non-animal based safety assessment of chemicals.

INTRODUCTION

The safety evaluation of chemicals is currently evolving from using animal toxicity tests towards the application of innovative non-animal based *in vitro* approaches to predict toxicity. This development is encouraged by initiatives such as the European Registration, Evaluation, Authorisation and restriction of Chemicals (REACH) (EC 2007), the Cosmetic Products Regulation (EC 2009) as well as the US National Research Council report on toxicity testing in the 21st century (National Research Council 2007). For many years, *in vitro* toxicity assays have been used for hazard identification only, including for example the detection of genotoxicity, and the ranking and prioritisation of compounds for further *in vivo* toxicity testing (Gülden and Seibert 2005). Translation of *in vitro* data to the *in vivo* situation is an important but limiting step for the use of *in vitro* outcomes in the regulatory risk assessment of chemicals, as *in vitro* derived toxicity outcomes as such do not always reflect *in vivo* toxicity values (Blauboer 2010; Punt et al. 2011). For example, in our study on the embryotoxic potencies of a series of phenols evaluated *in vitro* with the ES-D3 differentiation assay of the embryonic stem cell test (EST), it was concluded that the assay did not correctly rank the phenols according to their *in vivo* potency (Strikwold et al. 2012). Especially the toxicity of p-heptyloxyphenol was relatively higher in the EST than reported in *in vivo* studies in the literature as compared to the other phenols tested. In the EST p-heptyloxyphenol displayed a BMC₅₀ that was more than 3 orders of magnitude lower than that of phenol whereas *in vivo* BMD₁₀ values differed less than 3-fold (Strikwold et al. 2012). Kinetic differences between the *in vitro* and *in vivo* situation were hypothesised to provide a reason for the observed disparities (Strikwold et al. 2012).

Combining *in vitro* toxicity data with physiologically based kinetic (PBK) modelling applying reverse dosimetry has recently been shown to provide a promising approach to extrapolate *in vitro* concentration-response curves to *in vivo* dose-response curves from which points of departure (PoDs) for the risk assessment of chemicals can be derived (Louisse et al. 2010; Louisse et al. 2014; Strikwold et al. 2013). In this way kinetic differences between the *in vitro* and *in vivo* situation can be taken into account and *in vivo* dose-response curves suitable for deriving a PoD for risk assessment can be obtained based on *in vitro* data. However, as PBK models are generally data intense and their development often time consuming (Loizou and Hogg 2011), their application is often hampered. Applying *in silico* predictions, i.e. Quantitative Structure-Activity Relationships (QSARs) and *in vitro* kinetic experiments may aid the development of PBK models by predicting input values for kinetic parameters required, thereby also facilitating non-animal based safety assessment of chemicals.

For phenol, one of the congeners tested in our previous *in vitro* study on the embryotoxic potency of a series of phenols (Strikwold et al. 2012), *in vitro* PBK-based reverse dosimetry and subsequently dose-response modelling, provided a PoD that appeared to match the

range of in vivo derived PoDs (Strikwold et al. 2013). The aim of the present study was to translate in vitro embryotoxicity data for a series of phenols including p-heptyloxyphenol as previously obtained with the EST (Strikwold et al. 2012), to in vivo developmental toxicity values for the rat by PBK-based reverse dosimetry, using in silico and in vitro defined kinetic parameters. Ultimately, this should elucidate whether combining in vitro data with PBK modelling to predict in vivo values, can overcome differences that were observed between the in vitro and the in vivo relative potencies of different phenolic congeners, and especially whether this approach can overcome the deviating results for p-heptyloxyphenol. This may provide another proof-of-principle to assess the feasibility of this in vitro PBK approach for prospective toxicological safety evaluations of chemicals.

MATERIALS AND METHODS

COMPOUNDS AND MATERIALS

Phenol (99%), p-fluorophenol (99%), p-heptyloxyphenol (97%), p-methylketophenol (99%), antipyrine ($\geq 99\%$), fluorescein, Tris(hydroxymethyl)aminomethane (Tris) ($\geq 99.9\%$) and Dulbecco's Modified Eagle's medium (DMEM), uridine 5'-diphosphoglucuronic acid (UDPGA), alamethicin (98%), sodium taurocholate hydrate (97%), β -glucuronidase (Type 1x-A from *Escherichia coli*) and bovine serum albumin ($\geq 98\%$) were obtained from Sigma Aldrich (Steinheim, Germany). Acetonitrile (ULC/MS grade) and methanol (HPLC supra-gradient) were obtained from BioSolve (Valkenswaard, The Netherlands), dimethylsulfoxide (DMSO) ($\geq 99\%$) from Acros Organics (Geel, Belgium). Trifluoroacetic acid (TFA), hydrochloric acid (37%), magnesium chloride hexahydrate, potassium phosphate ($\geq 99\%$) and Transwell® inserts (0.4 μm pored polycarbonate membrane, 12 mm diameter) were purchased from VWR International GmbH (Darmstadt, Germany). Foetal calf serum (FCS) was purchased from HyClone-Perbio (Etten-Leur, The Netherlands). Penicillin, streptomycin, L-glutamine, minimal essential medium non-essential amino acids and trypsin / EDTA in PBS (final concentration 0.025% / 0.01%) were obtained from Gibco (Paisley, Scotland). Phosphate buffered saline (PBS), and Hank's balanced salt solution (HBSS), were obtained from Invitrogen (Breda, The Netherlands) and HEPES was from VWR (Radnor, USA).

BeWo choriocarcinoma cells subclone b30 were kindly provided by the Institute of Public Health of the Faculty of Health Sciences of the University of Copenhagen (Denmark) with permission from Dr. Alan Schwartz (Washington University, St Louis, MO). The provided cell line was confirmed to be mycoplasma negative. The colorectal adenocarcinoma (Caco-2) cells were obtained from ATCC (Middlesex, UK). Pooled liver microsomes from male Sprague-Dawley rats were obtained from BD Biosciences Gentest (Woburn, MA, USA).

GENERAL OUTLINE IN VITRO PBK APPROACH

The in vitro PBK approach to predict in vivo dose-response curves and a PoD for risk assessment using in vitro embryotoxicity data consisted of the following steps: (i) establishment of in vitro effective concentrations (EC_x) of the phenols in the EST, (ii) development of PBK models describing in vivo kinetic properties of the phenols in rat including derivation of PBK model parameters, (iii) sensitivity analysis of the PBK models, (iv) translation of in vitro EC_x values into in vivo external dose levels (ED_x) generating dose-response curves for developmental toxicity in rat and enabling the definition of a PoD for risk assessment and (v) evaluation of predictions performed with the in vitro PBK approach.

IN VITRO EMBRYOTOXICITY

Embryotoxicity data of phenol, p-fluorophenol, p-heptyloxyphenol and p-methylketophenol determined using the murine embryonic stem cell (ES-D3) differentiation assay of the EST by Strikwold et al. (2012), were used as a starting point for the in vitro PBK approach translating in vitro embryotoxicity data to in vivo toxicity values. The use of both the maximum concentration in foetal plasma (C_{max}) and the Area Under the foetal plasma concentration-time Curve (AUC) in the in vitro PBK approach was evaluated. The concentration of phenol and p-fluorophenol decreased in time in the EST culture medium (without cells) in a similar fashion, while p-methylketophenol and p-heptyloxyphenol were stable (Strikwold et al. 2012). Therefore, the AUC of the 10 day EST of p-methylketophenol and p-heptyloxyphenol was calculated by multiplying the test concentration by the duration of the experiment (AUC_{0-10d}), while the calculated AUC_{0-10d} for phenol and p-fluorophenol was reduced by 39% corresponding to the loss of phenol in the EST as reported by Strikwold et al. (2013).

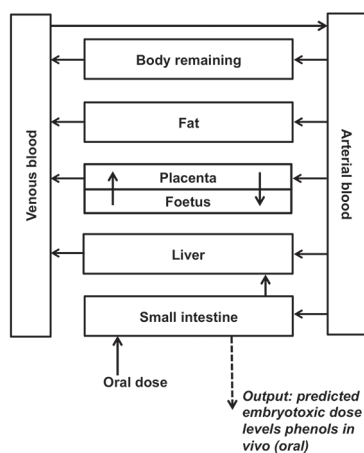


Figure 1 Schematic representation of the PBK models of the phenols.

RAT PBK MODEL STRUCTURES FOR PHENOLS

The rat PBK model for phenol developed by Strikwold et al. (2013) was used as a starting point to construct rat PBK models for the different phenols of the present study (Figure 1), with four major modifications. The first modification is that only liver glucuronidation of the phenolic compounds was taken into account in the present study to describe the metabolic conversions. This could be done because the sensitivity analysis of the previously developed PBK model of phenol by Strikwold et al. (2013), performed at an oral dose level of 150 mg/kg bw which is consistent with high oral dose levels that were applied in *in vivo* toxicity studies of the phenols (Kavlock 1990), identified that glucuronidation of phenol in the liver is the most influential metabolic pathway in the model. Moreover, *in vivo* kinetic studies towards the metabolism of phenol confirm the importance of this route, showing that the glucuronide conjugate is the predominant metabolite formed at high oral dose levels (Hiser et al. 1994). Furthermore, the metabolic parameters K_m and V_{max} of sulfation were not identified as a sensitive parameter in the PBK model for phenol at high oral dose levels and the V_{max} value for sulfation was very low (Strikwold et al. 2013), supporting the choice for glucuronidation as the metabolic and elimination pathway in the current PBK models. A second modification is that we have included *in vitro* transport experiments with Caco-2 cells to define the oral uptake constants of the different compounds of the present study, since the previously predicted plasma concentrations of phenol appeared to be quite sensitive to the oral absorption coefficient (k_a). A third modification is that a fat compartment was included in the PBK models for the different phenolic compounds, because p-heptyloxyphenol may readily be distributed to adipose tissue due to its relatively high lipophilicity. Finally, a placental/foetal compartment was added to the PBK models, including transport of the compound from the mother to the embryos/foetuses and back by simple diffusion. For the placental/foetal compartment, the number of embryos in one litter was considered to be 12 and they were treated as one unit for which the physiological parameters were calculated. Foetal-maternal diffusion was set equal to maternal-foetal diffusion. To include maternal-foetal diffusion in the PBK model, apparent permeability coefficients (P_{app}) across placental BeWo cells cultivated in a transwell system were derived *in vitro* and subsequently converted to *in vivo* diffusion transplacental clearance rates (l/h) (see section *In vitro* placental transport study). The PBK models were defined with parameters representative for gestational day 11 (GD11), facilitating evaluation of the PBK model predictions with available *in vivo* developmental toxicity data for rats exposed to phenol or p-substituted phenol at GD11.

An overview of the PBK model algorithms, which are similar for all the phenols, is included in Supplementary data A. Kinetic model calculations were performed by applying Rosenbrock's algorithms for solving stiff systems (Berkeley Madonna, version 8.3.18, UC Berkeley, CA, USA).

PBK MODEL PARAMETER VALUES

Physiological parameters

In the PBK models, organ weights of the pregnant rat were kept equal to values of a non-pregnant rat and placental and foetal weights were additionally included. The fractions of blood flow to the organs were set equal to that of the non-pregnant rat as well, although the fraction of blood flow to the compartment 'body remaining' was reduced to accommodate for the added blood flow to the placental/foetal compartment, with the total fraction not exceeding 1. Most physiological parameters were taken from Brown et al. (1997). The fraction of blood flow to the small intestine was calculated using reported blood flow rates for the specific parts of the splanchnic system by Delp et al. (1998). The volume of the placentas, the foetuses and the blood flow to the placentas were estimated by the algorithms of O'Flaherty et al. (1992). The volume of the foetuses included also the amniotic fluid volume of GD11 that was reported by Park and Shepard (1994) and Fisher (1993), because at this gestational day maternal-foetal exchange occurs via both the chorioallantoic placenta and the yolk sac placenta (Carney et al. 2004). All physiological parameters are presented in Table 1.

Table 1 Physiological data for the rat applied in the PBK models of the phenols.

Parameter	Percentage of body weight ^a	Percentage of cardiac output
Model compartments		
small intestine	1.4	7.5
liver	3.4	17.5 ^b
adipose tissue	7.0	7.0
arterial blood	1.85	
venous blood	5.55	
placentas		0.34
body remaining	71.8	67.66
Weight placentas (kg)	0.00079	
Weight foetuses and amniotic fluid (kg)	0.00034	
	(l/h/kg bw ^{0.74})	
Cardiac output	15	

^a Organ percentages of body weight without placenta and foetal compartment are reported because they were kept similar to non-pregnant rat values. The (weight of the) foetal-placental compartment is added separately. See text for more details.

^b Without flow from small intestine.

In silico predictions of physico-chemical and biochemical parameters

An overview of physico-chemical parameters that are used to predict biochemical and distribution parameters of the compounds are included in Table 2. Tissue plasma partition coefficients (Pt:p) were calculated using the algorithm of Berezhkovskiy (2004), which requires information on plasma protein binding, lipophilicity and acid-base properties (see Tables 2 and 3). The adipose tissue-plasma partition coefficients were calculated using the olive oil-water distribution coefficient ($D^*vo:w_{pH7.4}$) and the partition coefficients for the non-adipose tissues were calculated with the n-octanol-water partition coefficient (Pow) for the non-ionised species at pH 7.4. The value of $D^*vo:w_{pH7.4}$ was calculated using $\log Po:w$ and pKa according to the algorithms reported by Poulin and Theil (2002). The unbound fraction of the compound in plasma was calculated with the Simcyp model (Simcyp 2015), after which these values were converted to the unbound fraction in tissue using the algorithm of Poulin and Theil (2002). The Pt:p values of the placental compartment were set equal to the predicted liver:plasma partition coefficient and the Pt:p of the embryonic/foetal unit was a volume weighted whole body:plasma partition coefficient, in which the adipose tissue was omitted because of the low amount of fat in foetal rat (Sarr et al. 2012). Partitioning of the compounds between red blood cells and plasma (Prbc:p) was predicted with the algorithms of Paixão et al. (2009), and was subsequently used to calculate the partition coefficient of the compounds between blood and plasma (Pb:p) using the following equation:

$$Pb:p = (Prbc:p * HTC) + (1 - HTC)$$

where HTC corresponds to a hematocrit fraction of 0.45.

Table 2 Physico-chemical properties of the phenols.

Parameter	phenol	p-fluoro	p-heptyloxy	p-methylketo
MW (Da) ^a	94.11	112.10	208.30	136.15
Log Po:w ^a	1.54	1.84	4.41	1.40
pKa ^a	9.86	9.92	10.35	8.12
% ionised in serum (pH 7.4) ^b	0	0	0	16

^a Values from ACD/Labs (2015).

^b Calculated with Simcyp model (Simcyp 2015).

Table 3 In silico predicted biochemical and distribution parameters of the phenols for the rat.

Parameter	phenol	p-fluoro	p-heptyloxy	p-methylketo
Fu plasma (pH 7.4) (-) ^a	0.38	0.31	0.03	0.28
Partition coefficients ^b				
liver:plasma	0.81	0.96	7.99	0.64
intestine:plasma	0.97	1.20	11.57	0.74
adipose:plasma	0.83	1.42	84.38	0.39
placenta:plasma ^c	0.81	0.96	7.99	0.64
foetus:foetal plasma ^d	0.76	0.89	6.92	0.61
body remaining:plasma	0.75	0.87	6.67	0.61
blood:plasma ^e	0.72	0.70	1.48	0.67

^a Fraction unbound to plasma proteins (Fu). Calculated with Simcyp model (Simcyp 2015).

^b Calculated with algorithms of Berezhkovskiy (2004).

^c Assumed to be the same as the partition coefficient of the liver.

^d Whole body:plasma partition coefficient without adipose tissue (volume weighted).

^e Calculated with algorithms of Paixão et al. (2009).

In vitro intestinal transport study

Caco-2 cells (passages 37-40) were cultured in DMEM containing 25 mM HEPES (pH 7.4) supplemented with 10% (v/v) heat-inactivated FCS, 4500 mg/l glucose, 2 mM L-glutamine, 1% (v/v) minimal essential medium nonessential amino acids, 10,000 U/ml penicillin and 10 mg/ml streptomycin and maintained in polystyrene cell culture flasks (Corning, Amsterdam The Netherlands) in a 5% CO₂-humidified atmosphere at 37 °C. Cells were harvested after exposure to a trypsin-EDTA solution. Next, the cells were seeded onto Transwell® inserts (0.4 µm pored polycarbonate membrane, 12 mm diameter), at a density of 10⁵ cells/cm². Cell culture medium (0.5 ml and 1.5 ml in the apical and basolateral compartment, respectively), was changed every two days.

Compounds that were included in the transport experiments were phenol, p-fluorophenol, p-heptyloxyphenol, p-methylketophenol, antipyrine (passive transcellular control) and fluorescein (passive paracellular control) as well DMSO (solvent control). Stock solutions of the test compounds were prepared in DMSO, and tested at a final DMSO level in the transport buffer of 0.2%, except for p-heptyloxyphenol for which the final DMSO level was 0.5% due to the relatively lower solubility of this compound.

Transport experiments were performed between day 20 and 23 post-seeding. Prior to the transport experiments, the cell culture medium was removed and cells were equilibrated in HBSS for 30-45 min in a 5% CO₂-humidified atmosphere at 37 °C. In these 45 min, the integrity of the cell monolayer was examined by measuring the Trans Epithelial Electrical Resistance (TEER) of the cell layer using a Millicell ERS-2 Volt-Ohm Meter (Millipore, USA). Only cell layers with a TEER value between 500-1000 Ω.cm² were used for the transport experiments. The transport buffer for the apical compartment consisted of HBSS containing

10 mM HEPES (pH 6.5) and 10 mM sodium taurocholate and the transport buffer for the basolateral compartment consisted of HBSS (pH 7.4) with 30 mg/ml bovine serum albumin. At first, 1.5 ml pre-warmed (37 °C) transport buffer was added to the basolateral compartment. Then, the transport experiments were started by adding 0.5 ml pre-warmed transport buffer containing the test compound (100 µM) to the apical compartment. After 60 min incubation in a 5% CO₂-humidified atmosphere at 37 °C, a 75 µl sample was taken from the basolateral compartment and then from the apical compartment. Each sample was added to 150 µl ice-cold methanol, vortexed and put on ice immediately. The filters of the Transwell® inserts were washed one time with HBSS and two times with PBS, then cut out from the insert and added to 250 µl methanol 65% (v/v) and sonicated for 15 min by a Bandelin Sonorex RK100 sonicator (Berlin, Germany). Samples were analysed by UPLC-PDA (see section Quantification of analytes) for the presence of the test compound and possible metabolites.

TEER values were also measured at the end of the transport experiment, during the first washing step and compared to the TEER values measured before the transport experiment in order to assess toxicity of the test compound to the cell monolayer. Caco-2 monolayers were omitted from further analysis when the TEER value was reduced more than 15% during the transport experiments (Wang et al. 2014). The Caco-2 transport studies encompassed four independently performed experiments including three replicates in each assay.

The apparent permeability coefficients (P_{app}) (cm/s) were calculated using the following algorithm:

$$P_{app} = \frac{\frac{\Delta Q}{\Delta t}}{A * C_0}$$

where P_{app} is the apparent permeability coefficient (cm/s), $\Delta Q/\Delta t$ (nmol/s) is the amount of the test compound transported to the receiver chamber in a certain time period, A is the transwell membrane surface area (cm²) and C_0 is the initial concentration of the test compound in the donor compartment (µM).

In order to assess the validity of the P_{app} calculations for this experiment, the linearity of transport from the apical to the basolateral side was verified by taking samples from the basolateral side at $t=15, 30, 60$ and 90 min, at a test concentration of 100 µM. The amount of sample (50 µl) withdrawn from the basolateral side was replaced by a similar amount of Caco-2 transport medium, which was accounted for in assessing the linearity. The recovery of the test compound in each transport experiment was calculated with a mass balance equation, taking into account the amount of the test compound in the apical and basolateral compartment and the amount in the cells and/or filter of the Transwell® insert.

To extrapolate the in vitro derived apparent permeability coefficients (P_{app}) from the Caco-2 transport experiments to in vivo oral absorption coefficients (k_a), relative P_{app} ratios were calculated with phenol as the standard compound (P_{app} p-substituted phenol / P_{app} phenol), which were subsequently multiplied by the k_a value for phenol of 7.62/h obtained from the rat in situ intestinal perfusion study of Humphrey et al. (1980).

In vitro placental transport study

BeWo cells (passages 28-31) were cultured in DMEM with 4500 mg/ml glucose and supplemented with 10% (v/v) heat-inactivated FCS, 2 mM L-glutamine, 10,000 U/ml penicillin and 10 mg/ml streptomycin and maintained in polystyrene cell culture flasks (Corning, Amsterdam The Netherlands) in a 5% CO₂-humidified atmosphere at 37 °C. Cells were harvested after exposure to a trypsin-EDTA solution. Next, the cells were seeded onto Transwell® inserts (0.4 µm pored polycarbonate membrane, 12 mm diameter), with a density of 10⁵ cells/cm². Cell culture medium (0.5 ml and 1.5 ml in the apical and basolateral compartment, respectively) was changed daily.

Transport experiments were performed 6 days post-seeding. The transport buffer consisted of HBSS with 30 mg/ml bovine serum albumin (apical compartment) and 10 mg/ml bovine serum albumin (basolateral compartment) representing mid and late gestational maternal and embryonic/foetal rat plasma albumin levels, respectively (Honda et al. 2008; McMullin et al. 2008; Yeoh and Morgan 1974). The transport experiments were performed for the same compounds and according to the same method as described for the Caco-2 transport experiments, except that only cell layers with a TEER value > 190 Ω·cm² were used for the transport experiments. The BeWo transport studies encompassed four independently performed experiments including two replicates in each assay. Samples were analysed by UPLC-PDA (see section Quantification of analytes) for the presence of the test compound and possible metabolites. The apparent permeability coefficients were calculated using the same method as described for the Caco-2 transport experiments.

To extrapolate the in vitro derived apparent permeability coefficients (P_{app}) obtained from the BeWo transport experiments to in vivo transplacental clearance rates (CLPL), relative P_{app} ratios were calculated with antipyrine as the standard compound (P_{app} (p-substituted) phenol / P_{app} antipyrine) which were subsequently multiplied by the transplacental maternal-foetal antipyrine clearance rate of 0.18 l/h. This antipyrine clearance rate was obtained by converting the reported antipyrine transplacental clearance value of 0.448 l/h/kg for the rat at GD20 (Varma and Ramakrishnan (1985) to a value for GD11 via allometric scaling to maternal body weight (O'Flaherty et al. 1992) using a maternal body weight for GD11 reported by Buelke-Sam et al. (1982).

In vitro assays for glucuronidation of phenols by rat tissue

The formation of glucuronide metabolites of the p-substituted phenols was investigated in incubations with rat liver microsomes. Incubation mixtures consisted of 50 mM Tris-HCl (pH 7.4) and 10 mM MgCl₂, containing (final concentrations) rat liver microsomes (0.2 mg protein/ml) and 2 mM UDPGA. To obtain maximum glucuronidation activity, the microsomes were activated by preincubating the incubation mixture with 0.025 mg/ml alamethicin added from a 200 times concentrated stock solution in methanol, during 15 min on ice (Fisher et al. 2000). Subsequently, the incubations were started after a 1-min preincubation at 37 °C by addition of the substrate from a 200 times concentrated stock solution in DMSO and incubated in a shaking water bath at 37 °C for 45 min. The reactions were terminated by addition of ice-cold acetonitrile (20% v/v). In the blank incubation mixtures, UDPGA was omitted. Samples were analysed by UPLC-PDA (see section Quantification of analytes). No reference standards of the glucuronide metabolites were commercially available. Hence, the metabolites were identified as follows. At first, retention times from the UPLC-PDA chromatograms of the parent compound of the blank incubation were compared with the retention times of newly appearing peaks in chromatograms of the incubation mixtures, as the glucuronide conjugates are expected to elute earlier compared with their parent compounds due to their increased hydrophilicity. Secondly, the formation of the suggested glucuronide conjugate was confirmed by enzymatic deglucuronidation with β -glucuronidase. To this purpose a volume of 10 μ l of the incubation mixture of the glucuronidation assay (that was not terminated by the addition of ice-cold acetonitrile) was added to 90 μ l of 200 mM potassium phosphate (pH 6.2). Then, 4 μ l of glucuronidase (200 units/ml) was added and the mixtures were incubated for 60 min in a shaking water bath at 37 °C. The reactions were terminated by addition of ice-cold acetonitrile (20% v/v) and were put on ice. Control samples were treated under the same conditions, but without glucuronidase.

After identifying the formation of the glucuronide conjugates for the p-substituted phenols, incubations with rat liver microsomes were performed to quantify kinetic parameters, which are the maximum enzyme reaction rate (V_{max}) and the Michaelis-Menten constant (K_m). The conditions of the incubation assays were optimised to obtain linear reaction rates with respect to incubation time and protein concentration and non-limiting cofactor levels were applied. The optimised incubation mixtures consisted of 50 mM Tris-HCl (pH 7.4) with 10 mM MgCl₂, containing (final concentrations) 10 mM UDPGA and 0.1, 0.01 and 0.05 mg microsomal protein/ml for p-fluorophenol, p-heptyloxyphenol, and p-methylketophenol, respectively. To obtain maximum glucuronidation activity, the microsomes were activated by preincubating the incubation mixture with 0.025 mg/ml alamethicin added from a 200 times concentrated stock solution in methanol, during 15 min on ice (Fisher et al. 2000). Subsequently, the incubations were started after a 1-min preincubation at 37 °C by addition of the substrate from a 200 times concentrated stock solution in DMSO and incubated in a shaking water

bath of 37°C for 10 min for p-fluorophenol and 2.5 min for p-heptyloxyphenol and p-methylketophenol, respectively. The incubation experiments encompassed three or four independently performed experiments for each phenol.

Kinetic constants for the glucuronidation of the p-substituted phenols were derived by fitting the data to the standard Michaelis-Menten equation;

$$v = \frac{V_{max} * [S]}{K_m + [S]}$$

in which [S] represents the substrate concentration, V_{max} the maximum velocity and K_m the Michaelis-Menten constant for the formation of the glucuronide metabolites. Data analysis was accomplished using GraphPad Prism 5.0 software (GraphPad, San Diego, CA, USA). For the PBK model, the in vitro derived V_{max} values from rat liver microsomes were scaled to the in vivo situation using a reported microsomal protein yield of 38 mg/g rat liver (Chiu and Ginsberg 2011). The in vivo K_m value was assumed to be the same to the in vitro K_m value. Michaelis-Menten constants for phenol were taken from our previous study (Strikwold et al. 2013). The present study assumed unrestricted metabolism despite the high plasma protein binding of p-heptyloxyphenol, because the rapid metabolic turnover is assumed to clear the chemical so avidly that protein binding may not be rate limiting.

QUANTIFICATION OF ANALYTES

Samples from the BeWo and Caco-2 transport experiments were centrifuged at 13,000 rpm at 5°C for 15 min. Next 7.5 µl of the supernatant of each sample was analysed by UPLC (Waters Acquity). Samples from the glucuronidation assays were centrifuged at 15,000 rpm at 5°C for 5 min. Subsequently, 3.5 µl of the supernatant of each sample was analysed by UPLC, except for the incubations with p-heptyloxyphenol of which 10 µl was analysed by UPLC. All samples, except those from transport studies with fluorescein, were analysed on a Waters BEH C18 1.7 µm column, 2.1 x 50 mm, with nanopure water (0.1% TFA) (A) and pure acetonitrile (B) applying a gradient elution. The start condition was 100:0 (A:B), changing to 90:10 from 1 to 2 min, then to 10:90 from 2 to 4 min (or from 2 to 3 min when analysing samples for p-heptyloxyphenylglucuronide), remaining at this ratio for 0.5 min and then rapidly declining to the start condition. The flow rate was 0.6 ml/min. Peaks of the analytes were detected with a photodiode array detector (PDA, Waters). Analytes, except the glucuronide metabolites, were quantified with a linear calibration curve using peak areas obtained at the compounds' maximum wavelength. The glucuronide metabolites were, due to the absence of commercially available reference compounds, quantified with the calibration curve and at maximum wavelengths of their parent compound. Differences in the UV absorbance between the parent and the glucuronide conjugate at the selected wavelength

were quantified by comparing the peak areas of the parent compound from three different concentrations of the calibration curve with the peak areas of corresponding concentrations of the glucuronide conjugate, which were obtained from a complete glucuronidation of the parent compound in a glucuronidation experiment of 2 h. A noticeable difference between the peak area of the parent compounds and the glucuronide (average of three tested concentrations) was only observed for p-fluorophenol (absorbance of conjugate was 2-fold lower compared to the parent) and this difference was used to correct the measured absorbance of the parent compound from each point of the calibration curve. Fluorescein was quantified with a fluorescence SpectraMax M3 microplate reader (Molecular Devices, USA) with excitation and emission at 495 and 538 nm, respectively.

SENSITIVITY ANALYSES OF THE PBK MODELS

For each PBK model a local sensitivity analysis was performed to determine influential parameters. To this purpose, each parameter was changed in turn keeping the other ones constant (Chiu et al. 2007). The normalised sensitivity coefficient (SC) was calculated using the algorithm:

$$SC = \frac{(C' - C)}{(P' - P)} * \left(\frac{P}{C}\right)$$

where C is the initial outcome of the model, which in this case is the maximum foetal plasma concentration (C_{max}). C' is the output of the model after a 1% parameter change. P is the initial parameter value and P' is the parameter value modified by an increase of 1%. The sensitivity analysis was conducted for an oral exposure to a single dose of 2 and 200 mg/kg bw.

TRANSLATION OF IN VITRO EFFECT CONCENTRATIONS IN THE EST TO IN VIVO EFFECT CONCENTRATIONS

In vitro concentration-response data obtained with the EST were translated to in vivo dose-response values by applying PBK-based reverse modelling, performed as described by Strikwold et al. (2013) with some modifications. To correct for in vivo and in vitro differences in albumin and fat levels, each nominal in vitro effect concentration of p-heptyloxyphenol obtained from the EST from Strikwold et al. (2012) was translated to an in vivo effect concentration (EC_x) according to the extrapolation rules of Glden and Seibert (2003). In the extrapolation rule, a value of 0.99 was used for the fraction of p-heptyloxyphenol bound to albumin in the EST, which was obtained from a reported bound fraction of p-heptyloxyphenol in the culture medium of the whole embryo culture (WEC) assay (Fisher et al. 1993). In vivo albumin and fat levels that are used in the extrapolation rules were adjusted to values that correspond to embryos/foetuses during mid/late gestation. An in vivo lipid content of 0.11%

was applied based on foetal rat data (GD17) presented by Johansson (1983). An in vivo embryonic/foetal albumin level of 10 mg/ml was used representing albumin levels in mid and late gestation; GD10 (Yeoh and Morgan, 1974) and GD18 (Mcmullin et al. 2008). The vitro lipid fraction and albumin levels resembling the situation in the EST were 0.04% and 4.8 mg/ml, respectively (Verwei et al. 2006). For the other phenols, no correction according the extrapolation rules of Gülden and Seibert (2003) was applied, since it was found that in vitro cytotoxicity of phenol tested with the fibroblast-like embryonic mouse cell line Balb/c 3T3 clone A31 was not affected by differences in bovine serum albumin levels reflecting the in vitro and in vivo situation. It is assumed that this also applies for p-methylketophenol and p-fluorophenol as these compounds have a comparable log Po:w value as phenol, which is an important factor in albumin binding (Endo and Goss 2011).

Next, the maximum foetal plasma concentrations (C_{max}) in the PBK model were set equal to the effect concentrations from the EST (which was corrected by the extrapolation rule of Gülden and Seibert (2003) in case of p-heptyloxyphenol). In addition, the foetal plasma AUC in the PBK model were set equal to the AUC_{0-10d} from the EST. Applying in vitro PBK-based reverse dosimetry, provided in vivo effective dose levels (ED_x) from which an in vivo dose-response curve and a $BMDL_{05}$ was derived using the Environmental Protection Agency's (EPA) Benchmark Dose Software (BMDS) version 2.6. For each compound, the benchmark dose model selected was the one that provided the best fit determined as described by Strikwold et al. (2012).

EVALUATION OF THE DATA

The $BMDL_{05}$ predicted with the in vitro PBK approach were compared to the $BMDL_{05}$ (or NOAEL) derived from an in literature reported in vivo developmental toxicity study with rats that received phenol or p-substituted phenol at GD11 Kavlock (1990). The $BMDL_{05}$ values of the in vivo study were derived using the BMDS version 2.6. For each compound, the benchmark dose model was selected that provided the best fit as described by Strikwold et al. (2012). In addition, potency ratios were calculated (potency phenol / potency p-substituted phenol) from potency data obtained with the in vitro PBK approach ($BMDL_{05}$), and the in vivo developmental toxicity data (most critical in vivo endpoint) from Kavlock (1990) ($BMDL_{05}$ or NOAEL).

RESULTS

IN VITRO EMBRYOTOXICITY

Phenol and the p-substituted phenols showed a concentration-response related inhibition of differentiation of ES-D3 cells into beating cardiomyocytes in the EST (Figure 2) identifying the embryotoxic potential of the different compounds (Strikwold et al. 2012). The highest difference

in embryotoxic potential *in vitro* was observed between phenol and p-heptyloxyphenol, with the BMC₅₀ value being three orders of magnitude higher for phenol. The differences in BMC₅₀ values were much lower between phenol and the other p-substituted phenols, including p-fluorophenol and p-methylketophenol, namely 1.9-fold and 4.9-fold, respectively (Strikwold et al. 2012).

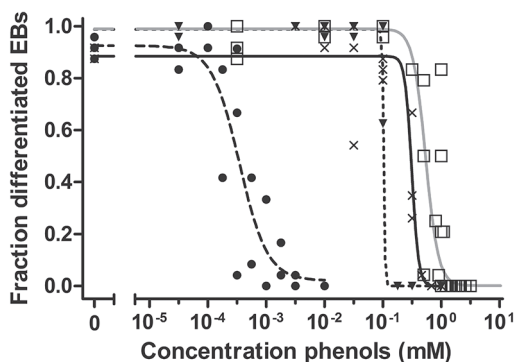


Figure 2 Concentration-response curves for phenol (grey line, □), p-fluorophenol (solid line, ×), p-heptyloxyphenol (dashed line, ●) and p-methylketophenol (dotted line, ▼) representing the inhibition of differentiation of the embryoid bodies (EBs) by the compound. Data obtained from Strikwold et al. (2012).

IN SILICO PREDICTIONS OF BIOCHEMICAL AND DISTRIBUTION PBK MODEL PARAMETERS

Physico-chemical parameters that are used for the prediction of PBK model parameters are outlined in Table 2 and the predicted biochemical and distribution model parameters are presented in Table 3. Notable differences between the compounds are the relatively high log Po:w value of 4.41 for p-heptyloxyphenol compared to log Po:w values < 1.84 for the other phenols. The tissue:plasma partition coefficients of p-heptyloxyphenol are substantially higher than those for the other phenols, especially the fat:plasma partition coefficient which is 84.4 for p-heptyloxyphenol and varies between 0.39-1.42 for the other phenols. The predicted fraction of phenols unbound to plasma albumin differs from 0.03 for p-heptyloxyphenol to 0.38 for phenol.

IN VITRO INTESTINAL TRANSPORT STUDY

Each phenol tested in the Caco-2 transport experiment showed a linear increase of the test concentration in the basal compartment for at least 60 min. The P_{app} values of the Caco-2 experiments are presented in Table 4. Transport of each of the test compounds is rapid, and the P_{app} values differ at maximum only 1.3-fold between the test compounds, ranging from

51.9 10^{-6} cm/s for p-methylketophenol to 40.2 10^{-6} cm/s for p-heptyloxyphenol. The average mass recovery of antipyrine was 93.4%. The mass recovery of phenol, p-fluorophenol, p-heptyloxyphenol and p-methylketophenol was on average 80.2%, 78.2% 70.4% and 82.1%, respectively.

Table 4 Mean apparent permeability ($P_{app} \pm SD$) obtained from Caco-2 and BeWo transport assays, predicted intestinal oral absorption coefficients (k_a) and predicted rat transplacental clearance values (CLPL) for the test compounds.

Compound	P_{app_Caco-2} (10^{-6} cm/s)	k_a^a (/h)	P_{app_BeWo} (10^{-6} cm/s)	CLPL ^c (l/h)
phenol	48.4 \pm 8.6	7.62 ^b	41.6 \pm 3.4	0.19
p-fluorophenol	47.7 \pm 13.8	7.52	34.2 \pm 3.3	0.15
p-heptyloxyphenol	40.2 \pm 3.9	6.34	5.9 \pm 1.7	0.026
p-methylketophenol	51.9 \pm 6.6	8.18	27.5 \pm 1.7	0.12
antipyrine	42.7 \pm 2.6	6.73	40.4 \pm 3.2	0.18 ^d

^a Predicted oral absorption coefficient (see section Materials and methods).

^b Uptake rate from in situ intestinal perfusion study in rat (Humphrey et al. 1980).

^c Predicted rat transplacental clearance (see section Materials and methods).

^d Transplacental clearance value obtained from in vivo rat study (Varma and Ramakrishnan 1985). (see section Materials and methods).

IN VITRO PLACENTAL TRANSPORT STUDY

Each phenol tested in the BeWo transport experiment showed a linear increase in concentration in the basal compartment for at least 60 min, after addition of the test compound to the apical side (final concentrations apical compartment 100 and 500 μ M). The mass balances showed that > 90% of the mass of each compound was conserved in each transport experiment. The P_{app} values are presented in Table 4. Transport is rapid for each of the compounds, except for p-heptyloxyphenol which showed a P_{app} value of 5.9 10^{-6} cm/s, which is 6.8-fold lower than the P_{app} value of antipyrine. The P_{app} values for the other phenols were comparable to antipyrine, showing a 1.03-fold higher and 1.2- and 1.5-fold lower P_{app} value compared to the value of the reference compound antipyrine for phenol, p-fluorophenol and p-methylketophenol, respectively. The transport of the paracellular control fluorescein was on average 11-fold lower compared to the passive transcellular control antipyrine indicating the integrity of the monolayer.

An interesting observation was that the P_{app} value for p-heptyloxyphenol obtained from the BeWo experiment was 6.8-fold lower than the P_{app} value from the Caco-2 experiment, while the P_{app} values for the other phenols were less than 2-fold lower in the BeWo assay and the P_{app} value from the BeWo experiment for antipyrine was only 1.1-fold lower than the P_{app} from the Caco-2 experiment.

IN VITRO GLUCURONIDATION OF P-SUBSTITUTED PHENOLS BY RAT LIVER MICROSOMES

Results from the incubation experiments showed that rat liver microsomes were able to metabolise the p-substituted phenols to their glucuronide conjugates. Metabolism of the p-substituted phenols followed Michaelis-Menten kinetics (Figure 3). The apparent K_m and V_{max} values of the rat liver microsomes and the (scaled) catalytic efficiencies are presented in Table 5. The compound p-heptyloxyphenol was far more efficiently converted by liver microsomes than the other phenols. The scaled catalytic efficiency (l/h/g liver) for glucuronidation of p-heptyloxyphenol was 145-fold higher than that of phenol. The scaled catalytic efficiencies of p-fluorophenol and p-methylketophenol were respectively 1.7-fold and 6.0-fold higher than that of phenol.

Table 5 Kinetic constants K_m and $V_{max} \pm SD$, and catalytic efficiencies of the formation of the glucuronide metabolite of the phenols in rat liver microsomes.

Compound	$K_{m(app)}^a$	$V_{max(app)}^b$	Catalytic efficiency ^c	Scaled $V_{max(app)}^d$	Scaled catalytic efficiency ^e
phenol	465 ± 66	90 ± 4	0.19	205	0.44
p-fluorophenol	314 ± 16	101 ± 1.6	0.32	231	0.74
p-heptyloxyphenol	2.1 ± 0.6	60 ± 4.5	28.0	137	63.8
p-methylketophenol	138 ± 17	160 ± 4.4	1.16	365	2.65

^a μM .

^b nmol/min/mg microsomal protein.

^c V_{max}/K_m (ml/min/mg protein in rat liver microsomes).

^d $\mu mol/h/g$ liver.

^e l/h/g liver.

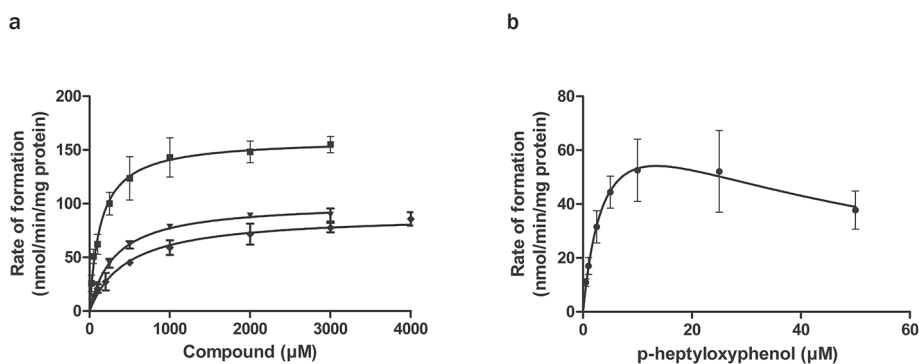


Figure 3 Concentration-dependent formation of the glucuronide conjugate of phenol (♦), p-fluorophenol (▼), p-methylketophenol (■) (panel a) and p-heptyloxyphenol (●) (panel b) in incubations with rat liver microsomes. Individual symbols represent mean activities of 3-4 independently performed experiments \pm SD.

SENSITIVITY ANALYSIS

The results of the sensitivity analysis performed at a high oral dose of 200 mg/kg bw (Figure 4) indicated that the most influential parameters for the phenol models are the volume of the liver, parameters related to glucuronidation in the liver (V_{max} , K_m and liver microsomal protein yield), the oral absorption coefficient, and the partition blood/plasma coefficient. The parameter K_m was of higher influence in the models of p-methylketophenol and p-heptyloxyphenol than in the other phenol models. In the model for p-heptyloxyphenol, parameters related to the intestine (volume intestine, flow to intestine and partition coefficient intestinal tissue:plasma) are more influential than in the models of the other phenols. Parameters related to the foetal/placental compartment do not highly influence the model outcome.

In general, the model outcomes are sensitive to similar parameters at a low oral dose of 2 mg/kg bw when compared to the analysis at 200 mg/kg bw. Parameters related to the intestine in the model for p-heptyloxyphenol are not of influence at a low dose of 2 mg/kg bw. Moreover, the values of sensitivity coefficients of the phenols for k_a , derived at a low dose of 2 mg/kg bw, are lower than the sensitivity coefficients derived at 200 mg/kg bw. The sensitivity coefficients for the microsomal protein content and the V_{max} for glucuronidation in the liver for p-fluorophenol, p-heptyloxyphenol and p-methylketophenol are lower than the sensitivity coefficients for these parameters derived at 200 mg/kg bw, while the sensitivity coefficients for phenol and p-fluorophenol for K_m are higher when compared to the sensitivity coefficients derived at 200 mg/kg bw.

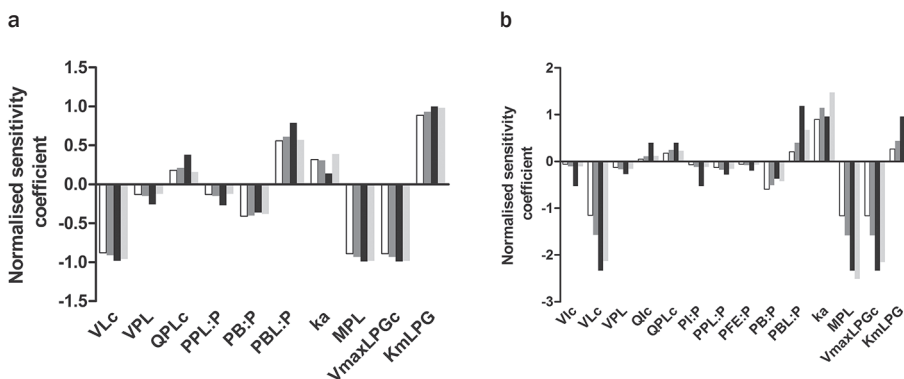


Figure 4 Normalised sensitivity coefficients for parameters of the PBK model for phenol (white bars), p-fluorophenol (dark grey bars), p-heptyloxyphenol (black bars) and p-methylketophenol (light grey bars) based on foetal C_{max} values from a single oral dose of 2.0 mg/kg bw (a) and 200 mg/kg bw (b). Normalised sensitivity coefficients ≥ 0.2 are presented. Vlc= fraction intestinal tissue, VLc=fraction liver tissue, VPL=volume placental tissue, Qlc=fraction intestinal flow, QPLc= fractional placental flow, Pl:P= partition coefficient intestine:plasma, PPL:P partition coefficient placenta:plasma, PFE:P=partition coefficient foetus:foetal plasma, PB:P=partition coefficient body remaining:plasma, PBL:P=partition coefficient blood:plasma, k_a =oral absorption coefficient, MPL=liver microsomal protein yield, $V_{max}LPGc$ =unscaled maximum rate of glucuronidation of phenols in liver, K_mLPG =Michaelis-Menten constant for glucuronidation of phenols in liver.

TRANSLATION OF IN VITRO-EFFECT CONCENTRATIONS IN THE EST TO IN VIVO DOSE LEVELS

In a first step the in vitro concentrations of p-heptyloxyphenol were converted to equivalent plasma concentrations using extrapolation rules of Gülden and Seibert (2003). Only a very small difference was observed between the in vitro effect concentrations from the EST and the estimated equivalent plasma concentrations, with the latter being 2.1-fold higher than the in vitro effect concentrations. In a second step, the in vivo effect concentrations were translated to external in vivo oral dose values using the PBK models thus defining a dose-response curve from which a PoD could be derived. The predicted dose-response curves based on C_{max} or the AUC_{0-10d} are presented in Figure 5. The $BMDL_{05}$ values for the phenols predicted by the in vitro PBK approach using C_{max} and the AUC_{0-10d} from the EST as a dose metric for reverse dosimetry are outlined in Table 6, together with the $BMDL_{05}$ values that were predicted from in vivo developmental toxicity data reported in literature. The in vivo experimental data and the PBK model based predictions were representative for exposure at GD11 since in the in vivo experimental study exposure was at GD11 and for the predictions the PBK model was defined using physiological parameters representative for GD11. Comparing the $BMDL_{05}$ values that were predicted with the in vitro PBK approach with the $BMDL_{05}$ values derived from in vivo data, indicates that the $BMDL_{05}$ that is based on C_{max} as a dose metric represents the in vivo $BMDL_{05}$ better than the $BMDL_{05}$ based on the AUC_{0-10d} for phenol and p-fluorophenol, while for p-methylketophenol both the $BMDL_{05}$ based on C_{max} and AUC_{0-10d} seem to represent the in vivo $BMDL_{05}$ well. The difference between the $BMDL_{05}$ values predicted with the in vitro PBK approach based on C_{max} of the EST as a dose metric and the $BMDL_{05}$ values obtained with in vivo developmental toxicity data vary less than 3.8-fold for these three phenols. For p-heptyloxyphenol, however, the $BMDL_{05}$ value based on AUC_{0-10d} of the EST as a dose metric represents the in vivo $BMDL_{05}$ somewhat better (1.9-fold difference) than the predicted $BMDL_{05}$ based on C_{max} (4.3-fold difference).

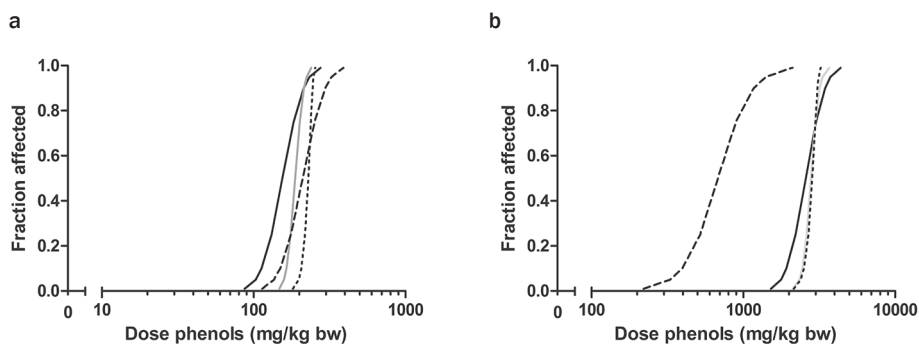


Figure 5 In vivo dose-response curves for developmental toxicity of phenol (solid black line), p-fluorophenol (solid grey line), p-heptyloxyphenol (dashed line) and p-methylketophenol (dotted line) in rat predicted by in vitro PBK-based reverse dosimetry. Panel **a** represents the predicted dose-response curves based on the nominal test concentration of the phenols relating C_{max} to developmental toxicity. Panel **b** represents the predicted dose-response curves relating the AUC_{0-10d} of the phenols to developmental toxicity.

Table 6 BMDL₀₅ values (mg/kg bw) for developmental toxicity of the phenols predicted with the in vitro PBK approach and BMDL₀₅ values derived from in vivo developmental toxicity data reported in the literature.

Compound	in vitro PBK approach		in vivo
	BMDL ₀₅ _{C_{max}}	BMDL ₀₅ _{AUC}	BMDL ₀₅ (or NOAEL) ^a
phenol	88	1536	333
p-fluoro	129	1892	183
p-heptyloxy	113	257	484
p-methylketo	186	2170	632

^a Derived from in vivo developmental toxicity data (most critical endpoint) from Kavlock (1990).

The potency ratios between phenol and p-fluorophenol, p-heptyloxyphenol and p-methylketophenol calculated based on the BMDL₀₅ values obtained with the in vitro PBK approach are graphically presented in Figure 6, together with the potency ratios obtained from the in vivo developmental toxicity study of Kavlock (1990) and the EST. The difference between the most and the least potent test compound in the EST, p-heptyloxyphenol and phenol, was three orders of magnitude (Strikwold et al. 2012), which does not reflect the potency ratio obtained from the in vivo developmental toxicity study which shows a small potency difference between the phenols (maximum 0.5-fold for the potency ratio based on the in vivo BMDL₀₅ or NOAEL). From Figure 6 it can be seen that the large difference in the toxic potency that was observed in the EST for p-heptyloxyphenol compared to phenol was greatly diminished, namely from 1553-fold in the EST to 0.8-fold in the in vitro PBK approach when based on the C_{max}. The potency ratio between phenol and p-fluorophenol and p-methylketophenol was changed from 1.9 to 0.7-fold and from 4.9 to 0.5-fold, respectively.

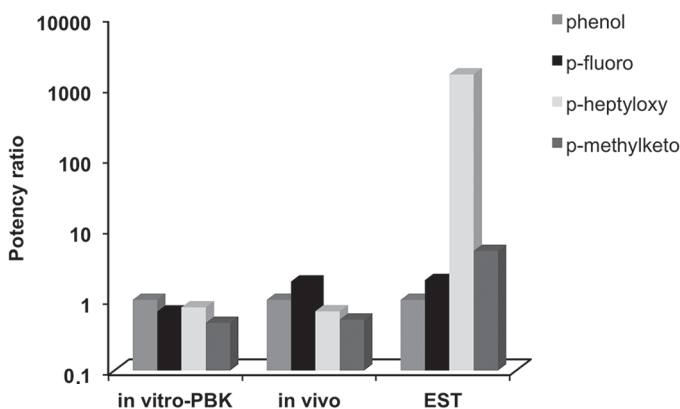


Figure 6 Potency of p-substituted phenols relative to phenol expressed as a potency ratio (potency ratio = potency phenol/potency p-substituted phenol), specified for the in vitro PBK approach (BMDL₀₅) using C_{max} as dose metric, the in vivo data (most critical endpoint) from Kavlock (1990) (BMDL₀₅ or NOAEL) and the EST (BMC₅₀).

DISCUSSION AND CONCLUSION

Translation of *in vitro* toxicity data to *in vivo* toxicity values is highly relevant in order to use *in vitro* data in the regulatory risk assessment of chemicals. In previous studies it was demonstrated that PBK-based reverse dosimetry converting *in vitro* concentration-response values to *in vivo* dose-response data could successfully be applied to predict a PoD for phenol (Strikwold et al. 2013), for all-trans-retinoic-acid (Louisse et al. 2014) and for some glycol-ethers (Louisse et al. 2010). The aim of the present study was to investigate whether PBK-based reverse dosimetry could be used to translate *in vitro* embryotoxicity data obtained with the EST for a series of phenols (Strikwold et al. 2012), to *in vivo* developmental toxic potency values for the rat, using only *in silico* and *in vitro* derived (kinetic) parameters and data from the literature, and if this approach could overcome differences in *in vitro* and *in vivo* relative potencies of different phenolic congeners observed by Strikwold et al. (2012). The PoDs predicted with the *in vitro* PBK approach differed only 3.8-fold from the PoDs derived from *in vivo* data from literature, when C_{\max} of the EST was considered to be the most appropriate dose metric for *in vitro* PBK-based reverse dosimetry for phenol and p-fluorophenol and the AUC_{0-10d} for p-heptyloxyphenol, while both C_{\max} and AUC_{0-10d} were appropriate metrics for p-methylketophenol. The large difference between the *in vitro* derived relative potency and the *in vivo* derived relative potency of p-heptyloxyphenol was reduced from 3 orders of magnitude for the EST data as such (Strikwold et al. 2012) to less than 2-fold after applying PBK-based reverse dosimetry to these EST data.

Results from our *in silico* and *in vitro* derived (kinetic) parameters, together with PBK modelling provide insight into the possible factors underlying the relative low toxic potency for p-heptyloxyphenol *in vivo* (Kavlock 1990) compared to the relatively high observed embryotoxic potency *in vitro* in the EST (Strikwold et al. 2012). This discrepancy may be due to three major factors that play a role *in vivo* but not in the EST *in vitro* model, including 1) the relatively rapid metabolism of p-heptyloxyphenol by glucuronidation, 2) the relatively low placental transport of p-heptyloxyphenol compared to the other phenols, and 3) the relatively high tissue:plasma partition coefficients of p-heptyloxyphenol. Of these three aspects, the rapid glucuronidation of the toxic parent compound p-heptyloxyphenol has the largest contribution to the improved relative potency prediction for this compound. The contribution of metabolism in diminishing the toxicity of p-heptyloxyphenol was also observed in the WEC assay where the embryotoxic potency of p-heptyloxyphenol was greatly reduced when hepatocytes were added to the WEC assay (Oglesby et al. 1992).

The affinity constant K_m for glucuronidation of the phenols in the liver was found to be an influential kinetic parameter in the sensitivity analysis. The K_m of p-heptyloxyphenol was much lower than the K_m of the other tested phenols, resulting in a very rapid glucuronidation and elimination of the toxic parent compound. The high lipophilicity of p-heptyloxyphenol may explain the high affinity for the enzyme.

Transport across the placenta was determined with the BeWo cell line, and provided high P_{app} values for each of the test compound, except for p-heptyloxyphenol for which the P_{app} value was 7.1-fold lower compared with phenol. The high P_{app} values are in line with in vivo studies in rats reporting that simple phenolic compounds may readily pass the placenta (Abu-Qare et al. 2000; Gray and Kavlock 1990). In general, cellular permeability increases with increasing lipophilicity, until a certain threshold (Li et al. 2013; Waterhouse 2003; Wils et al. 1994). It has been demonstrated in vitro with intestinal cells that transport may decrease for compounds with an octanol:buffer distribution coefficient > 3000 (Wils et al. 1994), which corresponds to our observations for p-heptyloxyphenol ($\log P_{ow} = 25704$ (ACD/Labs 2015) in the Caco-2 and the BeWo assays. Interestingly, the P_{app} value of p-heptyloxyphenol in the BeWo transport experiment was 7.1-fold lower than the P_{app} value of phenol while this was only 1.2-fold in the Caco-2 assay. The observed difference may be due to binding of p-heptyloxyphenol to albumin that is present in the apical medium of the BeWo assay but not in the apical medium of Caco-2 assay. These albumin levels were selected to reflect physiological conditions. The predicted P_{app} value in the BeWo assay for p-heptyloxyphenol may be somewhat lower than the in vivo value, as Li et al. (2013) observed that the relative P_{app} value of the highly albumin bound compound ketoprofen was 3.4-fold lower in the BeWo system with albumin, compared to the relative P_{app} determined with the ex vivo perfusion system that also included albumin. This difference possibly originates from differences in the fluid dynamics of both systems, which was static in the BeWo assay and is dynamic in the ex vivo perfusion system (Li et al. 2013).

Incorporating permeability data obtained from the BeWo transport system to semi-quantitatively predict placental transfer in the PBK models in the present study, presents an approach that has not been applied in PBK modelling before. The BeWo transport system was evaluated to be a valuable in vitro model to predict transport of compounds across the placenta (Li et al. 2013). Nonetheless, this approach may be explored further, investigating the applicability domain of the BeWo assay with respect to different chemical classes, i.e. lipophilic compounds, as well as the time of pregnancy to augment its utility.

The present study predicted the embryotoxic potency of the phenols with physiological parameters in the PBK model selected for GD11 because for this time point in vivo developmental toxicity data for evaluation of the predictions were available. The EST was used to represent a sensitive in vitro endpoint for developmental toxicity (Genschow et al. 2004), which ideally may represent the sensitivity of the embryo at the critical window for toxicity of the p-substituted phenols. Parameterisation of the PBK model for other gestational days is possible. Calculations with parameters adjusted to GD20 (data not shown) indicate little differences with GD11, providing a 1.04 to 1.8-fold higher BMDL₀₅ value for predictions made with the PBK parameters for GD20 than for GD11 for the different phenols. Based on these results, the predictions for GD11 may be regarded to represent a sensitive period.

In conclusion, PBK models were developed for a series of phenols, using in vitro, in silico data and data obtained from the literature only. Applying the in vitro PBK-based reverse dosimetry approach to overcome kinetic differences between the in vitro toxicity test system and the in vivo situation resulted in an improved prediction of the in vivo developmental toxic potency for this series of phenols. This approach has even overcome the large disparities that were observed between the in vitro and the in vivo relative potencies of p-heptyloxyphenol. Herewith, we provide another proof-of-principle that integrating in vitro toxicity data and PBK-based reverse dosimetry may be a promising approach for prospective toxicological safety evaluations of compounds, without performing animal testing.

REFERENCES

- Abu-Qare AW, Brownie CF, Abou-Donia MB (2000) Placental transfer and pharmacokinetics of a single oral dose of [¹⁴C]p-nitrophenol in rats. *Arch Toxicol* 74:388-396
- ACD/Labs (2015) Advanced Chemistry Development (ACD/Labs) Software V11.02 (© 1994-2015 ACD/Labs). Values taken from SciFinder.
- Berezhkovskiy LM (2004) Volume of distribution at steady state for a linear pharmacokinetic system with peripheral elimination. *J Pharm Sci* 93:1628-1640
- Blaauboer BJ (2010) Biokinetic modeling and in vitro-in vivo extrapolations. *J Toxicol Environ Health B Crit Rev* 13:242-252
- Brown RP, Delp MD, Lindstedt SL, Rhomberg LR, Beliles RP (1997) Physiological parameter values for physiologically based pharmacokinetic models. *Toxicol Ind Health* 13:407-484
- Buelke-Sam J, Nelson CJ, Byrd RA, Holson JF (1982) Blood flow during pregnancy in the rat: I. Flow patterns to maternal organs. *Teratology* 26:269-277
- Carney EW, Scialli AR, Watson RE, DeSesso JM (2004) Mechanisms regulating toxicant disposition to the embryo during early pregnancy: an interspecies comparison. *Birth Defects Res, Part C* 72:345-360
- Chiu WA, Barton HA, DeWoskin RS, Schlosser P, Thompson CM, Sonawane B, Lipscomb JC, Krishnan K (2007) Evaluation of physiologically based pharmacokinetic models for use in risk assessment. *J Appl Toxicol* 27:218-237
- Chiu WA and Ginsberg GL (2011) Development and evaluation of a harmonized physiologically based pharmacokinetic (PBPK) model for perchloroethylene toxicokinetics in mice, rats, and humans. *Toxicol Appl Pharmacol* 253:203-234
- Delp MD, Evans MV, Duan C (1998) Effects of aging on cardiac output, regional blood flow, and body composition in Fischer-344 rats. *J Appl Physiol* 85:1813-1822
- EC (2007) Corrigendum to Regulation (EC) No 1907/2006 of the European Parliament and of the Council of 18 December 2006 concerning the Registration, Evaluation, Authorisation and Restriction of Chemicals (REACH), establishing a European Chemicals Agency, amending Directive 1999/45/EC and repealing Council Regulation (EEC) No 793/93 and Commission Regulation (EC) No 1488/94 as well as Council Directive 76/769/EEC and Commission Directives 91/155/EEC, 93/67/EEC, 93/105/EC and 2000/21/EC. *Off J Eur Union* L136:3-280
- EC (2009) Regulation (EC) no 1223/2009 of the European parliament and of the council of 30 November 2009 on cosmetic products. *Off J Eur Union* L342:59-209
- Endo S and Goss KU (2011) Serum albumin binding of structurally diverse neutral organic compounds: data and models. *Chem Res Toxicol* 24:2293-2301
- Fisher HL, Sumler MR, Shrivastava SP, Edwards B, Oglesby LA, Ebron-McCoy MT, Copeland F, Kavlock RJ, Hall LL (1993) Toxicokinetics and structure-activity relationships of nine para-substituted phenols in rat embryos in vitro. *Teratology* 48:285-297
- Fisher MB, Campanale K, Ackermann BL, Vandenbranden M, Wrighton SA (2000) In vitro glucuronidation using human liver microsomes and the pore-forming peptide alamethicin. *Drug Metab Dispos* 28:560-566

- Genschow E, Spielmann H, Scholz G, Pohl I, Seiler A, Clemann N, Bremer S, Becker K (2004) Validation of the embryonic stem cell test in the international ECVAM validation study on three in vitro embryotoxicity tests. *Altern Lab Anim* 32:209-244
- Gray JA and Kavlock RJ (1990) A pharmacokinetic analysis of phenol in the pregnant rat: deposition in the embryo and maternal tissues. *Teratology* 41:561
- Gülden M and Seibert H (2003) In vitro-in vivo extrapolation: estimation of human serum concentrations of chemicals equivalent to cytotoxic concentrations in vitro. *Toxicology* 189:211-222
- Gülden M and Seibert H (2005) In vitro-in vivo extrapolation of toxic potencies for hazard and risk assessment - problems and new developments. *ALTEX* 22 (Special Issue 2):218-225
- Hiser MF, Kropscott BE, McGuirk RJ, Bus JS (1994) Pharmacokinetics, metabolism and distribution of ¹⁴C-phenol in Fischer 344 rats after gavage, drinking water and inhalation exposure. OTS0557473. Study ID: K-002727-022. Dow Chemical Company. Submitted to U.S. Environmental Protection Agency under TSCA Section 8D
- Honda T, Honda K, Kokubun C, Nishimura T, Hasegawa M, Nishida A, Inui T, Kitamura K (2008) Time-course changes of hematology and clinical chemistry values in pregnant rats. *J Toxicol Sci* 33:375-380
- Humphrey MJ, Filer CW, Jeffery DJ, Langley PF, Wadds GA (1980) The availability of carfecillin and its phenol moiety in rat and dog. *Xenobiotica* 10:771-778
- Johansson MBN (1983) Lipoproteins and lipids in fetal, neonatal and adult rat serum. *Biol Neonate* 44:278-286
- Kavlock RJ (1990) Structure-activity relationships in the developmental toxicity of substituted phenols: in vivo effects. *Teratology* 41:43-59
- Li H, van Ravenzwaay B, Rietjens IMCM, Lousse J (2013) Assessment of an in vitro transport model using BeWo b30 cells to predict placental transfer of compounds. *Arch Toxicol* 87:1661-1669
- Loizou G and Hogg A (2011) MEGen: a physiologically based pharmacokinetic model generator. *Front Pharmacol* 2: article 56
- Louise J, Bosgra S, Blaauboer BJ, Rietjens IMCM, Verwei M (2014) Prediction of in vivo developmental toxicity of all-trans-retinoic acid based on in vitro toxicity data and in silico physiologically based kinetic modeling. *Arch Toxicol* 89:1135-1148
- Louise J, de Jong E, van de Sandt JJM, Blaauboer BJ, Woutersen RA, Piersma AH, Rietjens IMCM, Verwei M (2010) The use of in vitro toxicity data and physiologically based kinetic modeling to predict dose-response curves for in vivo developmental toxicity of glycol ethers in rat and man. *Toxicol Sci* 118:470-484
- McMullin TS, Lowe ER, Bartels MJ, Marty MS (2008) Dynamic changes in lipids and proteins of maternal, fetal, and pup blood and milk during perinatal development in CD and wistar rats. *Toxicol Sci* 105:260-274
- National Research Council (2007) Toxicity testing in the 21st century: a vision and a strategy. The National Academy Press, Washington, DC
- O'Flaherty EJ, Scott W, Schreiner C, Beliles RP (1992) A physiologically based kinetic model of rat and mouse gestation: disposition of a weak acid. *Toxicol Appl Pharmacol* 112:245-256
- Oglesby LA, Ebron-McCoy MT, Logsdon TR, Copeland F, Beyer PE, Kavlock RJ (1992) In vitro embryotoxicity of a series of para-substituted phenols: structure, activity, and correlation with in vivo data. *Teratology* 45:11-33
- Paixão P, Gouveia LF, Morais JAG (2009) Prediction of drug distribution within blood. *Eur J Pharm Sci* 36:544-554
- Park HW and Shepard TH (1994) Volume and glucose concentration of rat amniotic fluid: effects on embryo nutrition and axis rotation. *Teratology* 49:465-469
- Poulin P and Theil FP (2002) Prediction of pharmacokinetics prior to in vivo studies. 1. Mechanism-based prediction of volume of distribution. *J Pharm Sci* 91:129-156
- Punt A, Schiffelers MJWA, Jean Horbach G, van de Sandt JJM, Groothuis GMM, Rietjens IMCM, Blaauboer BJ (2011) Evaluation of research activities and research needs to increase the impact and applicability of alternative testing strategies in risk assessment practice. *Regul Toxicol Pharmacol* 61:105-114
- Sarr O, Yang K, Regnault TRH (2012) In utero programming of later adiposity: the role of fetal growth restriction. *J Pregnancy* 2012:1-10
- Simcyp (2015) Simcyp prediction tools-fu. Available at: <https://members.simcyp.com/account/tools/fu/> [Last accessed: Dec 2015]
- Strikwold M, Spenkeliink B, Woutersen RA, Rietjens IMCM, Punt A (2013) Combining in vitro embryotoxicity data with physiologically based kinetic (PBK) modelling to define in vivo dose-response curves for developmental toxicity of phenol in rat and human. *Arch Toxicol* 87:1709-1723
- Strikwold M, Woutersen RA, Spenkeliink B, Punt A, Rietjens IMCM (2012) Relative embryotoxic potency of p-substituted phenols in the embryonic stem cell test (EST) and comparison to their toxic potency in vivo and in the whole embryo culture (WEC) assay. *Toxicol Lett* 213:235-242

Varma DR and Ramakrishnan R (1985) A rat model for the study of transplacental pharmacokinetics and its assessment with antipyrine and aminoisobutyric acid. *J Pharmacol Methods* 14:61-74

Verwei M, van Burgsteden JA, Krul CAM, van de Sandt JJM, Freidig AP (2006) Prediction of in vivo embryotoxic effect levels with a combination of in vitro studies and PBPK modelling. *Toxicol Lett* 165:79-87

Wang X, Wang W, Cheng G, Huang L, Chen D, Tao Y, Pan Y, Hao H, Wu Q, Wan D, Liu Z, Wang Y, Yuan Z (2014) High risk of embryo-fetal toxicity: Placental transfer of T-2 toxin and its major metabolite HT-2 toxin in BeWo cells. *Toxicol Sci* 137:168-178

Waterhouse RN (2003) Determination of lipophilicity and its use as a predictor of blood-brain barrier penetration of molecular imaging agents. *Mol Imaging and Biol* 5:376-389

Wils P, Warnery A, Phung-Ba V, Legrain S, Scherman D (1994) High lipophilicity decreases drug transport across intestinal epithelial cells. *J Pharmacol Exp Ther* 269:654-658

Yeoh GCT and Morgan EH (1974) Albumin and transferrin synthesis during development in the rat. *Biochem J* 144:215-224

SUPPLEMENTARY DATA A

MASS BALANCE ALGORITHMS AND PARAMETER SPECIFICATIONS OF THE PBK MODEL FOR PHENOL AND P-SUBSTITUTED PHENOLS IN THE RAT

The algorithms are similar for phenol, p-fluorophenol, p-heptyloxyphenol and p-methylketophenol. An example for the compound phenol below is presented.

4

COMPOUND	ABBREVIATION
phenol	ph
phenylglucuronide	pg

COMPARTMENT (TISSUE (T))	ABBREVIATION
Small intestine	I
Liver	L
Fat	F
Placenta	PL
Foetus	FE
Remaing body	B
Arterial	A
Venous	V
Blood	BL

VARIABLE	UNIT	ABBREVIATION
Blood flow rate to tissue	$l\ h^{-1}$	Q(T)
Cardiac output	$l\ h^{-1}$	QC
Concentration phenol in tissue or blood	μM	$C(T)_{ph}$
Partition coefficient tissue:plasma phenol	-	$P(T)_{ph}$
Volume of tissue or blood	l	V(T)
Amount phenol in tissue or blood	μmol	$A(T)_{ph}$
Maximum rate of formation metabolite (m) in tissue	$\mu mol\ h^{-1}$	$V_{max}(T)_m$
Michaelis-Menten constant for formation metabolite (m) in tissue	μM	$K_m(T)_m$
Uptake rate phenol intestine	h^{-1}	ka
Amount phenol taken up from the gut lumen	μmol	$Uptake_{ph}$
Amount phenol remaining in the gut lumen	μmol	AGL_{ph}
Clearance placenta	$l\ h^{-1}$	CLPL

SMALL INTESTINE

$$\frac{dA_{ph}}{dt} = \frac{dUptake_{ph}}{dt} + QI * \left(CA_{ph} - \frac{CI_{ph}}{PI_{ph}} * PBL_{ph} \right)$$

Uptake phenol from gut lumen

$$\frac{dUptake_{ph}}{dt} = - \frac{dAGL_{ph}}{dt} = ka * AGL_{ph}$$

$$AGL_{ph}(0) = \text{Oral dose}$$

LIVER COMPARTMENT

$$\frac{dAL_{ph}}{dt} = QL * CA + QI * \frac{CI_{ph}}{PI_{ph}} * PBL_{ph} - (QL + QI) * \frac{CL_{ph}}{PL_{ph}} * PBL_{ph} - \frac{VmaxL_{pg} * \frac{CL_{ph}}{PL_{ph}}}{KmL_{pg} + \frac{CL_{ph}}{PL_{ph}}}$$

$$CL_{ph} = \frac{AL_{ph}}{VL}$$

FAT COMPARTMENT

$$\frac{dAF_{ph}}{dt} = QF * \left(CA_{ph} - \frac{CF_{ph}}{PF_{ph}} * PBL_{ph} \right)$$

$$CF_{ph} = \frac{AF_{ph}}{VF}$$

PLACENTAL/FOETAL COMPARTMENT

Phenol in placental compartment

$$\frac{dAPL_{ph}}{dt} = QPL * \left(CA_{ph} - \frac{CPL_{ph}}{PPL_{ph}} * PBL_{ph} \right) + CLPL * \left(\frac{CFE}{PFE} - \frac{CPL}{PPL} \right)$$

$$CPL_{ph} = \frac{APL_{ph}}{VPL}$$

Phenol in foetal compartment

$$\frac{dAFE_{ph}}{dt} = CLPL * \left(\frac{CPL}{PPL} - \frac{CFE}{PFE} \right)$$

$$CFE_{ph} = \frac{AFE_{ph}}{VFE}$$

REMAINING BODY TISSUE

$$\frac{dAB_{ph}}{dt} = QB * \left(CA_{ph} - \frac{CB_{ph}}{PB_{ph}} * PBL_{ph} \right)$$

$$CB_{ph} = \frac{AB_{ph}}{VB}$$

ARTERIAL BLOOD COMPARTMENT

$$CA_{ph} = CV_{ph}$$

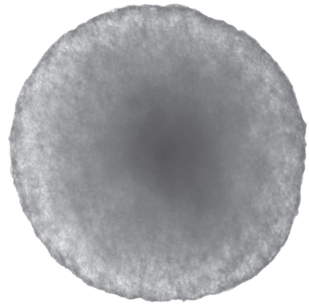
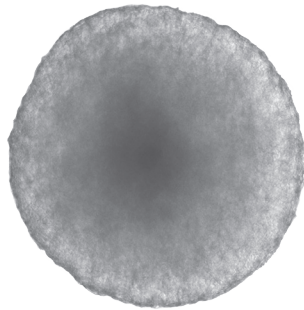
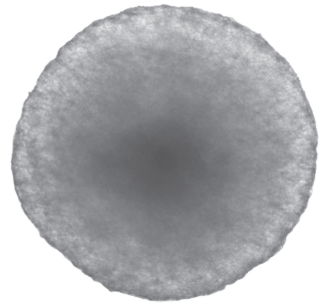
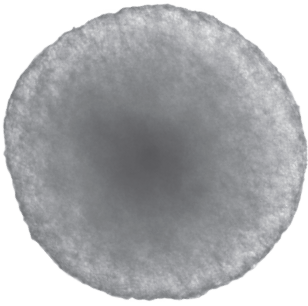
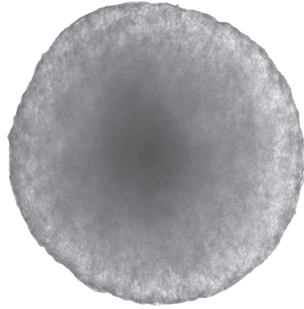
VENOUS BLOOD COMPARTMENT

$$\frac{dAV_{ph}}{dt} = (QL + QI) * \frac{CL_{ph}}{PL_{ph}} * PBL_{ph} + QF * \frac{CF_{ph}}{PF_{ph}} * PBL_{ph} + QPL * \frac{CPL_{ph}}{PPL_{ph}} * PBL_{ph} + QB * \frac{CB_{ph}}{PB_{ph}} * PBL_{ph} - QC * CV_{ph}$$

$$CV_{ph} = \frac{AV_{ph}}{VV}$$

Note: the maternal circulation is via blood, but exchange between mother and foetus is modelled to occur via plasma because that represents the BeWo system better. For the reverse dosimetry, the foetal plasma was set equal to the concentration in the EST.





CHAPTER 5

Development of a combined in vitro physiologically based kinetic (PBK) and Monte Carlo modelling approach to predict interindividual human variation in phenol induced developmental toxicity

**Marije Strikwold, Bert Spenkelink, Ruud A Woutersen, Ivonne MCM Rietjens, Ans Punt
Submitted for publication**

ABSTRACT

With our recently developed in vitro physiologically based kinetic (PBK) modelling approach we could extrapolate in vitro toxicity data to in vivo toxicity values applying PBK-based reverse dosimetry. This approach allows to make toxicity predictions directly for humans by taking human kinetic information into account. Ideally information on kinetic differences among human individuals within a population should also be considered. In the present study we demonstrated a modelling approach that integrated in vitro toxicity data, PBK modelling and Monte Carlo simulations to obtain insight in interindividual human kinetic variation and derive chemical specific adjustment factors (CSAFs) for phenol induced developmental toxicity as the endpoint of interest. The present study revealed that UGT1A6 is the primary enzyme responsible for the glucuronidation of phenol in humans followed by UGT1A9. Monte Carlo simulations were performed taking into account interindividual variation in glucuronidation by these specific UGTs and in the oral absorption coefficient which was shown to be another parameter with high influence on the phenol plasma concentrations predicted by the PBK model. Linking Monte Carlo simulations with PBK modelling, population variability in the maximum plasma concentration of phenol for the female human population could be predicted. This approach provided a CSAF for interindividual variation of 2.0 which covers the 99th percentile of the population. Based on this outcome, it was concluded that the default safety factor of 3.16 applied for interindividual human kinetic differences in the safety assessment of chemicals seems adequately protective. Dividing the dose-response curve data obtained with in vitro PBK-based reverse dosimetry, with the CSAF obtained for the 99th percentile provided a dose-response curve that reflects the consequences of the interindividual variability in phenol kinetics for the developmental toxicity of phenol. The strength of the presented approach is that it provides insight in the effect of interindividual variation in kinetics for phenol induced developmental toxicity, based on only in vitro and in silico testing.

INTRODUCTION

The development of alternatives to animal testing is a subject of increasing importance. Especially a number of recent regulatory decisions within the EU have made the development of non-animal based approaches in chemical risk assessment more important (EC 2007; EC 2009). In addition, alternatives to animal testing are also crucial for economic and ethical reasons and to meet the criticism about the human relevance of animal based safety tests. To enhance the development of non-animal approaches in risk assessment, we have recently developed an *in vitro* physiologically based kinetic (PBK) reverse dosimetry approach, which allowed prediction of *in vivo* developmental toxicity values for phenol and a series of *p*-substituted phenols from *in vitro* concentration-response curves obtained with the embryonic stem cell test (EST) (Strikwold et al. 2013; Strikwold et al. 2016). Within this approach *in vitro* toxicity data obtained with the EST were extrapolated to *in vivo* dose-response curves for developmental toxicity using *in vitro* PBK-based reverse dosimetry (Louisse et al. 2010; Louisse et al. 2014; Strikwold et al. 2013; Strikwold et al. 2016). The predicted points of departure (PoDs), that can be used as a starting point in the hazard and risk assessment of chemicals, differed less than 4-fold from the *in vivo* determined values (Strikwold et al. 2013; Strikwold et al. 2016). Similar promising results were obtained when applying this approach for a series of glycol ethers and for all-trans-retinoic-acid (Louisse et al. 2010; Louisse et al. 2014).

A major advantage of this *in vitro* PBK-based reverse dosimetry approach is that it provides the opportunity to make predictions directly for humans by taking PBK model parameters defined for humans into account. This implies that the *in vitro* PBK-based reverse dosimetry approach is not only relevant to reduce animal experiments but also to make the risk assessment more relevant to the human situation. Such human predictions are an important goal within the framework for toxicity testing in the 21st century as envisioned by the National Research Council (2007).

Within our recent work, we made predictions on developmental toxicity of phenol for an average human female, applying the *in vitro* PBK-based reverse dosimetry approach for phenol (Strikwold et al. 2013). However, this model did not take into account interindividual human variation in sensitivity towards the toxic effects, which may occur as a result of differences in kinetic processes between individuals. Although a default safety factor of 3.16 for interindividual human differences is often applied to account for such human variation in kinetics (IPCS 2005), having more detailed insights in possible interindividual variation might provide risk assessors with a reliable basis to derive human guidance values and assist in defining chemical specific adjustment factors (CSAFs). The aim of the present study was to demonstrate an approach that integrates *in vitro* toxicity data, PBK modelling and Monte Carlo simulations to assess the effects of human interindividual variation in kinetics for phenol induced developmental toxicity.

Phenol is a high production volume chemical that is mainly metabolised by glucuronidation and sulfation. Results from a previously published PBK model for phenol indicated that the glucuronidation pathway is an important determinant for blood phenol concentrations (Strikwold et al. 2013). UGT1A6 and UGT1A9 are likely to be involved in the glucuronidation of phenol because many p-substituted phenols are a substrate for these UGT forms (Ethell et al. 2002). Moreover, at least SULT1A1 and SULT1A3 are involved in the sulfation of phenol (Dajani et al. 1999). Genetic differences and lifestyle factors may influence the expression and activity of these enzymes, and hence may significantly influence the metabolism of phenol and the sensitivity towards phenol induced developmental toxicity. The sensitivity analysis of the PBK model of phenol (Strikwold et al. 2013) revealed that the oral absorption coefficient (k_a) and glucuronidation of phenol in the liver were parameters that influenced the maximum predicted phenol plasma concentration (C_{max}) to a major extent and were therefore included in the evaluation of interindividual variation in the present study.

To enable prediction of the effect of interindividual human kinetic variation in sensitivity to phenol induced developmental toxicity, information on the metabolic variation in phenol glucuronidation was generated with in vitro kinetic experiments using two approaches. At first, phenol glucuronidation was quantified using subcellular liver fractions of ten female individuals, which is often used as a first step when information about interindividual variation is lacking. The kinetic constants obtained for each female were used to define ten subject specific PBK models based on our previously developed PBK model for phenol (Strikwold et al. 2013), from which differences in plasma phenol levels of the ten individuals were calculated. Secondly, a Monte Carlo simulation was performed to predict interindividual variation in phenol plasma levels. To this end the variation in phenol glucuronidation was modelled based on data from in vitro kinetic experiments using UGT isoforms and human variation in expression of these UGT enzymes described in literature. Variation in phenol plasma concentrations obtained with both approaches was compared to each other. So far in both approaches, only variation in phenol glucuronidation was taken into account, next to the use of average values for the other model parameters. In a next step interindividual variation for the oral absorption coefficient, which according to the sensitivity analysis (Strikwold et al. 2013) also highly influenced the model outcome, was included in the Monte Carlo simulations as well. Based on the results obtained from the latter Monte Carlo simulation a CSAF (IPCS 2005) was derived that accounts for interindividual differences in phenol kinetics within the human population. Possible consequences of the results obtained for risk assessment are discussed.

MATERIALS AND METHODS

COMPOUNDS AND BIOLOGICAL MATERIALS

Phenol (99%), phenyl- β -D-glucuronide ($\geq 99\%$), propofol ($\geq 98\%$), propofol- β -D-glucuronide sodium salt (99.4%), serotonin ($\geq 98\%$), Tris(hydroxymethyl)aminomethane (Tris) ($\geq 99.9\%$), uridine 5'-diphosphoglucuronic acid (UDPGA) and alamethicin (98%) were obtained from Sigma Aldrich (Steinheim, Germany). Serotonin- β -D-glucuronide (97%) was obtained from Biozol (Eching, Germany). Acetonitrile (UPLC/MS grade) was obtained from BioSolve (Valkenswaard, The Netherlands), dimethylsulfoxide (DMSO) ($\geq 99\%$) from Acros Organics (Geel, Belgium). Trifluoroacetic acid (TFA), hydrochloric acid (37%) and magnesium chloride hexahydrate were purchased from VWR International GmbH (Darmstadt, Germany).

SupersomesTM (baculovirus insect microsomal preparations) with individually expressed human UGT 1A1, 1A9 and 2B7 enzymes were purchased from BD Biosciences (Belgium). SupersomesTM (baculovirus insect microsomal preparations) with individually expressed human UGT 1A3, 1A4, 1A6, 1A7, 1A8, 1A10, 2B4, 2B10, 2B15, 2B17 enzymes and pooled female human liver microsomes (21 donors) were purchased from Corning (Woburn MA, USA). Ten individual female human liver S9 homogenates were obtained from XenoTech (Lenexa, KS, USA).

GLUCURONIDATION OF PHENOL BY POOLED FEMALE HUMAN LIVER MICROSOMES AND INDIVIDUAL FEMALE HUMAN LIVER S9

Incubations were performed to determine the kinetic constants, namely the maximum enzyme reaction rate (V_{max}) and the Michaelis-Menten constant (K_m) for phenol glucuronidation with female human liver fractions. The incubation mixtures consisted of 50 mM Tris-HCl buffer (pH 7.4) with 10 mM $MgCl_2$, containing (final concentrations) 10 mM UDPGA, 0.5 mg microsomal protein/ml for assays with pooled female human liver microsomes or 0.5 mg S9 protein/ml for assays with ten individual female human liver S9 homogenates. To overcome enzyme latency the incubation mixtures were pre-treated for 15 min on ice, with the poreforming peptide alamethicin (0.025 mg/ml) added from a 200 times concentrated stock solution in methanol. Then, incubations were started after a 1-min pre-incubation at 37 °C by the addition of the substrate phenol (final concentrations ranging from 200 to 4000 μ M added from a 200 times concentrated stock solution in DMSO) and left in a shaking water bath of 37 °C for 10 min for the assays with pooled female human liver microsomes and with individual female human liver S9. The reactions were terminated with the addition of ice-cold acetonitrile (20% v/v) and subsequently put on ice. In the blank incubation mixtures, UDPGA was omitted. The ten human individual liver fractions were assumed to represent the female fertile population. To enable the collection of ten female samples, also females aged 57 and 66 year were included, knowing that older age does not affect glucuronidation activity (Court 2010).

GLUCURONIDATION OF PHENOL BY RECOMBINANT UGT ENZYMES

Supersomes™ with individually expressed UGT enzymes 1A1, 1A3, 1A4, 1A6, 1A7, 1A8, 1A9, 1A10, 2B4, 2B7, 2B10, 2B15, 2B17 were screened on the ability to glucuronidate phenol. Incubations were performed in 50 mM Tris-HCl buffer (pH 7.4 including 10 mM MgCl₂), containing (final concentrations) 0.5 mg protein/ml and 10 mM UDPGA. To overcome enzyme latency the incubation mixture was pre-treated for 15 min on ice, with the poreforming peptide alamethicin (0.025 mg/ml) added from a 200 times concentrated stock solution in methanol. Then, incubations were started after a 1-min pre-incubation at 37 °C by the addition of phenol (final concentration 1000 μM added from a 200 times concentrated stock solution in DMSO) and left in a shaking water bath of 37 °C for 45 min. The reactions were terminated with the addition of ice-cold acetonitrile (20% v/v) and subsequently put on ice. In the blank incubation mixtures UDPGA was omitted.

Kinetic constants V_{max} , K_m , the inhibition constant K_i or k , the latter representing the first-order kinetic rate constant in the absence of saturation (for details see section Enzyme kinetic parameters) were determined for those UGT enzymes that showed a sufficient turnover in the screening study, including UGT1A6, UGT1A7, UGT1A8, UGT1A9 UGT2B7. The final phenol concentrations ranged from 200 to 8000 μM depending on the UGT enzyme studied and were added to the incubation mixture from 200 times concentrated stock solutions in DMSO. Other incubation conditions were similar as used for the screening assay, except that the incubation period was 30 min. Based on the kinetic curves and the kinetic constants obtained together with the scaled catalytic efficiency (V_{max}/K_m), the contribution of the different UGTs to phenol glucuronidation in vivo was further evaluated and UGTs that were expected to contribute the most to phenol glucuronidation at relevant plasma concentrations of phenol were included in the Monte Carlo evaluation.

RELATIVE ACTIVITY FACTOR (RAF)

With the RAF approach (Crespi 1995) the glucuronidation activity of UGT enzymes can be scaled to female human liver microsomes enabling extrapolation of the in vitro determined activity to in vivo values. The V_{max} values obtained from the in vitro incubations with recombinant enzymes (nmol/min/mg protein) were scaled to the in vivo situation (μmol/h/g organ) using this RAF approach (Crespi 1995), according to the following equation:

$$Scaled V_{max_UGT} = V_{max_UGT(app)} / (1000 \text{ nmol}/\mu\text{mol}) * (60 \text{ min}/\text{h}) * \text{RAF}_{UGT} * \text{MPL}$$

in which MPL represents the microsomal protein yield of 32 mg/(g liver) (Barter et al. 2007). RAF_{UGT} corresponds to the ratio between the conversion of an enzyme specific probe substrate by the recombinant enzyme (Supersomes™) and by pooled female human liver microsomes (HLM). The RAF is determined according to the following equation:

$$RAF = \frac{v \text{ HLM probe}}{v \text{ Supersome}^{\text{TM}} \text{ probe}}$$

in which, v represents the metabolic turnover of an enzyme specific probe substrate. The probe used to determine the RAF for UGT1A6 was serotonin (Krishnaswamy et al. 2003) and the probe for UGT1A9 was propofol (Court 2005). To determine the RAF values for UGT1A6 and UGT1A9, incubations were performed as described for phenol glucuronidation using HLM or the SupersomesTM (both pre-treated with alamethicin to reduce enzyme latency), using a concentration of 0.1 mg protein/ml for HLM and 0.1 mg protein/ml SupersomesTM for serotonin with an incubation time of 30 min, and a concentration of 0.1 mg protein/ml for HLM and 0.1 mg protein/ml for SupersomesTM for propofol with an incubation time of 15 min. The applied final probe concentrations in the incubations were 4000 μM for serotonin and 25 μM for propofol, taking into account recommendations about appropriate probe concentrations reported by Court (2005). In the blank incubation mixtures, UDPGA was omitted.

The performance of the RAF approach was evaluated by comparing the sum of scaled catalytic efficiencies (V_{max}/K_m) of the individual isoenzymes UGT1A6 and UGT1A9 to the scaled catalytic efficiency that was determined with kinetic constants obtained from pooled female human liver microsomes.

QUANTIFICATION OF COMPOUNDS AND GLUCURONIDE CONJUGATES

Samples of the incubation experiments with phenol, propofol and serotonin as substrate were centrifuged at 14,000 rpm for 5 min. Subsequently 3.5 μl were analysed by UPLC-PDA (Waters Acquity) according to the method for phenol and phenylglucuronide described previously by Strikwold et al. (2013). Phenylglucuronide was quantified by its peak area using a linear calibration curve ($R^2 > 0.999$) made using a commercially available reference compound. Chromatogram peaks of propofol glucuronide and serotonin glucuronide from samples of the incubation experiments were identified using commercially available reference standards. The RAFs were calculated based on the peak areas of the glucuronides that were formed after incubating the probes.

ENZYME KINETIC PARAMETERS

Kinetic parameters describing enzymatic conversions were defined based on the in vitro metabolism data obtained in the present study using GraphPad (GraphPad Prism 5.0 software, San Diego, CA, USA). The best model fit was selected from the Michaelis-Menten model, substrate inhibition model, and linear curve fitting based on visual inspection of the curves. Subsequently, the relevant enzyme kinetic parameters (V_{max} for the maximum enzyme reaction rate, Michaelis-Menten constant K_m , inhibition constant K_i or k representing the first-order kinetic rate constant) were estimated. In vitro derived $V_{\text{max(app)}}$ values were scaled to the

in vivo situation using a protein yield of 32 mg/g liver (Barter et al. 2007) for in vitro studies with microsomes and Supersomes™ and 143 mg/S9 (Medinsky et al. 1994) for in vitro studies with S9. In vivo K_m values were assumed to be the same as K_m values obtained from the in vitro experiments. The catalytic efficiencies of the enzyme were defined by V_{max}/K_m .

PBK MODELS, MONTE CARLO SIMULATIONS AND SENSITIVITY ANALYSIS

Our previously developed PBK model for phenol in humans (Strikwold et al. 2013) was used as starting point in the present study to evaluate the effect of human interindividual variation in kinetics for phenol induced developmental toxicity. The kinetic constants derived in the present study from incubations with the pooled human female liver samples were used in the PBK model. Subsequently a sensitivity analysis was performed using the same approach as described by Strikwold et al. (2013) to determine parameters that influenced the model outcome.

Then, interindividual variability in phenol glucuronidation was assessed using a population of ten female individuals. To this purpose, the kinetic constants (V_{max} and K_m) for liver glucuronidation obtained from incubations with individual female human liver S9 homogenates were included in the PBK model for phenol (Strikwold et al. 2013). With the PBK models, maximum phenol plasma concentrations (C_{max}) at an oral dose level of 25 mg/kg bw were calculated for each individual.

To enable prediction of kinetic variation in a larger human population, interindividual variability was assessed by linking the PBK model of phenol (Strikwold et al. 2013) with Monte Carlo simulations. To this end, a PBK model was developed in which the kinetic constants for glucuronidation of phenol were described with the kinetic constants obtained in the present study from incubations with recombinant UGT enzymes. Together with literature reporting human variation in expression of these UGT enzymes, Monte Carlo simulations could be performed on interindividual human differences in glucuronidation of phenol in the liver. The Monte Carlo simulations were performed in connection with the PBK model to simulate phenol plasma concentrations that could occur in the human female population at an oral dose of 25 mg/kg bw, when taking interindividual human variation in the maximum glucuronidation rate (V_{max}) of phenol in the liver into account. The predicted variation in the C_{max} of phenol at an oral dose level of 25 mg/kg bw obtained with the Monte Carlo simulation was compared to the C_{max} values of phenol predicted by the individual PBK models for the ten individuals at an oral dose level of 25 mg/kg bw. So far, only variation in phenol glucuronidation was taken into account in both approaches, next to the use of average values for the other model parameters.

In addition to the analysis above, a Monte Carlo simulation was performed that in addition to variation in UGT expression, also included the interindividual human variation in the oral absorption coefficient (k_a), because the sensitivity analysis revealed this to be another

parameter of major influence (Strikwold et al. 2013). No interindividual human variation in the remaining model parameters was included since they were shown by the sensitivity analysis to be of limited influence.

For the Monte Carlo modelling, a total of 10,000 simulations were performed. The distributions were truncated at ± 3 SD by excluding individuals with a V_{\max} value for UGT1A6 and/or UGT1A9 and/or a k_a value higher or lower than three times the SD of the geometric mean values from the Monte Carlo simulation. This resulted in a final population of 9956 and 9907 individuals for respectively simulations with variation in UGTs and simulations with variation in both UGTs and k_a . In each simulation, the values of the model parameters V_{\max} for UGT1A6 and UGT1A9 and the k_a were randomly taken from the log-normal distribution. The log-normal distribution of a parameter was defined by the mean (μ_w) and the standard deviation (σ_w) according to the equations defined by Zhang et al. (2007):

$$\mu_w = \ln \frac{\mu_x}{\sqrt{1 + CV_x^2}}$$

and

$$\sigma_w^2 = \ln(1 + CV_x^2)$$

where μ_x represents the average of V_{\max_UGT} or k_a and CV_x is the coefficient of variation for each of the values. In the simulation, the parameters were allowed to vary independently from one another. The average k_a value was 7.62/h which was obtained from the rat in situ intestinal perfusion study of Humphrey et al. (1980) and assumed to be applicable for human. The average value for the apparent V_{\max} of UGT1A6 and UGT1A9 were experimentally obtained in the present study amounting 7.3 and 9.7 nmol/min/mg protein, respectively. The coefficients of variation (CV) representing interindividual variation in the glucuronidation activity by UGT1A6 and UGT1A9 amounting to 76% and 55% respectively, were taken from the literature (Court 2010) and attributed to the V_{\max} values of these UGTs in the PBK model. The CV for k_a was assumed to be 30% representing a moderate level of variation (Covington et al. 2007).

Model predictions with Monte Carlo simulations were performed with Berkeley Madonna (version 8.3.18, UC Berkeley, CA, USA). The population distribution generated with the Monte Carlo simulation was statistically analysed with GraphPad (GraphPad Prism 5.0 software, San Diego, CA, USA) to calculate the geometric mean, and different percentiles of the C_{\max} values of phenol obtained from the Monte Carlo analysis. The population distribution enabled the prediction of the CSAF, which was obtained by dividing the percentile (90th and 99th of the population) of C_{\max} by the geometric mean of C_{\max} (IPCS 2005).

REVERSE DOSIMETRY AND DOSE-RESPONSE ANALYSIS

In analogy to our previous study (Strikwold et al. 2013), reverse dosimetry was applied using the maximum plasma concentration (C_{\max}) as appropriate dose metric. To this end each concentration tested in the EST (EC_x), was set equal to the maximum plasma concentration of unconjugated phenol in the PBK model for the average female that used kinetic constants determined using pooled female liver samples, providing effective external oral dose levels (ED_x) (Strikwold et al. 2013). From these ED_x values, an in vivo dose-response curve was derived and a 95% lower confidence limit of the benchmark dose at 5% benchmark response ($BMDL_{05}$) using the Benchmark Dose Software (BMDS) version 2.6 from the Environmental Protection Agency (EPA). Calculations were performed with the logProbit model because this model provided the best fit for our previous predicted dose-response curve for phenol in humans (Strikwold et al. 2013). Subsequently, the dose-response curve of a sensitive individual in the population, represented by the 99th percentile obtained from the Monte Carlo simulations, was visualised by applying the CSAF (99th percentile of C_{\max}) to the dose-response curve of the average population, assuming linear kinetic processes at these dose levels.

RESULTS

FORMATION OF PHENYLGLUCURONIDE BY POOLED FEMALE HUMAN LIVER MICROSOMES AND INDIVIDUAL FEMALE HUMAN LIVER S9

Table 1 presents the kinetic constants K_m , V_{\max} and the scaled catalytic efficiencies for glucuronidation as obtained in incubations with pooled female human liver microsomes and individual female liver S9 preparations. The K_m and V_{\max} for the glucuronidation of phenol obtained with pooled female microsomes were 771 μM and 64 $\mu\text{mol/h/g}$ liver, respectively.

The average V_{\max} and K_m of the ten individuals amounted to 976 μM and 78 $\mu\text{mol/h/g}$ liver, respectively. The difference between the highest and lowest K_m value predicted for the ten females is 4.8-fold. Interestingly, the K_m value of individual H_217 is 257 μM which is relatively low compared to the K_m values obtained with the pooled females ($K_m = 771 \mu\text{M}$) and the K_m values obtained with the other individual liver samples (mean $K_m = 976 \mu\text{M}$). The difference between the highest and lowest scaled V_{\max} values of the individuals is 2.3-fold. The mean scaled V_{\max} of the ten individuals is reasonably in accordance with the scaled V_{\max} obtained from incubations with pooled female liver microsomes, namely 78 versus 64 $\mu\text{mol/h/g}$ liver respectively. The kinetic constants obtained for the ten females were used in the PBK models for the individuals, of which the model predictions were used to assess the consequences of interindividual differences in glucuronidation of phenol for the resulting C_{\max} values.

The coefficients of variation (CVs) of the in vitro determined V_{\max} and K_m of the ten individuals were 32% and 30%, respectively and the resulting CV for the scaled catalytic

efficiency (V_{\max}/K_m) of the ten females was 79%. This relative high CV for the scaled catalytic efficiency is caused by female H_217 which has a relative low K_m value of 257 μM , but a V_{\max} value comparable to the other individuals. Removing this subject from the dataset provides a CV of 36% for the scaled catalytic efficiency, hence providing a moderate variation in glucuronidation activity for the individuals.

Table 1 Kinetic constants K_m , $V_{\max} \pm \text{SD}$ and catalytic efficiencies for the formation of the metabolite phenylglucuronide of phenol in incubations with pooled and individual female human liver fractions.

Human source	$K_{m(\text{app})}^{\text{a}}$	$V_{\max(\text{app})}^{\text{b}}$	In vitro catalytic efficiency ^c	Scaled $V_{\max(\text{app})}^{\text{d}}$	Scaled catalytic efficiency liver ^e	Age	Race ^f
<u>Pooled microsomes</u>							
	771 \pm 147	33.4 \pm 1.9	43.3	64.1	83.2	33-78	C, AA, H
<u>Individual S9</u>							
H_120	842 \pm 190	6.3 \pm 0.46	7.5	54.4	64.6	57	C
H_251	1213 \pm 337	13.0 \pm 1.3	10.7	111.4	91.8	42	C
H_280	1098 \pm 433	11.8 \pm 1.6	10.8	101.2	92.2	36	C
H_291	1224 \pm 437	5.6 \pm 0.73	4.5	47.7	39.0	18	C
H_393	1024 \pm 426	11.0 \pm 1.6	10.8	94.6	92.3	30	C
H_428	1115 \pm 105	11.5 \pm 0.39	10.3	98.7	88.5	57	C
H_177	1169 \pm 376	6.1 \pm 0.73	5.2	52.3	44.7	45	C
H_205	786 \pm 200	10.7 \pm 0.87	13.7	92.2	117.3	48	C
H_217	257 \pm 72	9.2 \pm 0.54	36.0	79.2	308.4	66	C
H_220	1035 \pm 451	5.7 \pm 0.86	5.5	49.1	47.5	33	C
<u>Statistics</u>							
Mean \pm SD	976 \pm 292	9.1 \pm 2.9	11.5	78.1	98.6		
CV (%)	30	32			79		

^a μM .

^b nmol/min/mg protein in tissue fraction.

^c $\mu\text{l}/\text{min}/\text{mg}$ protein in tissue fraction.

^d $\mu\text{mol}/\text{h}/\text{g}$ liver.

^e ml/h/g liver.

^f C=Caucasians; AA=African American; H=Hispanic.

FORMATION OF PHENYLGLUCURONIDE BY RECOMBINANT UGT ENZYMES

Incubations with cDNA recombinant expressed UGT enzymes were performed to determine which UGT enzymes are able to glucuronidate phenol. Figure 1 presents the formation of phenol glucuronide for each tested UGT during 45 min of incubation under similar conditions. Especially UGT1A6 and UGT1A9 were able to form phenylglucuronide, followed by UGT2B7.

Extrahepatic UGT1A7, UGT1A8 and UGT1A10, which are amongst others differentially expressed in oesophagus, stomach, small intestine, colon, bile duct, lung and kidney (Tukey and Strassburg 2000; Ohno and Nakajin 2009), were also able to glucuronidate phenol, as well as UGT1A1 and UGT2B15. Each of these extrahepatic UGTs and UGT1A1 and 2B15 showed a conversion that was lower than 5% of the sum of phenylglucuronide formed by all individual tested UGTs, under similar screening conditions. Glucuronidation of phenol was not detected for UGT1A3, UGT1A4, UGT2B4, UGT2B10 and UGT2B17 during the 45 min of incubation.

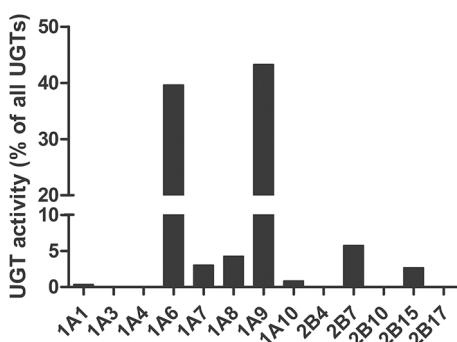


Figure 1 Activity of human UGT isoenzymes for the glucuronidation of phenol tested with Supersomes™ (baculovirus expressed insect microsomal preparations). UGT isoenzyme activity is expressed as the percentage of the sum of the individual UGT isoenzyme activities tested under similar screening conditions (see section Materials and methods). Isoenzyme activities are average values obtained from 2 or 3 independent experiments.

Determination of the contribution of each individual UGT *in vivo* required a correction of V_{max} of each UGT by the respective RAF. To determine the V_{max} and other kinetic values, the rate of glucuronidation by UGT1A6, UGT1A7, UGT1A8, UGT1A9, and UGT2B7 with increasing concentrations of phenol was determined of which the results are presented in Figure 2. The kinetic constants V_{max} , K_m , K_i and k , together with the RAFs and the (scaled) catalytic efficiencies of the UGTs are presented in Table 2. The RAFs determined in the present study for UGT1A6 and UGT1A9 were 3.4 and 0.57 respectively. The RAF for UGT2B7, which is an average of three RAF values from literature is 1.7 (Al-Subeihi et al. 2015; Kato et al. 2012; Saabi et al. 2013). At present no specific probes for UGT1A7, UGT1A8 and UGT1A10 are available, which hampers determination of RAFs for these enzymes. As the metabolic conversion by these enzymes is observed to be lower than for UGT1A6 and UGT1A9 (i.e. lower catalytic efficiency) and as UGT1A7, UGT1A8 and UGT1A10 are only present in extrahepatic tissues these enzymes were not included in the PBK model to evaluate interindividual differences using Monte Carlo simulations. UGT2B7 did not show saturation kinetics, and

showed a linear increase in the rate of glucuronidation with an increasing phenol concentration up to at least 8000 μM . Taking into account the relatively low scaled catalytic efficiency of 1.44 ml/h/g liver for UGT2B7 compared to the scaled catalytic efficiencies of 43.2 and 20.8 ml/h/g liver for UGT1A6 and UGT1A9 respectively, together with the relative low glucuronidation activity of UGT2B7 at phenol concentrations below 1000 μM (Figure 2) which are physiologically relevant, no major contribution of UGT2B7 towards the glucuronidation of phenol in the female human liver was expected.

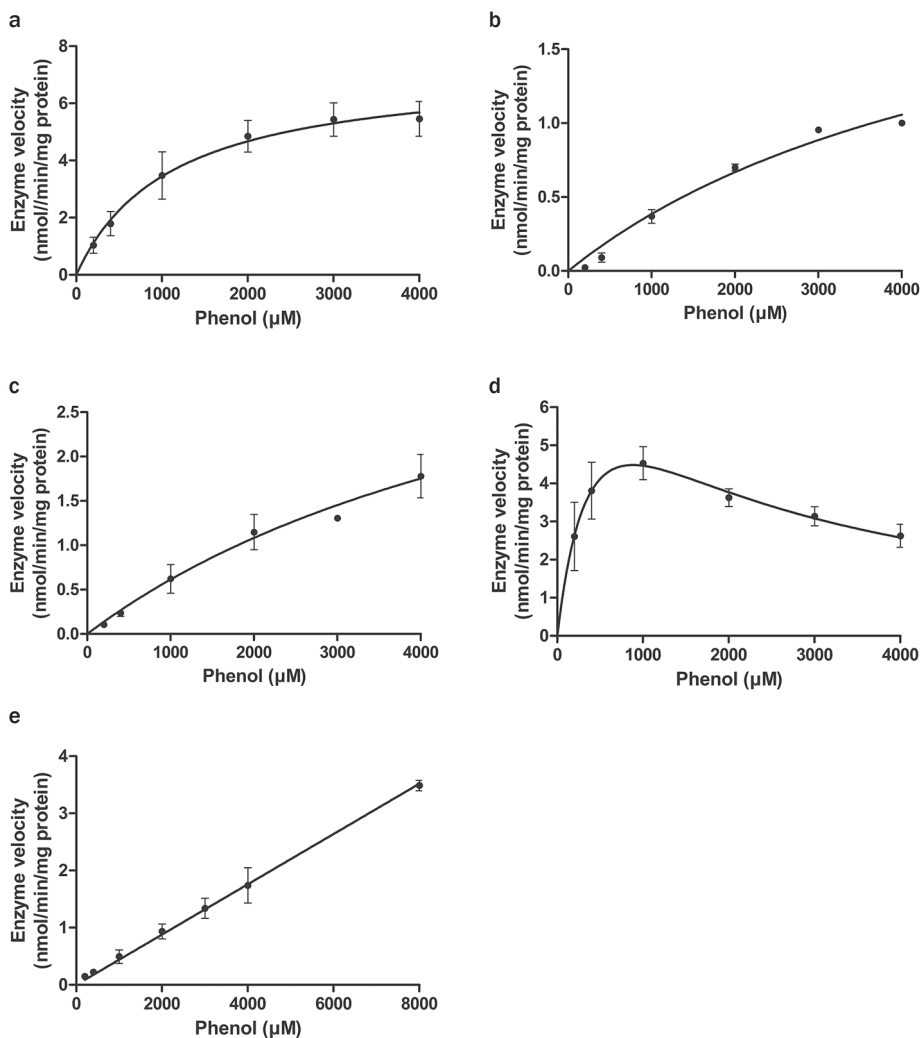


Figure 2 Concentration dependent formation of phenylglucuronide by cDNA recombinant expressed UGT enzymes: a UGT1A6 (n=3 \pm SD), b UGT1A7 (n=2 \pm SD), c UGT1A8 (n=2 \pm SD), d UGT1A9 (n=2 \pm SD), e UGT2B7 (n=3 \pm SD).



Both, UGT1A6 and UGT1A9 have a much higher affinity (reflected by a lower K_m) for phenol compared to the other UGT enzymes. Incubations with UGT1A9 with phenol concentrations above 900 μM resulted in substrate inhibition, but this concentration is above phenol plasma concentrations at relevant dose levels. When taking into account the kinetic plots of the UGTs and the scaled catalytic efficiencies which are corrected by the RAF, UGT1A6 and UGT1A9 are estimated to be the UGTs predominantly contributing to the glucuronidation of phenol in the female human liver and these UGTs were thus included in our PBK model to evaluate interindividual differences using Monte Carlo simulations.

To evaluate the performance of the RAF approach to estimate phenol glucuronidation in female human liver, the sum of the scaled catalytic efficiencies of the individual enzymes UGT1A6 and UGT1A9 was compared to the scaled catalytic glucuronidation efficiency that was measured with pooled female human liver microsomes. It can be concluded that the RAF approach performed reasonably well with the sum of the scaled catalytic efficiencies of the individual enzymes UGT1A6 and UGT1A9 predicting 77% of the total catalytic glucuronidation efficiency that was measured with pooled female human liver microsomes.

Table 2 Kinetic constants V_{\max} , $K_m \pm \text{SD}$, K_i , k , RAF values and catalytic efficiencies of the formation of the metabolite phenylglucuronide of phenol in Supersomes™.

Enzyme	$V_{\max(\text{app})}^{\text{a}}$	$K_{\text{m}(\text{app})}^{\text{b}}$	$K_{\text{i}(\text{app})}^{\text{c}}$	$k_{(\text{app})}^{\text{d}}$	In vitro catalytic efficiency ^e	RAF ^f	Scaled $V_{\max(\text{app})}^{\text{g}}$	Scaled catalytic efficiency liver ^h
UGT1A6	7.3 \pm 0.6	1108 \pm 239	N/A	N/A	6.6	3.4	47.8	43.2
UGT1A7	2.5 \pm 0.6	5565 \pm 1985	N/A	N/A	0.45	- ^j		
UGT1A8	4.6 \pm 1.5	6475 \pm 3096	N/A	N/A	0.71	- ^j		
UGT1A9	9.7 \pm 3.3	509 \pm 288	1529 \pm 834	N/A	19.0	0.57	10.6	20.8
UGT2B7	- ^j	- ^j	N/A	0.44E-3	0.44	1.7 ^k		1.44

^a nmol/min/mg protein.

^b μM .

^c μM .

^d nmol/min/mg protein/ μM substrate.

^e $\mu\text{l}/\text{min}/\text{mg}$ protein. In case of UGT2B7 the catalytic efficiency is defined by the slope of the linear relation between the rate of formation as a function of the substrate concentration.

^f -

^g $\mu\text{mol}/\text{h}/\text{g}$ liver.

^h ml/h/g liver.

ⁱ Could not be derived because of linear kinetics.

^j No specific probe available.

^k Average of three RAF values from literature (Al-Subeihi et al. 2015; Kato et al. 2012; Saabi et al. 2013).

N/A: not applicable.

PBK MODELLING, MONTE CARLO SIMULATIONS AND CSAF

Given that in the present study the phenol PBK model was defined with some updated kinetic parameters an updated sensitivity analyses was performed (See supplementary data A). This analysis confirmed that especially the kinetics for glucuronidation of phenol in the liver and the oral absorption coefficient k_a were parameters that influenced the maximum predicted phenol plasma concentration (C_{max}).

Two methods were applied to evaluate the influence of interindividual variation in glucuronidation on phenol plasma concentrations in the female human population. At first, variation in phenol plasma levels was determined for a group of ten human females. With the kinetic constants obtained in the present study for the ten female subjects, PBK models were developed for each individual female. Figure 3 presents the predicted phenol plasma C_{max} for each female at an oral dose of 25 mg/kg bw obtained with the PBK model. The geometric mean phenol plasma C_{max} of the ten females is predicted to be 152 μM and the difference between the highest and the lowest C_{max} of phenol is 3.2-fold. The geometric CV of the predicted C_{max} values is 36%.

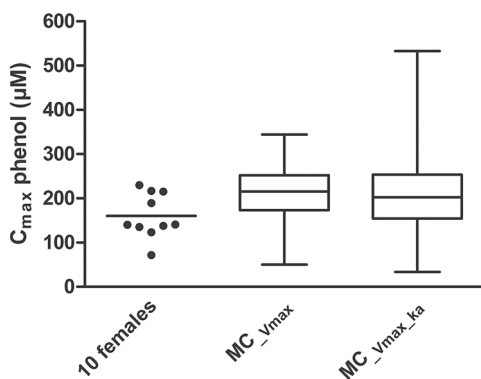


Figure 3 Box and whisker plot representing the distribution of maximum plasma concentrations of phenol (C_{max}) at an oral dose of 25 mg/kg bw predicted with the PBK models for the ten females (dots represent values for individual females) and distributions predicted with PBK models linked with Monte Carlo (MC) simulation for 9956 individuals with a PBK model with interindividual variation in the V_{max} of UGT1A6 and UGT1A9 and for 9907 individuals with interindividual variation in the V_{max} of UGT1A6 and UGT1A9 and in the k_a for oral absorption. The whiskers represent the minimum and maximum phenol plasma C_{max} of each population.

Secondly, a Monte Carlo simulation ($n=9956$) was performed at an oral dose of 25 mg/kg bw to evaluate the interindividual variation in phenol plasma concentrations that could occur in a larger female human population, taking interindividual variation in phenol glucuronidation by UGT1A6 and UGT1A9 into account. The distribution of parameters used in the Monte Carlo simulations is included in Table 3. Figure 3 presents a box and whisker plot visualising the

spread in the C_{max} of phenol for this population. The geometric mean phenol plasma C_{max} is 202 μM , which is 1.3-fold higher than the geometric mean for the ten individuals. The difference between the highest and the lowest phenol plasma C_{max} predicted with the Monte Carlo simulations is 6.8-fold, is larger than the difference in C_{max} of 3.2-fold observed for the 10 individuals. The geometric CV of the predicted C_{max} values is 31%, which is comparable to the geometric CV of the 10 individuals. Comparing the phenol plasma C_{max} predicted for the ten individuals and the Monte Carlo simulations with variation in UGT, indicates that the small group of ten individuals reasonably represents the geometric mean phenol plasma kinetics of a large population, but that for defining the outer boundaries of the population distribution which are relevant to identify sensitive individuals, a Monte Carlo simulation appears more appropriate.

Table 3 Distribution of parameters used in the Monte Carlo simulations.

Parameter	Mean	CV (%)	Min-max simulation values	Fold-variation
$V_{max_UGT1A6(\text{app})}^a$	7.3	76	0.76 - 43.8	57
$V_{max_UGT1A9(\text{app})}^a$	9.7	55	1.81 - 39.6	22
ka^b	7.62	30	3.0 - 17.6	5.8

^a nmol/min/mg protein.

^b /h, value obtained from the rat in situ intestinal perfusion study of Humphrey et al. (1980).

In a subsequent step, C_{max} of phenol in the female population at an oral dose of 25 mg/kg bw was calculated with the PBK model linked with the Monte Carlo analysis (n=9907) that included not only variation in UGT1A6 and UGT1A9 activity but also variation in ka . A box and whisker plot visualising the spread of C_{max} of this analysis is included in Figure 3, and Figure 4 presents the frequency distribution of the predicted C_{max} of phenol. The geometric mean of the C_{max} of phenol in the simulated population is 194 μM and the median C_{max} in this population is 202 μM . The difference between the highest and the lowest C_{max} value in the simulated population at the dose of 25 mg/kg bw is 15.8-fold. Comparing the Monte Carlo predictions with and without ka as a variable parameter indicates that introducing variation in ka in the Monte Carlo analysis increased the difference between the highest and lowest predicted C_{max} value in the population distribution from 6.8-fold to 15.8-fold. This result also demonstrates that variation in ka provides an important contribution to variation in the population distribution of the C_{max} of phenol. Overall, the Monte Carlo simulation including variation in V_{max} of the UGTs and ka provides the best insight in interindividual differences in the kinetics of phenol.

The data now obtained for the distribution of the plasma C_{max} of phenol in the population can be used to obtain a chemical specific adjustment factor (CSAF) for the interindividual

variation in the kinetics of phenol. Such a CSAF can be defined based on the ratio of the 90th or the 99th percentile of the population distribution divided by the mean value (IPCS 2005). For this analysis the results obtained with Monte Carlo simulations that included variation in UGT1A6, UGT1A9 and k_a were used. The geometric mean, the 90th and the 99th percentiles of the plasma C_{max} of phenol are 194, 303 and 391 μM , respectively. The CSAF thus obtained amounted to 1.6 when using the 90th percentile, while the CSAF amounted to 2.0 when the 99th percentile was used thus including even the most sensitive individuals. The CSAF of 2.0 could replace the default uncertainty factor of 3.16 that accounts for interindividual human kinetic differences (IPCS 2005).

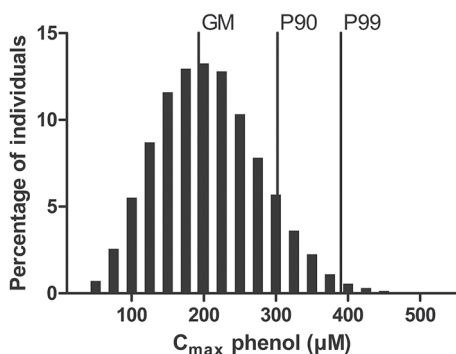


Figure 4 Frequency distribution for the maximum predicted plasma concentration (C_{max}) of phenol in 9907 individuals after Monte Carlo simulation including variation in V_{max} of UGT1A6, UGT1A9 and k_a with our PBK model for phenol at an oral dose of 25 mg/kg bw. The GM, P90 and P99 represent the geometric mean, the 90th and the 99th percentile of the distribution corresponding to 194, 303 and 391 μM phenol in plasma.

DOSE-RESPONSE ANALYSIS

In an additional step the PBK models were used to analyse the consequences of the detected interindividual variation in C_{max} values for the predicted in vivo dose-response curves for the developmental toxicity of phenol in human. To this end, the in vitro effect concentrations that were previously obtained with the EST (Strikwold et al. 2012) were converted to in vivo effective doses applying PBK-based reverse dosimetry. First reverse dosimetry was applied using the PBK model for the average female human based on the average kinetic constants derived from the incubations with pooled female human liver microsomes in the present study. The resulting dose-response curve is presented in Figure 5. The BMDL_{05} derived from this dose-response curve of the average female was 27 mg/kg bw and can serve as a PoD for the risk assessment. In a next step the interindividual variation in C_{max} and k_a values was taken into account by dividing the dose-response curve data with the CSAF obtained for the 99th percentile. The curve thus obtained (Figure 5) reflects the consequences of the

interindividual variability in phenol kinetics for the ultimate dose-response curve for human developmental toxicity presenting the curve for the most sensitive females in the population.

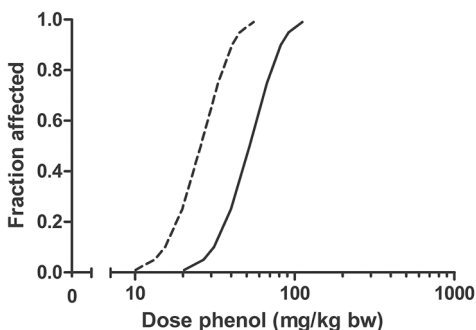


Figure 5 Dose-response curve (95% lower confidence limit) predicted with the in vitro PBK approach, visualising the average (solid black line) and the susceptible (dashed black line) individuals of the human population. The curve for the susceptible individuals in the population is derived by applying the CSAF (99th percentile of C_{max}) to the dose-response curve of the average population.

DISCUSSION

The present study aimed to demonstrate an approach that combines in vitro toxicity data, PBK modelling and Monte Carlo simulations to assess the consequences of human interindividual variation in kinetics for phenol induced developmental toxicity. The sensitivity analysis of the PBK model of phenol for the average female population as predicted in the present study revealed that especially the oral absorption coefficient (k_a) and glucuronidation of phenol in the liver were parameters that influenced the maximum predicted phenol plasma concentration (C_{max}) and these parameters were therefore included in the evaluation of interindividual variation in the present study. At first, glucuronidation of phenol was determined with ten individual human female liver fractions and the kinetic constants obtained were used to define individual PBK models of phenol for each female which were used to predict phenol plasma levels. Secondly, to enable prediction of interindividual variation in a larger human population, Monte Carlo simulations were performed in connection with our PBK model for phenol, simulating interindividual human variation on the basis of the conversion of phenol by UGT enzymes and literature reported information on variation in expression of these enzymes. In a final step also variability in the oral absorption coefficient was included in the analyses.

UGT enzymes involved in glucuronidation of phenol have not been fully characterised before. Our studies with SupersomesTM revealed that UGT1A1, UGT1A6, UGT1A7, UGT1A8,

UGT1A9, UGT1A10, UGT2B7 and UGT2B15 are intrinsically able to glucuronidate phenol. The present study revealed that UGT1A6 is the primary UGT responsible for the glucuronidation of phenol in the liver followed by UGT1A9. The scaled catalytic efficiency of the other enzymes capable to glucuronidate phenol was lower than that of UGT1A6 and UGT1A9, which implies that these UGT enzymes will not contribute to the *in vivo* glucuronidation of phenol to a significant extent. The importance of UGT1A6 and UGT1A9 in the glucuronidation of phenol is in line with the involvement of these UGT enzymes in the glucuronidation of a series of *p*-substituted phenols (Ethell et al. 2002).

In the present study variability in phenol glucuronidation was assessed based on *in vitro* kinetic data obtained with experiments using UGT isoforms and human variation in expression of these UGT derived from the literature from a human liver bank of 54 people (man and woman) (Court 2010). Court (2010) did not find any significant effect of gender, age (when age > 20 years) and smoking on the glucuronidation activity in the liver by UGT1A6 and UGT1A9. However, consuming alcohol was associated with an increased glucuronidation of the specific probes serotonin (UGT1A6) and propofol (UGT1A9). Additionally, drug intake, diet or environmental factors (Guillemette 2003) may also influence the activity of UGT enzymes as well as genetic polymorphisms. As no gender differences were observed for UGT1A6 and UGT1A9 (Court 2010) the reported CVs were considered adequate and used to simulate developmental toxicity in the female population in the Monte Carlo modelling.

Within the present study the focus was on including variability in the most sensitive parameters that influence the model outcome. For this reason, the kinetic constants for glucuronidation of phenol and the oral uptake rate constant were varied in the Monte Carlo simulations. Little information exists on variation in uptake of compounds from the intestine, whereas from our Monte Carlo analysis with and without variation in k_a it can be concluded that variation in k_a provides an important contribution to variation in the population distribution of C_{max} of phenol. It is expected that oral absorption of the phenols is driven by passive diffusion. Factors like gastric emptying time, gastrointestinal motility, bile secretion and pH may in general influence passive diffusion (Martinez and Amidon 2002), but it is unknown if these factors give rise to the CV of 30% that was applied in the present study representing a moderate level of variation (Covington et al. 2007), or whether the CV of 30% should be considered a worst case approach to model interindividual variability in k_a . Further research towards interindividual variation in the oral uptake rate may be undertaken to define a CV representing variation in the human population for this parameter.

For phenol, the population distribution of the phenol plasma concentration generated by the Monte Carlo simulation including variation in UGT1A6, UGT1A9 and k_a provided information to predict a CSAF, which was calculated by the ratio of C_{max} of phenol at the 99th percentile and the geometric mean, resulting in a CSAF of 2.0. Comparing the CSAF of 2.0 derived in the present study to the default uncertainty factor of $10^{0.5}$ (=3.16) for interindividual

human kinetic differences shows that for phenol the default safety factor is adequately protective. The CSAF could replace the default uncertainty factor for interindividual kinetic differences of 3.16 when one would derive a human health-based guidance value for phenol.

Reverse dosimetry was applied with the PBK model for the average individual providing an in vivo dose-response curve from which a BMDL₀₅ of 27 mg/kg bw for the average female in the population was derived. When this BMDL₀₅ is used as a PoD for deriving a health-based guidance value, in addition to the CSAF of 2.0 for interindividual human kinetic differences, also other uncertainty factors may be needed. This includes first of all an uncertainty factor of 10^{0.5} (=3.16) accounting for human variability in toxicodynamics. Furthermore, one could argue that because the extrapolation was based on in vitro toxicity data obtained with cells of animal origin (mouse ES-D3 cells) an additional uncertainty factor of 10^{0.4} (=2.5) should be applied for interspecies differences in toxicodynamics. The default uncertainty factor of 10^{0.6} (=4.0) accounting for interspecies kinetic differences (IPCS 2005) can be omitted because the PBK model of phenol describes the kinetics directly for humans. The total uncertainty factor thus obtained amounts 15.9 and applying this factor to the PoD of 27 mg/kg bw that was derived from the in vivo dose-response curve of phenol for the average female population predicted with in vitro PBK-based reverse dosimetry would provide a guidance value of 1.7 mg/kg bw/d. This value is 3.4-fold higher than the TDI of 0.5 mg/kg bw/d derived from a BMDL₁₀ of 52 mg/kg bw for maternal toxicity obtained from a developmental toxicity study (Argus 1997) using an overall uncertainty factor of 100 (EFSA 2013). This difference is mainly due to the use of a CSAF of 2.0 instead of the default value of 3.16 and not applying the uncertainty factor of 4.0 accounting for interspecies kinetic differences because the PBK model for phenol directly applies for humans. Thus, the difference is not caused by the fact that the PoD was derived from an in vitro-PBK based alternative approach, instead of taken from an in vivo developmental toxicity study.

It can be argued whether an additional uncertainty factor should be applied to account for uncertainties regarding the use of the in vitro PBK approach, for example regarding differences in sensitivity between an in vitro toxicity assay and an in vivo system toward a test compound and uncertainties that may result from PBK models that are just defined by in vitro and silico predicted input parameters. So far, PoDs for developmental toxicity predicted with the in vitro PBK approach are within a 10-fold difference compared to in vivo reported developmental toxicity PoDs (Louisse et al. 2010; Louisse et al. 2014; Strikwold et al. 2013; Strikwold et al. 2016). Based on these data it might be advocated to replace the default uncertainty factor of 2.5 for interspecies toxicodynamic differences by a factor of 10 when a PoD is used that is derived with the in vitro PBK approach (when cells from animal origin are used). Applying this uncertainty factor of 10 together with the CSAF of 2.0 for interindividual differences in human kinetics and the uncertainty factor of 3.16 that accounts for interindividual human dynamic differences, provides a total uncertainty factor of 63.2,

resulting in a guidance value of 0.43 mg/kg bw/d for phenol which closely resembles the current TDI of 0.5 mg/kg bw/d.

Finally, it is of importance to stress that during pregnancy, biochemical and physiological changes occur which may possibly affect phenol plasma levels. In humans, glucuronidation is controlled by a wide array of nuclear receptors of which some are influenced by sex specific hormones (i.e. estradiol, progesterone) (Jeong 2010), which change during the course of pregnancy and may possibly lead to an increased glucuronidation. The present study did not explicitly take into account variation in UGT activity during pregnancy, because refining model predictions is not straightforward when the glucuronidation activity changes during the course of pregnancy. However, since results indicate that glucuronidation in humans may increase during pregnancy (Miners et al. 1986), phenol plasma levels may be lower than predicted in the current study where the kinetic parameters for the PBK model were determined for the non-pregnant female population for which data and microsomal samples were available. Given that increased glucuronidation will result in lower and thus less toxic plasma levels of phenol it can be concluded that the results obtained are adequately protective.

In conclusion, this study exemplifies a modelling approach to integrate in vitro toxicity data, PBK modelling and Monte Carlo simulations to predict safe human guidance values taking into account interindividual human kinetic variation. The strength of this approach is that it provides a risk assessment that is directly relevant to the human situation, based on only in vitro and in silico data.

SUPPLEMENTARY DATA A

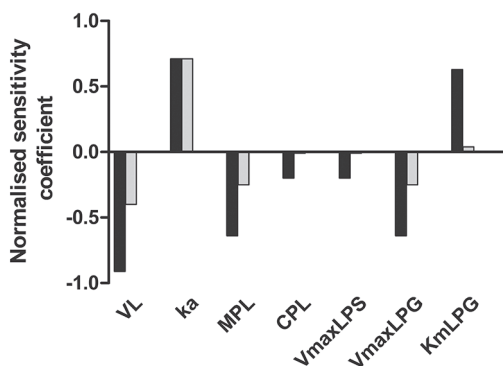


Figure S1 Normalised sensitivity coefficient for parameters of the PBK model of phenol in human based on C_{max} values obtained after a single oral dose of 1.5 mg/kg bw (black bars) and 150 mg/kg bw (grey bars). Normalised sensitivity coefficients ≥ 0.2 are presented. VL=fraction liver tissue, ka=oral absorption coefficient, MPL=liver microsomal protein yield, CPL=liver cytosolic protein yield, VmaxLPS=unscaled maximum rate of sulfation of phenol in liver, VmaxLPG= unscaled maximum rate of glucuronidation of phenol in liver, KmLPG=Michaelis-Menten constant for glucuronidation of phenol in liver.

REFERENCES

- Al-Subeihi AAA, Alhusainy W, Kiwamoto R, Spenkelink B, van bladeren PJ, Rietjens IMCM, Punt A (2015) Evaluation of the interindividual human variation in bioactivation of methyleugenol using physiologically based kinetic modeling and Monte Carlo simulations. *Toxicol Appl Pharmacol* 283:117-126
- Argus (1997) Oral (gavage) developmental toxicity study of phenol in rats. Protocol Number: Argus 916-011. Argus Research Laboratories, Inc., Horsham, PA
- Barter ZE, Bayliss MK, Beaune PH, Boobis AR, Carlile DJ, Edwards RJ, Houston JB, Lake BG, Lipscomb JC, Pelkonen OR, Tucker GT, Rostami-Hodjegan A (2007) Scaling factors for the extrapolation of in vivo metabolic drug clearance from in vitro data: reaching a consensus on values of human microsomal protein and hepatocellularity per gram of liver. *Curr Drug Metab* 8:33-45
- Court MH (2005) Isoform-selective probe substrates for in vitro studies of human UDP-glucuronosyltransferases. *Methods Enzymol* 400:104-116
- Court MH (2010) Interindividual variability in hepatic drug glucuronidation: studies into the role of age, sex, enzyme inducers, and genetic polymorphism using the human liver bank as a model system. *Drug Metab Rev* 42:209-224
- Covington TR, Gentry PR, Van Landingham CB, Andersen ME, Kester JE, Clewell HJ (2007) The use of Markov chain Monte Carlo uncertainty analysis to support a public health goal for perchloroethylene. *Regul Toxicol Pharmacol* 47:1-18
- Crespi CL (1995) Xenobiotic-metabolizing human cells as tools for pharmacological and toxicological research. *Advances in Drug Research*. Academic Press, New York, pp 179-235
- Dajani R, Cleasby A, Neu M, Wonacott AJ, Jhoti H, Hood AM, Modi S, Hersey A, Taskinen J, Cooke RM, Manchee GR, Coughtrie MWH (1999) X-ray crystal structure of human dopamine sulfotransferase, *SULT1A3*. Molecular modeling and quantitative structure-activity relationship analysis demonstrate a molecular basis for sulfotransferase substrate specificity. *J Biol Chem* 274:37862-37868
- EC (2007) Corrigendum to Regulation (EC) No 1907/2006 of the European Parliament and of the Council of 18 December 2006 concerning the Registration, Evaluation, Authorisation and Restriction of Chemicals (REACH), establishing a European Chemicals Agency, amending Directive 1999/45/EC and repealing Council Regulation (EEC) No 793/93 and Commission Regulation (EC) No 1488/94 as well as Council Directive 76/769/EEC and Commission Directives 91/155/EEC, 93/67/EEC, 93/105/EC and 2000/21/EC. *Off J Eur Union* L136:3-280
- EC (2009) Regulation (EC) No 1223/2009 of the European parliament and of the council of 30 November 2009 on cosmetic products. *Off J Eur Union* L342:59-209
- EFSA (2013) Scientific Opinion on the toxicological evaluation of phenol. *EFSA Journal* 11:3189, 44 pp
- Ethell BT, Ekins S, Wang J, Burchell B (2002) Quantitative structure activity relationships for the glucuronidation of simple phenols by expressed human *UGT1A6* and *UGT1A9*. *Drug Metab Dispos* 30:734-738
- Guillemette C (2003) Pharmacogenomics of human UDP-glucuronosyltransferase enzymes. *Pharmacogenomics J* 3:136-158
- Humphrey MJ, Filer CW, Jeffery DJ, Langley PF, Wadds GA (1980) The availability of carfecillin and its phenol moiety in rat and dog. *Xenobiotica* 10:771-778
- IPCS (2005) Chemical-specific adjustment factors for interspecies differences and human variability: guidance document for use of data in dose/concentration-response assessment. World Health Organization, Geneva
- Jeong H (2010) Altered drug metabolism during pregnancy: Hormonal regulation of drug-metabolizing enzymes. *Expert Opin Drug Metab Toxicol* 6:689-699
- Kato Y, Nakajima M, Oda S, Fukami T, Yokoi T (2012) Human UDP-glucuronosyltransferase isoforms involved in haloperidol glucuronidation and quantitative estimation of their contribution. *Drug Metab Dispos* 40:240-248
- Krishnaswamy S, Duan SX, Von Moltke LL, Greenblatt DJ, Court MH (2003) Validation of serotonin (5-hydroxytryptamine) as an in vitro substrate probe for human UDP-glucuronosyltransferase (*UGT*) 1A6. *Drug Metab Dispos* 31:133-139
- Louisse J, Bosgra S, Blaauboer BJ, Rietjens IMCM, Verwei M (2014) Prediction of in vivo developmental toxicity of all-trans-retinoic acid based on in vitro toxicity data and in silico physiologically based kinetic modeling. *Arch Toxicol* 89:1135-1148
- Louisse J, de Jong E, van de Sandt JJM, Blaauboer BJ, Woutersen RA, Piersma AH, Rietjens IMCM, Verwei M (2010) The use of in vitro toxicity data and physiologically based kinetic modeling to predict dose-response curves for in vivo developmental toxicity of glycol ethers in rat and man. *Toxicol Sci* 118:470-484
- Martinez MN and Amidon GL (2002) A mechanistic

approach to understanding the factors affecting drug absorption: a review of fundamentals. *J Clin Pharmacol* 42:620-643

Medinsky MA, Leavens TL, Csanády GA, Gargas ML, Bond JA (1994) In vivo metabolism of butadiene by mice and rats: A comparison of physiological model predictions and experimental data. *Carcinogenesis* 15:1329-1340

Miners JO, Robson RA, Birkett DJ (1986) Paracetamol metabolism in pregnancy. *Br J Clin Pharmacol* 22:359-362

National Research Council (2007) Toxicity testing in the 21st century: a vision and a strategy. The National Academy Press, Washington, DC

Ohno S and Nakajin S (2009) Determination of mRNA expression of human UDP-glucuronosyltransferases and application for localization in various human tissues by real-time reverse transcriptase-polymerase chain reaction. *Drug Metab Dispos* 37:32-40

Saabi AA, Allorge D, Sauvage FL, Tournel G, Gaulier JM, Marquet P, Picard N (2013) Involvement of UDP-glucuronosyltransferases UGT1A9 and UGT2B7 in ethanol glucuronidation, and interactions with common drugs of abuse. *Drug Metab Dispos* 41:568-574

Strikwold M, Spenkelink A, de Haan LHJ, Woutersen RA, Punt A, Rietjens IMCM (2016) Integrating in vitro data and physiologically based kinetic (PBK) modeling to assess the in vivo potential developmental toxicity of a series of phenols. Submitted for publication

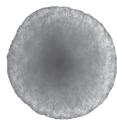
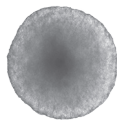
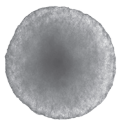
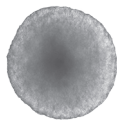
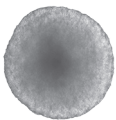
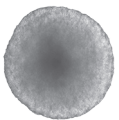
Strikwold M, Spenkelink B, Woutersen RA, Rietjens IMCM, Punt A (2013) Combining in vitro embryotoxicity data with physiologically based kinetic (PBK) modelling to define in vivo dose-response curves for developmental toxicity of phenol in rat and human. *Arch Toxicol* 87:1709-1723

Strikwold M, Woutersen RA, Spenkelink B, Punt A, Rietjens IMCM (2012) Relative embryotoxic potency of p-substituted phenols in the embryonic stem cell test (EST) and comparison to their toxic potency in vivo and in the whole embryo culture (WEC) assay. *Toxicol Lett* 213:235-242

Tukey RH and Strassburg CP (2000) Human UDP-glucuronosyltransferases: metabolism, expression, and disease. *Annu Rev Pharmacol Toxicol* 40:581-616

Zhang X, Tsang AM, Okino MS, Power FW, Knaak JB, Harrison LS, Dary CC (2007) A physiologically based pharmacokinetic/pharmacodynamic model for carbofuran in sprague-dawley rats using the exposure-related dose estimating model. *Toxicol Sci* 100:345-359





CHAPTER 6

**General discussion and future
perspectives**

OVERVIEW

Alternatives to animal testing are increasingly important for toxicological safety assessments of chemicals. Especially a number of recent regulatory shifts within the European Union (EU) have made the development of non-animal based approaches in chemical risk assessment more important (EC 2007; EC 2009), as well as economical limitations, ethical objections and concerns about the predictivity of animal based safety tests. During the past decades, many *in vitro* assays have been developed to test the toxicity of compounds, but until now they are mainly used for screening and prioritising chemicals with limited applications in quantitative risk assessment. An important reason for the limited use of *in vitro* data in current risk assessment practice is that *in vitro* toxicity outcomes are not directly applicable to the *in vivo* situation. More specifically, *in vitro* derived concentration-response curves cannot provide an *in vivo* dose-response curve from which a point-of-departure (PoD) for the risk assessment can be derived. Converting *in vitro* effective toxicity concentrations into *in vivo* effective dose levels by applying physiologically based kinetic (PBK) modelling was the major aim of the present thesis. In the present thesis we demonstrated the potential of a combined *in vitro* PBK-based modelling approach to translate *in vitro* toxicity data to *in vivo* toxicity values for rat and human predicting *in vivo* dose-response curves that allow definition of a PoD for risk assessment. We used *in silico* and *in vitro* defined PBK model parameters, and assessed interindividual variability by combining the *in vitro* PBK approach with Monte-Carlo simulations.

The present thesis focussed on predicting developmental toxicity using the murine embryonic stem cell differentiation test (EST) as a representative *in vitro* assay for this endpoint. Phenol and a series of *p*-substituted phenols were selected as the model compounds, representing a series of compounds that have not been evaluated before in the EST. The selected phenols have different chemical properties regarding lipophilicity and reactivity.

In chapter 2 we first evaluated the applicability of the EST to test the potential embryotoxicity for the selected series of phenols. To this purpose, toxicity data obtained with the EST for the phenols were compared to potency data reported for these compounds in the literature in the whole embryo culture (WEC) assay, being another *in vitro* assay for developmental toxicity. Next, the *in vitro* potency data generated with the EST were also compared to literature data reporting results from *in vivo* developmental toxicity tests. We found that the potency ranking of the EST was identical to the potency ranking of the WEC assay. However, the compound *p*-heptyloxyphenol was relatively more potent in the EST compared to the WEC assay, which may possibly result from the different endpoints that were used to define embryotoxicity and differences in the kinetic behaviour of the test compound in both assays. Furthermore, we found that the EST did not provide a similar potency ranking for the phenols when compared to *in vivo* developmental toxicity data obtained from literature.

The reason for the observed disparities may be diverse, and insight into the causes of these disparities is necessary to ultimately enhance the applicability of the EST in practice (Spielmann et al. 2006). For the present set of phenols, we hypothesised that combining *in vitro* derived toxicity values with kinetic data describing the absorption, distribution, metabolism and excretion (ADME) of the phenols *in vivo* may (partly) explain the disparities observed between the *in vitro* and the *in vivo* relative embryotoxic potencies. Such an integration of *in vitro* toxicity data with kinetic modelling may improve predictions of *in vitro* derived embryotoxic potency data of the test compounds, and theoretically may also be applied to quantitatively predict *in vivo* effective dose levels as well as PoDs enhancing the applicability of *in vitro* assays for quantitative risk assessment purposes.

In chapter 3 of the present thesis we demonstrated that combining *in vitro* embryotoxicity data derived from the EST with PBK modelling based reverse dosimetry, could indeed adequately translate *in vitro* effect concentrations to *in vivo* effective dose levels from which a PoD could be derived, with phenol as the model compound of interest. We developed PBK models for phenol in rat and human based on data obtained from *in silico* and *in vitro* experiments and data from the literature. Important parameters describing the ADME of phenol *in vivo* were the oral absorption coefficient and the metabolism of phenol. Glucuronidation and sulfation of phenol in different organs were included in the PBK models for rat and human based on *in vitro* data obtained from incubations with rat and human subcellular organ fractions. *In vitro* effect-concentrations obtained with the EST were translated to *in vivo* effective dose levels applying PBK-based reverse dosimetry, from which an *in vivo* dose-response curve and a PoD was derived. The predicted PoD for phenol fell within the variation of PoDs obtained from studies reported for developmental toxicity of phenol in the rat, indicating the applicability of this approach for quantitative hazard and risk assessment purposes.

After providing a proof-of-principle for the extrapolation of *in vitro* toxicity data to the *in vivo* situation using PBK-based reverse dosimetry for the compound phenol, it was investigated in chapter 4 of this thesis whether the *in vitro* PBK-based reverse dosimetry approach would also be successful for predicting *in vivo* potential developmental toxicity of the *p*-substituted phenolic congeners tested in the EST. Furthermore it was investigated whether the approach could overcome the difference observed between the *in vitro* and *in vivo* derived relative embryotoxic potencies for the phenols, particularly for *p*-heptyloxyphenol. The PBK model for phenol in the rat was used as a starting point to construct PBK models for the phenols that were included in this study. Adjustments that were made consisted of modelling glucuronidation in the liver as the sole route of metabolism as this was found to be the principle metabolic pathway and addition of a fat compartment because of the relatively high lipophilicity of *p*-heptyloxyphenol. Moreover, we also included *in vitro* transport experiments to predict the relative oral absorption of the phenols, and added a placental/foetal

compartment to quantify transfer of the compounds from mother to foetus and vice versa. With the *in vitro* PBK-based reverse dosimetry approach we could overcome the disparities that were observed between the *in vitro* and the *in vivo* relative potencies of the phenols, also for the compound p-heptyloxyphenol for which relative toxicity compared to phenol was more than three orders of magnitude higher in the EST while differed less than one order of magnitude *in vivo* (chapter 2). The most important parameter underlying the improved prediction for p-heptyloxyphenol, when combining the results of the EST with PBK modelling based reverse dosimetry, was the relatively rapid metabolism of this compound by glucuronidation. Moreover, the relatively low placental transport of heptyloxyphenol and the relatively high tissue:plasma partition coefficient of p-heptyloxyphenol compared to those for the other phenols were factors that contributed to an improved prediction.

In chapter 3 we have applied the *in vitro* PBK approach to predict developmental toxicity of phenol for the average human. In this chapter we did not take into account the variation in the population that might occur in sensitivity to developmental toxicity of phenol, as a result of interindividual human variation in kinetics, while such information may be valuable for risk assessors to derive human guidance values. In chapter 5 of this thesis we demonstrated an approach that combines *in vitro* toxicity data, physiologically based kinetic (PBK) modelling and Monte Carlo simulations to assess the effects of human interindividual variation in kinetics for phenol induced developmental toxicity. We used two approaches to obtain insight in interindividual differences in phenol glucuronidation. One approach involved *in vitro* quantification of the kinetic constants for glucuronidation of phenol using subcellular liver samples from ten individual females. The kinetic constants obtained for each female were included in our previously developed PBK model for phenol (Strikwold et al. 2013). The predicted difference between the maximum phenol plasma concentrations (C_{max}) of the ten individual females was limited (3.2-fold). The other approach involved quantification of glucuronidation of phenol by UGT enzymes. The UGT specific kinetic constants obtained were included in the PBK model of phenol (Strikwold et al. 2013) together with information about the variation in activity of these UGTs in the population. Subsequently, Monte Carlo simulations were performed generating a population distribution of the C_{max} of phenol, which showed a 6.8-fold difference between the highest and the lowest predicted C_{max} value, which is higher than the difference in C_{max} observed for the ten females. In a next step interindividual variation for the oral absorption coefficient, which according to the sensitivity analysis (Strikwold et al. 2013) also highly influenced the model outcome, was included in the Monte Carlo simulations as well providing a 15.8-fold difference between the highest and the lowest predicted C_{max} value. Based on the results obtained from the latter Monte Carlo simulation a chemical specific adjustment factor (CSAF) of 2.0 was derived, that covers interindividual human kinetic variation. Based on this outcome, it was concluded that the default safety factor of 3.16 applied for interindividual human kinetic differences in the safety assessment of

chemicals seems adequate protective. Then, PBK-based reverse dosimetry was applied in which the *in vitro* effect concentrations obtained from the EST were set equal to *in vivo* plasma concentrations using C_{\max} as an appropriate dose metric, generating effective dose levels. Benchmark dose modelling provided a dose-response curve and a PoD (BMDL₀₅) for the risk assessment. Dividing the dose-response curve data obtained with *in vitro* PBK-based reverse dosimetry, with the CSAF obtained for the 99th percentile of the population provided a dose-response curve that reflects the consequences of the interindividual variability in phenol kinetics for the developmental toxicity of phenol presenting the dose-response curve for the most sensitive individuals. Altogether, we demonstrated an approach that provided a toxicity estimate that is directly relevant to the human situation including interindividual variation, which can be applied for the risk assessment of chemicals, without the need for animal testing.

Overall, this thesis demonstrated the potential of the combined *in vitro* PBK approach to translate *in vitro* toxicity data to *in vivo* toxicity values for rat and human and to predict *in vivo* dose-response curves and define a PoD for risk assessment. The next sections discuss the most critical steps in the presented approach in some more detail, together with some important future perspectives. Topics discussed include especially:

- The use of the EST for predicting developmental toxicity *in vitro*
- PBK modelling considerations
- The use of different kinetic reverse dosimetry approaches to perform *in vitro* to *in vivo* extrapolations (IVIVE)
- The possibility to take interindividual variations into account and
- Future perspectives

THE USE OF THE EST FOR PREDICTING DEVELOPMENTAL TOXICITY IN VITRO

A first topic to discuss in some more detail is the use of the EST for predicting developmental toxicity, both in comparison to the WEC assay, being another *in vitro* assay for developmental toxicity as well as in comparison to *in vivo* developmental toxicity.

COMPARISON EST AND WEC ASSAY

For the series of phenols included in the present thesis, the toxic potency data obtained with the EST were close to the toxic potency data reported in the WEC assay, except for

p-heptyloxyphenol which was much more potent in the EST compared to the WEC assay. Reasons for the difference in the observed toxicity between the assays for p-heptyloxyphenol may be multiple, of which some may be related to the lipophilic nature of p-heptyloxyphenol ($\log D_{7.0} = 4.4$ (ACD/Labs 2015)). Inconsistent in vitro results between the EST and the WEC assay have also been observed for the lipophilic compound retinoic acid ($\log D_{7.0} = 4.0$ (ACD/Labs 2015)), for which the EC_{50} in the EST was 80-fold lower than the EC_{50} in the WEC assay (Louisse et al. 2011). Moreover, the EST appeared also to be up to 11-fold more sensitive than the WEC assay towards a series of six triazoles (de Jong et al. 2011) which have moderately high $\log D_{7.0}$ values varying between 2.7 and 3.9 (ACD/Labs 2015).

As discussed in chapter 2, the lower albumin fraction in the EST compared to the WEC assay may result in a higher free fraction of p-heptyloxyphenol in the EST, which may enhance toxicity. In addition, it was reported that phenols easily reach the conceptus and especially p-heptyloxyphenol was found to accumulate in the WEC assay (Fisher et al. 1993), indicating that the yolk sac hardly forms any barrier for compounds to move from the medium to the conceptus in the WEC assay and that the affinity for the conceptus is high, especially for the lipophilic compound p-heptyloxyphenol (Fisher et al. 1993). Such an accumulation of the compound may also occur in the embryonic stem cells and/or embryonic bodies of the EST and enhance the toxicity of p-heptyloxyphenol. In addition, it may be hypothesised that the embryonic stem cells and the embryonic bodies of the EST have a larger surface area-to-volume ratio than the rat conceptus in the WEC assay, enhancing uptake of lipophilic compounds from the culture medium into the cells. As a result the cells of the EST may be more exposed to lipophilic compounds that have a large affinity for the cellular content/membrane and hence may be more vulnerable for toxicity than the conceptus in the WEC assay. Moreover, it has been shown that cell density may impact the free concentration; more cells would result in a lower amount of chemical per cell, diminishing toxicity (Gülden et al. 2010). Additionally it has been proposed that expressing toxicity as moles per cell would facilitate the comparison between assays carried under different experimental conditions (Doskey et al. 2015). However, providing such a dose metric is difficult for the EST, because of significant changes in cell number during the course of the assay.

Another difference between the assays that may result in a more sensitive outcome of the EST compared to the WEC assay, is the different exposure window. In the EST applied in the present study (De Smedt et al. 2008), chemical exposure of the embryonic cells started at single cell suspension and continued ten days in which the cells developed into an embryoid body, subsequently forming contracting cardiomyocytes after plating on non-adherent petri-dishes. In the rat WEC assay, the conceptus (including decidual tissue and an intact yolk sac) (ECVAM 2010) is placed in culture medium containing the test compound at gestational day (GD) 9.5 (ECVAM 2010) or GD10 (Oglesby et al. 1992), and generally cultured for 48-h. Thus, the EST and the WEC assay may encompass different events in the developing embryo, with

possibly different sensitivity windows for exposure. Another important difference between the assays is the *in vitro* endpoint tested, which in the EST is differentiation of stem cells into beating cardiomyocytes, while the test outcomes of the WEC assay also include morphological endpoints, which on first sight may better reflect adverse outcomes of developmental toxicity *in vivo*. In spite of this, the EST appeared to work well also for compounds known to induce malformations *in vivo* (de Jong et al. 2009).

Overall, for most of the phenolic test compounds included in this thesis comparison of the EST with the WEC assay did not reveal large differences in the toxicity outcome between the assays, except that the EST was more sensitive towards the lipophilic compound p-heptyloxyphenol. Considering that the EST is a sensitive test, it may be regarded a suitable assay to study embryotoxicity. Nonetheless, it is recommended to further explore how *in vitro* kinetic processes i.e. related to lipophilicity should be accounted for when applying the EST in the hazard or quantitative risk assessment of chemicals.

PREDICTIVE CAPACITY OF THE EST FOR IN VIVO DEVELOPMENTAL TOXICITY FOR THE PHENOLS

Another issue to discuss when considering the use of the EST for predicting developmental toxicity *in vitro* is the predictivity of the EST for the model compounds used for the present studies. The phenols studied in the present thesis, may be regarded as weak embryo toxicants *in vivo* as developmental effects were reported to occur at relatively high oral dose levels (developmental NOAEL or BMD₁₀ > 40 mg/kg bw) (chapter 2). Our studies showed a limited ability of the EST to correctly predict the relative embryotoxic potency of the phenols, especially regarding p-heptyloxyphenol. Two validation studies using a diverse set of compounds, tested the performance of the EST and provided variable results regarding the ability of the assay to correctly predict *in vivo* developmental toxicity (Genschow et al. 2004; Marx-Stoelting et al. 2009).

One very important aspect that may limit the predictive capacity of the EST is the lack of metabolic capacity of the assay. This was clearly demonstrated in the present thesis, in which metabolism was an important parameter describing the *in vivo* kinetics of the phenols in the PBK models and which revealed that, when translating *in vitro* toxicity data to *in vivo* developmental toxicity values applying PBK-based reverse dosimetry, the predictive performance of the EST for the phenols improved. Apart from metabolism, other reasons that might explain the poor predictivity of the EST may be related to the absence of a well defined applicability domain for the EST which is further discussed below.

APPLICABILITY DOMAIN OF THE EST

When using the EST for predicting *in vivo* developmental toxicity it is also important to consider its applicability domain. The applicability domain of a bioassay may involve the chemical

structure, and/or biological space for which it is applicable to make predictions for new compounds (Hartung et al. 2004; Judson et al. 2013). Thus, the applicability domain of an assay may include a statement about the toxicity endpoint that is being predicted and physico-chemical properties or structural fragments of compounds for which the test is applicable. Carefully defining an applicability domain may be difficult for *in vitro* toxicity assays, because the number of compounds tested is often relatively small (Judson et al. 2013). This especially holds for the classical EST, which is not a high-throughput assay. At present, the applicability domain of the EST is not well defined. Considerations about the developmental toxicity endpoints that might be detected by the EST are discussed in some more detail below.

DEVELOPMENTAL TOXICITY ENDPOINTS IN RELATION TO THE EST

In the classical EST, differentiation of the embryonic stem cells into beating cardiomyocytes is evaluated after 10 days of chemical exposure. This is a simplified endpoint of embryogenesis/developmental toxicity. It has been shown that embryoid bodies, which are formed during the assay, can generate cells from the three different germ layers (ectoderm, endoderm and mesoderm) (Keller 1995), suggesting similarities with *in vivo* cellular processes for cardiac differentiation (van der Laan et al. 2012). Additionally, the EST resembles the functional interaction between different cells types like sinus node, ventricular and atrial cells (Tandon and Jyoti 2012). The EST may cover early events in development and differentiation, but lack the ability to test for morphological effects (Spielmann et al. 2006; van der Laan et al. 2012). Moreover, the EST is not able to mimic all complex pathways of developmental toxicity, which may limit its applicability. For example, it has been stated that the murine EST roughly covers a time window of the first GD5-10 in the rat (Ozolinš. 2010). Adverse effects of chemicals on embryonic developments that occur after this period, such as neural differentiation, may possibly remain undetected in the classical EST as has been observed for the compound methylmercury (He et al. 2012; Stummann et al. 2008).

From the example of methylmercury, and as has been outlined by others (Dreisig et al. 2013; Piersma et al. 2013), it may become clear that the EST cannot function as a stand-alone assay to test developmental toxicity. Enlarging the applicability domain to predict toxicity that reflect a wide array of developmental toxic effects can be achieved by testing additional *in vitro* endpoints (using embryonic stem cells), for example on neurodevelopmental toxicity (Theunissen et al. 2013), developmental bone toxicity measured by osteoblast formation and calcification of osteoblasts (Kuske et al. 2012) and endocrine disruptive endpoints (Jomaa et al. 2014). Toxicity could be identified using a combination of different read-outs like transcriptomic and proteomic profiles and flow cytometric, functional, physiological and morphological biomarkers (Garcia-Käufer et al. 2014; Louise et al. 2012).

In addition, (in vitro) assays testing placental transport of compounds (i.e. with BeWo cells in a so-called transwell system) and effects of compounds on the functioning of the placenta should be considered, because an altered placenta function may affect the wellbeing of the foetus (Myllynen et al. 2005). Current in vitro assays however, do not cover the variety of endpoints of the placenta, requiring the development of biomarkers for placental toxicity (Vähäkangas et al. 2014).

Altogether, different in vitro assays each covering a different sensitive aspect of foetal and embryonic development, could be applied in combination with the EST in a tiered approach to optimise the strategy for in vitro developmental toxicity testing (Kroese et al. 2015; Piersma et al. 2013).

PBK MODELLING CONSIDERATIONS

In chapter 3, 4 and 5 we translated in vitro outcomes of the phenols obtained in the EST to in vivo toxicity values applying PBK-based reverse dosimetry. PBK modelling forms an essential link in this extrapolation step, describing the ADME of a compound. Important steps that determine the quality of the PBK model are the definition of the PBK model structure and the selection of input parameters of the PBK model. These topics affecting the quality of the predictions made will be discussed in some more detail.

SELECTION AND PREDICTION OF RELEVANT INPUT PARAMETERS OF THE PBK MODELS FOR THE PHENOLS

To comply with the replacement, reduction and refinement (3Rs) principle in the most optimal way in the present thesis, all the parameters required for the PBK models, except the oral absorption coefficient in the PBK model of phenol (chapter 3), were predicted with in vitro and in silico approaches. Selecting such an in vitro approach to predict the kinetic properties of interest may not be straightforward. For instance, in the present thesis, transport across the small intestine to ultimately predict the oral absorption of the phenols (chapter 4) was quantified with transport studies using Caco-2 cells, but other approaches like the parallel artificial membrane permeability assay (PAMPA) (Kansy et al. 2004), or the use of MDCK cells (Volpe 2011; Wang et al. 2014) could also have been considered. For the phenols, for which passive diffusion is likely to be the most dominant transport route, selecting a different approach would probably provide comparable results. However, when transfer is facilitated by transporters, a more specific selection of the cellular system to be used may be required. Clearly, the applicability and the performance may differ per assay and depends on the physico-chemical properties of the test compound, and the species to be modelled. However,

for many *in vitro* tests the applicability domain is not (well) defined yet and efforts need to be undertaken to achieve this. Defining the applicability domain for *in vitro* ADME assays, in analogy to Quantitative Structure-Activity Relationships (QSARs) (Fjodorova et al. 2008), may therefore be valuable.

Evaluating the PBK models with a sensitivity analysis revealed that, apart from the oral absorption coefficient, glucuronidation of phenol in the liver is an influential parameter on the model outcome, both for phenol as well as for the *p*-substituted phenols. The capacity of the liver to glucuronidate the phenols was derived from *in vitro* assays with subcellular fractions from rat and human livers. The metabolic constants obtained from these experiments were extrapolated to *in vivo* relevant values and included in the PBK model. The resulting PBK model predictions provided adequate phenol plasma levels, which were quantitatively evaluated by comparing the values of the compound phenol to *in vivo* plasma levels reported for this compound in the literature. From these results, it is believed that the approach applied in the present thesis to predict metabolism of phenols *in vivo* was appropriate, not only for phenol, but also for the *p*-substituted phenols.

Metabolic formation of hydroquinone was not selected as a parameter to be included in the PBK models of the phenols. In literature, it has been hypothesised that some of the adverse effects of phenol might be due to its hydroxylated metabolite hydroquinone (Bruce et al. 2001). *In vivo*, only at higher oral doses of phenol (150 mg/kg bw) hydroquinone was present in elevated levels in urine being excreted as the corresponding glucuronide conjugate (Hiser et al. 1994). A developmental NOAEL of 100 mg/kg bw was established for hydroquinone in rats (Health Council of the Netherlands 2012; Krasavage et al. 1992) that received hydroquinone orally during GD6-16. Developmental NOAELs of phenol, derived by studies that used comparable species and dosage regimens as used for deriving the NOAEL of hydroquinone, were 60 and 120 mg/kg bw (Argus 1997; Jones-Price et al. 1983). Given that the *in vivo* embryotoxic effects were only observed at relatively high oral dose levels of hydroquinone comparable or higher than embryotoxicity values reported for phenol, it seems unlikely that the adverse effects of phenol detected *in vivo* can be ascribed to the (limited) formation of hydroquinone in the metabolic pathway of phenol.

It is also of interest to note that when phenol and hydroquinone were added together in the WEC assay, a synergistic toxic effect was observed (Chapman et al. 1994). The authors hypothesised that this effect might be due to the fact that phenol enhances the reaction of hydroquinone to benzoquinone providing free radical intermediates (Chapman et al. 1994). Chapman et al. (1994), however, did not report addition of antioxidants to the WEC assay, while hydroquinone is unstable due to auto-oxidation. Considering that the antioxidant GSH may prevent auto-oxidation of hydroquinone (Moridani et al. 2002) and is present in rat and human blood and tissues up to millimolar concentrations (Jain and Flora 2012; Pastore et al. 2003), we do not expect that synergism has an (important) role on phenol induced

developmental toxicity *in vivo*. Moreover, the metabolic profile reported for an *in vivo* kinetic study in rat with low to high oral doses of phenol (1.5, 15 and 150 mg/kg bw) did not report formation of benzoquinone (metabolites) (Hiser et al. 1994). Taken together, it is assumed that the parent compound phenol itself is responsible for the developmental toxicity observed and that its plasma and/or tissue concentrations can be expected to provide an adequate descriptor for prediction of the toxic effects that are observed *in vivo*.

As illustrated for phenol, defining metabolism, both qualitatively and quantitatively is an essential step when developing a PBK model. For phenol, the major metabolic pathways are well known and reported in literature, but, when extending the approach to other compounds, it is good to realise that for many compounds such kinetic information is lacking. A first step is then elucidating the reactions involved in metabolism of the compound and the products that are formed. *In silico* tools, like the expert systems Meteor (Lhasa Ltd., Leeds, UK), StarDrop (Optibrium Ltd., Cambridge, UK), and MetaSite (Molecular Discovery Ltd., Middlesex, UK) (T'Jollyn et al. 2011) may be helpful to identify molecular sites liable to metabolism and the type of metabolites expected to be formed. Subsequently, *in vitro* metabolic assays, followed by chemical metabolic profiling can be applied to confirm and/or refine these predictions and define the pathways quantitatively *in vitro* as well as to define the related kinetic constants required for the PBK models. It should be recognised that this may be labour intensive, but as was clear from the proof-of-principle provided in the present thesis, it is an indispensable aspect to define and parameterise the PBK models required to translate *in vitro* toxicity values to *in vivo* dose levels.

PBK MODELLING OF A PLACENTAL/FOETAL COMPARTMENT

In the PBK models described in chapter 4, we included a newly developed placental/foetal compartment that models placental transfer based on *in vitro* transport experiments with BeWo cells and partitioning of the compound in the embryo/foetus using partition coefficients. This approach comprises an important but currently lacking aspect in the extrapolation of *in vitro* derived embryotoxicity values to the *in vivo* situation. The measured transfer of the phenols across the BeWo cells was rapid, except for *p*-heptyloxyphenol for which transport *in vitro* was less rapid compared to the other phenols possibly due to binding to albumin in the apical compartment of the transport assay as discussed in chapter 4. The transport of *p*-heptyloxyphenol may be somewhat larger *in vivo*, because of prevailing dynamic fluid conditions *in vivo*, opposed to the static situations in the BeWo assay (Li et al. 2013), although such a relation should be further explored. The predicted foetal plasma concentrations for all phenols were close to maternal levels, except for *p*-heptyloxyphenol, for which the foetal concentrations were predicted to be lower than maternal plasma levels. This result seems to be in line with data reported in the literature for phenol and *p*-nitrophenol for which foetal and maternal plasma levels were reported to be similar indeed (Abu-Qare et al. 2000; Gray and Kavlock 1990).

An additional feature of the placental/foetal compartment in our PBK model is that it may aid in elucidating whether the embryotoxic effect is a result of a direct action of the compound or maternally mediated, although this was not the scope of the present thesis. For some of the phenols, embryotoxicity *in vivo* occurred at a similar or somewhat higher dose level than maternal weight changes, which may raise the question whether embryotoxic effects observed *in vivo* are due to indirect maternal effects or are induced by a more direct action of the compound. Disentangling whether embryotoxic effects observed *in vivo* are due to a direct action of the compound or mediated by maternal toxicity is difficult (Daston et al. 2010), but it may be important for the risk assessment (Spielmann et al. 2006). This aspect can be especially of importance when defining the most sensitive endpoint for risk assessment or for classification and labelling of a compound. With respect to phenol, for which both foetal and maternal toxicity has been reported, it is of interest to note that our experiments with the EST indicate that the phenols have the potency to cause embryotoxic effects. The transport studies with BeWo cells showed that the phenols may readily pass placental cells facilitating foetal exposure. Including a placental/foetal compartment in the PBK model provided foetal systemic concentrations that were close to maternal concentrations (except for p-heptyloxyphenol). Thus, it may be hypothesised that embryotoxicity observed *in vivo* at maternally toxic doses could still be mediated by a direct action of the compound since we predicted that the embryo/foetus itself is exposed to the compound, even at concentrations similar to those in maternal plasma in the case of phenol, p-fluorophenol and p-methylketophenol. For p-heptyloxyphenol *in vivo* dose levels causing maternal toxicity were lower than the dose levels causing embryotoxic effects (Kavlock 1990), which is in line with the difference in maternal and foetal circulating concentrations predicted with our *in vitro* PBK approach. Altogether, including a placental/foetal compartment in PBK modelling may provide valuable information to refine the toxicological assessment of developmental toxicants.

Taken together, the definition of the PBK model structure and the selection of input parameters of the PBK model are aspects that can greatly affect the quality of the PBK model and the PBK-based reverse dosimetry prediction, especially regarding input parameters that are influential on the model outcome. Developing and applying *in silico* and *in vitro* tools to predict *in vivo* kinetic processes that have a well defined applicability domain is essential. This holds especially true for approaches in predictive toxicology, where *in vivo* kinetic data are lacking for most compounds to be tested.

THE USE OF DIFFERENT KINETIC REVERSE DOSIMETRY APPROACHES TO PERFORM IN VITRO TO IN VIVO EXTRAPOLATIONS (IVIVE)

Another aspect that determines the quality and applicability of the in vivo toxicity predictions using in vitro toxicity data is the choice for the approach that is applied to perform kinetic reverse dosimetry. To illustrate this, the in vitro PBK approach is briefly compared other in vitro in vivo extrapolation approaches, and the different characteristics of the approaches are discussed. In addition, the selection of the dose metric used in kinetic reverse dosimetry is also addressed.

COMPARISON OF KINETIC REVERSE DOSIMETRY APPROACHES

The present thesis used PBK models to translate in vitro toxicity data to in vivo toxicity values. Recently, other approaches have been reported which also apply reverse dosimetry modelling to link the in vitro effect concentration to an in vivo oral effective dose level (Rotroff et al. 2010; Wetmore et al. 2012; Wetmore et al. 2013; Wetmore et al. 2015). These authors described a high throughput-in vitro in vivo extrapolation (HT-IVIVE) approach for risk assessment, in which at least two in vitro kinetic parameters were measured, namely protein binding and hepatic metabolic clearance. These data were included in the simple kinetic equation of Wilkinson and Shand (1975) to calculate the steady state concentration of a parent compound (C_{ss} (μM)) in plasma at a low dose exposure level of 1 mg/kg bw/d. Subsequently, this relation is used to calculate an oral equivalent dose of EC_{50} values obtained from in vitro kinetic (toxicity) studies.

In general, the in vitro PBK approach applied in the present thesis describes the ADME processes in more detail than the HT-IVIVE. Important differences between the models are related to the description of the kinetics of the metabolic processes, the selection of (additional) compartments (i.e. a foetal compartment), the description of the distribution of a compound within an organism and the selection of the dose metric. An overview of the main differences between the in vitro PBK approach applied in the present thesis and the HT-IVIVE approach (Rotroff et al. 2010; Wetmore et al. 2012; Wetmore et al. 2013) is presented in Table 1.

In general, the HT-IVIVE approach may provide a more conservative toxicity estimate (Thomas et al. 2013). It should be realised, however, that this may not always be the case and depends on the kinetic processes to be modelled in connection with model characteristics and the model input parameters. For example, in the in vitro PBK approach we included Michaelis-Menten kinetics (or substrate inhibition when applicable) to describe the metabolism of the phenols, while the HT-IVIVE approach assumes linear metabolic kinetic

processes and uses a metabolic clearance that was derived with the substrate depletion method at a low concentration of either 1 or 10 μM . When a similar clearance value is applied for situations where higher plasma concentrations prevail than the 1 or 10 μM , the HT-IVIVE approach will underestimate the metabolic turnover, resulting in a higher internal (plasma) concentration of the parent compound, but lower concentrations of a metabolite than actually is the case. This provides a conservative toxicity estimate when the parent compound is responsible for toxicity but would lead to an underestimation of the risk when the metabolite is the toxic entity. With this respect it is important to note that the HT-IVIVE approach is not able to predict toxicity values induced by metabolites of the parent compound that is modelled, as it only makes predictions based on the parent compound and not based on the metabolites. With in vitro PBK-based reverse dosimetry, however, it is possible to model the formation of metabolites and predict in vivo toxicity values based on the metabolites formed (Louisse et al. 2010). Another example which may lead to under prediction of the risk is bioaccumulation of the toxic compound in a target organ, which is not modelled with the HT-IVIVE approach. This was, however, also not included in our PBK model, because the phenols were not expected to accumulate.

Overall, the characteristics of the in vitro PBK and the HT-IVIVE approaches affect the applicability of each approach for the risk assessment of chemicals. The HT-IVIVE approach is a generic model especially suitable to provide a first tier toxicity estimate that can be characterised by a higher degree of uncertainty, and predictions are based on more conservative assumptions (Thomas et al. 2013). The PBK model developed in the present thesis is applicable for a higher tier toxicological assessment, although PBK models may also be applied in the first tier when they have more generic characteristics, for example modelling only a limited number of compartments.

Table 1 Overview of differences in the characteristics of the kinetic models applied in the in vitro PBK and the HT-IVIVE reverse dosimetry approaches.

Model characteristic	In vitro PBK approach present thesis ^a	HT-IVIVE approach ^{a,b}
Absorption		
Oral uptake	First order (but can be adjusted) 100% bioavailability, but can be adjusted based on Caco-2	Zero-order 100% bioavailability, but can be adjusted based on Caco-2
Distribution		
Partition coefficients	Y	N
Target organs for safety testing	Y	N
Placental/foetal compartment	Y	N
Blood-brain-barrier	Can be implemented	N
Binding to specific target molecules	Can be implemented	N
Prediction target organ concentration	Y (i.e. concentrations in liver or in foetus)	N
Metabolism		
Hepatic metabolism	In vitro derived kinetic constants from enzyme kinetic studies considering different models (i.e. Michaelis-Menten, substrate inhibition model)	Clearance value determined in vitro at a low concentration assuming linear metabolic kinetics (See text for details)
Non-specific binding to microsomes	Y	N
Prediction of target specific formation and levels of reactive metabolites	Y	N
Excretion		
Glomerular filtration rate	Not included, because regarded quantitatively not relevant for phenol	Included
Other		
Dose metric for reverse dosimetry	C_{max} , AUC ^c Can be adjusted to C_{ss} for comparison	C_{ss}
Time	Time dependent analysis i.e. to see when C_{ss} is established	One time (data) point (steady state)
Inter- and intraspecies modelling	Y	N
Route-to-route extrapolations	Can be implemented	N
Evaluation repeated dosing regimens	Can be implemented	N

^a Included (Y) or not included (N) in the kinetic reverse dosimetry approach.

^b Approach presented by Rotroff et al. (2010) and Wetmore et al. (2012, 2013, 2015).

^c Maximum test concentration (C_{max}); area under the concentration-time curve (AUC); steady state concentration (C_{ss}). For more details, see section Selection of dose-metric for the in vitro to in vivo extrapolation.

SELECTION OF DOSE-METRIC FOR THE IN VITRO TO IN VIVO EXTRAPOLATION

The choice of an adequate dose metric to be used, for example the maximum test concentration (C_{max}) or the area under the concentration-time curve (AUC), is an important step when performing extrapolations from in vitro toxicity data to in vivo toxicity values. It has been advocated that for reversible (toxic) reactions the peak concentration may be the appropriate metric but that for irreversible toxic actions the AUC may be preferred due to an increase in effect over time (Groothuis et al. 2015).

Daston (2010) reported that developmental toxicity is likely to be dependent on the peak concentration. For the present set of phenols, the PBK model based reverse dosimetry predicted in vivo toxicity values corresponded better to the in vivo toxicity values obtained from the literature when extrapolations were based on C_{max} values instead of the AUC (chapter 3 and 4). This dose-metric corresponds to the observation that toxicity of the phenols is associated with a polar narcosis mechanism (Hansch et al. 2000; Yi and Liu 2005) for which C_{max} is regarded an appropriate dose metric (Groothuis et al. 2015).

It has been suggested by some authors (Daston et al. 2010) to multiply the applied test concentration by the duration of the assay to obtain an AUC. This approach may be used as a first screening to assess differences between the dose metrics i.e. C_{max} or AUC on the model predictions when applying PBK-based reverse dosimetry. However, an important next step may be characterisation of the behaviour of the test compound in the in vitro assay, as in vitro kinetic processes may influence the AUC as was shown in the present thesis (chapters 2 and 3). It is likely that the test design of the EST, by using the hanging drop technique in the first three days of the assay, attributes to evaporation of (semi)-volatile compounds, as phenol disappeared rapidly during the first culturing day, while evaporation was much less after 3 days when phenol was present in petri dishes and 24-well plates. Moreover, it remains also to be seen how the dose metrics C_{max} and AUC will affect toxicity predictions when considering different in vitro assays such as the EST and the WEC assay which have large differences in the test duration, namely 10 days versus 48 hours.

An additional step in establishing the appropriate dose metric, may be investigating the behaviour of the concentration-response curves at different durations of exposure to evaluate whether a change in the AUC in vitro results in a change in the prediction of toxicity. It should be kept in mind, however, that changes in concentration-response curves may also be induced by a specific window of heightened susceptibility of cells towards the test compound during an assay, especially when the in vitro assay encompasses different processes regarding proliferation and differentiation like the EST.

Thus, identifying an appropriate dose metric for the PBK model based in vitro to in vivo translation is not straightforward, especially not in predictive toxicology when no information about the in vivo effect is available. Therefore, further insight in the relation of different dose metrics and toxic effects, preferably mechanistically based, is required.

THE POSSIBILITY TO TAKE INTERINDIVIDUAL VARIATIONS INTO ACCOUNT

Another aspect that is discussed in some detail in this chapter concerns the possibility to take interindividual variations into account to predict variation in toxicity. PBK models provide the opportunity to evaluate the effect of interindividual kinetic differences in toxicity. This can be achieved by defining PBK models for different individuals using (experimentally derived) kinetic constants from different humans, or by modelling variation in a (larger) population linking PBK modelling with Monte Carlo simulations using information on the level of variation of the kinetic parameters of interest in the human population, as was demonstrated for phenol in the present thesis.

The sensitivity analysis of the model performance revealed that especially glucuronidation and the oral absorption coefficient mainly influenced the predicted levels of phenol in plasma, hence interindividual variation in these kinetic processes was simulated. Individuals with a reduced UGT1A6 and UGT1A9 activity together with an increased oral absorption are regarded a sensitive subgroup for phenol induced developmental toxicity. However, our results indicate that when the oral absorption and glucuronidation by UGT1A6 and UGT1A9 are predominant kinetic processes, the default uncertainty factor of 3.16 which is applied in the risk assessment of chemicals to account for human kinetic differences (IPCS 2005; IPCS 2010) may be adequately protective for phenol induced developmental toxicity.

Multiple factors may influence the sensitivity of individuals towards a chemical, for example life-stage, gender, life style factors, disease status, environmental exposure, drug intake, as well as the genetic make up (Guillemette 2003). A number of these factors are expressed in the coefficients of variation of the activity of UGT enzymes that were used in the present thesis to predict variability in phenol glucuronidation using Monte Carlo simulations. Nonetheless, it should be recognised that the databank of 54 individuals (Court 2010) from which this information originates may not cover the full spectrum of variability in UGT enzyme activity in the population, including the variation caused by genetic variations in the population. With the increasing use of molecular techniques, more and more genetic variations are discovered (UGT Alleles Nomenclature Home Page 2015), but the effect of specific alleles on the UGT activity has only been defined for a selective number of variants. Further defining the influence of polymorphisms on the glucuronidation activity as well as the allele frequency in the population, may refine predictions of interindividual human variation in toxicity as presented in this thesis.

A topic that needs further attention in the prediction of interindividual human variation in toxicity is the variability between humans in the response of a chemical at the target site, such as receptor binding or signal transduction. This so called toxicodynamic difference may

result from factors like disease-status, genetic variability and drug or environmental exposure. At present, information about variations in responses caused by interindividual toxicodynamic differences is scarce. However, using a range of human cell lines from different individuals for instance obtained from biobanks and using in vitro disease models in toxicological research, which are becoming more and more available, may generate information about interindividual differences in dynamic toxicological responses. Variation in toxicological responses can for example be included in the in vitro in silico approach to further refine population based predictions on the toxicity of a chemical.

Overall, integrating in vitro toxicity data, PBK modelling and Monte Carlo simulations provided a unique approach to predict interindividual differences in developmental toxicity. The approach may provide a reliable basis to derive human guidance values and support population health based risk assessment, which is one of the goals outlined by the next generation (NexGen) framework for risk science (Krewski et al. 2014).

FUTURE PERSPECTIVES

The present thesis demonstrated that the in vitro PBK approach was able to predict in vivo PoDs for a series of phenols that are close to in vivo derived toxicity values and appeared to be a promising strategy to extrapolate in vitro toxicity values to in vivo relevant levels. The ultimate goal may be to apply the in vitro PBK approach in predictive toxicity for compounds for which no or little in vivo toxicity data are available for the endpoint of interest. Reaching that point requires sufficient confidence in the prediction together with regulatory acceptance, which may partly go hand-in-hand. This can be achieved by providing more examples, for different substances and different toxicity endpoints.

Based on this consideration, it would be interesting to test the validity of the in vitro PBK approach for other toxicity endpoints. Subsequently, a complete toxicological risk assessment for a set of compounds could be evaluated to see if the critical toxicological endpoint defined in vivo is picked up by the in vitro PBK approach. Within this context, phase I and II of the ToxCast program of the US-EPA (Dix et al. 2007), in which about 1000 unique compounds are being tested in several hundred in vitro tests including toxicity assays, may generate valuable information in the upcoming years. At present a subset of the in vitro toxicity data has been extrapolated to in vivo toxicity values using the method of Wilkinson and Shand (1975) (Wetmore et al. 2012; Wetmore et al. 2013; Wetmore et al. 2015), but this may possibly be extended in the future. Extrapolations generated so far including our approach, may support the definition of endpoints and groups of compounds for which IVIVE extrapolations are promising, but may also define bottlenecks and/or uncertainties that need to be eliminated.

Furthermore, to enlarge the future applicability of the presented in vitro PBK approach,

the method should also be tested for compounds that enter the body via the dermal or the inhalation route, in conjunction with *in vitro* assays that quantify uptake via these ports of entry. Moreover, we demonstrated a new non-animal based approach to quantify placental transfer using BeWo cells together with predicting the partitioning of the chemical in the foetus with PBK modelling, which provided adequate predictions for the phenols. However, more research is required to define the applicability domain for this method, focussing on changes in the developing embryonic/foetal compartment during pregnancy and the influence of physico-chemical properties of the compounds for which the method would be applicable.

At present extrapolating *in vitro* toxicity values to *in vivo* toxicity levels has predominantly been performed using *in vitro* toxicity data generated by *in vitro* models using cells from animal origin. A next step can be the use of human cells, which in potential may closer mimic human biological responses than animal cells (Tandon and Jyoti 2012), and may perhaps, eventually, eliminate the interspecies safety factor that accounts for differences in interspecies toxicodynamics in the risk assessment of chemicals. Within this context, the use of induced pluripotent stem cells (iPSC) may have an advantage over immortalised human cells because iPSC may better mimic essential features of primary human cells and may circumvent ethical concerns regarding the use of embryonic stem cells (Yap et al. 2015). Furthermore, three-dimensional (3D) cell cultures in addition to two-dimensional (2D) cultures may be considered as 3D cultures potentially may represent more tissue functions that are present in the *in vivo* micro environment like cellular communication (Fey and Wrzesinski 2012), and provide opportunities to include various cell types in one model (Roth and Singer 2014). Moreover, it has been shown that 3D microtissues with liver cells had a prolonged life-time and viability, extending possibilities to test chronic chemical exposure (Messner et al. 2013), which is an important bottleneck in current *in vitro* toxicity testing. Moreover, the organ-on-a-chip which is a microdevice for culturing living cells that are continuously perfused, may encapture many advantages that were outlined above for the different cell culture technologies, like multicellular architecture, tissue-tissue interaction, together with simulating the tissue and organ physiology (Bhatia and Ingber 2014). Taken together, the developments in *in vitro* cell culture technology of which some are briefly discussed have the potential to improve *in vitro* toxicity testing in the (near) future, hence refining the extrapolation of *in vitro* effect concentrations to *in vivo* toxicity values.

A final factor that needs to be considered in the further development of the *in vitro* PBK approach for predicting PoDs and using them in a subsequent risk assessment is the way in which related uncertainties can be taken into account. To account for the extra uncertainties associated with the *in vitro* PBK-based *in vivo* predictions, an additional safety factor may be introduced when deriving safe exposure levels for the risk assessment of chemicals. Such a safety factor may specify uncertainties related to the *in vitro* toxicity assay selected, as well as uncertainties implicit in the *in silico* toxicokinetic methods. Applying such an additional

safety factor may be a starting point to enhance the use of the in vitro PBK model approach in practice, while determining the size of such an uncertainty factor may have to await the development and evaluation of more proofs of principle.

FINAL CONCLUSIONS

The present thesis showed that combining in vitro toxicity data with kinetic processes is indispensable to improve in vivo toxicity predictions, which are based on in vitro toxicity data. We demonstrated that combining in vitro toxicity data with PBK-based reverse dosimetry adequately predicted in vivo developmental toxicity values for a series of phenols. The results obtained demonstrate the possibility of the approach to improve toxic potency estimates as well as to provide quantitative toxicity estimates like a PoD, the latter solving a major bottleneck hampering the application of in vitro approaches in the risk assessment of chemicals. Moreover, this thesis is an important step forward to ultimately implement the envisioned paradigm shift away from studying apical endpoints in animal studies for the safety testing of chemicals, towards an approach that is cheaper, non-animal based and more directly relevant for humans.

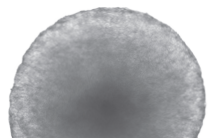
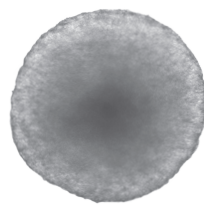
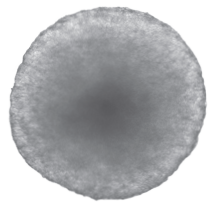
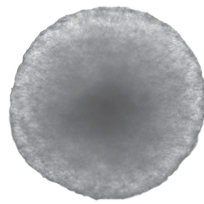
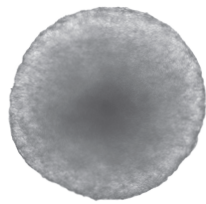
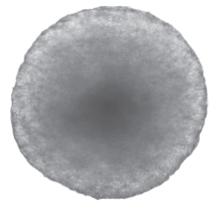
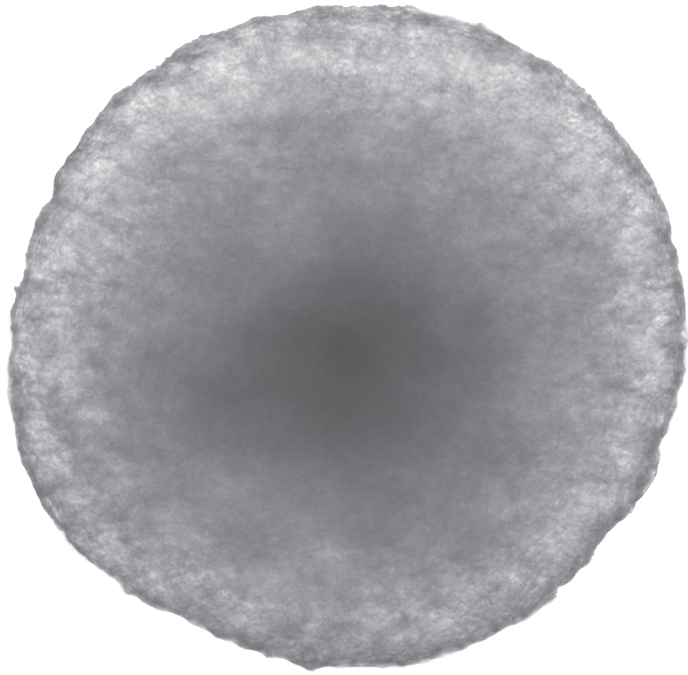
REFERENCES

- Abu-Qare AW, Brownie CF, Abou-Donia MB (2000) Placental transfer and pharmacokinetics of a single oral dose of [¹⁴C]p-nitrophenol in rats. *Arch Toxicol* 74:388-396
- ACD/Labs (2015) Advanced Chemistry Development (ACD/Labs) Software V11.02 (© 1994-2015 ACD/Labs). Values taken from SciFinder.
- Argus (1997) Oral (gavage) developmental toxicity study of phenol in rats. Protocol Number: Argus 916-011. Argus Research Laboratories, Inc., Horsham, PA
- Bhatia SN and Ingber DE (2014) Microfluidic organs-on-chips. *Nat Biotechnol* 32:760-772
- Bruce W, Meek ME, Newhook R (2001) Phenol: hazard characterization and exposure-response analysis. *J Environ Sci Health, Part C: Environ Carcinog Ecotoxicol Rev* 19:305-324
- Chapman DE, Namkung MJ, Juchau MR (1994) Benzene and benzene metabolites as embryotoxic agents: effects on cultured rat embryos. *Toxicol Appl Pharmacol* 128:129-137
- Court MH (2010) Interindividual variability in hepatic drug glucuronidation: studies into the role of age, sex, enzyme inducers, and genetic polymorphism using the human liver bank as a model system. *Drug Metab Rev* 42:209-224
- Daston GP, Chapin RE, Scialli AR, Piersma AH, Carney EW, Rogers JM, Friedman JM (2010) A different approach to validating screening assays for developmental toxicity. *Birth Defects Res, Part B* 89:526-530
- De Jong E, Barenys M, Hermesen SAB, Verhoef A, Ossendorp BC, Bessems JGM, Piersma AH (2011) Comparison of the mouse Embryonic Stem cell Test, the rat Whole Embryo Culture and the Zebrafish Embryotoxicity Test as alternative methods for developmental toxicity testing of six 1,2,4-triazoles. *Toxicol Appl Pharmacol* 253:103-111
- De Jong E, Lousse J, Verwei M, Blaauboer BJ, van de Sandt JJM, Woutersen RA, Rietjens IMCM, Piersma AH (2009) Relative developmental toxicity of glycol ether alkoxy acid metabolites in the embryonic stem cell test as compared with the in vivo potency of their parent compounds. *Toxicol Sci* 110:117-124

- De Smedt A, Steemans M, De Boeck M, Peters AK, van der Leede B, Van Goethem F, Lampo A, Vanparys P (2008) Optimisation of the cell cultivation methods in the embryonic stem cell test results in an increased differentiation potential of the cells into strong beating myocard cells. *Toxicol in Vitro* 22:1789-1796
- Dix DJ, Houck KA, Martin MT, Richard AM, Setzer RW, Kavlock RJ (2007) The toxcast program for prioritizing toxicity testing of environmental chemicals. *Toxicol Sci* 95:5-12
- Doskey CM, van 't Erve TJ, Wagner BA, Buettner GR (2015) Moles of a substance per cell is a highly informative dosing metric in cell culture. *PLoS ONE* 10
- Dreisig K, Taxvig C, Kjærstad MB, Nellemann C, Hass U, Vinggaard AM (2013) Predictive value of cell assays for developmental toxicity and embryotoxicity of conazole fungicides. *Altox* 30:319-330
- EC (2007) Corrigendum to Regulation (EC) No 1907/2006 of the European Parliament and of the Council of 18 December 2006 concerning the Registration, Evaluation, Authorisation and Restriction of Chemicals (REACH), establishing a European Chemicals Agency, amending Directive 1999/45/EC and repealing Council Regulation (EEC) No 793/93 and Commission Regulation (EC) No 1488/94 as well as Council Directive 76/769/EEC and Commission Directives 91/155/EEC, 93/67/EEC, 93/105/EC and 2000/21/EC. *Off J Eur Union* L136:3-280
- EC (2009) Regulation (EC) No 1223/2009 of the European parliament and of the council of 30 November 2009 on cosmetic products. *Off J Eur Union* L342:59-209
- ECVAM (2010). INVITTOX protocol no 123. Embryotoxicity testing in post-implantation whole embryo culture (WEC) - method of Piersma. Available at: <http://ecvam-dbalm.jrc.ec.europa.eu/>.
- Fey SJ and Wrzesinski K (2012) Determination of drug toxicity using 3D spheroids constructed from an immortal human hepatocyte cell line. *Toxicol Sci* 127:403-411
- Fisher HL, Sumler MR, Shrivastava SP, Edwards B, Oglesby LA, Ebron-McCoy MT, Copeland F, Kavlock RJ, Hall LL (1993) Toxicokinetics and structure-activity relationships of nine para-substituted phenols in rat embryos in vitro. *Teratology* 48:285-297
- Fjodorova N, Novich M, Vrachko M, Smirnov V, Kharchevnikova N, Zholdakova Z, Novikov S, Skvortsova N, Filimonov D, Poroikov V, Benfenati E (2008) Directions in QSAR modeling for regulatory uses in OECD member countries, EU and in Russia. *J Environ Sci Health, Part C: Environ Carcinog Ecotoxicol Rev* 26:201-236
- Garcia-Käuffer M, Gartiser S, Hafner C, Schiwy S, Keiter S, Gründemann C, Hollert H (2014) Genotoxic and teratogenic effect of freshwater sediment samples from the Rhine and Elbe River (Germany) in zebrafish embryo using a multi-endpoint testing strategy. *Environ Sci Pollut Res* 22:16341-16357
- Genschow E, Spielmann H, Scholz G, Pohl I, Seiler A, Clemann N, Bremer S, Becker K (2004) Validation of the embryonic stem cell test in the international ECVAM validation study on three in vitro embryotoxicity tests. *Altern Lab Anim* 32:209-244
- Gray JA and Kavlock RJ (1990) A pharmacokinetic analysis of phenol in the pregnant rat: Deposition in the embryo and maternal tissues. *Teratology* 41:561
- Groothuis FA, Heringa MB, Nicol B, Hermens JLM, Blaau-boer BJ, Kramer NI (2015) Dose metric considerations in in vitro assays to improve quantitative in vitro-in vivo dose extrapolations. *Toxicology* 332:30-40
- Guillemette C (2003) Pharmacogenomics of human UDP-glucuronosyltransferase enzymes. *Pharmacogenomics J* 3:136-158
- Gülden M, Jess A, Kammann J, Maser E, Seibert H (2010) Cytotoxic potency of H2O2 in cell cultures: Impact of cell concentration and exposure time. *Free Radical Biol Med* 49:1298-1305
- Hansch C, McKarns SC, Smith CJ, Doolittle DJ (2000) Comparative QSAR evidence for a free-radical mechanism of phenol-induced toxicity. *Chem-Biol Interact* 127:61-72
- Hartung T, Bremer S, Casati S, Coecke S, Corvi R, Fortaner S, Gribaldo L, Halder M, Hoffmann S, Roi AJ, Prieto P, Sabbioni E, Scott L, Worth A, Zuang V (2004) A modular approach to the ECVAM principles on test validity. *Altern Lab Anim* 32:467-472
- He X, Imanishi S, Sone H, Nagano R, Qin XY, Yoshinaga J, Akanuma H, Yamane J, Fujibuchi W, Ohsako S (2012) Effects of methylmercury exposure on neuronal differentiation of mouse and human embryonic stem cells. *Toxicol Lett* 212:1-10
- Health Council of the Netherlands (2012) Hydroquinone and benzoquinone. Health-based recommended occupational exposure limit. Publication no. 2012/27. Health Council of the Netherlands, The Hague
- Hiser MF, Kropscott BE, McQuirk RJ, Bus JS (1994) Pharmacokinetics, metabolism and distribution of ¹⁴C-phenol in Fischer 344 rats after gavage, drinking water and inhalation exposure. OTS0557473. Study ID: K-002727-022. Dow Chemical Company. Submitted to U.S. Environmental Protection Agency under TSCA Section 8D
- IPCS (2005) Chemical-specific adjustment factors for interspecies differences and human variability: guidance document for use of data in dose/concentration-response assessment. World Health Organization, Geneva

- IPCS (1999) Principles for the assessment of risks to human health from exposure to chemicals. World Health Organization, Geneva
- Jain A and Flora SJS (2012) Dose related effects of nicotine on oxidative injury in young, adult and old rats. *J Environ Biol* 33:233-238
- Jomaa B, Hermsen SAB, Kessels MY, van den Berg JHJ, Peijnenburg AACM, Aarts JMMJG, Piersma AH, Rietjens IMCM (2014) Developmental toxicity of thyroid-active compounds in a zebrafish embryotoxicity test. *Altex* 31:303-317
- Jones-Price C, Ledoux TA, Reel JR, Fisher PW, Langhoff-Paschke L, Marr MC, Kimmel CA (1983) Teratologic evaluation of phenol in CD rats. PB83-247726. National Technical Information Service (NTIS), Washington, DC
- Judson R, Kavlock R, Martin M, Reif D, Houck K, Knudsen T, Richard A, Tice RR, Whelan M, Xia M, Huang R, Austin C, Daston G, Hartung T, Fowle III JR, Wooge W, Tong W, Dix D (2013) Perspectives on validation of high-throughput assays supporting 21st century toxicity testing. *Altex* 30:51-66
- Kansy M, Avdeef A, Fischer H (2004) Advances in screening for membrane permeability: high-resolution PAMPA for medicinal chemists. *Drug Discovery Today: Technol* 1:349-355
- Kavlock RJ (1990) Structure-activity relationships in the developmental toxicity of substituted phenols: in vivo effects. *Teratology* 41:43-59
- Keller GM (1995) In vitro differentiation of embryonic stem cells. *Curr Opin Cell Biol* 7:862-869
- Krasavage WJ, Blacker AM, English JC, Murphy SJ (1992) Hydroquinone: a developmental toxicity study in rats. *Fundam Appl Toxicol* 18:370-375
- Krewski D, Westphal M, Andersen ME, Paoli GM, Chiu WA, Al-Zoughool M, Croteau MC, Burgoon LD, Cote I (2014) A framework for the next generation of risk science. *Environ Health Perspect* 122:796-805
- Kroese ED, Bosgra S, Buist HE, Lewin G, van der Linden SC, Man HY, Piersma AH, Rorije E, Schulpen SHW, Schwarz M, Uibel F, van Vugt-Lussenburg BMA, Wolterbeek APM, van der Burg B (2015) Evaluation of an alternative in vitro test battery for detecting reproductive toxicants in a grouping context. *Reprod Toxicol* 55:11-19
- Kuske B, Pulyanina PY, zur Nieden NI (2012) Embryonic stem cell test: stem cell use in predicting developmental cardiotoxicity and osteotoxicity. In: Harris C and Hansen JM (eds.) *Developmental toxicology: methods and protocols, Methods in molecular biology*, 889. Springer, New York, pp 147-179
- Li H, van Ravenzwaay B, Rietjens IMCM, Lousse J (2013) Assessment of an in vitro transport model using BeWo b30 cells to predict placental transfer of compounds. *Arch Toxicol* 87:1661-1669
- Louisse J, de Jong E, van de Sandt JJM, Blaauboer BJ, Woutersen RA, Piersma AH, Rietjens IMCM, Verwei M (2010) The use of in vitro toxicity data and physiologically based kinetic modeling to predict dose-response curves for in vivo developmental toxicity of glycol ethers in rat and man. *Toxicol Sci* 118:470-484
- Louisse J, Gönen S, Rietjens IMCM, Verwei M (2011) Relative developmental toxicity potencies of retinoids in the embryonic stem cell test compared with their relative potencies in in vivo and two other in vitro assays for developmental toxicity. *Toxicol Lett* 203:1-8
- Louisse J, Verwei M, Woutersen RA, Blaauboer BJ, Rietjens IMCM (2012) Toward in vitro biomarkers for developmental toxicity and their extrapolation to the in vivo situation. *Expert Opin Drug Metab Toxicol* 8:11-27
- Marx-Stoelting P, Adriaens E, Ahr HJ, Bremer S, Garthoff B, Gelbke HP, Piersma A, Pellizzer C, Reuter U, Rogiers V, Schenk B, Schwengberg S, Seiler A, Spielmann H, Steemans M, Stedman DB, Vanparys P, Vericat JA, Verwei M, van de Water F, Weimer M, Schwarz M (2009) A review of the implementation of the embryonic stem cell test (EST). The report and recommendations of an ECVAM/ReProTect Workshop. *Altern Lab Anim* 37:313-328
- Messner S, Agarkova I, Moritz W, Kelm JM (2013) Multi-cell type human liver microissues for hepatotoxicity testing. *Arch Toxicol* 87:209-213
- Moridani MY, Cheon SS, Khan S, O'Brien PJ (2002) Metabolic activation of 4-hydroxyanisole by isolated rat hepatocytes. *Drug Metab Dispos* 30:1063-1069
- Myllynen P, Pasanen M, Pelkonen O (2005) Human placenta: a human organ for developmental toxicology research and biomonitoring. *Placenta* 26:361-371
- Oglesby LA, Ebron-McCoy MT, Logsdon TR, Copeland F, Beyer PE, Kavlock RJ (1992) In vitro embryotoxicity of a series of para-substituted phenols: structure, activity, and correlation with in vivo data. *Teratology* 45:11-33
- Ozolinš. TRS (2010) De-risking developmental toxicity-mediated drug attrition in the pharmaceutical industry. In: Xu JJ and Urban L (eds.) *Predictive toxicology in drug safety*. Cambridge University Press, Cambridge, pp 153-182
- Pastore A, Federici G, Bertini E, Piemonte F (2003) Analysis of glutathione: implication in redox and detoxification. *Clin Chim Acta* 333:19-39
- Piersma AH, Bosgra S, van Duursen MBM, Hermsen SAB, Jonker LRA, Kroese ED, van der Linden SC, Man H, Roelofs MJE, Schulpen SHW, Schwarz M, Uibel F, van Vugt-Lussenburg BMA, Westerhout J, Wolterbeek APM,

- van der Burg B (2013) Evaluation of an alternative in vitro test battery for detecting reproductive toxicants. *Reprod Toxicol* 38:53-64
- Roth A and Singer T (2014) The application of 3D cell models to support drug safety assessment: Opportunities & challenges. *Adv Drug Delivery Rev* 69-70:179-189
- Rotroff DM, Wetmore BA, Dix DJ, Ferguson SS, Clewell HJ, Houck KA, LeCluyse EL, Andersen ME, Judson RS, Smith CM, Sochaski MA, Kavlock RJ, Boellmann F, Martin MT, Reif DM, Wambaugh JF, Thomas RS (2010) Incorporating human dosimetry and exposure into high-throughput in vitro toxicity screening. *Toxicol Sci* 117:348-358
- Spielmann H, Seiler A, Bremer S, Hareng L, Hartung T, Ahr H, Faustman E, Haas U, Moffat GJ, Nau H, Vanparys P, Piersma A, Sintes JR, Stuart J (2006) The practical application of three validated in vitro embryotoxicity tests. *Altern Lab Anim* 34:527-538
- Strikwold M, Spenkelink B, Woutersen RA, Rietjens IMCM, Punt A (2013) Combining in vitro embryotoxicity data with physiologically based kinetic (PBK) modelling to define in vivo dose-response curves for developmental toxicity of phenol in rat and human. *Arch Toxicol* 87:1709-1723
- Stummann TC, Hareng L, Bremer S (2008) Embryotoxicity hazard assessment of cadmium and arsenic compounds using embryonic stem cells. *Toxicology* 252:118-122
- T'Jollyn H, Boussey K, Mortishire-Smith RJ, Coe K, De Boeck B, Van Bocxlaer JF, Mannens G (2011) Evaluation of three state-of-the-art metabolite prediction software packages (Meteor, MetaSite, and StarDrop) through independent and synergistic use. *Drug Metab Dispos* 39:2066-2075
- Tandon S and Jyoti S (2012) Embryonic stem cells: An alternative approach to developmental toxicity testing. *J Pharm BioAll Sci* 4:96-100
- Theunissen PT, Pennings JLA, van Dartel DAM, Robinson JF, Kleinjans JCS, Piersma AH (2013) Complementary detection of embryotoxic properties of substances in the neural and cardiac embryonic stem cell tests. *Toxicol Sci* 132:118-130
- Thomas RS, Philbert MA, Auerbach SS, Wetmore BA, Devito MJ, Cote I, Rowlands JC, Whelan MP, Hays SM, Andersen ME, Meek MEB, Reiter LW, Lambert JC, Clewell III HJ, Stephens ML, Zhao QJ, Wesselkamper SC, Flowers L, Carney EW, Pastoor TP, Petersen DD, Yauk CL, Nong A (2013) Incorporating new technologies into toxicity testing and risk assessment: moving from 21st century vision to a data-driven framework. *Toxicol Sci* 136:4-18
- UGT Alleles Nomenclature Home Page 2015. Available at: <https://www.pharmacogenomics.pha.ulaval.ca/ugt-alleles-nomenclature/>.
- Vähäkangas K, Loikkanen J, Sahlman H, Karttunen V, Repo J, Sieppi E, Kummu M, Huuskonen P, Myöhänen K, Storvik M, Pasanen M, Myllynen P, Pelkonen O (2014) Biomarkers of toxicity in human placenta. In: Gupta RC (ed.) *Biomarkers in Toxicology*. Academic Press/Elsevier, Amsterdam, pp 325-360
- Van der Laan JW, Chapin RE, Haenen B, Jacobs AC, Piersma A (2012) Testing strategies for embryo-fetal toxicity of human pharmaceuticals. Animal models vs. in vitro approaches. A workshop report. *Regul Toxicol Pharmacol* 63:115-123
- Volpe DA (2011) Drug-permeability and transporter assays in Caco-2 and MDCK cell lines. *Future Medicinal Chemistry* 3:2063-2077
- Wang M, Zhang Y, Sun B, Sun Y, Gong X, Wu Y, Zhang X, Kong W, Chen Y (2014) Permeability of exendin-4-loaded chitosan nanoparticles across MDCK cell monolayers and rat small intestine. *Biol Pharm Bull* 37:740-747
- Wetmore BA, Wambaugh JF, Allen B, Ferguson SS, Sochaski MA, Setzer RW, Houck KA, Strobe CL, Cantwell K, Judson RS, LeCluyse E, Clewell III HJ, Thomas RS, Andersen ME (2015) Incorporating high-throughput exposure predictions with dosimetry-adjusted in vitro bioactivity to inform chemical toxicity testing. *Toxicol Sci* 148:121-136
- Wetmore BA, Wambaugh JF, Ferguson SS, Li L, Clewell III HJ, Judson RS, Freeman K, Bao W, Sochaski MA, Chu TM, Black MB, Healy E, Allen B, Andersen ME, Wolfinger RD, Thomas RS (2013) Relative impact of incorporating pharmacokinetics on predicting in vivo hazard and mode of action from high-throughput in vitro toxicity assays. *Toxicol Sci* 132:327-346
- Wetmore BA, Wambaugh JF, Ferguson SS, Sochaski MA, Rotroff DM, Freeman K, Clewell HJ, Dix DJ, Andersen ME, Houck KA, Allen B, Judson RS, Singh R, Kavlock RJ, Richard AM, Thomas RS (2012) Integration of dosimetry, exposure, and high-throughput screening data in chemical toxicity assessment. *Toxicol Sci* 125:157-174
- Wilkinson GR and Shand DG (1975) A physiological approach to hepatic drug clearance. *Clin Pharmacol Ther* 18:377-390
- Yap MS, Nathan KR, Yeo Y, Lim LW, Poh CL, Richards M, Lim WL, Othman I, Heng BC (2015) Neural differentiation of human pluripotent stem cells for nontherapeutic applications: toxicology, pharmacology, and in vitro disease modeling. *Stem Cells Int* 2015:1-11
- Yi ZS and Liu SS (2005) Support vector machines for prediction of mechanism of toxic action from multivariate classification of phenols based on MEDV descriptors. *Internet Electron J Mol Des* 4:835-849



CHAPTER 7

Summary

Many efforts have been undertaken over the past decades to develop *in vitro* tests for a wide range of toxicological endpoints as an alternative to animal testing. The principle application of *in vitro* toxicity assays still lies in the hazard assessment and the prioritisation of chemicals for further toxicity testing. The *in vitro* toxicity outcomes are hardly used in quantitative risk assessment of chemicals, for example to predict health-based guidance values like an acceptable or tolerable daily intake (ADI or TDI). An important reason for this limited use is that an *in vitro* toxicity assay cannot provide a complete *in vivo* dose-response curve from which a point of departure (PoD) for risk assessment, like a no observed adverse effect level (NOAEL) or a 95% lower confidence limit of the benchmark dose (BMDL) can be derived. Translation of *in vitro* toxicity data to the *in vivo* situation is of paramount importance to overcome these constraints. Physiologically based kinetic (PBK) models, which mathematically describe the absorption, distribution, metabolism and excretion (ADME) of a compound in an organism, can be used to extrapolate *in vitro* derived toxicity data to *in vivo* toxicity values.

The aim of the present thesis was to demonstrate the potential of a combined *in vitro* PBK-based approach to translate *in vitro* toxicity data to *in vivo* toxicity values for rat and human predicting *in vivo* dose-response curves that allow definition of a PoD for risk assessment. This translation was carried out by applying PBK-based reverse dosimetry, using *in silico* and *in vitro* defined kinetic parameters, and by combining the *in vitro* PBK approach with Monte Carlo simulations to assess interindividual variability. The present thesis focused on the prediction of *in vivo* developmental toxicity. The ES-D3 differentiation assay of the embryonic stem cell test (EST) was selected as a representative *in vitro* assay for this toxicity endpoint. Phenol and a series of para-substituted phenols being p-fluorophenol, p-heptyloxyphenol, p-mercaptophenol and p-methylketophenol were chosen as model compounds.

Chapter 1 introduces the methods and concepts that are used in the present thesis, namely *in vitro* developmental toxicity testing, PBK modelling and Monte Carlo simulations. Also the general outline of the *in vitro* PBK approach using reverse dosimetry is presented. Furthermore, a brief description of the ADME properties of each phenol that is included in the present thesis is given.

In **chapter 2** the applicability of the EST as an alternative assay to predict developmental toxicity for the selected phenols was evaluated. The embryotoxic potencies of the phenols obtained with the EST were compared with potency data reported in the literature for the WEC assay, providing a similar potency ranking. The results suggest that the EST can identify the intrinsic embryotoxic potency of the phenols. However, when comparing the potency ranking of the EST to *in vivo* reported potency data on developmental toxicity of the phenols, it was concluded that the EST was not able to correctly rank the phenols according these *in vivo* potency data. Only phenol was correctly ranked, being the least potent congener, while the relative toxic potency of p-heptyloxyphenol was overestimated in the EST, when compared to the *in vivo* derived relative potency value. It was hypothesised that combining *in vitro* toxicity

data with kinetic modelling could improve the *in vivo* toxicity prediction.

In **chapter 3** we combined *in vitro* toxicity data from the EST with PBK-based modelling for the compound phenol. For this purpose, PBK models were developed that describe the ADME of phenol in rat and human. The PBK models were parameterised with *in vitro* and *in silico* data and data taken from the literature. Evaluation of the PBK models pointed out that the oral absorption coefficient and phenol glucuronidation are influential model parameters for the predicted phenol plasma concentration. PBK-based reverse dosimetry was applied to translate the *in vitro* effect concentrations obtained from the EST to *in vivo* effective dose levels from which an *in vivo* dose-response curve was generated allowing the prediction of a PoD for risk assessment. The predicted PoD thus obtained for the rat lies within the range of PoDs for phenol obtained from *in vivo* developmental toxicity data from the literature. The results demonstrate the potential of PBK-based reverse dosimetry to translate *in vitro* toxicity data to *in vivo* toxicity values that can be used for quantitative hazard and risk assessment purposes, like deriving safe exposure levels.

In **chapter 4** it was explored whether PBK-based reverse dosimetry could also successfully extrapolate *in vitro* toxicity data obtained in the EST to *in vivo* developmental toxicity values for a series of para-substituted phenols. It was of interest if this approach could overcome the differences observed between the *in vitro* and *in vivo* derived relative embryotoxic potencies for the phenols, especially for p-heptyloxyphenol. For each phenol, a PBK model for the rat was developed. *In silico* methods were selected and applied to predict input values for a number of PBK model parameters. *In vitro* assays were performed to predict metabolism of the test compounds and transport across the intestinal and the placental barrier. After completing the PBK models, reverse dosimetry was applied generating *in vivo* developmental toxicity data for each of the phenols from which a PoD was derived. These PoDs appeared to differ less than 3.8-fold from PoDs derived for the phenols from *in vivo* toxicity data available in the literature. The large difference that was observed between the *in vitro* and the *in vivo* relative embryotoxic potency for the phenols, especially for p-heptyloxyphenol, was reduced to a large extent after applying the *in vitro* PBK-based reverse dosimetry approach. Our modelling approach pointed towards metabolism by glucuronidation as the most important factor underlying the relative low toxic potency for p-heptyloxyphenol *in vivo* compared to the relatively high observed embryotoxic potency *in vitro*. Altogether, the results showed the feasibility of the PBK-based reverse dosimetry approach to properly extrapolate *in vitro* toxicity outcomes to *in vivo* toxicity values.

In **chapter 5** we demonstrated a modelling approach that integrates *in vitro* toxicity data, PBK modelling and Monte Carlo simulations to predict the effects of human interindividual variation in kinetics for phenol induced development toxicity. Incubations with recombinant uridine diphosphate glucuronyltransferases (UDPGTs) revealed that the enzymes UGT1A6 and UGT1A9 were mainly responsible for glucuronidation of phenol. Kinetic constants

describing the glucuronidation of phenol by UGT1A6 and UGT1A9 were included in the PBK model of phenol together with information about the variation in activity of these UGTs in the population and information on the interindividual variation for the oral absorption coefficient. Monte Carlo simulations in connection with PBK modelling provided a population distribution of phenol plasma concentrations, from which chemical specific adjustment factors (CSAFs) were calculated that cover interindividual human kinetic variation. It was concluded that the default safety factor of 3.16 applied for interindividual human kinetic differences in the safety assessment of chemicals is adequate protective, given that the predicted CSAF lies within this value. Dividing the dose-response curve data obtained with in vitro PBK-based reverse dosimetry with the CSAF provided a dose-response curve that reflects the consequences of the interindividual variability in phenol kinetics for the developmental toxicity of phenol. Altogether, this chapter presented a non-animal based approach to predict interindividual human variation in sensitivity to phenol induced developmental toxicity.

Chapter 6 discusses prominent aspects of the in vitro PBK-based reverse dosimetry approach. The items discussed encompass the selection of the EST as an alternative in vitro assay to predict developmental toxicity, different considerations regarding PBK modelling, the use of different kinetic reverse dosimetry approaches to perform in vitro toxicity to in vivo toxicity extrapolations (IVIVE) and the possibility to take interindividual variations into account. Finally, future perspectives related to the application of the PBK-based reverse dosimetry to predict in vivo toxicity values from in vitro toxicity data are outlined.

In conclusion, this thesis demonstrated that the approach of combining in vitro toxicity data with PBK-based reverse dosimetry has the potential to overcome a major bottleneck in the hazard and risk assessment of chemicals, since it was not only able to improve in vitro toxic potency estimates but more importantly it provided adequate quantitative toxicity estimates such as a PoD. Altogether this thesis contributes to the replacement of apical endpoints in animal studies for the safety testing of chemicals, towards an approach that is cheaper, non-animal based and more directly relevant for humans.

ACKNOWLEDGEMENTS

First of all I would like to express my gratitude to my promotors Ivonne Rietjens and Ruud Woutersen, and my co-promotor Ans Punt. I enjoyed our pleasant meetings with our lively and fruitful discussions and appreciated the space you gave me to share my thoughts with you. Ivonne, during my MSc project at the toxicology department, you asked me if I had plans to participate in a PhD program, which triggered me to explore the possibilities. I am grateful that you helped in the preparations which resulted in this PhD project, thank you! During the project you kept me focussed and I highly appreciated your critical views and I am very thankful for the dedication that you expressed to my PhD trajectory. Ruud, thank you for your always so calm and friendly support, and just like Ivonne your prompt replies to the drafts and emails no matter if you were in Zeist, Parma or Luxembourg. Ans, thank you for all your support, even when you changed jobs. I always felt very welcome to step into your office starting a 'PBK talk', which I enjoyed very much. You were a good sparring partner, thanks a lot!

Bert and Laura, I am happy that you both accepted being my paranymf. Bert, thank you for always being so helpful and friendly. Nothing was too much for you, taking samples in the weekend or, at the end of my PhD, starting up the UPLC so I could focus on my experiments. I also enjoyed our conversations of anything and everything. Laura, working together on Caco-2 and BeWo transport experiments was not only efficient, but also a lot of fun! Laura, I would also like to thank you and Ad for your hospitality, it was great that I could stay over in your house when I was in Wageningen for some days, also enjoying the nice dinners you prepared.

I also would like to thank the other (former) colleagues at the toxicology department; Jochem (thanks for introducing me to the EST), Reiko, Nynke, Alexandros, Wasma, Hequn (thanks for helping me with my first BeWo experiment), Jonathan, Karsten, Samantha, Hans, Rungnapa, Rozaini, Ans S., Arif, Erryana, Irene, Letty, Lidy, Myrthe, Suzanne, Ignacio, Nico, Sebas, Barae, Aziza and Si. Although I was not based in Wageningen and dropped by irregularly I always felt very welcome and at home indicating the great atmosphere at the department.

I would like to express my gratitude to TNO were I could perform the EST experiments, with special thanks for Mariska and Birol for changing cell culture medium, saving me a trip from Groningen to Zeist.

I also would like to thank my colleagues from Van Hall Larenstein University of Applied Sciences (too much to name you all individually). Thank you for your interest and good fellowship. Wendy Zuidema-Haans, a special thanks to you, for facilitating my PhD research where possible.

Thanks a lot to my dear friends Arianne & Gijs, Chantal & Irma and my family members Martijn & Annelies where I could stay whenever I was in Zeist or in Wageningen for performing experiments. Thank you for your generous hospitality and the nice evenings we had!

I would like to express my sincere gratitude to my parents Chris and Agnes, my sister Saskia and my parents in law Sytze and Laura and my brother and sister in law Jan Peter and

Carina for their interest, love and support. I also much appreciate you took great care for our children Minke & Maureen at busy times, thank you!

Ynske, you are the love of my life! Your love, support, care and humour in the past years were priceless. We share so many precious moments, together and with our wonderful children Warner*, Minke and Maureen, who gave us a deeper understanding and sense about the beauty of life. I am so happy to experience that with you.

ABOUT THE AUTHOR

CURRICULUM VITAE

Marije Strikwold was born June 19, 1978 in Eelde. After completing her secondary education at the Sint Maartens College in Haren (Gn), she started with the study Environmental Sciences at the Van Hall Instituut in Leeuwarden. Her final thesis was about the integration of a soil information system with a human exposure model for soil contamination. After her graduation in 2000, she started as a consultant at the Van Hall Instituut Business Center, where she developed exposure models for human risk assessment of soil contamination and trained people, nationally and internationally, to apply these models in practice. From 2003-2008 Marije studied Biomedical Sciences at the Institute for Risk Assessment Sciences (IRAS) at Utrecht University, next to her job as a consultant. As part of this study she performed a research project concerning an epidemiological analysis to predictors of dust and endotoxin levels and asthma related health endpoints at IRAS. She also performed a research project at Wageningen University at the subdepartment of toxicology, where she developed and validated ecotoxicological Quantitative Structure-Activity Relationships (QSAR) for a series of phenols. She conducted her MSc thesis at the National Institute for Public Health and the Environment (RIVM) where she studied differences in six European crop consumption models.

In 2010, Marije started her PhD programme at Wageningen University, which she combined with her job as a consultant, and from 2011 with her job as a lecturer in toxicology at the Life Sciences & Technology department of Van Hall Larenstein University of Applied Sciences in Leeuwarden. During this period, her Postgraduate Education in Toxicology was completed, which enables her to become registered as a Toxicologist by the Netherlands Society of Toxicology (NVT) and the European Society of Toxicology (EUROTOX). Currently, Marije holds a full-time position as a lecturer and researcher at Van Hall Larenstein University of Applied Sciences, where she participates in the applied research groups Food, Health and Safety and Sustainable Water Systems.

LIST OF PUBLICATIONS

PEER REVIEWED PUBLICATIONS

Strikwold M, Spenkeliink B, Woutersen RA, Rietjens IMCM, Punt A (2013) Combining in vitro embryotoxicity data with physiologically based kinetic (PBK) modelling to define in vivo dose-response curves for developmental toxicity of phenol in rat and human. *Arch Toxicol* 87:1709-1723

Strikwold M, Woutersen RA, Spenkeliink B, Punt A, Rietjens IMCM (2012). Relative embryotoxic potency of p-substituted phenols in the embryonic stem cell test (EST) and comparison to their toxic potency in vivo and in the whole embryo culture (WEC) assay. *Toxicol Lett* 213:235-24.

Gehring U, Strikwold M, Schram-Bijkerk D, Weinmayr G, Genuneit J, Nagel G, Wickens K, Siebers R, Crane J, Doekes G, Di Domenicantonio R, Nilsson L, Priftanji A, Sandin A, El-Sharif N, Strachan D, van Hage M, von Mutius E, Brunekreef B; ISAAC Phase Two Study Group (2008) Asthma and allergic symptoms in relation to house dust endotoxin: Phase Two of the International Study on Asthma and Allergies in Childhood (ISAAC II). *Clin Exp Allergy* 38:1911-1920

Strikwold M, Spenkeliink A, de Haan LHJ, Woutersen RA, Punt A, Rietjens IMCM. Integrating in vitro data and physiologically based kinetic (PBK) modelling to assess the in vivo potential developmental toxicity of a series of phenols (submitted)

Strikwold M, Spenkeliink A, Woutersen RA, Rietjens IMCM Punt A. Development of a combined in vitro physiologically based kinetic (PBK) and Monte Carlo modelling approach to predict interindividual human variation in phenol induced developmental toxicity (submitted)

ABSTRACTS

Strikwold M, Punt A, Woutersen RA, Spenkeliink A, de Haan LHJ, Rietjens IMCM (2014) Assessment of potential embryotoxicity of a series of p-substituted phenols by an integrated QSAR-in vitro-PBK approach. In: *The 18th International Congress on In Vitro Toxicology ESTIV2014*:234

Strikwold M, Woutersen RA, Spenkeliink A, Rietjens IMCM, Punt A (2013) Extrapolating In vitro Embryotoxicity Data Towards In vivo Dose-response Curves And A Point Of Departure For Risk Assessment Using An In vitro-PBK Approach. In: *Annual meeting of the Netherlands Society of Toxicology (NVT)*

Strikwold M, Woutersen RA, Spenkelink B, Rietjens IMCM, Punt A (2013) Extrapolating in vitro embryotoxicity data toward in vivo exposure levels using a combined in vitro-physiologically based kinetic modeling approach. In: *The Toxicologist: Supplement to Toxicological Sciences* 132, Society of Toxicology. Abstract no 2458

Strikwold M and Zvinavashe E (2007) Improvement and development of QSAR's for phenols. *Chem-Biol Interact* 169:141

Smit PJ and Strikwold M (2003) Development of human exposure models depending on decision making process. In: *Proc SETAC Europe 13th Annual Meeting*:70

CONFERENCE PROCEEDINGS

Strikwold M, Smit PJ, Boeije LFM, Moet D, van Loenhout R, van der Plas R (2008) Sludge? Please in my backyard! In: *Proc 10th Int Conf ConSoil*:283-291

Strikwold M and Smit PJ (2005) Different users, different risk assessments; comparison of practical application of risk assessment models by different users. In: *Proc 9th Int Conf ConSoil*:1235-1240

Strikwold M and Swartjes FA (2005) Influence of different model algorithms and input values on exposure via crop consumption for 6 European models. In: *Proc 9th Int Conf ConSoil*:944-949

Smit PJ and Strikwold M (2005) Why do we apply human risk assessment models; an investigation of motives and consequences for development. In: *Proc 9th Int Conf ConSoil*:1170-1171

Strikwold M and Smit PJ (2003) Practical application of the human risk assessment model RISC-HUMAN in risk based land management. In: *Proc 8th Int Conf ConSoil*:3092-3095

Otte PF, Lijzen JPA, Smit PJ, Strikwold M. (2003). Evaluation of the Procedure to Determine the Remediation Urgency. In: *Proc 8th Int Conf ConSoil*:957-961

Smit PJ, Strikwold M, Lijzen JPA, Otte PF (2003). Seven years remediation of urgency method: bottlenecks to be eliminated. In: *Proc 8th Int Conf ConSoil*:585-591

OVERVIEW OF COMPLETED TRAINING ACTIVITIES

DISCIPLINE SPECIFIC ACTIVITIES

Courses

Cell Toxicology, Postgraduate Education in Toxicology (PET), 2014

Pathobiology, PET, 2013

Food Toxicology, PET, 2013

Mutagenesis and Carcinogenesis, PET, 2012

Organ Toxicology, PET, 2011

Medical and Forensic Toxicology, PET, 2011

Reproduction Toxicology, PET, 2011

Meetings

18th International Congress on In Vitro Toxicology (ESTIV), Egmond aan Zee, The Netherlands, 2014
(oral presentation)

53th Annual meeting of the American Society of Toxicology, Phoenix, USA, 2014

52th Annual meeting of the American Society of Toxicology, San Antonio, USA, 2013
(oral presentation)

Safety Evaluation Ultimately Replacing Animal Testing (SEURAT-1), Data analysis group Webinar
(oral presentation), 2013

Annual conference, Netherlands Society of Toxicology, 2015, 2013 (oral presentation), 2010

Mini-seminar Food Health and Safety, Van Hall Larenstein University of Applied Sciences 2015
(oral presentation)

Mini-seminar Sustainable Water Systems, Van Hall Larenstein University of Applied Sciences, 2015
Dutch Society of Toxicology PhD student symposia, 2010, 2011, 2013-2015

GENERAL COURSES

Risk Assessment, PET, 2010

Laboratory Animal Science (B), PET, 2012

Talented oriented coaching, NHL University of Applied Sciences, 2014

OPTIONAL ACTIVITIES

Attending scientific presentations, Division of Toxicology Wageningen University, 2010-2015

Research and literature discussion presentations, Van Hall Larenstein University of Applied Sciences, 2010-2015

Preparation Research Proposal, 2009

APPROVED BY THE GRADUATE SCHOOL VLAG

The studies described in this thesis were conducted within a collaborative project of Wageningen University, TNO and Van Hall Larenstein University of Applied Sciences. The research described in this thesis was funded through the programme Alternatives to Animal Experiments III of The Netherlands Organisation for Health Research and Development (ZonMw) (project number 114011002).

Financial support from Wageningen University and Van Hall Larenstein University of Applied Sciences for printing this thesis is gratefully acknowledged.

Printing: GVO drukkers & vormgevers B.V., Ede, The Netherlands

Layout and thesis cover: J Ontwerp

Marije Strikwold, 2016

